Thermal Stress and Bleaching in the Cnidarian-Dinoflagellate Symbiosis: The Application of Metabolomics

Katie E. Hillyer

A thesis
submitted to the Victoria University of Wellington
in fulfilment of the requirements for the degree of
Doctor of Philosophy

Victoria University of Wellington
(2016)

Abstract

Reef-building corals form critical ecosystems, which provide a diverse range of goods and services. Their success is based on a complex symbiosis between cnidarian host, dinoflagellate algae (genus *Symbiodinium*) and associated microorganisms (together termed the holobiont). Under functional conditions nutrients are efficiently recycled within the holobiont; however, under conditions of thermal stress, this dynamic relationship can dysfunction, resulting in the loss of symbionts (bleaching). Mass coral bleaching associated with elevated temperatures is a major threat to the long-term persistence of coral reefs. Further study is therefore necessary in order to elucidate the cellular and metabolic networks associated with function in the symbiosis and to determine change elicited by exposure to thermal stress. Metabolomics is the study of small compounds (metabolites) in a cell, tissue or whole organism. The metabolome comprises thousands of components, which will respond rapidly to change, reflecting a combination of genotype, phenotype and the environment. As a result, the study of these metabolic networks serves as a sensitive tool for the detection and elucidation of cellular responses to abiotic stress in complex systems.

This thesis presents outputs of gas chromatography-mass spectrometry-based metabolite profiling techniques, which have been applied to the study of thermal stress and bleaching in the cnidarian-dinoflagellate symbiosis. In **Chapter 2** these techniques were developed and applied to the model symbiotic cnidarian *Aiptasia* sp., and its homologous symbiont (*Symbiodinium* ITS 2 type B1), to characterise both ambient and thermally-induced metabolite profiles (amino and non-amino organic acids) in both partners. Thermal stress, symbiont photodamage and associated bleaching, resulted in characteristic modifications to the free metabolite pools of both partners. These changes differed between partners and were associated with modifications to central metabolism, biosynthesis, catabolism of stores and homeostatic responses to thermal and oxidative stress.

In **Chapter 3** metabolite profiling techniques (focussing this time on carbohydrate pools) were once again applied to the study of thermally-induced changes to the free pools of the coral *Acropora aspera* and its symbionts (dominant *Symbiodinium* ITS 2 type C3) at differing stages of symbiont photodamage and thermal stress. Additionally, targeted analysis was employed to quantify these changes in terms of absolute amounts. Once again exposure to elevated temperatures resulted in symbiont photodamage, bleaching and characteristic modifications to the free metabolite pools of symbiont and host, which differed between partners and with the duration of thermal stress. These changes were associated with increased turnover of a number of networks including: energy-generating pathways, antioxidant networks, ROS-associated damage and damage signalling, and were also indicative of potential alterations to the composition of the associated microbial holobiont.

Finally in **Chapter 4**, metabolite profiling techniques optimized in **Chapter 2** and **3** were coupled to ^{13}C labelling in both *Aiptasia* sp. and *A. aspera*, in order to further investigate the questions raised in these preceding studies. Once again changes were observed to central metabolism, biosynthesis and alternative energy-generation modes in symbiont and host, in both symbioses. Interestingly however, in all cases there was continued fixation of carbon, production- and translocation of mobile products by the remaining symbionts *in hospite*. This suggests that even during the later stages of bleaching, symbionts are, at least in part, metabolically functional in terms of photosynthate provision.

This study therefore serves as an important first step in developing the application of metabolomics-based techniques to the study of thermal stress in the cnidarian-dinoflagellate symbiosis. The power of these techniques lies in the capacity to simultaneously assess rapid and often post-translational change in a highly repeatable and quantitative manner. With the use of these methods, this study has shown how metabolic, homeostatic and acclimatory networks interact to elicit change in each partner of the symbiosis during thermal stress and how these responses vary between symbiotic partners. Further understanding of these networks, individual sensitivities- and enhanced resistance to thermal stress are essential if we are to better understand the capacity of coral reefs to acclimate and persist in the face of climate change.

Contributions and publications

Chapter two:

This chapter is formatted as a stand-alone manuscript based on a published study.

Hillyer, K. E., Tumanov, S., Villas-Bôas, S. and Davy, S. K. (2015). Metabolite profiling of symbiont and host during thermal stress and bleaching in a model cnidarian-dinoflagellate symbiosis. *Journal of Experimental Biology*, jeb. 128660.

R.A. Keyzers assisted with GC-MS analysis of preliminary samples at the School of Chemistry and Physical Sciences, VUW. Sample preparation and GC-MS analysis of experimental samples were undertaken at the Centre for Genomics, Proteomics and Metabolomics, School of Biological Sciences, University of Auckland, New Zealand. S. Tumanov assisted with the sample processing, GC-MS and data analysis. M. Han assisted with the PAPi analysis. S. Villas-Boas and S.K. Davy advised on the experimental design, sample processing, data analysis, interpretation and writing.

Chapter three:

This chapter is formatted as a stand-alone manuscript based on a publication in preparation.

Molecular analysis of symbiont ITS 2 type and write up of this analysis were carried out by S. Wilkinson. D. Dias produced **Figure 3.4** and assisted with **Sections 3.2.5** to **3.2.8**. Morgan Han assisted with PAPi analysis. Sample preparation and GC-MS analysis were undertaken at Metabolomics Australia, The University of Melbourne, Australia. A. Lutz assisted with the sample processing set-up. D. Dias, N. Jayasinghe and H. Mendis assisted with the GC-MS analysis and data analysis. U. Roessner and S.K. Davy advised on the experimental design, data analysis, interpretation and writing.

Chapter four:

This chapter is formatted as a stand-alone manuscript based on a publication in preparation.

R.A. Keyzers assisted with GC-MS analysis of preliminary samples at the School of Chemistry and Physical Sciences, VUW. D. De Souza, S. O'Callaghan, D. Callahan and U. Roessner, Bio21 Institute, The University of Melbourne, Australia, assisted with data analysis and interpretation of preliminary data. Sample preparation and GC-MS analysis were undertaken at Metabolomics Australia, The University of Melbourne, Australia. A. Lutz assisted with the sample processing set-up. D. Dias, N. Jayasinghe and H. Mendis assisted with the GC-MS analysis and data analysis. D. Dias assisted with **Section 4.2.6**. U. Roessner and S.K. Davy advised on the experimental design, data analysis, interpretation and writing.

Acknowledgements

This thesis would not have been possible without the generous aid of so many people that I have come to meet over its course. Thank you firstly to those that have patiently endured and coaxed my transformation from the proverbial caterpillar into the somewhat-more biochemistry savvy metabolomics trainee, namely Rob Keyzers, all of those at the Centre for Genomics, Proteomics and Metabolomics, School of Biological Sciences, University of Auckland and Metabolomics Australia, The University of Melbourne, Australia. Particular heartfelt thanks to Niru Jayasinghe, Himasha Mendis, Dan Dias, Adrian Lutz, Sergey Tumanov, Silas Vilas Boas and Ute Roessner, there is no way I could I have done this without you! Thanks should also be extended to the Davy Lab Group, past and present, for their positivity, creative thinking and words of kindness along the way.

Thanks also go to DHL for defrosting the samples for Chapter 3 and 4 v1, allowing me the opportunity for the new and improved data Chapter 3 and 4 v2 and the creation of the collaboration with the most excellent Melbourne group. Thanks to all the staff at Heron Island Research Station, in particular to Dani, Liz and Pauline, who made sure that I was able to do it all over again and that stay number two went so smoothly. A big thank you also to everyone at Khalid bin Sultan Living Oceans Foundation, in particular to Dr Andrew Bruckner, Alex Dempsey and Phillip Renard (the accommodating dive buddy). I feel so incredibly grateful for the experiences joining the research missions gave me. Keep up the great work guys!

Similarly, I should also acknowledge my long-suffering family, friends and flatties for their continued love, unwavering support and understanding of my academic adventures. I blame my dad for getting me hooked on the sea from a young age and whose love for the ocean and everything in it (almost!) rivals my own.

I'd also like to thank my supervisor Prof. Simon Davy for his patient encouragement, wise words and support when things got tough, not to mention his exceptional understanding of just how to play the academic game. I still have a lot to learn, but I have had a great start.

Thank you all.

Table of Contents

List of figures

List of tables

List of abbreviations

3PGA 3-phosphoglycerate

AMDIS Automated Mass Spectral Deconvolution and Identification System

AsC Ascorbate

ATP Adenosine triphosphate

CoA Coenzyme A

CCM Carbon concentrating mechanism

Chl Chlorophyll

DHA Docosahexaenoic acid

DIC Dissolved inorganic carbon

DIN Dissolved inorganic nitrogen

DPA Docosapentaenoic acid

EI Electron ionization

FC Fold change

Fd Ferredoxin

FDR False discovery rate

FFA Free fatty acid

FIS Freshly isolated symbionts

FSW Filtered seawater

F_v/F_m Maximum quantum yield of photosystem II

G3P Glyceraldehyde 3-phosphate

GC-MS Gas chromatography – mass spectrometry

Gln Glutamine

Glu Glutamate

GOGAT Glutamine:2-oxoglutarate aminotransferase

GS Glutamine synthetase

GSH Glutathione

HPLC High performance liquid chromatography

HSP Heat shock protein

ITS Internal transcribed spacer

KEGG Kyoto Encyclopedia of Genes and Genomes

LC-MS Liquid chromatography – mass spectrometry

LIN Liquid nitrogen

MAA Mycosporine-like amino acid

MCF Methyl chloroformate

MD Metabolite Detector

MFA Metabolic flux analysis

MID Mass isotopomer distribution

MOX Methoxyamine

MSTFA N-Methyl-N-(trimethylsilyl) trifluoroacetamide

MQ MilliQ ultrapure water

MUFA Monounsaturated fatty acid

m/z Mass-to-charge ratio

NAD Nicotinamide adenine dinucleotide

NADP Nicotinamide adenine dinucleotide phosphate

NMR Nuclear magnetic resonance

NO Nitric oxide

NTFD Non-Targeted Tracer Fate Detection

PAM Pulse amplitude modulated

PAPi Pathway activity profiling

PC Principal component

PCA Principal components analysis

PS I Photosystem I

PS II Photosystem II

PUFA Polyunsaturated fatty acid

RI Retention index

ROS Reactive oxygen species

RT Retention time

RUBP Ribulose-1,5-biphosphate

SEM Standard error mean

SFA Saturated fatty acid

TAG Triacylglycerol

TCA Tricarboxylic acid

TMS Trimethylsilyl

Chapter 1 General introduction

1.1 Global scale goods and services of coral reefs

A coral reef system, the Great Barrier Reef, is the single living structure visible from outer space, however the value of coral reefs lies not only in the scale of the habitats that they create, but also in the variety of species that these ancient systems foster. Reef-building (hermatypic) corals can typically be found within coastal tropical latitudes between 25°S and 25°N, in areas of low nutrients, turbidity and suitable water biochemistry, which enable reef structures to accrete (Johannes et al., 1983; Hoegh-Guldberg, 1999) (**Fig. 1.1**). Coral reef systems are both highly efficient and incredibly diverse, likened to those of terrestrial rainforests for the sheer abundance and range of species that they support (Connell, 1978; Crossland et al., 1991). These species extend to the surrounding low-lying, coastal communities, for which in many developing countries, coral reef habitats provide a valuable source of protein, income and coastal protection (Moberg and Folke, 1999; De Groot et al., 2002) (**Fig. 1.2**). These ancient habitats also offer significant opportunities for bio-prospecting and the development of pharmaceuticals, in addition to their inherent social and cultural worth (Spurgeon, 1992; Moberg and Folke, 1999).

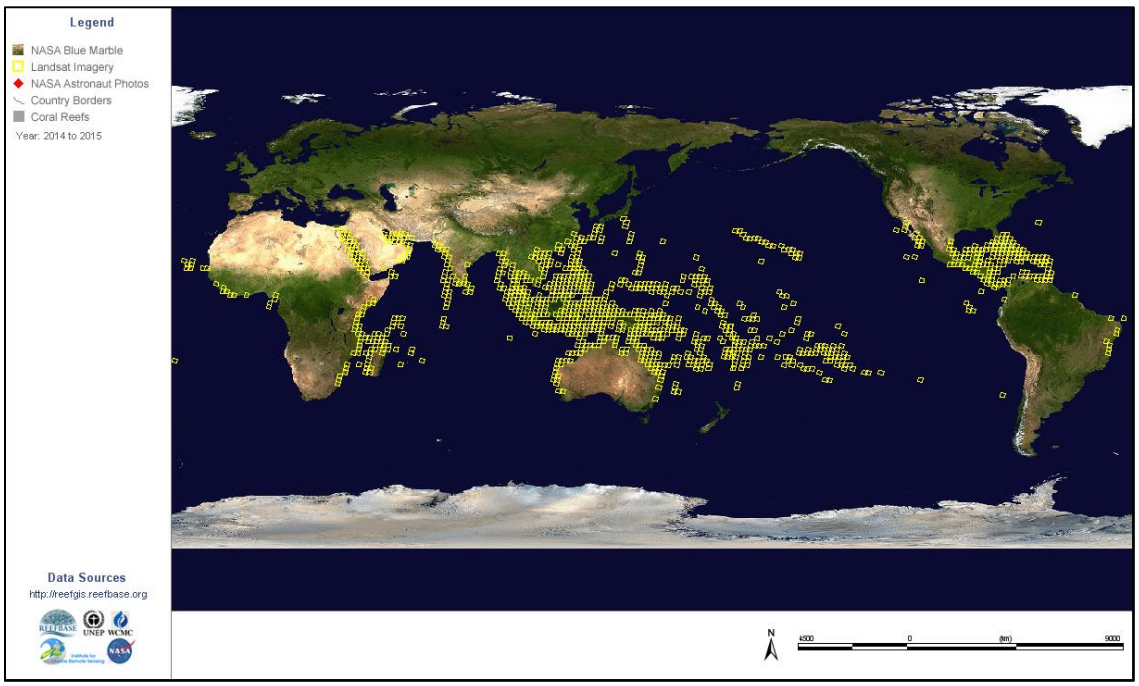

Fig. 1.1: The global distribution of tropical coral reefs. Source: ReefBase http://www.reefbase.org

1.2 The coral symbiosis

Hermatypic corals comprise the stony corals of the order Scleractinia (phylum Cnidaria). These corals secrete calcareous skeletons, which form the basis of coral reef systems, however a diverse range of taxa are important in a reef's resistance to stress and long-term successful persistence (Hughes et al., 2003; Nyström et al., 2008; Hughes et al., 2010). These range from tiny calcareous algae, which help cement the reef structure preventing erosion, to grazing fish species, which are important for controlling excessive growth of fleshy algal species that can outcompete corals (Hughes, 1994; Mumby et al., 2006). However, central to the success of hermatypic corals is the mutually beneficial relationship of the cnidarian host with dinoflagellate symbionts, of the genus *Symbiodinium* (Muscatine and Hand, 1958; Muscatine and Cernichiari, 1969; Yellowlees et al., 2008).

Fig. 1.2: An aerial view of the island of Bora Bora, French Polynesia, exemplifying a spectacular barrier reef system. Image courtesy of A. Bruckner/Khaled bin Sultan Living Oceans Foundation.

Symbiosis in its most basic sense is the living together of two species (De Bary, 1879). This relationship exists on a continuum of benefit and complexity, from opportunistic parasitism (where one partner gains at the expense of the other), to obligate mutualism (where both partners benefit in some form and symbiosis is necessary for persistence), and often these relationships are both ancient and highly

specific (Herre et al., 1999). The basis of successful mutualism lies not only in the exchange of goods at a net benefit to each partner, but also in the capacity of at least one partner to acquire novel capabilities, for instance the fixation of nitrogen in legumes (Doebeli and Knowlton, 1998; Herre et al., 1999). As a result of their benefits, mutualistic symbioses between photosynthetic algal symbionts and invertebrate hosts are widespread in both marine and freshwater environments (Trench, 1993; Venn et al., 2008). In benthic marine taxa, *Symbiodinium*-invertebrate associations predominate, which in addition to cnidarians, include representatives of species of sponge, bivalve, gastropod and flatworm (Trench, 1993; Venn et al., 2008). In addition to their primary dinoflagellate symbionts, each host will also form associations with a diverse and specific array of microorganisms, together forming the so-called 'holobiont' (Rohwer et al., 2002; Thompson et al., 2015).

1.2.1 The cnidarian host

As cnidarians, reef-building corals have a relatively simple body plan; each individual (polyp) consists of a central body cavity (coelenteron) and oral disc, which is surrounded by a ring of tentacles (**Fig.1.3**) (Veron, 2000). The body wall comprises two cell layers, the outer epidermis and the inner gastrodermis; these tissues are separated by an acellular layer called the mesogloea. Each individual polyp is located within an enclosed area of skeleton (corallite); these corallite structures and indeed the polyps they house vary greatly in size and shape according to species (Porter, 1976). Species range from solitary to colonial, and are capable of reproducing both sexually and asexually (Richmond and Hunter, 1990; Harrison, 2011). Individuals may reproduce through asexual division and fragmentation, or sexually, either *via* broadcast spawning, or brooding their larvae (Fadlallah, 1983; Richmond and Hunter, 1990; Hall and Hughes, 1996). Colony growth form is also highly plastic, and morphology may vary according both to species and environmental variables, such as depth, turbidity and wave exposure (Goreau, 1959; Chappell, 1980).

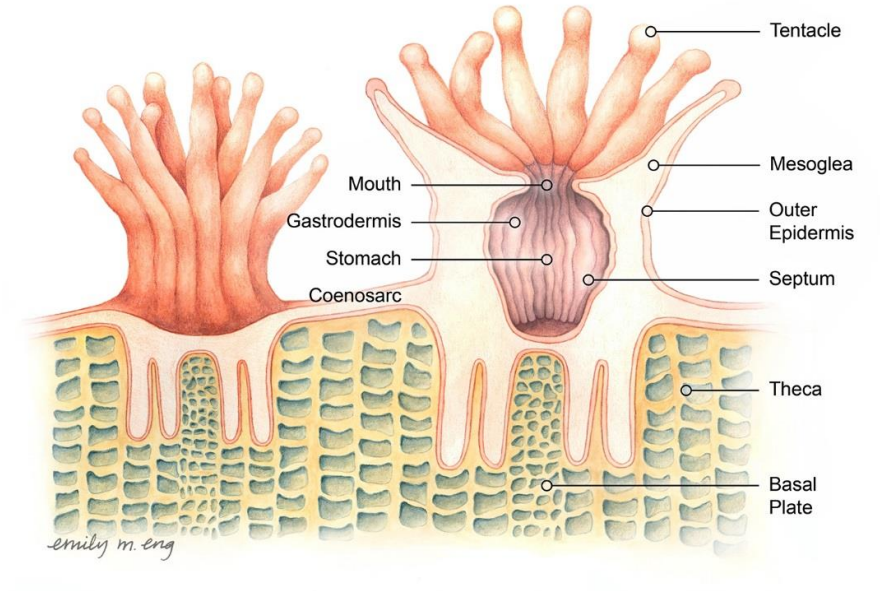

Fig. 1.3: Cross-section of a coral polyp. Image by Emily M. Eng, www.emilymeng.com. Reproduced with permission of the artist.

1.2.2 The dinoflagellate symbiont

The *Symbiodinium* are an ancient and highly genetically diverse genus of dinoflagellates (LaJeunesse, 2001; Coffroth and Santos, 2005). Currently, there are nine described clades (A-I), each containing multiple sub-clades ('types'), which are equivalent to species in their genetic variation (Coffroth and Santos, 2005; Pochon et al., 2006; Pochon and Gates, 2010). Each type differs somewhat in physiology and ecological range, with varying environmental optima and geographic distributions (LaJeunesse, 2001; Baker, 2003). Key morphological and physiological differences include the structure of cell membranes (Tchernov et al., 2004; Díaz-Almeyda et al., 2011), antioxidant capacity (Krueger et al., 2014), modes of carbon concentration (Brading et al., 2013), free metabolite pools (Klueter et al., 2015), photophysiology and photoprotective mechanisms (Iglesias-Prieto et al., 1991; Hill et al., 2012; Suggett et al., 2015).

In symbiosis, the dinoflagellate algae are encapsulated within a host-derived membrane (symbiosome), located within the gastrodermal cells of each polyp (Wakefield and Kempf, 2001) (**Fig. 1.4**). *In hospite*, *Symbiodinium* are in a vegetative state, with major cellular structures including a cellulose cell wall, typical

eukaryotic organelles (nucleus and mitochondria), a lobed chloroplast with an associated pyrenoid and storage compartments, such as starch granules, and lipid bodies (Freudenthal, 1962; Trench, 1971; Schoenberg and Trench, 1980) (**Fig. 1.5**). When *in hospite*, the symbiont cells typically divide mitotically, forming daughter cells, which are subsequently encapsulated in their own symbiosomes (Trench, 1993).

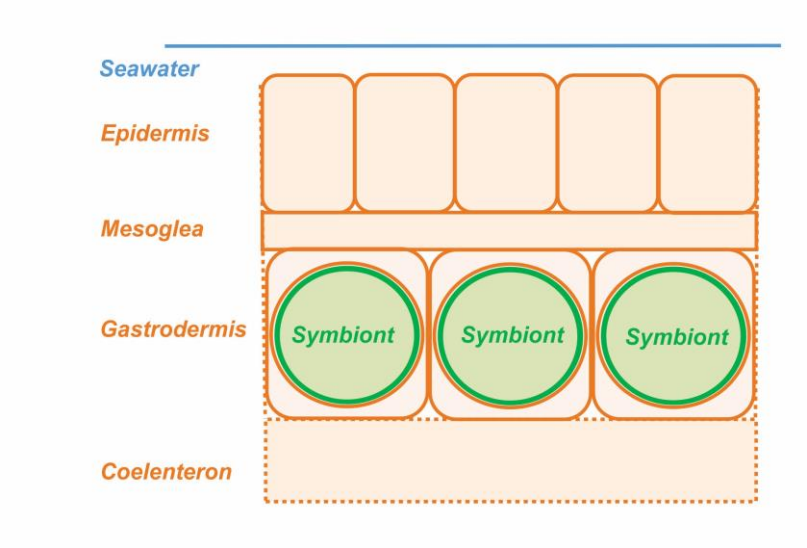

Fig. 1.4: Simplified schematic showing the cnidarian tissue structure. From the upper epidermis which is exposed to the surrounding seawater, to the acellular mesogloea, to the gastrodermal cells which enclose the symbiont cell. The gastrodermis lines the coelenteron space or gastrovascular cavity. N.B. not to scale.

1.2.3 The holobiont

Reef-building corals exhibit differing scales of specificity and flexibility in the partnerships that they form with *Symbiodinium* clades and types, and *vice versa* (Baker, 2003; LaJeunesse et al., 2010; Silverstein et al., 2012). Typically however, cnidarian-dinoflagellate symbioses are dominated by *Symbiodinium* spp. in clades A–D, with the capacity for association with multiple different types concurrently (Baker, 2003; Silverstein et al., 2012). However, clones of a single *Symbiodinium* type, specific to a host species and location, dominate and, excluding environmental perturbation (see below), community composition is typically highly stable over time (Thornhill et al., 2009; Pettay et al., 2011; Arif et al., 2014).

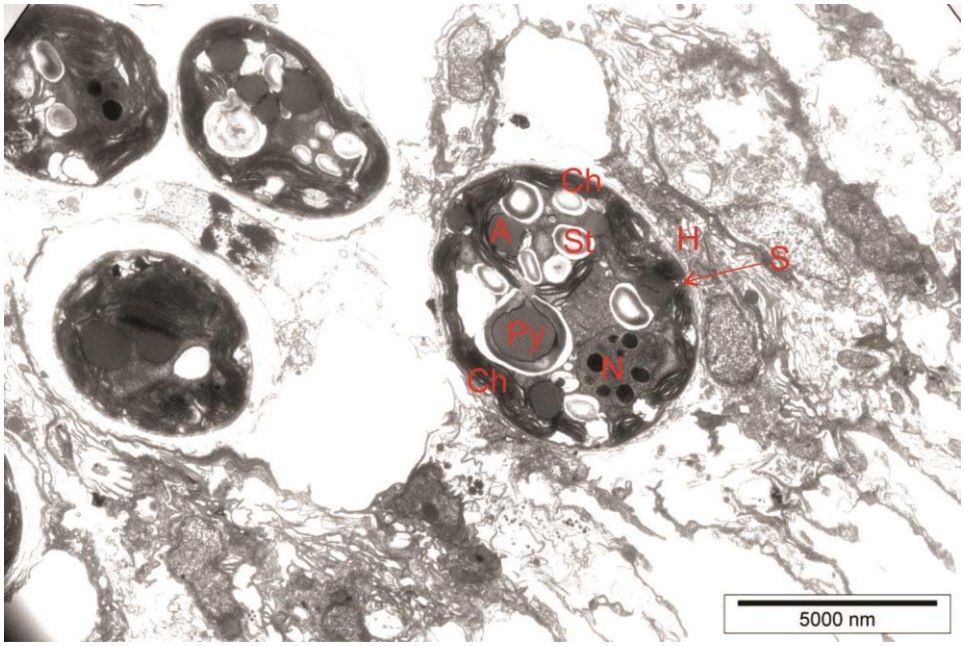

Fig. 1.5: Transmission electron micrograph of *Symbiodinium* cells *in hospite* in the sea anemone *Aiptasia* sp. showing major organelles and structures. Chloroplast (Ch), nucleus (N), pyrenoid (Py), starch (St), accumulation body (A), symbiosome membrane (S) and host tissue (H). Micrograph courtesy of Ashley Sproles.

Symbiotic dinoflagellates are originally acquired *via* one of two modes of transmission, largely based on reproductive mode of the parent: vertical in species that brood their larvae, or horizontal in spawning species (Richmond and Hunter, 1990; Baird et al., 2009b). In vertical transmission, symbionts are passed from parent to offspring, *via* either egg, or brooded larvae (Weis et al., 2001; Thornhill et al., 2006). In horizontal transmission, there is direct uptake, establishment and maintenance of suitable *Symbiodinium* cells from the environment by fertilised larvae and juvenile corals (Little et al., 2004; Gómez-Cabrera et al., 2008; Harii et al., 2009). In some cases however, there may be opportunity for brooding species to also acquire novel types from horizontal transmission (Byler et al., 2013).

Typical symbiont density *per* host cell averages 1-2 cells (Muscatine et al., 1998), with symbiont population size thought to be actively controlled by the host *via* mechanisms such as nutrient limitation and the breakdown and expulsion of excess algal cells (Falkowski et al., 1993; Baghdasarian and Muscatine, 2000; Dunn et al., 2002). However, environmental drivers, such as light and thermal stress, or external

stressors may drastically alter the typical balance of both symbiont composition and density (Hoegh-Guldberg and Smith, 1989; Coffroth and Santos, 2005; LaJeunesse et al., 2015) (**Section 1.4**).

The most common and widespread associations in the Pacific are those dominated by the diverse group of clade C *Symbiodinium* (Baker, 2003; LaJeunesse et al., 2004). Populations in the Caribbean associate more commonly with *Symbiodinium* in clades A, B and C (LaJeunesse et al., 2003). However, other less abundant types (such as members of clade D) may fulfil important ecological niches, such as increasing bleaching thresholds under elevated temperatures (Coffroth and Santos, 2005; Berkelmans and van Oppen, 2006) (**Section 1.4**). However, the functional significance of these alternative types and the capacity for natural switching between types remains the subject of some debate (Loram et al., 2007; Cantin et al., 2009; Jones and Berkelmans, 2011; Stat and Gates, 2011; LaJeunesse et al., 2015).

In addition to *Symbiodinium*, each coral will host a specific consortium of microorganisms, forming a coral holobiont (Forest et al., 2002; Rosenberg et al., 2007). These microbiota include bacteria, archaea, fungi, viruses, protists and other algae, which are thought to function in preventing pathogenic infection, the recycling of nutrients and in coral development (Rosenberg et al., 2007).

1.3 Metabolic function

1.3.1 Host-supplied inorganic nutrients

The success of the cnidarian-dinoflagellate symbiosis is based upon the bi-directional exchange of nutrients between symbiont and host (Muscatine and Hand, 1958; Muscatine and Porter, 1977; Yellowlees et al., 2008). These nutrients are sourced from a highly effective combination of symbiont autotrophy and host heterotrophy. In the first instance, as symbionts are encapsulated within the symbiosome without free access to the surrounding seawater, dissolved inorganic nutrients must be supplied to the algal cells in order to fuel carbon fixation, nitrogen assimilation and symbiont growth (Miller and Yellowlees, 1989). As such, necessary translocated compounds from host to symbiont include dissolved inorganic carbon (DIC), dissolved inorganic nitrogen (DIN), phosphorus and other inorganic nutrients (Miller and Yellowlees, 1989; Yellowlees et al., 2008).

Carbon is fixed in the dinoflagellate *via* the C3 pathway of the Calvin cycle, during which the chloroplast-associated enzyme ribulose-1,5-bisphosphate carboxylase/oxygenase (Rubisco) catalyses the conversion of ribulose-1,5-bisphosphate (RuBP) to two molecules of 3-phosphoglycerate (3PGA) (Streamer et al., 1993). 3PGA is then converted into metabolic intermediates such as hexose phosphates, aspartate, malate and glucose (Streamer et al., 1993). Unusually, the *Symbiodinium* possess an alternate type (type II) of Rubisco, which has a relatively low specificity for CO_2 *versus* O_2 (Rowan et al., 1996). Therefore, under aerobic and oxygenic conditions, in order for the dinoflagellate to effectively fix carbon, Rubisco must be surrounded with a high concentration of CO_2. Under typical conditions (pH 8.2), DIC is present in seawater predominantly as bicarbonate (HCO_3^-) ions (ca. 2.1 mM), with the availability of aqueous CO_2 being relatively low in contrast (12 μM) (Allemand et al., 1998; Brading et al., 2013). However, as charged ions, the more abundant bicarbonate cannot freely permeate cell membranes, necessitating cellular mechanisms in both symbiont and host to concentrate both CO_2 and bicarbonate *via* carbon concentrating mechanisms (CCMs) (Allemand et al., 1998). These CCMs include bicarbonate transporters, membrane-bound proton (H^+) pumps and the enzyme carbonic anhydrase, which catalyses the inter-conversion of bicarbonate to CO_2 (Yellowlees et al., 1993; Leggat et al., 1999; Bertucci et al., 2010; Brading et al., 2013).

In contrast to DIC, under typical conditions in the oligotrophic waters which surround coral reefs, levels of DIN and phosphorus are low (<1 μM), however in order to fuel effective symbiont cell function and growth, both elements must be supplied to the dinoflagellate (Miller and Yellowlees, 1989; Smith and Muscatine, 1999). DIN in seawater is predominantly available as both ammonium (NH_4^+) and nitrate (NO_3^-) ions. In the case of nitrate, the ion must first be reduced by the enzyme nitrate reductase, a process which requires reduced ferredoxins (Fd) from the photosynthetic transport chain, or NAD(P)H (in non-photosynthetic organisms) (Dagenais-Bellefeuille and Morse, 2013). NH_4^+ may be directly assimilated *via* the glutamine synthetase/glutamine:2-oxoglutarate aminotransferase (GS/GOGAT) cycle (Miller and Yellowlees, 1989; Pernice et al., 2012). In this cycle, NH_4^+ is added to glutamine (Gln) to produce glutamate (Glu), consuming ATP; Glu is then reduced back to Gln with either reduced-Fd, or NAD(P)H (Dagenais-Bellefeuille and Morse,

2013). The capacity to assimilate nitrogen in this way is present in both symbiont and the host, however the process is much more rapid in the dinoflagellate (Swanson and Hoegh-Guldberg, 1998; Pernice et al., 2012). Ammonia (NH_3) is also produced by the host in relative abundance as a bi-product of heterotrophic metabolism, however the mechanisms controlling the movement of NH_4^+ ions from host to symbiont are not yet entirely resolved (Wang and Douglas, 1999; Pernice et al., 2012). Evidence suggests that NH_4^+ is recycled in the symbiosis, as heterotrophic feeding of the host reduces the requirement for symbiont-derived assimilation of the ion from the surrounding water (Falkowski et al., 1993; Grover et al., 2002; Davy et al., 2006). The host may also actively maintain a concentration gradient surrounding the symbiosome, in order to facilitate passive diffusion of NH_4^+ to the symbiont (D'Elia et al., 1983; Miller and Yellowlees, 1989; Wang and Douglas, 1998; Pernice et al., 2012). The presence of potential active NH_4^+ transporters has also been detected in the dinoflagellate (Leggat et al., 2007).

Organic phosphorus may be taken up by host heterotrophy, whereas inorganic phosphate is thought to be concentrated and transported from surrounding seawater by carrier-mediated active transport in the cnidarian host, with active uptake from host to symbiont also mediated by a similar carrier (Godinot et al., 2009; Godinot et al., 2011). As both nitrogen and phosphorus are essential for symbiont growth and division, and given that *Symbiodinium* cells *in hospite* typically have slower rates of growth and division relative to when they are under optimal conditions *in vitro* (Miller and Yellowlees, 1989; Muscatine et al., 1989; Smith and Muscatine, 1999; Davy et al., 2012), the host may manipulate the supply of these elements to maintain optimal rates of mobile product translocation (see below) and control symbiont proliferation (Cook et al., 1988; Falkowski et al., 1993; Smith and Muscatine, 1999; Kopp et al., 2013; Jiang et al., 2014). In addition, ambient levels of DIN and DIP may also play an important role in both calcification and photosynthetic rate and maintaining cell density during exposure to thermal stress (Ezzat et al., 2016).

1.3.2 Symbiont-derived carbon-rich photosynthate

Following the fixation of inorganic carbon *via* the Calvin cycle in the dinoflagellate symbiont (as discussed above) and the production of organic carbon-rich products, these compounds will have a number of fates: they may then either be metabolised by the algae, stored, or translocated to the host (Streamer et al., 1993) (**Fig. 1.6**).

Under functional conditions, however, this translocation is thought to comprise over 40% (and potentially more than 90%) of the algal-derived photosynthetic products, exceeding the normal metabolic needs of the host (Muscatine and Cernichiari, 1969; Muscatine et al., 1984; Tremblay et al., 2014). Symbiont-derived carbon-rich mobile products are then directly metabolised by the host in respiratory pathways, whereas nitrogen-rich products are used in biosynthesis pathways, such as calcification, growth and reproduction (Tanaka et al., 2006; Bachar et al., 2007; Kopp et al., 2015).

A range of mechanisms have been suggested that may allow the host to control this high rate of transfer from the symbiont: 1) As the host is thought to maintain the symbiont in a state of nitrogen and phosphorus limitation, high C:N:P ratios will lead to arrested symbiont growth and cell division. This leads to the accumulation of carbon rich energy stores (such as lipid bodies), and this excess carbon may in turn then be made available to the host (Wang and Douglas, 1998; Smith and Muscatine, 1999; Jiang et al., 2014); 2) The host maintains an acidic environment around the symbiosome membrane *via* a proton pump (H^+ ATPase), that leads to enhanced production of CO_2 and correspondingly increased photosynthesis and translocation of mobile products (Barott et al., 2015), aided *via* mechanisms such as membrane-bound active transporters, including ABC transporters (Peng et al., 2010; Barott et al., 2015); 3) A chemical(s) ('host release factor'; HRF) is produced by the host that stimulates photosynthate release (Trench, 1971; Sutton and Hoegh-Guldberg, 1990; Gates et al., 1995; Grant et al., 1997; Withers et al., 1998). Muscatine (1967) discovered that by incubating freshly isolated symbionts (FIS) with host homogenate, the subsequent release of photosynthate into the incubation media was increased. Studies later proposed that a number of host-derived compounds including amino acids were responsible for eliciting this response in the algae (Sutton and Hoegh-Guldberg, 1990; Gates et al., 1995; Wang and Douglas, 1997; Cook and Davy, 2001), however no such response was detected in a subsequent study (Withers et al., 1998). It should also be noted that studies investigating the presence and role of HRF in the symbiosis were carried *in vitro* (rather than *in hospite*) and primarily detected glycerol as the major released compound (this is discussed in more detail below). The mechanisms that primarily control photosynthate release therefore remain to be entirely resolved.

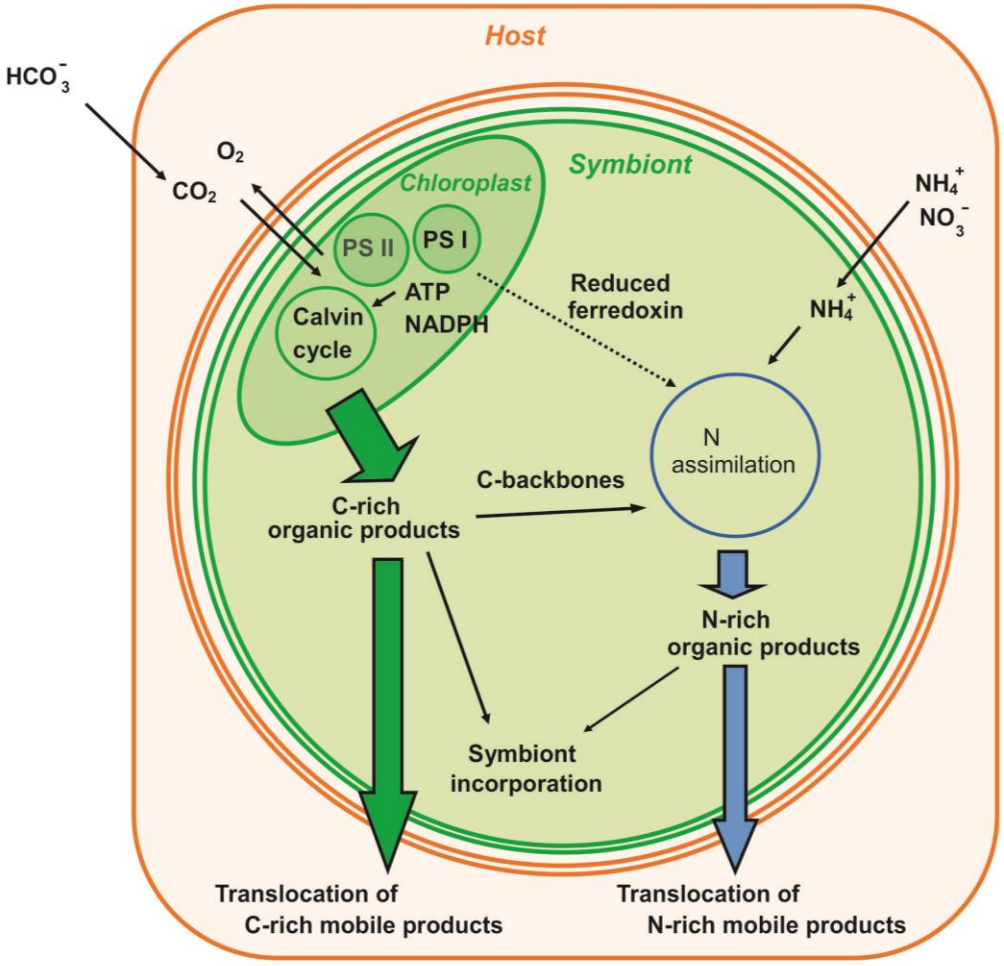

Fig. 1.6: Simplified schematic of the principal modes of carbon fixation and nitrogen assimilation in the functional cnidarian-dinoflagellate symbiosis under photosynthesising conditions. Inorganic carbon (in the form of bicarbonate ions, HCO_3^-) is concentrated *via* carbon concentrating mechanisms (principally the enzyme carbonic anhydrase) and transported to the symbiont, where it is fixed from CO_2 in the Calvin cycle, eventually producing carbon-rich products (carbohydrates, fatty acids and lipids). These carbon-rich products may either be used in symbiont respiration or incorporation, or translocated to the host. Carbon backbones and reduced ferredoxins produced during the turnover of photosynthesis are then used in nitrogen assimilation. Nitrogen assimilation in the symbiont occurs predominantly from ammonium (NH_4^+) and to a lesser extent nitrate (NO_3^-) *via* the glutamine synthetase/glutamine:2-oxoglutarate aminotransferase (GS/GOGAT) cycle. In turn, nitrogen assimilation will produce nitrogen-rich mobile products (amino acids and proteins) which are translocated to the host.

1.3.3 Mobile compounds

Both the quantity and composition of symbiont-derived mobile products have been subjects of interest since Muscatine and Hand (1958) provided the first proof that dinoflagellate symbionts *in hospite* under photosynthesising conditions, fix carbon and translocate organic products to the cnidarian host. von Holt and von Holt (1968) provided further insight into the rates of translocation and the composition of labelled fractions; following *in hospite* incubations under photosynthesising and non-photosynthesising conditions within a number of cnidarian-dinoflagellate symbioses, the authors detected up to one third of total photosynthate present in the host after 3 hours. The major labelled fractions in the host varied according to species, however label was detected in lipid, amino acid and polar fractions. Subsequent studies also found significant light-enhanced lipogenesis in the symbiosis, coupled to accumulations of labelled lipids (fatty acids, wax ester and triglyceride) in host tissues, and translocation of lipid droplets as mobile compounds was suggested (Patton et al., 1977; Kellogg and Patton, 1983). These lipid droplets were comprised primarily of wax esters (ca. 83%), with triacylglycerol, diacylglycerol ethers, free fatty acids, free sterols and phospholipids (Kellogg and Patton, 1983).

However, owing to the complexity of the endosymbiosis, neither absolute quantities nor identities of the *in hospite* mobile products have been entirely resolved (Yellowlees et al., 2008; Davy et al., 2012). Early studies typically tackled the issue with the use of FIS from a number of cnidarian-dinoflagellate symbioses. FIS were incubated with radiotracers, principally ^{14}C-bicarbonate under photosynthesising and non-photosynthesising conditions, with and without the addition of host homogenate (Muscatine, 1967; Muscatine and Cernichiari, 1969; Trench, 1971). Label was subsequently detected in released organic products within the incubation medium and these compounds were postulated as the major products translocated to the host. These early studies identified large pools of glycerol which was released into the incubation medium and contributed up to 95% of the labelled products detected (Muscatine, 1967; Muscatine and Cernichiari, 1969; Trench, 1971). Other labelled products, albeit in much smaller proportions, included alanine, glucose, fumaric acid, succinic acid, glycolic acid, lipids and two other unidentified organic acids (Muscatine, 1967; Muscatine and Cernichiari, 1969; Trench, 1971). Interestingly however, both Muscatine and Cernichiari (1969) and Trench (1971) detected glucose as the major

labelled product in the intracellular pools of the dinoflagellate. Further to this an *in hospite* labelling study by Schmitz and Kremer (1977) also detected glucose as the major labelled product in the intact symbiosis of symbiont and host extract. Glucose comprised between 7-33% of the labelled fraction of symbiont intracellular pools (Muscatine and Cernichiari, 1969; Trench, 1971). Additional labelling was detected in a number of carbohydrates, amino acids and intermediates, including sugar phosphates, mannose, aspartate, glycine, serine, alanine, glycerol, glutamic acid, glycolipids and TCA cycle intermediates (Muscatine and Cernichiari, 1969; Trench, 1971; Schmitz and Kremer, 1977).

These early studies provided valuable insight into the relative nutritional importance of the algal symbionts, identifying a number of key candidate mobile compounds, however a major limitation (with the exception of Schmitz and Kremer, 1977) was the use of viable (i.e. non-metabolically quenched) FIS incubated in seawater (Ishikura et al., 1999). Upon removal from the host and re-suspension *in vitro*, the algae experience considerable changes in environmental conditions from those *in hospite*, especially with respect to osmotic pressure (Ishikura et al., 1999). Acclimation to osmotic stress in the live algae inevitably involves the production of compatible solutes in large quantities, which are in turn released into incubation media; a major such solute in the dinoflagellate is glycerol (Mayfield and Gates, 2007; Suescún-Bolívar et al., 2012). Given that this compound also forms a minimal portion of the dinoflagellate intracellular pool under typical conditions *in hospite*, the role of glycerol as a mobile product in the symbiosis is likely to have been overstated in these early studies (Ishikura et al., 1999; Burriesci et al., 2012).

More recent studies *in hospite* have also aimed to identify candidate carbon-rich mobile products translocated from symbiont to host in a range of cnidarian-dinoflagellate symbioses (Whitehead and Douglas, 2003; Burriesci et al., 2012). In an elegant study, Whitehead and Douglas (2003) labelled exogenously supplied substrates which were provided to the anemone *Anemonia viridis* under non-photosynthesising conditions. Where host metabolism of these substrates matched that of control individuals incubated under photosynthesising conditions, they were considered ‘mobile compounds’, concluding that glucose and the organic acids succinate and/or fumarate (or metabolically allied compounds) function in this role in the symbiosis. Complementary to these conclusions was a study by Burriesci et al.

(2012), which following *in hospite* incubations with the stable isotope ^{13}C, detected rapid labelling of glucose in host pools in the anemone *Aiptasia* sp.. It was concluded by the authors that glucose is therefore likely to be the major translocated product in the cnidarian-dinoflagellate symbiosis. Other labelled products identified in this study, and corresponding detection times following incubation with the tracer, are summarised in **Table 1.1**.

Table 1.1 Labelled compounds and their time of detection in the host under photosynthesising conditions in the anemone *Aiptasia* sp. (adapted from Burriesci et al., 2012).

Metabolite	Time detected
Glucose	2 min
Succinate	1 h
Threonine	1 h
Glutamine	1 h
Mannose	1 h
Inositol type 1	1 h
Inositol type 2	1 h
Glycerol	24 h
Glutamic acid	24 h
Pentaric acid	24 h
Glycine	1 week
Beta-Alanine	1 week

Given that corals comprise of a high percentage of lipids (ca. 34% dry weight), further work (Papina et al., 2003; Dunn et al., 2012; Imbs et al., 2014; Kopp et al., 2015) has aimed to build on the work of Patton et al. (1977) and Kellogg and Patton (1983) to establish in more detail what role lipids play in the symbiosis. Papina et al. (2003) detected high proportions of polyunsaturated fatty acids (PUFAs) from the extracts of both dinoflagellate symbiont and coral host, with a number of fatty acids considered specific to the dinoflagellates (namely C18:4n-3, C22:5n-3 and C22:6n-3). However, these compounds were also detected to a lesser extent in host tissue and therefore considered indicative of translocation of these groups in the symbiosis. Further to this, the detection of a number of PUFAs considered characteristic of the host (for example C22:5n-6, and C18:2n-7) in symbiont pools also suggests that there is reciprocal translocation from host to symbiont (Imbs et al., 2014).

Recently Kopp et al. (2015) investigated both carbon fixation and nitrogen assimilation in a coral symbiosis at the cellular level, with the application of nano

secondary ion mass spectrometry (nanoSIMS) technology. This was coupled to pulse-chase ^{13}C-bicarbonate and ^{15}N incubations. The authors observed rapid incorporation of ^{13}C into symbiont starch granules and lipid droplets under photosynthesising conditions. These stores were then mobilised in symbiont dark respiration. Labelled carbon was subsequently translocated to the host where it was observed to accumulate into lipid droplets and glycogen deposits, and after a lag of 3 h, the translocation of labelled nitrogenous compounds to the host was also detected.

NanoSIMS techniques have also been applied to more in-depth studies of nitrogen metabolism in the coral symbiosis (Pernice et al., 2012; Kopp et al., 2013). Pernice et al. (2012) demonstrated that both symbiont and host cells were capable of directly assimilating NH^+ *via* a GS/GOGAT-like cycle (as discussed in **Section 1.3.1**), however the *Symbiodinium* cells did so at a much greater rate (up to 23 times more). Symbionts rapidly assimilated NH_4^+ and synthesised labelled glutamine and glutamate, and these compounds were in turn re-mobilised into nitrogenous compounds, such as proteins, amino acids and purines, with later translocation to the host of these nitrogenous products. Earlier studies by Wang and Douglas (1999) with the application of ^{14}C-labelled glucose, aspartate and glutamate incubations, suggested that translocated amino acids in the *Aiptasia* symbiosis include histidine, isoleucine, leucine, lysine, phenylalanine, tyrosine and valine.

1.4 A globally threatened system

Coral reefs are one of the oldest ecosystems in the world, existing for over 250 million years (Pandolfi, 2011). In their natural state they are considered to be highly persistent, or ecologically resilient and resistant to change (Holling, 1973; Nyström et al., 2008). However, these systems are increasingly under the influence of human activities at local, regional and global scales, with approximately 75% of the world's reefs considered either threatened, or destroyed (Hughes et al., 2010; Burke et al., 2011). Major global-scale stressors for coral reefs include increased seawater temperatures, extreme weather, disease, sea level rise and ocean acidification, coupled to destructive regional and local-scale activities, such as over-fishing, poor

waste-water management and coastal development (Hoegh-Guldberg et al., 2007). Cumulatively, these drivers are not only eroding the natural capacity of coral reef ecosystems for resistance to change, but also impeding recovery following disturbance (Hughes, 1994; Nyström et al., 2008). This eroded capacity to cope has resulted in widespread declines in live coral cover worldwide and a major phase shift at many sites, from live coral to algal-dominated communities (Hughes, 1994; Hoegh-Guldberg, 1999; Hughes et al., 2003; Hughes et al., 2007).

However, of these stressors, elevated water temperatures, which in turn lead to mass bleaching events, pose the single biggest threat to the persistence of coral reefs as we know them worldwide (Baker et al., 2008; Carpenter et al., 2008; Lesser, 2011). These bleaching events have been increasing in frequency, severity and duration and are projected to continue increasing, with harmfully frequent bleaching events projected to occur by 2030 (Pandolfi et al., 2003; Donner et al., 2005; Baker et al., 2008; Pandolfi et al., 2011). Recent models also predict widespread degradation coral reef systems, which is likely to affect approximately 90% of coral reefs by 2050 (Frieler et al., 2013; Kwiatkowski et al., 2015).

1.4.1 Coral bleaching

Coral bleaching is the breakdown and loss of symbiont photosynthetic pigments and/or whole cells, resulting in a pale, white, or brightly coloured coral appearance, due to the exposure of host skeleton and tissues (Weis, 2008; Weis, 2010). The bleaching response may be elicited by a range of abiotic and biotic stressors, that include disease, eutrophication, turbidity, changes in salinity, high/low light and high/low water temperatures (Hoegh-Guldberg and Smith, 1989; Glynn, 1996; Brown, 1997b). Thermally-induced bleaching is a major issue for scleractinians, as they typically exist at, or close to, their maximum temperature thresholds (Coles and Jokiel, 1977; Jokiel and Coles, 1990). Where exceeded, individuals will be exposed to thermal stress and bleaching is likely to occur (Hoegh-Guldberg, 1999; Baker et al., 2008). Typically, temperatures of only 1°C above monthly means at a given site will result in thermal stress, and where these temperature anomalies are prolonged and cumulatively exceed ≥ 4°C heating weeks (i.e. ≥ 4°C for one week, or ≥ 1°C for four weeks), a significant bleaching event is considered likely to occur (Eakin et al., 2009).

Interestingly, this mechanism is by no means uniform at a given site, time-point or within a given species. Variations in the occurrence, extent and severity of bleaching can largely be explained by a combination of abiotic and biotic factors, including changes in the combined holobiont (genotype and phenotype), individual sensitivities to a given stressor (Baker, 2003; Abrego et al., 2008; Weis, 2010), and small-scale spatial differences, such as shading, upwelling/downwelling and turbidity at a given location (Glynn, 1996). Most corals contain 1-5 x 10^6 dinoflagellate symbionts *per* cm^2 of live coral surface and between 2-20 pg chlorophyll *a per* symbiont cell (Glynn, 1996). Bleaching will result in the loss of typically between 60-90% of symbionts, with those symbionts in turn losing on average between 50-80% of their photosynthetic pigments (Glynn, 1996). If suitable conditions resume, then symbiont communities will slowly repopulate the host, by cell division *in hospite* and/or *via* uptake from the environment (Toller et al., 2001; Lewis and Coffroth, 2004; LaJeunesse et al., 2010).

The drivers and cellular mechanisms of coral bleaching have been a major focus of study since the threats posed to reef persistence by mass bleaching were first highlighted (see reviews in Glynn, 1996; Brown, 1997b). However, owing both to the complexity of the holobiont and variability in its response to a given stressor, central aspects remain to be fully resolved, such as for instance the role of the host in the process (Wooldridge, 2014; Krueger et al., 2015). One central mechanism thought to drive bleaching under conditions of high temperatures and high light levels, is the excessive generation of reactive oxygen species (ROS) by the dinoflagellate *in hospite*, known as the oxidative theory of coral bleaching (reviewed in Weis, 2008) (discussed in **Section 1.4.2**). Although ROS perform important and highly conserved roles in both normal cell function and in damage signalling, ROS species are in themselves damaging where rates of production exceed the capacity of antioxidant networks (D'Autreaux and Toledano, 2007; Brosché et al., 2010; Suzuki et al., 2012). The oxidative theory is therefore based on bleaching as a host immune-like response to minimise exposure to ROS generated by photoinhibited and dysfunctional photosymbionts (Dunn et al., 2007; Weis, 2008). However increasing evidence also supports the view that in many instances expelled *Symbiodinium* are photosynthetically viable (Hill and Ralph, 2007) and that symbiont-derived ROS does not accumulate in the host *in hospite* during bleaching, but rather oxidative stress in

the host may result from host metabolism itself (Krueger et al., 2015) (discussed in **Section 1.4.3**).

1.4.2 Photosynthesis as a source of oxidative stress

The photosynthetic pigments of *Symbiodinium* comprise chlorophyll *a*, chlorophyll *c1* and/or *c2*, the major xanthophylls peridinin or fucoxanthin (or fucoxanthin derivatives), diadinoxanthin and diatoxanthin (Venn et al., 2006). Collectively these pigments absorb energy (light) and transfer this energy to the electron transport chain. In linear electron flows this energy is then used in turn to reduce NADP to NADPH from PS II to PS I, and create a proton motive force across the chloroplast membrane generating ATP (reviewed in Roth, 2014). Cyclic electron flows are also generated at PS I, generating ATP only. Both ATP and NADPH are then used to fuel the fixation of carbon in the Calvin cycle, *via* the action of the enzyme Rubisco (Roth, 2014) (**Section 1.3**).

At low light levels, maximum quantum efficiency (φmax) is achieved when the rate of photosynthesis increases linearly with increasing light absorption (reviewed in Smith et al., 2005). However, as light intensity continues to increase, there is a decline in photosynthetic efficiency and the relationship between photosynthesis and absorbed light becomes nonlinear. This decline in the turnover of photosynthesis is due primarily to a reduction of components of the electron transport chain and an increase of protective mechanisms, which dissipate energy instead (Smith et al., 2005). These protective mechanisms include re-emitting the energy as fluorescence, as heat (non-photochemical quenching, NPQ) *via* the xanthophyll cycle, or finally *via* the generation of triplet chlorophyll, through which a number of ROS species are produced. As dinoflagellates are regularly exposed to short-term increases in light levels (such as during the middle of the day), which saturate photosystems, NPQ plays in important role in responding to change *via* dynamic photoinhibition (reversible photoprotective processes) (Brown et al., 1999; Hoegh-Guldberg and Jones, 1999; Warner and Berry-Lowe, 2006). However, where energy levels exceed rates at which NPQ are capable of dissipating, then ROS are produced, leading to damage at a number of sites termed photoinactivation (see below), including the D1 protein of PS II (Warner et al., 1999). These systems have therefore evolved a number of complex repair and antioxidant responses to limit photoinactivation and repair this ROS-associated damage to PS II (Lesser, 2006; Krueger et al., 2014)

(**Section 1.4.3**). However, if under non-typical conditions (high light and heat) the rate of damage exceeds that of repair, a photosynthetic system is said to be photoinhibited and the turnover of photosynthesis will be reduced (Warner et al., 1999). Photodamage may also be sustained as a result of high temperatures, below light levels normally required to saturate photosynthesis, owing to inhibition of this repair to the D1 protein of PS II (Takahashi et al., 2004; Takahashi and Murata, 2008).

An additional strategy for the dissipation of excess electrons at PS I is alternative electron flows, which *via* the Mehler reaction deflect electrons from the chloroplast, reducing O_2 to superoxide radicals and subsequently to hydrogen peroxide by superoxide dismutase (Roberty et al., 2014). Eventually, hydrogen peroxide is detoxified to water *via* the action of ascorbate peroxidase (**Fig. 1.7**). However, in order for the cycle to be effective, ascorbate must be recycled *via* the action of reduced ferredoxin. Without these electron carriers, ascorbate is not effectively recycled, and ROS will accumulate within the chloroplast (Smith et al., 2005).

Further to this, ROS produced during increased turnover of alternative electron flows and as a result of the saturation of photosynthesis, coupled to elevated temperatures may also cause damage to Rubisco (Jones et al., 1998; Lilley et al., 2010), thylakoid membranes (Tchernov et al., 2004; Hill et al., 2009; Díaz-Almeyda et al., 2011), antenna proteins (Hill et al., 2012), the oxygen evolving complex (Hill and Ralph, 2008) and PS I (Hoogenboom et al., 2012) leading to further photoinhibition. Damage to Rubisco may then lead to a break down in the Calvin cycle and sink limitation, where there is a reduction in the consumption of ATP and NADPH from PS I, leading to the backup of excitation energy at PS II (Jones et al., 1998; Lilley et al., 2010). Although this breakdown in the activity of the Calvin cycle has recently been shown not to be a key driver of bleaching, it does lead to a decline in the generation of downstream products, which in turn has implications for cellular metabolic function and repair (Bhagooli, 2013; Hill et al., 2014). Further to this, ROS-associated damage sustained to the thylakoid membranes of the chloroplast may also lead to the uncoupling of the electron transport chain and a breakdown in the production of ATP (Tchernov et al., 2004). This limitation of ATP would restrict the turnover of the Calvin cycle and carbon assimilation, and generate yet more ROS as a result.

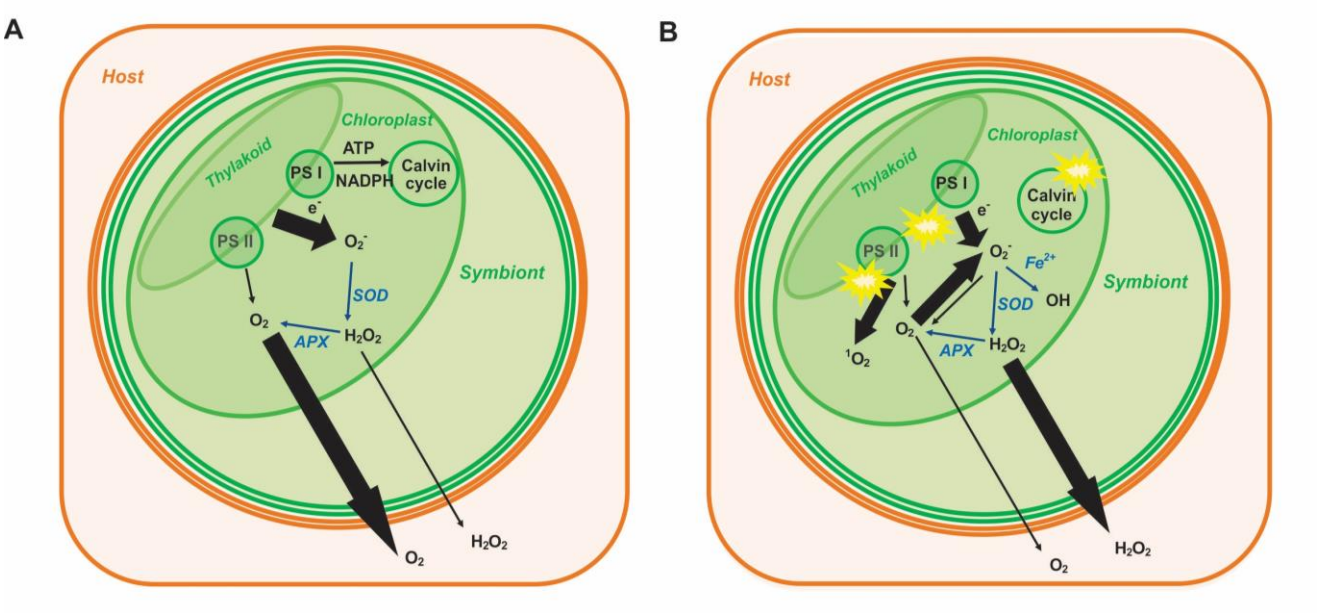

Fig. 1.7: Schematic of oxygen-evolving pathways in *Symbiodinium* under growth conditions (A) and thermal and light stress (B). Under functional conditions, photosystem I (PS I) and photosystem II (PS II) produce large quantities of oxygen which diffuse into the host. Reactive oxygen species (ROS), such as hydrogen peroxide (H_2O_2) and superoxide (O_2^-), are effectively converted to oxygen by the enzymes superoxide dismutase (SOD) and ascorbate peroxidase (APX). Under thermal and light stress, damage occurs at the D1 protein of PSII, in the Calvin cycle and on the thylakoid membranes. This damage leads to the increased activity of alternative electron flows and *via* the Mehler reaction, the production of large amounts of ROS in the form of singlet oxygen ($^1O_2$) and O_2^-. These overwhelm antioxidant responses and initiate a cascade, leading to the production of further unstable ROS species, including the more persistent H_2O_2. (Adapted from Weis, 2008).

1.4.3 Respiration as a source of oxidative stress

Exposure to elevated temperatures will also result in an increase in rates of cellular respiration in both partners, and in the symbiont this will result in increases in the ratio of respiration to photosynthetic rate (Coles and Jokiel, 1977; Clark and Jensen, 1982). These energetic requirements will therefore necessitate the generation of energy from alternative sources, leading to increases in the turnover of alternative networks, such as associated with the breakdown of energy stores (Coles and Jokiel, 1977; Clark and Jensen, 1982). Thermal acclimation and homeostatic responses will also require the generation of a number of complex and metabolically-costly cellular-level changes in symbiont and host (Brown, 1997a). As a consequence of this increase in the turnover of respiratory and acclimatory networks, ROS will also be

generated at the mitochondria, endoplasmic reticulum and microbodies (peroxisomes and glyoxysomes) of both symbiont and host (Lesser, 2006).

Cumulatively, this enhanced generation of ROS at multiple sites leads to increased turnover of enzymic and non-enzymic antioxidant responses to maintain oxidative state (see **Section 1.4.4** below), however changes in host responses can be independent of those in the symbiont, indicating a disparity in oxidative state between partners (Krueger et al., 2015).Where antioxidant responses are overwhelmed; ROS are no longer detoxified and therefore accumulate at sites of production, causing further damage and escalating into a positive feedback loop (Lesser, 1996; Roberty et al., 2015). As charged molecules, most species of ROS are unable to permeate the lipid bilayer, and they therefore accumulate at sites of production, causing lipid peroxidation, DNA damage and modifications to cellular proteins (Gill and Tuteja, 2010). Eventually, this damage will extent to components of the lipid bilayer of cellular membranes, leading to lipid peroxidation, the leakage of ROS from sites of accumulation and the generation of further unstable and cytotoxic molecules, such as oxylipins (Lesser, 2006). Both ROS and oxylipins are highly conserved damage-signalling molecules (Weis, 2008; Lõhelaid et al., 2015), and lead to enhanced cell death *via* mechanisms such as necrosis, apoptosis, autophagy and to the expulsion of symbiont cells during bleaching (Dunn et al., 2004; Weis, 2008).

1.4.4 Acclimation to thermal stress

A number of mechanisms may be employed to increase resistance to bleaching, to acclimate to unfavourable conditions, and finally to improve recovery following bleaching. Principal amongst these is minimising the degree of exposure to the causative abiotic stressors (**Section 1.4**), namely light, heat and ROS. The main mechanisms are summarised in **Fig 1.8**. In the first instance photoprotective pigments serve to limit excess exposure to both visible and UV light in sessile marine organisms (Shick and Dunlap, 2002). Major accessory and photoprotective pigments in the cnidarian-dinoflagellate symbiosis, include carotenoids, fluorescent pigments and mycosporine-like amino acids (MAAs) (Salih et al., 2000; Venn et al., 2006; Rosic and Dove, 2011; Strychar and Sammarco, 2011). In the dinoflagellate both the ratios and sizes of these photoprotective pigments may be altered to acclimate to differing conditions (Venn et al., 2006; Warner and Berry-Lowe, 2006; Strychar and

Sammarco, 2011). Similarly enzymatic and non-enzymatic cellular antioxidants and heat shock proteins (HSPs) are important in maintaining oxidative state and cellular function (Downs et al., 2002; Krueger et al., 2014; Roberty et al., 2015; Wietheger et al., 2015). Cell function and structure may also be maintained *via* modifications to fatty acid metabolism, lipogenesis and the structure of cellular membranes (Tchernov et al., 2004; Papina et al., 2007; Díaz-Almeyda et al., 2011; Leal et al., 2013) and the production of compatible solutes such as sugar alcohols, betaines and dimethylsulfoniopropionate (DMS) (Mayfield and Gates, 2007; Yancey et al., 2010).

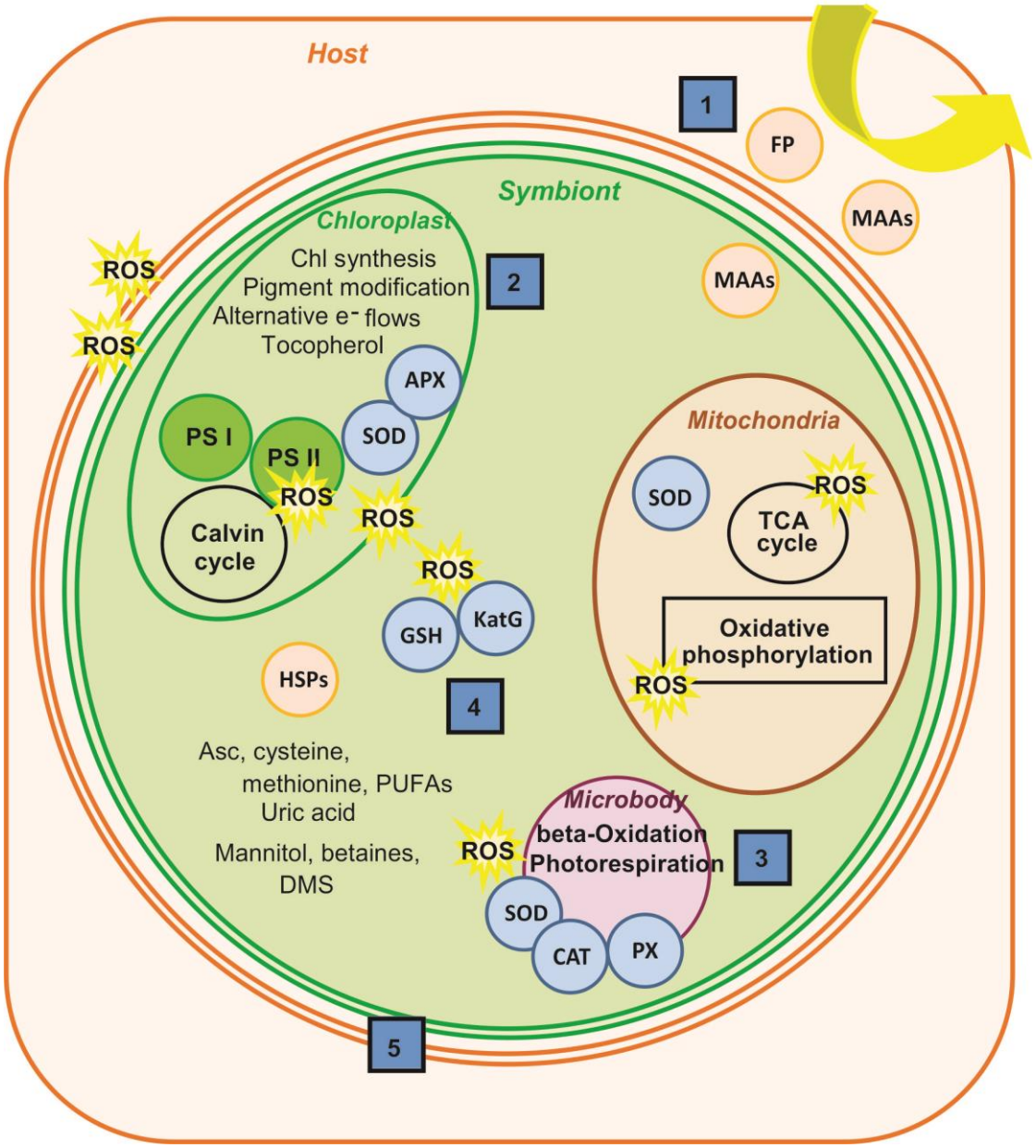

Fig. 1.8 (previous page): Summary of major known symbiont metabolic and cellular protective and acclimation mechanisms to thermal and oxidative stress. 1. MAAs and florescent proteins (FP) absorb and reflect excess light energy; 2. Photoprotective accessory pigments and alternate electron flows divert excess energy from the chloroplast; 3. Enzymatic and non-enzymatic antioxidants are located at sites of high ROS production namely the chloroplast, mitochondria and cell cytoplasm. 4. Intracellular pools of heat shock proteins (HSPs) and compatible solutes serve to maintain cell structure and function, 5. Membrane structure may also be altered, with increases in saturation and stability at high temperatures. SOD superoxide dismutase, APX ascorbate peroxidase, KatG catalase peroxidase, GSH glutathione, Chl chlorophyll, AsC ascorbate, DMS dimethylsulphate, PUFA polyunsaturated fatty acid, CAT catalase, PX peroxidase.

1.5 Gaps in our knowledge

Given the threats facing coral reefs and the importance of the metabolic interactions that underpin their success, it is perhaps surprising how little attention stress-related shifts in intracellular metabolite pools and mobile-product exchange in the symbiosis have received. To date, only a single study has characterised metabolite profiles associated with an environmental stressor within the symbiosis, and this was focussed on the effect of nutrient enrichment on secondary metabolites in the soft coral *Sarcophyton ehrenbergi* (Fleury et al., 2000). The authors found that the ratio of bioactive, or stress metabolites (terpenes) to energy-storage metabolites (lipids) varied with nutrient enrichment (phosphorus and nitrogen). It was postulated that increased nitrogen availability to the algal symbiont resulted in uncontrolled symbiont growth and reductions in mobile-product translocation to the host.

Great advances in our knowledge of cellular interactions in the cnidarian-dinoflagellate symbiosis have been made in recent years, particularly within the ‘omics fields (genomics, transcriptomics, proteomics and metabolomics). However, major gaps remain in a number of aspects central to the function and dysfunction of the symbiosis (Edmunds and Gates, 2003; Davy et al., 2012). In particular further study is required in order to elucidate central metabolic pathways and metabolic interactions in the functional symbiosis and to establish how these networks are affected by thermal stress. A more holistic approach is necessary to better understand the complex and dynamic metabolic changes in the holobiont during periods of thermal stress. These data are essential for understanding how the

symbiosis will persist in to the future. Gaps in knowledge in each partner and the symbiosis as a whole during thermal stress and bleaching include:

1. What are the changes to central metabolism and costs associated with acclimation to these conditions?
2. What are the roles of intracellular free metabolite pools and metabolic pathways in cellular homeostasis, cell signalling and acclimation to thermal stress?
3. How are mobile compound exchange and down-stream pathways affected?
4. Are there heat responsive compounds that may serve as specific indicators of these stressors?

1.6 The application of metabolomics

Metabolomics is the study of the diverse group of small molecules (<1500 kDa in molecular weight) found in a cell, biofluid, tissue, or organism. The metabolome is the complete set of these molecules and consists of a chemically diverse mix of compounds (Oliver et al., 1998). These compounds are the products of enzyme-catalysed reactions and fall into two main groups: primary metabolites and secondary metabolites (Roessner et al., 2006). Primary metabolites comprise those directly associated with metabolism, namely growth, development and reproduction, and secondary metabolites typically perform specific ecological roles (Roessner et al., 2006). Metabolic reactions can be divided into anabolic and catabolic reactions. Typically, anabolic reactions, which synthesise complex molecules from simple compounds, require energy in the form of ATP, NADPH or NADH. In contrast, the degradation of these compounds by catabolism will release energy (Roessner et al., 2006).

The metabolome is highly dynamic, responding rapidly to change *via* the turnover of pathways, or metabolic flux (Grüning et al., 2010). As many pathways are self-regulating, acting in competing and interacting pathways, alterations to free metabolite pools and shifts in associated metabolic pathways are typically post-translational (Fiehn et al., 2000; Roessner et al., 2006). Free metabolite pools therefore typically reflect an organism, tissue or cell's first response to its

environment, and the interaction of genotype and phenotype (i.e. the metabolome) (**Fig. 1.9)**

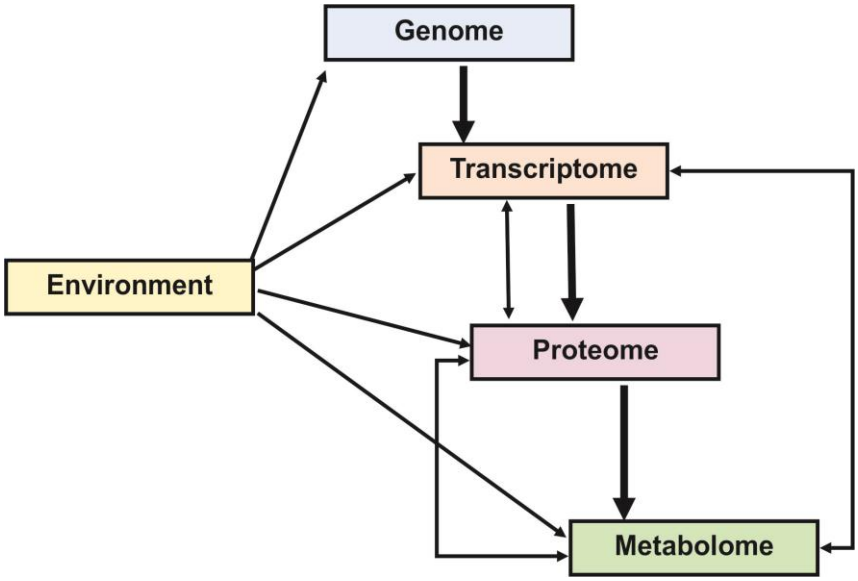

Fig. 1.9: The organisation of the 'omes'. Showing the flow of information from genome to metabolome, and their interaction with one another and the environment. Amended from Griffin and Shockcor (2004).

Typically, the metabolome is highly resilient with high functional redundancy (Grüning et al., 2010; Gu et al., 2012). Perturbations to the metabolic network can result in modifications, or total exclusions of a given pathway, resulting in shifts not only in metabolite pools, but in the mechanisms for the generation of cellular energy, or biosynthesis (Grüning et al., 2010). In addition to their primary roles, free metabolite pools may also perform important secondary functions in cellular homeostasis, such as serving as compatible solutes, or messenger molecules (Wahid et al., 2007; Guy et al., 2008). Levels of individual compounds in free metabolite pools therefore represent their dynamic roles as intermediates, or end-points, and in maintaining cellular homeostasis. Due to the sheer number of metabolites, each reflecting a particular aspect of metabolism in the cell, tissue or organism of interest, it is possible to rapidly detect low-level and ecologically-relevant cellular changes in complex systems (Fiehn, 2002; Lankadurai et al., 2013). The application of metabolomics-based techniques therefore provides an excellent tool for the assessment of sub-acute and complex stressors in environmental studies (Viant, 2007; Viant, 2008).

1.6.1 Measuring the metabolome

Due to the complexity of the metabolome, it is not currently possible to simultaneously measure its entire suite of metabolites (Villas-Bôas et al., 2005; Dettmer et al., 2007). This is mainly due to its high turnover rate, sheer number of compounds, large range of concentrations and differing chemical properties (polarity, stability, volatility and solubility) (Roessner et al., 2006; Dettmer et al., 2007). As a result, many metabolites remain unidentified, particularly within complex systems, such as the cnidarian-dinoflagellate symbiosis. Therefore metabolomic studies typically focus on certain aspects of the metabolome, or focus on a widely studied and well characterised model system. As a result, the majority of studies fall into two main categories: comparative studies that apply untargeted qualitative comparisons between samples (metabolite profiling) and quantitative studies, which focus on a particular group of compounds, or a single compound (target analysis) (Nielsen et al., 2006; Roessner et al., 2006).

The methods and analytical platforms applied will also be dependent on the objectives of the study. The main platforms for the identification and quantitation of these small molecules fall into three major categories, namely GC-MS, liquid-chromatography mass spectrometry (LC-MS) and NMR spectroscopy (Smedsgaard et al., 2006). The advantages and disadvantages of each of these methods are mainly based upon their sensitivity and repeatability (**Table 1.2**) (Villas-Bôas et al., 2005). Metabolomics *via* the application of GC-MS is capable of the simultaneous analysis of a broad range of metabolite classes, and produces data with high reproducibility and high accuracy, it therefore provides an excellent platform for the untargeted assessment of multiple metabolite groups (Villas-Bôas et al., 2005).

Table 1.2 Major metabolomics analysis platforms, advantages and disadvantages (adapted from Villas-Bôas et al., 2005).

Analysis platform	✓ Advantages	× Disadvantages
GC-MS	✓ Simultaneous analysis of a range of metabolite groups ✓ High chromatographic resolution ✓ Highly repeatable ✓ Relatively rapid	× Unable to analyse thermally unstable compounds × Requirement for derivatization of non-volatile groups × Identification requires known standards and/or library comparison × Average sensitivity – requiring relatively large amount of biomass (> 100 mg dry weight) for detection of compounds in low abundance
LC-MS	✓ High detection sensitivity ✓ No requirement for derivatization ✓ Relatively rapid ✓ Average to high chromatographic resolution ✓ Analysis of thermo-labile compounds	× Difficulty in effectively separating multiple classes × Matrix effects
NMR	✓ Very high structural resolution ✓ Direct unbiased quantification	× Low resolution × Small dynamic range × Low sensitivity

1.6.2 GC-MS analysis

In GC-MS, gas chromatography (GC) is used to separate the analytes. The metabolites are then identified using their molecular mass and fragmentation pattern *via* mass spectrometry (MS). This analytical system is reviewed in detail in Smedsgaard et al. (2006), but a brief introduction will be provided here:

A small volume (ca. 1 µL) of each sample in liquid phase is first injected into the GC. The sample is evaporated in a heated injector and the mix of analytes is then directed into the GC. The GC comprises a capillary column, with a carrier gas to separate the molecules in gas phase. The differing chemical properties of the analytes result in differing affinities for the column's stationary phase (the distribution coefficient, *K*) and therefore separation as the sample travels down the column in the carrier gas. This causes the analytes to elute from the column at different times.

Once the compounds are eluted from the GC, they travel into the MS. In the MS they are ionized into component ions, which are then directed to a detector. The most common ionization mode is *via* electron impact, so-called electron ionization (EI). In EI, the analytes are bombarded with free electrons from a source, resulting in the production of molecule fragments. The gas phase reaction can be described with the following equation:

$M + e^- = M^{+\bullet} + 2e$

Where M is the analyte molecule being ionized, e^- is the electron and $M^{+\bullet}$ is the resulting ion.

The fragment ions are then separated and detected by a mass analyser, using their mass-to-charge ratios (*m/z*). Following detection of the fragment ions, the *m/z* data and retention time are reported in digital format as chromatograms (**Fig. 1.10**). Retention time is a means of qualitative identification, relating to the time between injection and detection of a target compound peak. However, retention time will vary according to a number of factors, including analysis conditions and those relating to the column including its type, dimensions, degradation and any associated contamination. As such, retention time will vary between machines and even between analytical runs on a single machine.

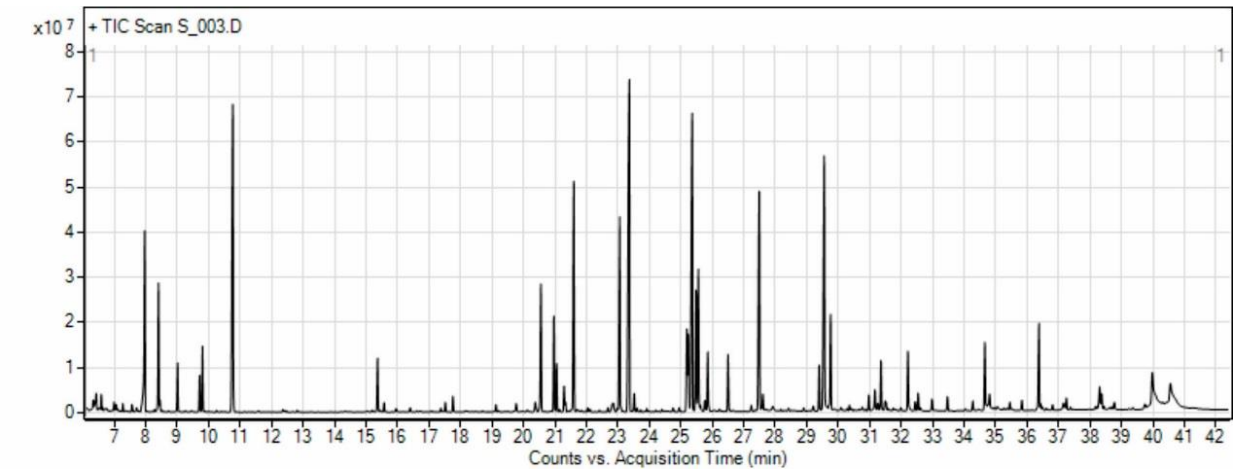

Fig. 1.10: A typical GC-MS chromatogram. Showing target compound peak intensity (y axis) and retention time (mins) (x axis).

Where an unknown compound, or an untargeted analysis is run, putative identification may be possible *via* comparison with commercially available libraries, such as that of the National Institute of Standards and Technology (NIST) (http://chemdata.nist.gov/). This is due to the specific pattern of the mass spectra produced, which may be matched to corresponding known compounds (**Fig. 1.11**). However, in order for an analyte to be confirmed it must be matched against a known standard run on the same machine (Sansone, 2007; Kanani et al., 2008). Internal standards are also applied in order to control for any variation in the analysis between samples, such as retention time shifts and for targeted quantification of a compound (Kanani et al., 2008). Relative quantity of a metabolite (i.e. for comparative studies) may be determined based upon the peak area, or height. However for absolute quantitation of a compound known standards must be run and individual calibration curves produced for each analyte of interest.

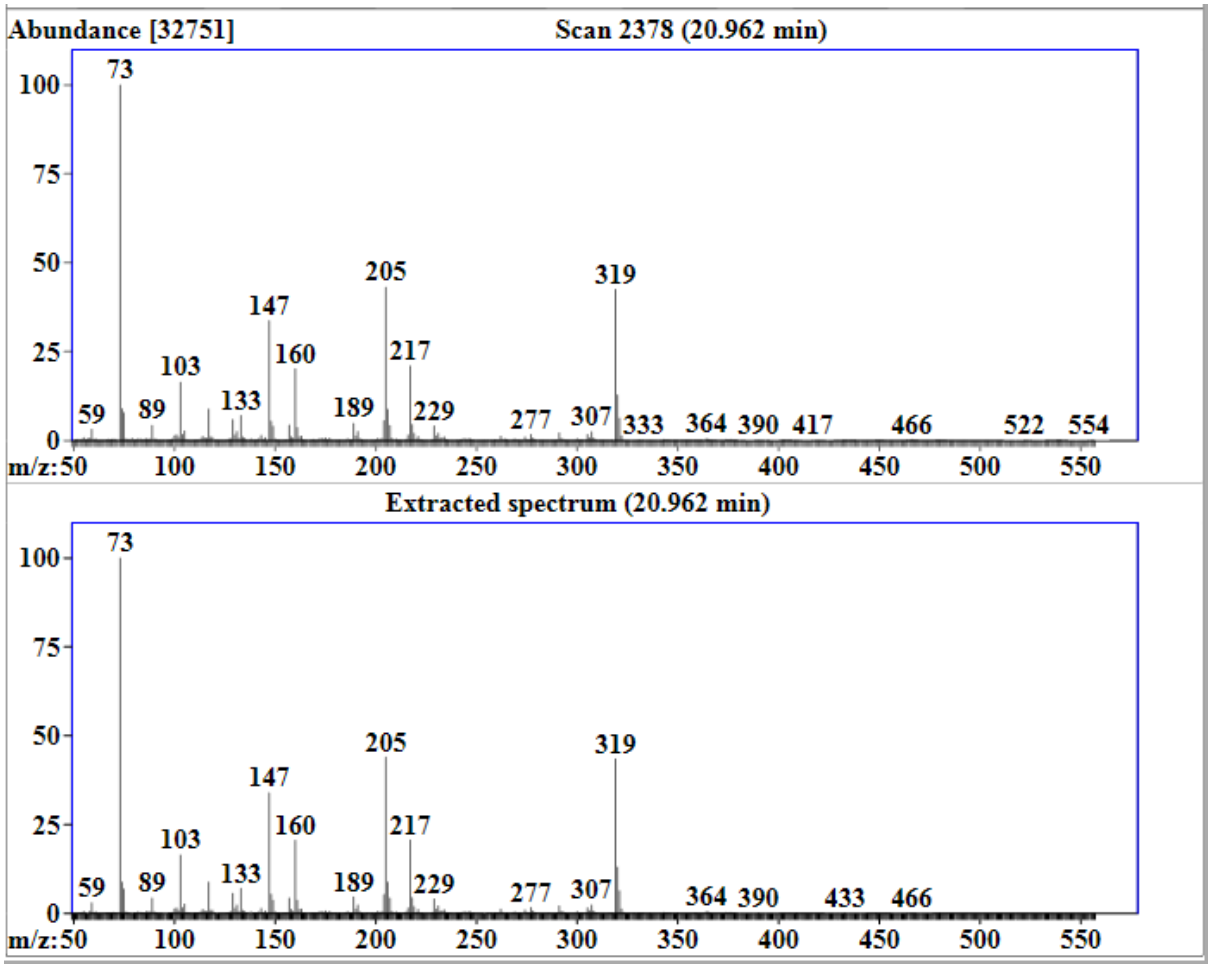

Fig. 1.11: A chromatogram for an unknown compound (top), matched with a known standard (bottom), positively confirming an identification of the monosaccharide galactose.

1.6.3 ^{13}C tracer experiments

^{13}C tracer experiments are based on the application of carbon labelling, *via* incubations *in vivo* or *in vitro* with ^{13}C-enriched media. Labelled carbons are then distributed over the metabolic network and enrichment of the metabolite pools may then be measured (Roessner et al., 2006). As ^{13}C is naturally present in the environment, background levels of the heavy isotope must be identified and quantified, in order to accurately estimate enrichment (Wiechert, 2001; Klein and Heinzle, 2012). A compound with *n* carbon atoms, however, may be labelled on all, some or none of its carbon atoms (isotopomer). Therefore, the number of isotopomers of a compound can be represented as 2^n, either labelled or unlabelled in each carbon position (Wiechert, 2001).

Each isotopomer will represent a fraction of the total pool of a given metabolite. The labelling state of a metabolite therefore represents the distribution across all of these compounds. This distribution will in turn be determined by the turnover of chemical pathways of the respective metabolite; for instance, different pathways may result in the same end-product, but with differing sites of cleavage and therefore different isotopomers (Zamboni et al., 2009) (**Fig. 1.12)**. Typically, most studies apply ^{13}C-labelling to systems when equilibrium is reached between labelled and unlabelled compounds (i.e. an isotopically steady state), with in-depth knowledge of the system under study, this enables actual rates of label distribution and fluxes to be quantified (Wiechert, 2001; Roessner et al., 2006). However, non-stationary, or kinetic labelling studies are also increasingly being applied to uncover changes in the kinetics of enrichment of metabolite pools and to trace unknown pathways in lesser studied systems (Roessner et al., 2006; Young et al., 2011).

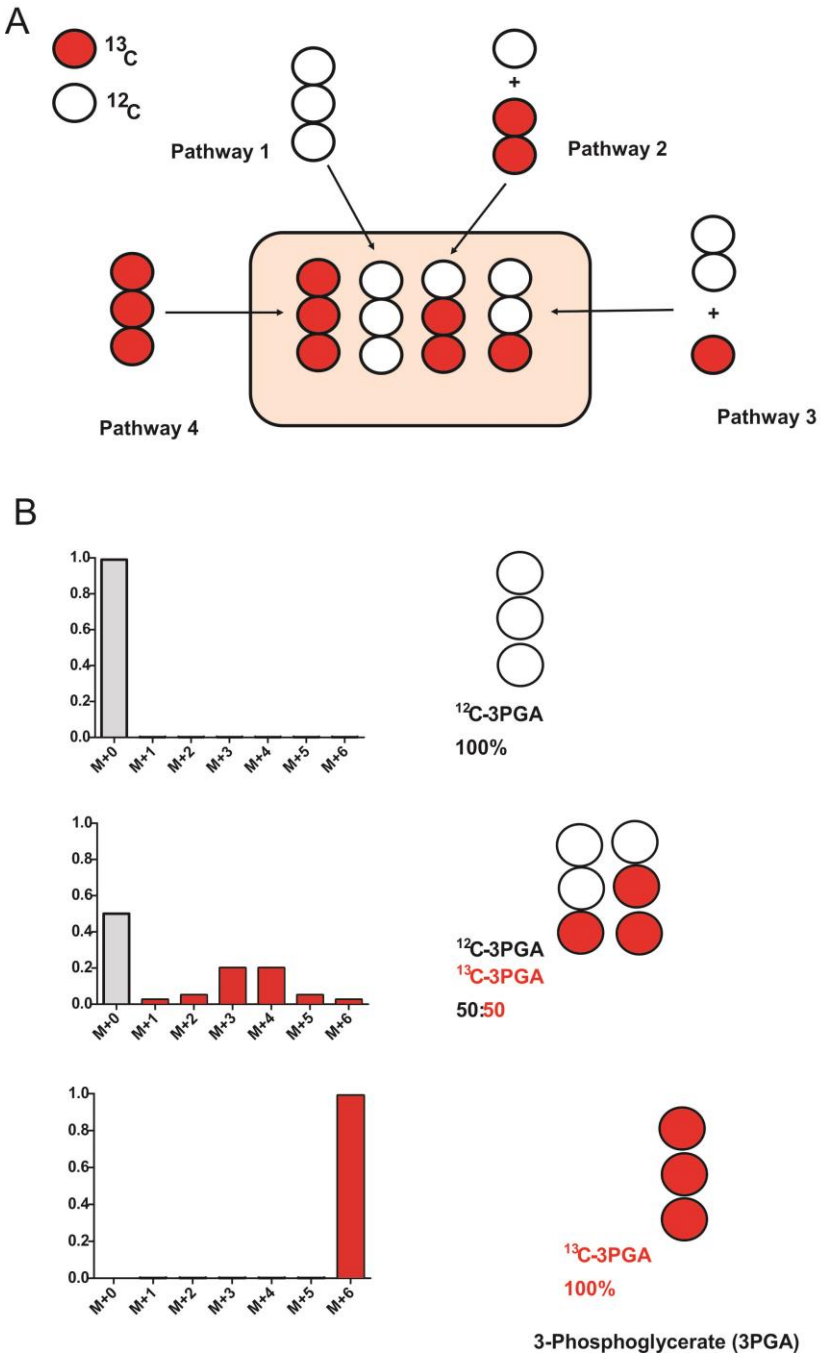

Fig. 1.12: Tracing metabolism with the application of ^{13}C isotope tracer. A) A simplified metabolic network; each pathway produces the same end product, but with a unique labelling pattern (isotopomer). B) Simplified mass isotopomer distributions, of 100% unlabelled to 100% labelled 3-phosphoglycerate; isotopomers have the same chemical formula, but different molecular weights, owing to the incorporation of heavy isotopes, denoted as M+1, M+2, M+3 etc, in order of increasing weight and label incorporation. Figure adapted from Duckwall et al. (2013).

1.6.4 Application to the study of thermal stress

The metabolomics techniques outlined above have been widely applied to both clinical and environmental studies (Viant et al., 2003; Griffin and Shockcor, 2004; Kaplan et al., 2004; Guy et al., 2008; Viant, 2008). Individual metabolites and entire metabolite profiles associated with a given stressor have been identified in a number of systems, including heat stress-associated shifts in metabolism in terrestrial plants (Kaplan et al., 2004; Guy et al., 2008), invertebrates (Malmendal et al., 2006; Michaud et al., 2008) and marine organisms, such as steelhead trout (*Oncorhynchus mykiss*) (Viant et al., 2003) and the red abalone (*Haliotis rufescens*) (Rosenblum et al., 2005) (**Table 1.3**). These studies primarily identified a number of highly conserved changes associated with exposure to thermal stress, within a number of metabolite groups. Notably, these included accumulations of heat-responsive compounds associated with changes to the turnover of carbon fixation, central metabolism (such as glycolysis and the TCA cycle), amino acid and fatty acid metabolism, biosynthesis and cellular homeostasis (osmotic and oxidative state).

The application of metabolomics to the study of the cnidarian-dinoflagellate symbiosis is also receiving increased attention (Fleury et al., 2000; Gordon and Leggat, 2010; Burriesci et al., 2012; Gordon et al., 2013; Sogin et al., 2014; Klueter et al., 2015). Metabolite profiles and mobile products of the sea anemone *Aiptasia* sp. and its dinoflagellate symbiont have already been characterised using these approaches (Burriesci et al., 2012). The study identified glucose to be a major translocated mobile compound in the symbiosis, opposing the long-established theory that glycerol served as the major mobile compound (Muscatine, 1967; Muscatine and Cernichiari, 1969) (**Section 1.3.3**). A second recent study has also characterised the metabolite profiles of different *Symbiodinium* types in culture and their responses to changes in temperature (Klueter et al., 2015). Although a number of compounds were not fully identified, the study detected accumulations of multiple heat-responsive metabolites, including sterols, fatty acids and monosaccharides. Interestingly, both thermally- and light-induced accumulations of two inositol isomers were highly consistent between types. As such this compound may be indicative of a conserved response to these abiotic stressors between *Symbiodinium* types. It was postulated by the authors that these accumulated compounds could be inositol

phosphates, which have major roles in calcium signalling pathways and the induction of encystment (Klueter et al., 2015).

As discussed in **Section 1.5**, major gaps still remain in our understanding of change elicited to central and homeostatic pathways in both symbiont and host during thermal stress and bleaching (Edmunds and Gates, 2003; Davy et al., 2012). Metabolomics-based techniques offer an excellent platform for investigating both thermally induced responses and the complex metabolic interactions that underpin the function of holobiont, particularly when coupled to stable isotope labelling.

Table 1.3 Metabolites associated with thermal stress from a range of systems

System	Analytical platform	Heat-responsive compounds	Reference
Microorganism: *Escherichia coli*	NMR	Reductions of glucose, coupled to accumulations of leucine, isoleucine, valine, lactate, N-acetyl alanine, dimethylamine and methylamine, alanine, α-aminoadipate, glutamate, succinate and glucosylglyceric acid.	(Ye et al., 2012)
Terrestrial plant: Kentucky bluegrass (*Poa Pratensis*) and hybrid bermudagrass (*Cynodon transvaalensis* × *Cynodon dactylon*')	GC-MS	36 heat responsive compounds consisting of organic acids, amino acids, sugars and sugar alcohols. Differential accumulation of a number of compounds in the more heat resistant hybrid, namely: seven sugars (sucrose, fructose, galactose, floridoside, melibiose, maltose and xylose), a sugar alcohol (inositol), six organic acids (malic acid, citric acid, threonic acid, galacturonic acid, isocitric acid and methyl malonic acid) and nine amino acids (Asn, Ala, Val, Thr, *γ*-Aminobutyric acid, Ile, Gly, Lys and Met).	(Du et al., 2011)
Terrestrial plant: *Arabidopsis thaliana*	GC-MS	Alteration of 143 polar metabolites including: amino acids (Asn, Leu, Ile, Thr, Ala, Leu, and Val). Fumarate and malate (oxaloacetate precursors). Amine-containing metabolites (3-Ala, 4-aminobutyric acid [GABA], and putrescine). Carbohydrates including maltose, sucrose, raffinose, galactinol, myoinositol, and cell-wall monosaccharides.	(Kaplan et al., 2004)
Terrestrial plant: Bentgrass *Agrostis* spp.	GC-MS	Organic acids (lactic acid, threonic acid, and aminomalonic acid) and sugars (glucose, fructose, sucrose, and maltose) and amino acids (valine, alanine, proline, aspartic acid, aminobutyric acid, and asparagines), organic acids (threonic acid, gluconic acid, and citric acid), and sugars (fructose, floridoside, and turanose)	(Xu et al., 2013)
Terrestrial	NMR	16 metabolites: alanine, β-alanine, glutamate, glutamine,	(Malmendal et al.,

System	Analytical platform	Heat-responsive compounds	Reference
invertebrate: Fruitfly, *Drosophila melanogaster*		isoleucine, leucine, proline, tyrosine, valine, acetate, choline, glucose, glycogen, ATP, NAD, and a fatty acid-like metabolite.	2006)
Terrestrial invertebrate: Antarctic midge, *Belgica antarctica*	GC-MS	Elevated ketoglutarate and putrescine	(Michaud et al., 2008)
Marine invertebrate: Red abalone*, Haliotis rufescens*	NMR	Nine amino acids (alanine, glutamine, isoleucine, leucine, lysine, phenylalanine, tryptophan, tyrosine, valine), two carbohydrates (glucose and glycogen).	(Rosenblum et al., 2005)
Marine vertebrate: Steelhead trout, *Oncorhynchus mykiss*	NMR	Phosphocreatine, ATP and glycogen, lactate, glucose, phosphocholine, glycine and alanine.	(Viant et al., 2003)

1.7 Aims and objectives

The main aim of this thesis was to investigate change in free metabolite pools, mobile compound exchange and downstream pathways within the cnidarian-dinoflagellate symbiosis associated with thermal stress and bleaching. Principally, the study aimed to identify heat-responsive compounds and metabolic pathways within each partner of the symbiosis.

To address this aim, the study had three specific objectives:

1. To characterise the metabolite profiles of both partners of a model cnidarian-dinoflagellate symbiosis (*Aiptasia* sp. and its homologous symbiont, *Symbiodinium* ITS 2 type B1) under control conditions, and to identify changes associated with exposure of the intact symbiosis to thermal stress and bleaching.

   The associated hypotheses were: a) Symbiont and host pools would differ in terms of the composition of their metabolite profiles under non-stressful conditions; b) the two partners would differ in their responses to thermal stress; and c) heat-responsive metabolites and pathways would be associated with altered metabolic mode during photoinhibition and the maintenance of cellular homeostasis.

2. To build on the model system approach, by characterising the metabolite profiles of symbiont and host in a common reef-building coral (*Acropora aspera* and symbiont *Symbiodinium* ITS 2 type C3) in response to thermal stress, and early and late-phase bleaching.

   The associated hypotheses were: a) Symbiont and host would differ in terms of the composition of their metabolite profiles under non-stressful conditions; b) symbiont and host would differ in their responses to thermal stress; c) heat-responsive metabolites and pathways would be associated with altered metabolic mode during photoinhibition and the maintenance of cellular homeostasis; and d) responses would differ with increased exposure to thermal stress and associated symbiont photoinhibition.

3. To trace carbon fixation, downstream mobile product exchange and pathway end-points in symbiont and host in the *Aiptasia* sp. model system and *A. aspera*, to determine any difference in metabolic function of the symbiosis associated with thermal stress, and early- and late-phase bleaching.

   The associated hypotheses were: a) Thermal stress would alter carbon fixation, label incorporation, quantity and composition of mobile compounds exchanged from symbiont to host; b) shifts in label incorporation in downstream pathways in each partner would occur as a result; and c) these changes would differ with thermal-stress duration.

These objectives fall into the three respective chapters that form the experimental basis of this thesis (**Chapters 2-4**). **Chapter 5** provides a general discussion of the outputs of these chapters and proposed further work.

The methods applied were based upon untargeted and targeted metabolite profiling *via* the use of GC-MS, coupled to incubations with a stable isotope tracer (^{13}C).

Chapter 2 Metabolite profiling of symbiont and host in a model cnidarian-dinoflagellate symbiosis during thermal stress and bleaching

2.1 Introduction

The cnidarian-dinoflagellate symbiosis underpins the success of reef-building (scleractinian) corals in nutrient-poor tropical waters (Muscatine and Cernichiari, 1969; Yellowlees et al., 2008). In symbiosis, dinoflagellate algae of the genus *Symbiodinium* are encapsulated within a host-derived membrane (symbiosome), located within the cnidarian host's gastrodermal cells (Wakefield and Kempf, 2001). In successful symbiosis, there is a complex bi-directional exchange of both organic and inorganic compounds (Muscatine and Hand, 1958; Miller and Yellowlees, 1989; Davy et al., 2012). The photosynthetic symbionts translocate organic products of carbon fixation and nitrogen assimilation to the host, including sugars, sugar alcohols, amino acids and lipids (Muscatine and Cernichiari, 1969; Whitehead and Douglas, 2003; Kopp et al., 2015). In return, the host provides access to dissolved inorganic nutrients (DIC, DIN and phosphorus) and may also exchange host derived amino acids, lipids and fatty acids (Wang and Douglas, 1999; Imbs et al., 2014). The functional holobiont also comprises a specific suite of associated microbial consortia, which are also thought to contribute to these nutritional interactions (Rohwer et al., 2002).

The symbiosis is highly efficient and adapted to relatively wide thermal regimes, however sea water temperatures are rising and continue to do so, regularly exceeding critical temperature thresholds (Hoegh-Guldberg, 1999; Hughes et al., 2003). This in turn necessitates costly acclimation responses in symbiont and the host, with a re-organization of cell metabolism and structure (Kaplan et al., 2004). In symbiosis, this process will occur in each partner individually, but as change is elicited in the downstream exchange of mobile compounds between partners, it will affect the holobiont as a whole (Clark and Jensen, 1982; Jokiel and Coles, 1990). Acclimation responses will vary according to the holobiont genotype and phenotype, however they include enzymatic and non-enzymatic antioxidants, photoprotective compounds such as fluorescent proteins and accessory pigments, heat shock proteins (HSPs), compatible solutes, and structural modifications to maintain cell and

organelle stability and function (Lesser, 2006; Baird et al., 2009a). Further to their roles in central metabolism, free metabolite pools will function in the *de novo* synthesis of these protective compounds. In addition, they have direct roles as intracellular antioxidants, chelating agents, compatible solutes and cellular signals (Guy et al., 2008; Grüning et al., 2010). Even with costly acclimation responses in place, where elevated temperatures are prolonged, and/or severe, thermal stress will lead eventually to dysfunction of the symbiosis. Specifically, the accumulation of reactive oxygen species (ROS) in symbiont and host, and the breakdown and loss of dinoflagellate symbionts, *via* bleaching (Weis, 2008).

Despite the importance of coral reefs and bleak projections for their future under climate change, major gaps remain in our understanding of how this dynamic and complex symbiosis is affected by high temperature stress and bleaching (Edmunds and Gates, 2003; Davy et al., 2012). In particular, data elucidating changes to mobile compound exchange and downstream pathways in the holobiont are lacking. Less still is known of the secondary roles of many primary metabolites in cellular acclimation, or how these compounds may serve to alter resistance to stress. Metabolomics is a widely used approach for the study of abiotic stressors within clinical research, and increasingly in environmental monitoring (Viant, 2008; Lankadurai et al., 2013). Metabolomics refers to the analysis of low molecular weight metabolites within a cell, tissue or biofluid (the “metabolome”) (Viant, 2007). The metabolome of an organism is a downstream product of genotype, phenotype and environmental drivers (Fancy and Rumpel, 2008; Spann et al., 2011). Given a variable of interest, it is therefore possible to detect fine scale change in a rapid and quantitative manner. Furthermore, by calculating accompanying pathway rate changes, insight can also be gained into wider downstream physiological effects. At the simplest level, one such method for estimating pathway turnover involves the comparison of metabolite abundance and role in particular pathways, producing a hypothetical estimate of pathway activity, which may then be compared between conditions (Aggio et al., 2010). Due to the diversity of the metabolome, no one method is currently capable of capturing all metabolite classes, due to their differing characteristics (Viant, 2008). However, with the application of gas chromatography-mass spectrometry (GC-MS) metabolite profiling, it is possible to simultaneously

analyse a relatively large number of metabolite groups in a high throughput, repeatable, sensitive and cost-effective manner (Villas-Bôas et al., 2005).

This study applied GC-MS metabolite profiling and pathway activity analysis to the tropical sea anemone *Aiptasia* sp. (of unknown Pacific origin) and its *in hospite* homologous symbiont (*Symbiodinium minutum*, ITS2 type B1) (Starzak et al., 2014). This anemone is a widely used model system for the study of the cnidarian-dinoflagellate symbiosis (Weis, 2008). The main aim was to investigate heat-stress induced modifications to the intracellular pools of both partners. The methods were therefore optimized to focus on pools of amino and non-amino organic acids (in particular fatty acids). These compounds not only play important roles in the functional metabolism of the holobiont, but have also been previously shown to respond to heat treatment, principally in the maintenance of homeostasis, cell structure, cell signalling and cell death (Díaz-Almeyda et al., 2011; Imbs and Yakovleva, 2012; Leal et al., 2013).

2.2 Materials and methods

Specimens of the sea anemone *Aiptasia* sp. were maintained in the lab in 1 µm filtered seawater (FSW) at 25°C, with light provided by AQUA-GLO T8 fluorescent bulbs at ≈ 95 µmol quanta m^{-2} s^{-1} (light:dark ≈ 12h:12h). Anemones were fed twice a week with freshly hatched *Artemia* sp. nauplii. Prior to the experiment, anemones were rinsed repeatedly with FSW to remove external contaminants. Individuals were acclimated and starved in 25 L aquaria (light regime as above) for seven days prior to sampling, to ensure that any *Artemia* nauplii had been digested and expelled. Following acclimation, the treatment aquaria were ramped to 32°C ± 0.4°C over a period of 48 h (≈ 1°C 8 h^{-1}). Once the target temperature was attained, it was maintained for six days for the treatment group. A control group was maintained at 25°C ± 0.5 °C.

Dark-adapted maximum yield of PS II (F_v/F_m) was measured with a diving PAM fluorometer (Walz, Effeltrich, Germany), following a 30 min dark adaptation at the end of the daily light cycle. PAM settings were maintained over the course of the experiment at: measuring light 4, saturation intensity 4, saturation width 0.6 s, gain 2

and damping 2. Measurements were taken a standard distance of 5 mm from each sample. Mean estimates with standard error (S.E.M) were calculated based on single measurements from ten individuals *per* treatment at each time point. These same individuals were maintained for daily measurements over the course of the experiment and were not sampled for metabolite profiles.

Sampling for metabolite profiling was undertaken at 0 d (pre-heat ramp) and after 6 d of heat treatment exposure. Three replicate samples were taken at each time point for each treatment. Each individual sample comprised a total of six individuals, to ensure sufficient biomass for metabolite identification (n = 3 x 6 anemones *per* time point and treatment). Individuals for metabolite analysis were immediately quenched by snap freezing in liquid nitrogen and transferred to a -80°C freezer for storage.

2.2.1 Host and Symbiodinium separation

Frozen individuals were pooled into single samples and ground with a pestle and mortar, which was chilled with the addition of liquid nitrogen. Once homogenised, 2.4 mL chilled MilliQ water (at 4°C) was added, the sample thoroughly vortexed, and a 400 µL aliquot taken for host protein, *Symbiodinium* cell counts and chlorophyll *a* analysis. The remaining homogenate was then centrifuged at 1,150 x *g* for 5 min at 4°C to pellet the algal symbionts.

The supernatant containing the host fraction was removed, snap-frozen in liquid nitrogen and freeze-dried overnight. The algal pellet was re-suspended in 3 mL chilled MilliQ water and re-centrifuged at 1,150 x *g* for 5 min at 4°C, and the supernatant discarded. This washing procedure was repeated twice and the resulting algal pellet was freeze-dried overnight. It should be noted that MilliQ water alone was employed for separation and purification phases due to the interaction of buffer precipitates (phosphates) and antifreezes (such as glycerol and ethylene glycol) with the metabolites of interest (K. Hillyer and J. Matthews, unpublished data).

2.2.2 Protein quantification, cell counts and chlorophyll a

Symbiodinium cell densities were quantified using Improved Neubauer haemocytometer counts (Boeco, Germany), with a minimum of six replicate cell counts *per* sample (to a confidence interval below 10%). Cell density was normalised to soluble protein content, which was assessed by the Bradford assay (Bradford, 1976) carried out on the supernatant of centrifuged (16000 x *g* for 20 min) host

fractions (triplicate measurements). Symbiont chlorophyll *a* content was quantified by dimethylformamide extraction undertaken in the dark at 4°C (Moran, 1982) and measured with an ELISA microplate reader (Enspire® 2300, Perkin-Elmer, Waltham, MA, USA) (triplicate measurements) at wavelengths of 663.8 nm, 646.8 nm and 750 nm.

2.2.3 Extraction

Once dry, 1 mL 50% cold MeOH (at -20°C) was added to each of the samples, which were also spiked with 20 µL of the internal standard d_4-alanine (at 10 mM). Methanol-chloroform washed aluminium beads were added and the samples vortexed for 1 min, frozen and re-vortexed for a further minute. This process was repeated twice for the symbiont samples, to ensure that the cells were fully lysed, identifiable by the orange colour of the extract. Samples were then centrifuged at 3220 x *g* for 6 min at -9°C, and the supernatants collected and stored on dry ice. The extraction was then repeated with the further addition of 1 mL 80% cold MeOH (at -20°C) to the pellet. This second extract was then combined with the first and the pooled sample freeze-dried overnight. The algal pellet and host cell debris were retained and dried in a drying oven at 100°C, to a constant dry weight.

2.2.4 MCF derivatization

Derivatization was *via* methyl chloroformate (MCF) with the method adapted from Smart et al. (2010). When completely dry, symbiont samples were re-suspended in 200 µL of NaOH (1M) and transferred to silanised glass tubes (CTS-1275, Thermo Fisher Scientific, USA). After this, a 50 µL aliquot was taken from each sample to produce a pooled sample. To the remaining sample, 167 µL of MeOH and 34 µL of pyridine were added, followed by 20 µL of MCF, and the solution vortexed for 30 s. A further 20 µL of MCF was then immediately added and the samples vortexed for another 30 s. Next, 400 µL chloroform was added to each sample and the mixture vortexed for 10 s. Finally, 400 µL sodium bicarbonate (50 mM) was added to halt the reaction and the samples vortexed for another 10 s. Derivatization and preparation of the pooled host sample was as for the symbiont, but all derivatization volumes were doubled, except in the case of chloroform. Samples were then centrifuged at 1,150 x *g* for 5 min and the upper aqueous phase discarded. Any remaining water was then removed from the sample with the addition of sodium sulphate. The remaining extract was then transferred to GC vials for GC-MS analysis.

An isotope-labelled derivative for each metabolite found in the sample was prepared *via* chemical derivatization of the pooled sample (algae/host) using isotope-labelled derivatizing reagents, namely deuterium-labelled methyl chloroformate (d-MCF) (MT001, Omics Ltd, Auckland, New Zealand) and deuterium-labelled methanol (methanol-d_4). A 50 µL aliquot of the relevant d-MCF-derivatized pooled sample (symbiont/host) was then spiked into each of the MCF-derivatized samples prior to GC-MS analysis.

2.2.5 GC-MS analysis

GC-MS was used for identification, semi-quantitation and absolute quantitation of metabolites. This involved use of a Thermo Scientific Trace GC Ultra gas chromatograph coupled to an ISQ mass spectrometer with a programmable temperature vaporising (PTV) injector.

GC-MS instrument parameters were based on Smart et al. (2010). Briefly, 1 µL of sample was injected using a CTC PAL autosampler into a Siltek™ 2 mm ID straight unpacked inlet liner. The injector was set to 260°C, constant temperature splitless mode with a pressure surge of 180 kPa for 1 min, and column flow of 1.0 mL min^{-1} in constant flow mode. Purge flow was set to 25 mL min^{-1}, 1.2 min after injection.

The column was a fused silica ZB-1701 30 m, 0.25 mm ID, 0.15 µm film thickness (86% dimethylpolysiloxane, 14% cyanopropylphenyl, Phenomenex). Carrier gas was ultra-high purity grade helium (99.9999%, BOC). GC oven temperature programming started isothermally at 45°C for 2 min; increased 9°C min^{-1} to 180°C, held 5 min; increased 40°C min^{-1} to 220°C, held 5 min; increased 40°C min^{-1} to 240°C, held 11.5 min; increased 40°C min^{-1} to 280°C, held 2 min. The transfer line to the MSD was maintained at 250°C, and the source at 230°C. The detector was turned on 5.5 min into the run under electron-impact ionisation mode, at 70 eV electron energy, with the electron multiplier set with no additional voltage relative to the autotune value. Solvent blanks were run for every 10-12 samples to monitor instrument carryover. Mass spectra were acquired in scan mode from 38 to 550 amu, at a rate of 5120 amu sec^{-1}.

2.2.6 Data analysis and validation

Metabolite data extraction and analysis were undertaken based on the protocol described in Smart et al. (2010) with the use of Automated Mass Spectral

Deconvolution and Identification System (AMDIS) (http://chemdata.nist.gov/mass-spc/amdis/) and R software, including the packages Metab, Metab-Q and PAPi (Aggio et al., 2010; Tumanov et al., 2015b), and the software package MetaboAnalyst (Xia et al., 2009; Xia et al., 2012). Compound identification was based on an in-house library of MS spectra. Derivative peak areas were used to quantify the concentrations of individual metabolites. MCF data were then normalized to the final area of the internal standard (d_4-alanine) and sample fraction dry weight. For quantitative data, Metab-Q was used to extract abundances of analytes from chromatograms. Metab-Q is an in-house software written in R-environment (http://www.r-project.org/) that generates a .csv file with individual analyte abundances using an AMDIS report. This script requires the XCMS library (Smith et al., 2006) and can process data files in NetCDF and mzXML formats. Metab-Q is a free software package that can be downloaded from the Metabolomics Laboratory webpage (The University of Auckland, New Zealand) (http://metabolomics.auckland.ac.nz/index.php/projects/26). Data were then normalised to sample dry weight.

Data were tested for normality and homogeneity, and log transformed where appropriate. IBM SPSS Statistics (v20) was used for both repeated-measures ANOVA (RMANOVA) and ANOVA. RMANOVA was used to test for differences in maximum quantum yields between treatment groups and days (repeat measurements were from the same individuals, which were set aside in each treatment). ANOVA was used to test for differences in heat stress indicators between treatments and sampling days. Statistical significance between the abundance of metabolite treatment means was determined by univariate tests (t-test) in MetaboAnalyst. Differences were considered significant at the $P < 0.05$ probability level. Fold change (FC) analysis was used to compare the absolute value change between group means, before data normalization was applied. Principal components analysis (PCA) using the normalised, log-transformed and auto-scaled metabolite data was undertaken with MetaboAnalyst. PCA analysis was used to summarize the multivariate metabolite data, capturing the variables that explained the greatest variation (principal components, PC) in each treatment group. The key-contributing metabolites, as determined by their contribution to the PCA plots, can be identified by their loadings values, as summarised in the corresponding loadings plots.

Pathway activity analysis using the Pathway Activity Profiling (PAPi) package was undertaken to compare activities using the normalized and transformed metabolite data following the methods described in Aggio et al. (2010). Briefly, using the normalized abundance data for each treatment at day 6 as input, the PAPi package calculates activity scores of individual pathways from the Kyoto Encyclopedia of Gene and Genomes (KEGG) database. These activity scores are based on the relative changes in compounds (control vs treatment) associated with each pathway of interest. This algorithm is based on two main assumptions: i) if a given pathway is active in a cell or organism, more intermediates associated with that pathway will be detected; and ii) there will be a lower abundance of associated pathway intermediates, due to high turnover and *vice versa* during low activity (Aggio et al., 2010). The resulting activity score therefore serves as an indicator of the likelihood that a pathway is active within a cell, or organism under a given condition, without the requirement for absolute quantitation such as during more detailed flux analysis. Resulting pathway activity scores were inverted to make interpretation in plotted figures more intuitive, i.e. an increase in activity score representing an increase in the predicted pathway activity. Independent sample t-tests (two-tailed) were used to test for differences between activity scores between treatment groups, with equal variance assumed.

2.3 Results

A total of 50 compounds comprised largely of amino and non-amino organic acids were identified *via* GC-MS analysis of the polar and semi-polar extracts of the dinoflagellate (symbiont) and cnidarian (host) fractions. These compounds consisted of 18 amino acids, 11 organic acids and amides, 3 monounsaturated fatty acids (MUFA), 12 polyunsaturated fatty acids (PUFA), 5 saturated fatty acids (SFA) and 1 peptide (**Table S2.1**).

2.3.1 Ambient metabolite profiles

Under ambient conditions, symbiont and host profiles differed to a high degree (PC1, 63.1%) in the relative composition of their free metabolite pools (**Fig. 2.1**; **Table S2.2**). Symbiont profiles were largely composed of a mix of SFAs, MUFA and PUFAs.

The most abundant of these - palmitic acid (C16_0), oleic acid (C18_1n) and 11,14,17-eicosatrienoic acid (C20_3n) - were present at concentrations of between 880 pg μg^{-1} and 640 pg μg^{-1} symbiont dry weight. Those distinctive of the symbiont profile included the PUFAs 11,14,17-eicosatrienoic acid (C20_3n), gamma-linolenic acid (C18_3n), 13,16-docosadienoic acid (C22_2n), and 11,14-eicosadienoic acid (C20_2n), and the SFAs myristic acid (C14_0) and dodecanoic acid (C12_0) (**Fig. 2.1**).

Host profiles were dominated by a more diverse range of metabolite groups, including SFAs, MUFAs, organic acids and amino acids (**Fig. 2.1**; **Table S2.2**). The most abundant metabolite was the organic acid citrate, at 3270 pg μg^{-1} host dry weight, followed by the amino acid glutamic acid, the SFA C16_0 and the tripeptide glutathione, which ranged between 1800 pg μg^{-1} and 900 pg μg^{-1} host dry weight. Characteristic metabolites of the host profile included the tripeptide glutathione, the amino acids isoleucine, methionine, cysteine and serine, the organic acids itaconic acid and citric acid (**Fig. 2.1**).

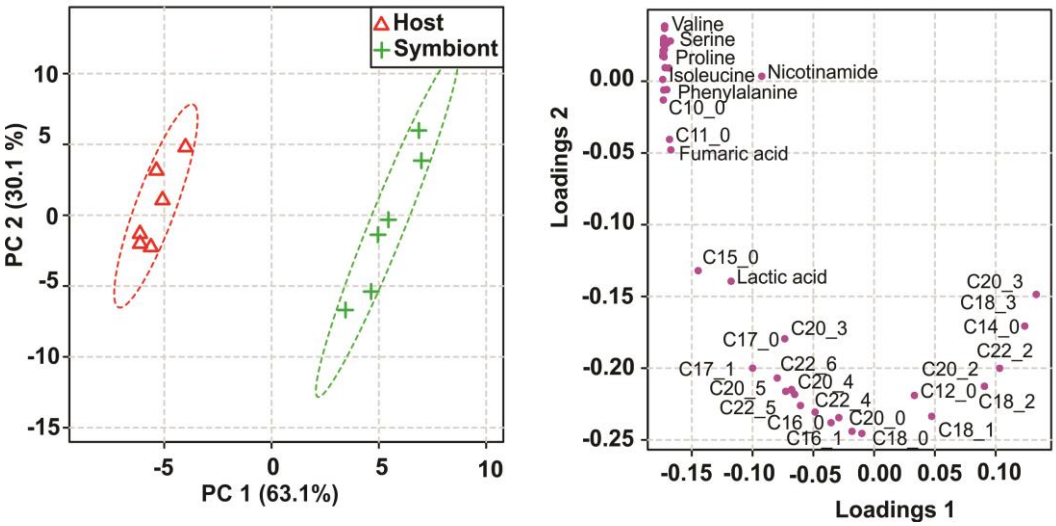

Fig. 2.1: PCA scores plot, with 95% confidence intervals (left) and loadings plot (right) of metabolite profile data for dinoflagellate symbiont (symbiont) and cnidarian host samples (host) under ambient conditions.

2.3.2 Heat stress indicators

Exposure to 32°C for 6 days resulted in significant declines in the maximum quantum yield of PS II (F_v/F_m; **Fig. 2.2**), which differed with treatment (RMANOVA, time x temperature $F_{6,108} = 12.93$, $P < 0.001$). After 6 days, F_v/F_m within the treatment group declined ca. 25% to 0.49 ± 0.04, compared to 0.64 ± 0.02 in the control.

Symbiodinium cell density also declined significantly in the heat treatment group (one-way ANOVA, $F_{3,20} = 23.283$, $P < 0.001$). Elevated temperature treatment caused a 69% reduction in symbiont density after 6 days (from 4.79 x10^6 cells mg^{-1} protein ± 3.42 x10^5 S.E. to 1.46 x10^6 cells mg^{-1} protein ± 1.55 x10^5 S.E.), while there was no significant decline in the control (Tukey HSD *post hoc*, $P = 0.992$). Chlorophyll *a* concentration *per* cell, however, remained unaffected by temperature, with values ranging from approximately 1.21 to 0.82 pg chl *a* $cell^{-1}$ (one-way ANOVA, $F_{3,20} = 1.295$, $P = 0.304$).

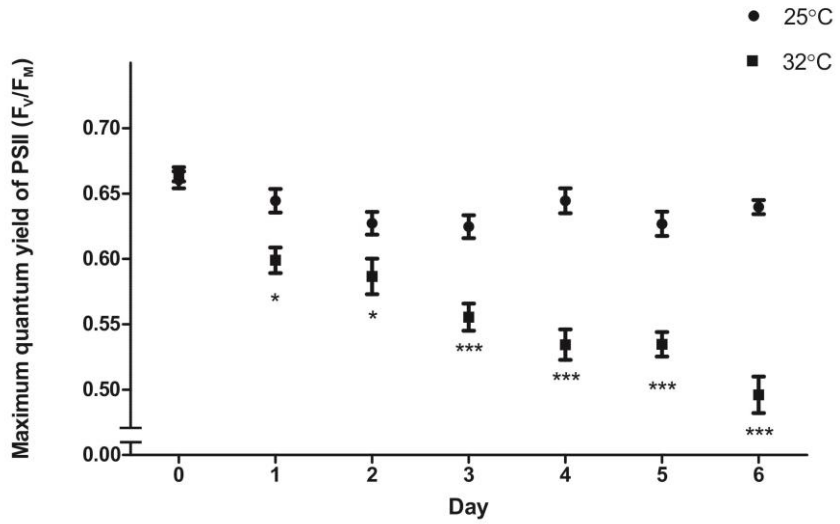

Fig. 2.2: Daily measurements of maximum quantum yield (F_v/F_m) of photosystem II of individuals (*n* = 10 per treatment) at 25°C and 32°C. Values are mean ± S.E.M. Asterisks denote significant results between treatments at each time point, RMANOVA, pairwise post-hoc with Bonferroni correction, * $P < 0.05$, *** $P < 0.001$.

2.3.3 Heat treatment metabolite profiles

For both symbiont and host, heat treatment caused a shift in metabolite profile, as indicated by the clear separation of the 6 d heat treatment groups within the PCA score plots (**Fig. 2.3**). For the symbiont, the heat treatment group was separated

along the negative axis of both PC1 and PC2 (PC 1, 72.3%, PC2, 11.7%) (**Fig. 2.3**). For the host fraction, the greatest variance in the data set was accounted for by within-group variability (PC 1, 52.7%), heat treatment explained a second level of variance in the data set (PC 2, 16.4%) (**Fig. 2.3**). Metabolite profiles of the 6 d controls and 0 d pre-heat treatment groups closely resembled one another, as reflected in their similar principal component scores and the spatial overlap of these groups in the PCA score plots.

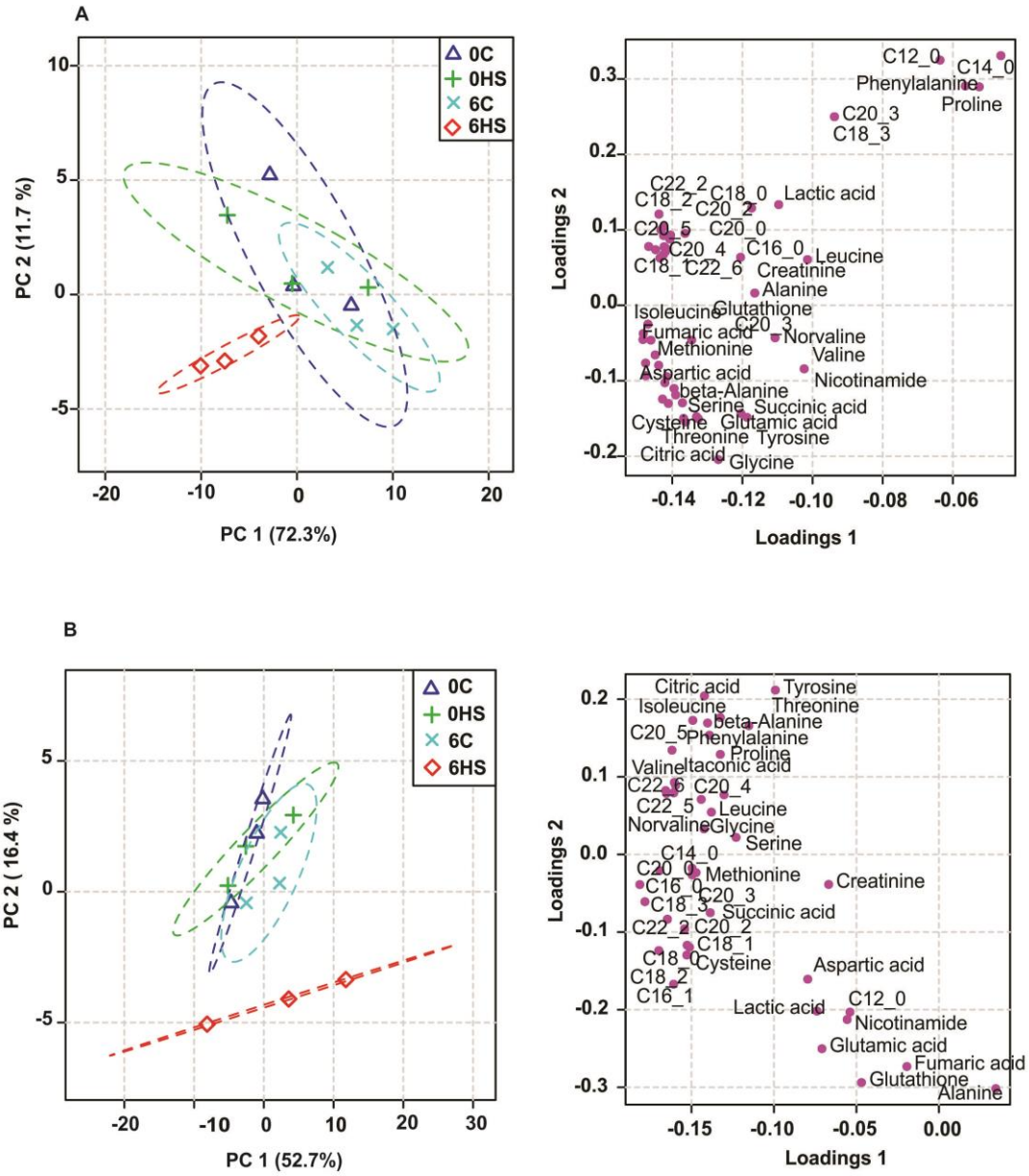

Fig. 2.3: Symbiont (A) and host (B) PCA score plots, with 95% confidence intervals (left) and metabolite loadings plots (right). 0C, day 0 control; 0HS, day 0 heat stress; 6C, day 6 control; 6HS, day 6 heat stress.

2.3.4 Heat responsive metabolites in the symbiont

The metabolites contributing the greatest to the heat treatment effect in the symbiont metabolite pools are summarised in **Fig. 2.4**. Briefly, they include the organic acid succinic acid and the amino acids valine, norvaline, threonine and methionine (**Fig. 2.4**). Those typical of the control included the saturated fatty acids myristic acid (C14_0) and dodecanoic acid (C12_0).

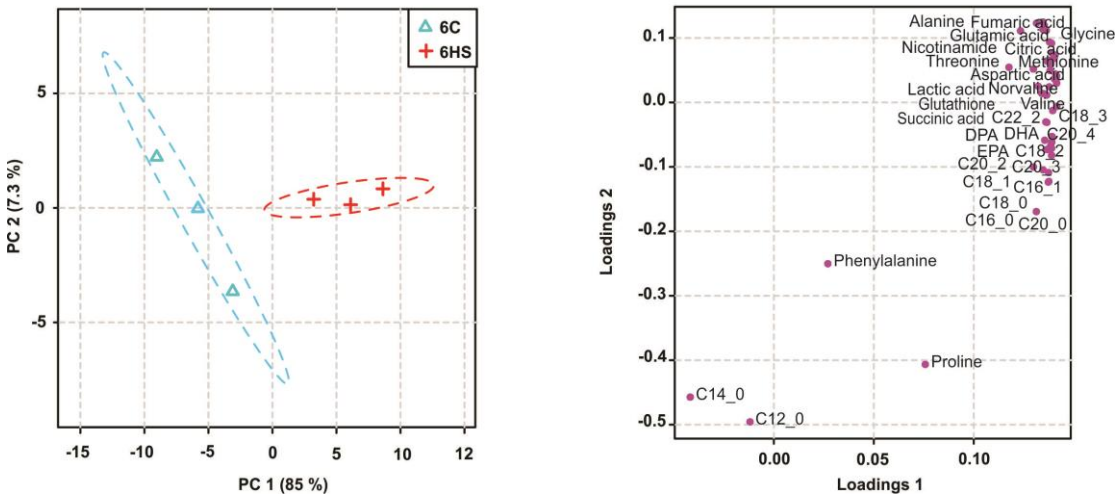

Fig. 2.4: Symbiont PCA score plots, with 95% confidence intervals (left) and metabolite loadings plots (right). 6C, day 6 control; 6HS, day 6 heat stress.

With respect to quantitative data of individual compounds, significant concentration increases and fold changes were detected for multiple metabolite groups (**Table S2.3**). Notably, the organic acids lactate, fumarate, citrate and succinate, the amino acids glycine, beta-alanine, threonine, valine, norvaline and methionine, and the PUFAs alpha- and gamma-linolenic acid (C18_3n) and 11,14,17-eicosatrienoic acid (C20_3n) (**Fig. 2.5**).

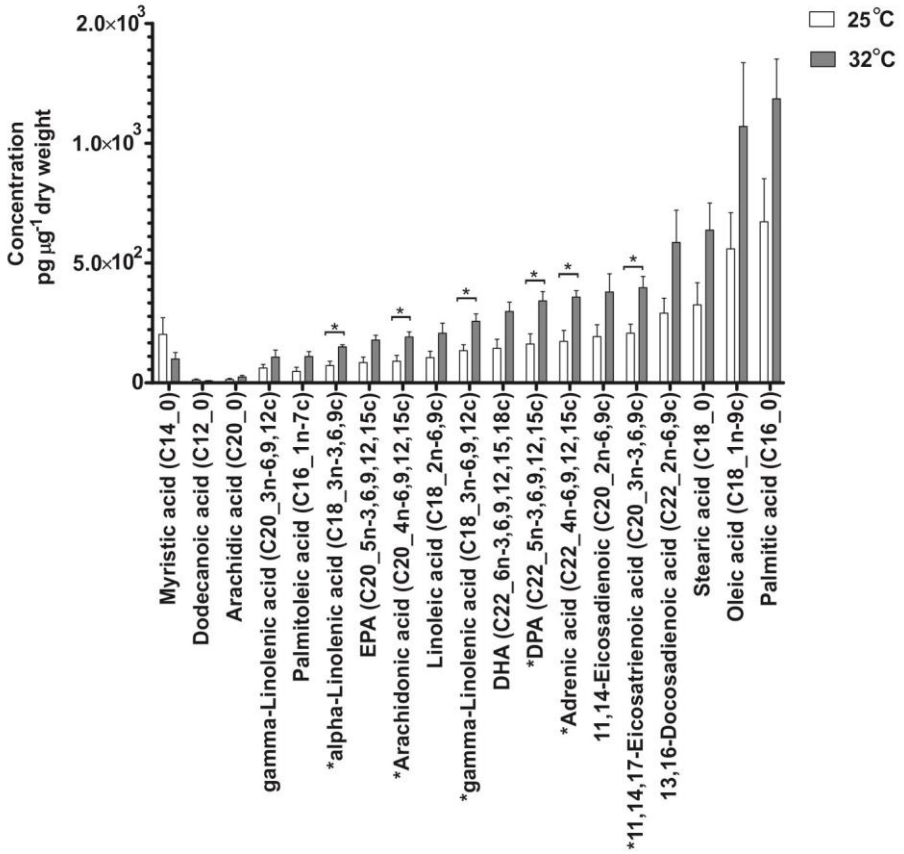

Fig. 2.5: Concentration of individual compounds in symbiont free fatty acid pools *per* µg dry weight during ambient conditions (25°C) and following exposure to thermal stress (32°C for 6 d) from the anemone *Aiptasia* sp. t-test concentration x treatment, * $P < 0.05$

As a result of these relative alterations in pools between ambient and heat stress groups, multiple activity changes to downstream networks were estimated, especially those associated with central metabolism, fatty acid metabolism and cellular homeostasis (**Fig. 2.6**). Principally, activity reductions for pathways associated with glycolysis, oxidative phosphorylation and the TCA cycle. Coupled to these modifications to central metabolism, declines in the activity of biosynthesis pathways for a number of amino acids and fatty acids were estimated. A reduction in the on-going metabolism of a number of amino acids and cellular antioxidants including, glutathione and nicotinamide was also estimated and therefore considered indicative of accumulations of these groups with thermal stress.

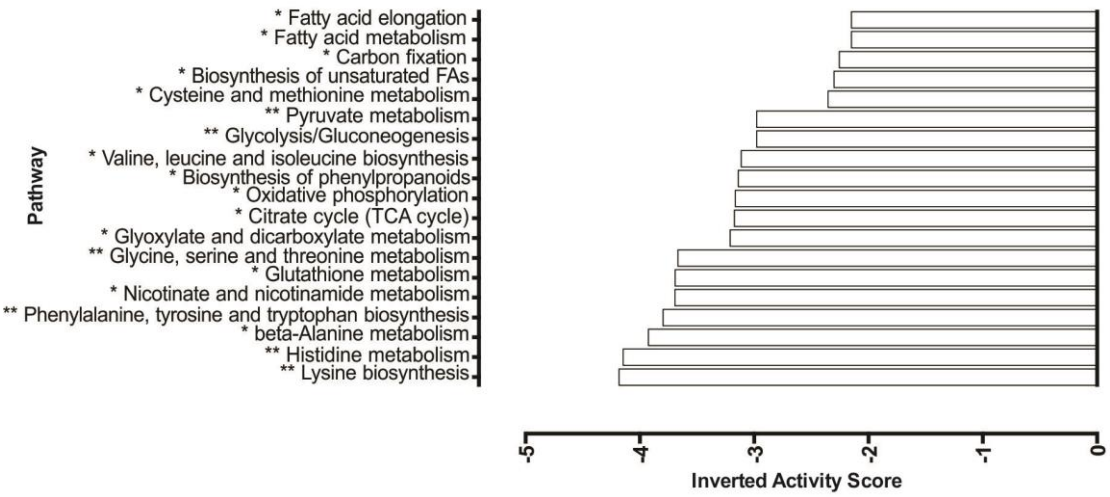

Fig. 2.6: Relative change in key symbiont metabolite pathway activities following 6 days of heat stress at 32°C. (PAPi activity analysis 6 d control v 6 d heat treatment, t-test activity score x treatment, 2-tailed ** $P < 0.005$, * $P < 0.05$).

2.3.5 Heat responsive metabolites in the host

Key metabolites that contributed to the metabolite profile of thermally-stressed anemone tissues included the SFA dodecanoic acid (C12_0), the nucleotide precursor nicotinamide, the tripeptide glutathione, and the organic acids lactate and fumarate (**Fig. 2.7** and **Fig. 2.8**).

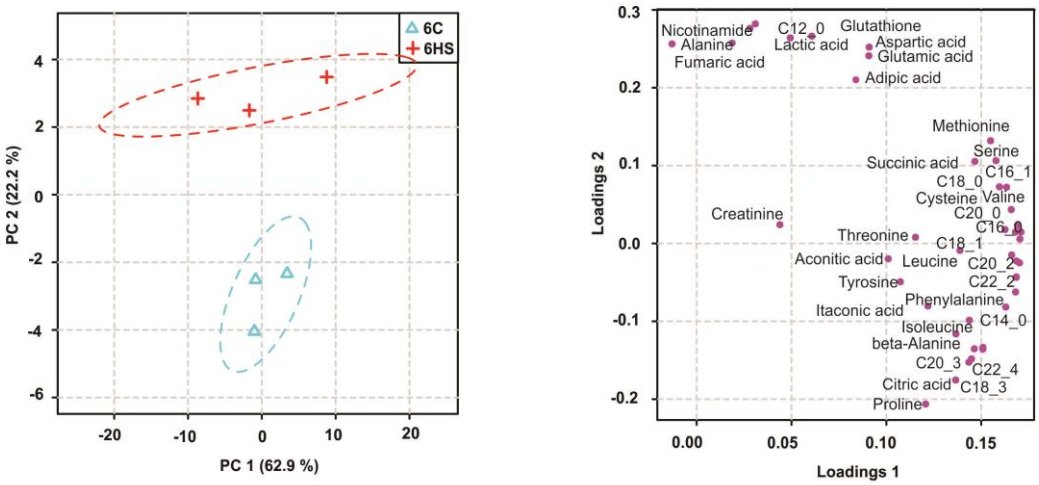

Fig. 2.7: Host PCA score plots, with 95% confidence intervals (left) and metabolite loadings plots (right). 6C, day 6 control; 6HS, day 6 heat stress.

Similarly, significant concentration increases and fold changes were detected for the same compounds, in addition to the amino acids alanine and glutamic acid (**Table S2.4**).

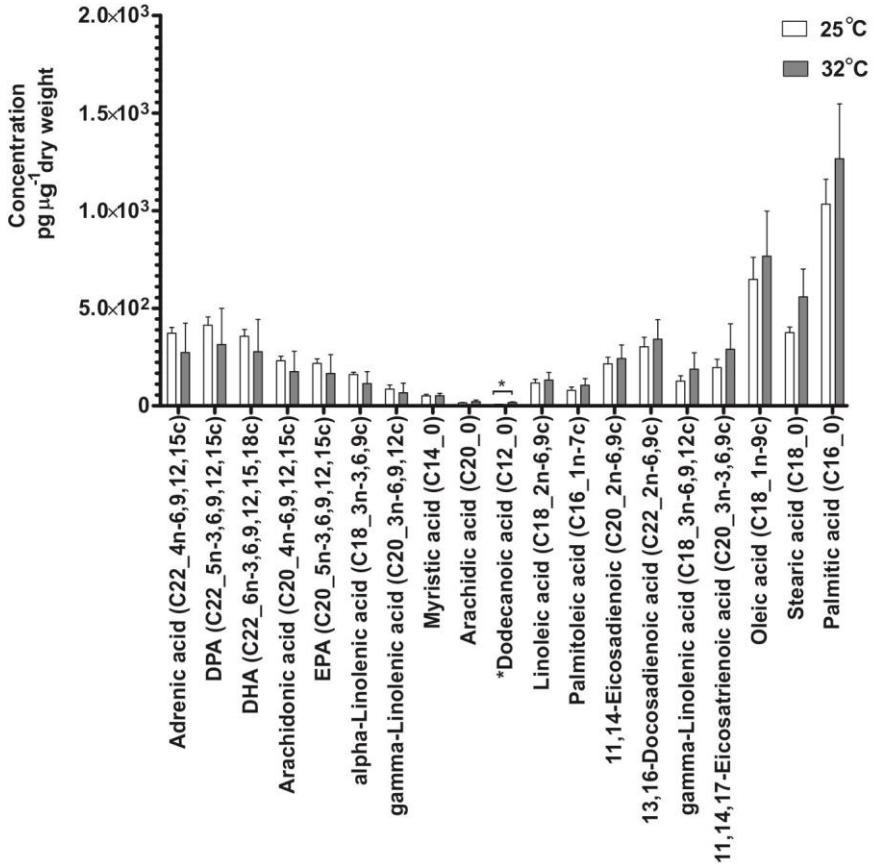

Fig. 2.8 Concentration of individual compounds in host free fatty acid pools *per* µg dry weight during ambient conditions (25°C) and following exposure to thermal stress (32°C for 6 d) from the anemone *Aiptasia* sp. t-test concentration x treatment, * $P < 0.05$

Alterations to pathway turnover were estimated for a number of central networks as a result of temperature treatment (**Fig. 2.9**). Briefly, relative increases in pathways linked to the generation of energy *via* gluconeogenesis, namely the TCA cycle, CoA biosynthesis and oxidative phosphorylation were estimated, coupled to declines in glycolysis and pyruvate metabolism. These alterations coincided with increased activity of the metabolism of a number of fatty acids and amino acids. Increased activity of networks associated with lipid signalling pathways were also detected,

namely those associated with the oxidation of the fatty acids arachidonic acid (C20_4) and linoleic acid (C18_2). Correspondingly, reduced metabolism of cellular antioxidants, including glutathione and thiol-containing amino acids were estimated indicative of accumulations of these groups in the heat stressed host.

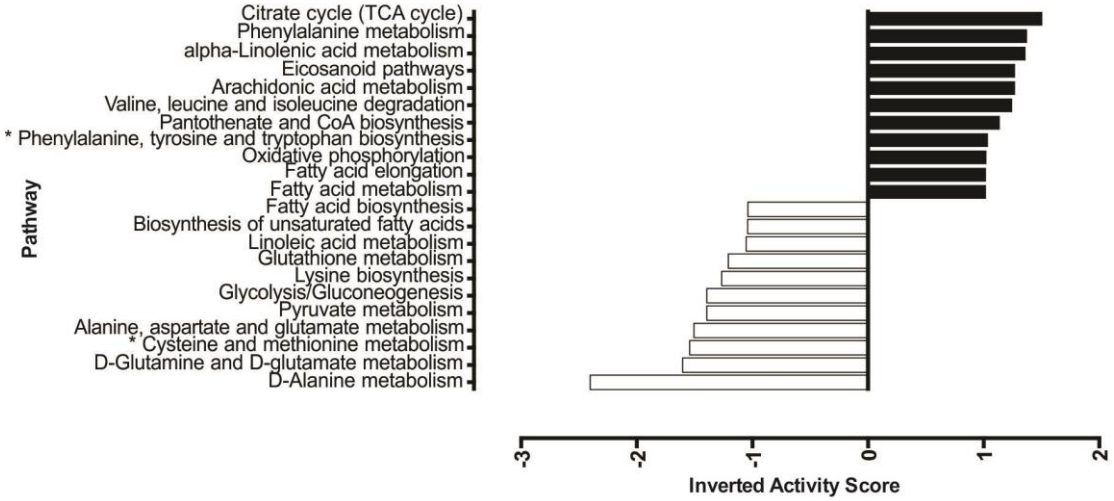

Fig. 2.9: Relative change in key host metabolite pathway activities following 6 days of heat stress at 32°C (PAPi activity analysis 6 d control v 6 d heat treatment, t-test activity score x treatment, 2-tailed ** $P < 0.005$, * $P < 0.05$).

2.4 Discussion

This study characterised metabolite profiles, in both partners of a model cnidarian-dinoflagellate symbiosis, during ambient conditions and following exposure to elevated temperature. Heat treatment (32°C for 6 days) resulted in thermal stress and breakdown of the symbiosis (bleaching). Marked, thermally induced changes in the pools of intracellular free metabolites in both partners were observed. Associated with these modifications, alterations to the activities of central metabolic pathways, such as glycolysis and gluconeogenesis were identified, in addition to those associated with nitrogen assimilation, biosynthesis, cellular homeostasis and cell signalling (**Fig. 2.10**).

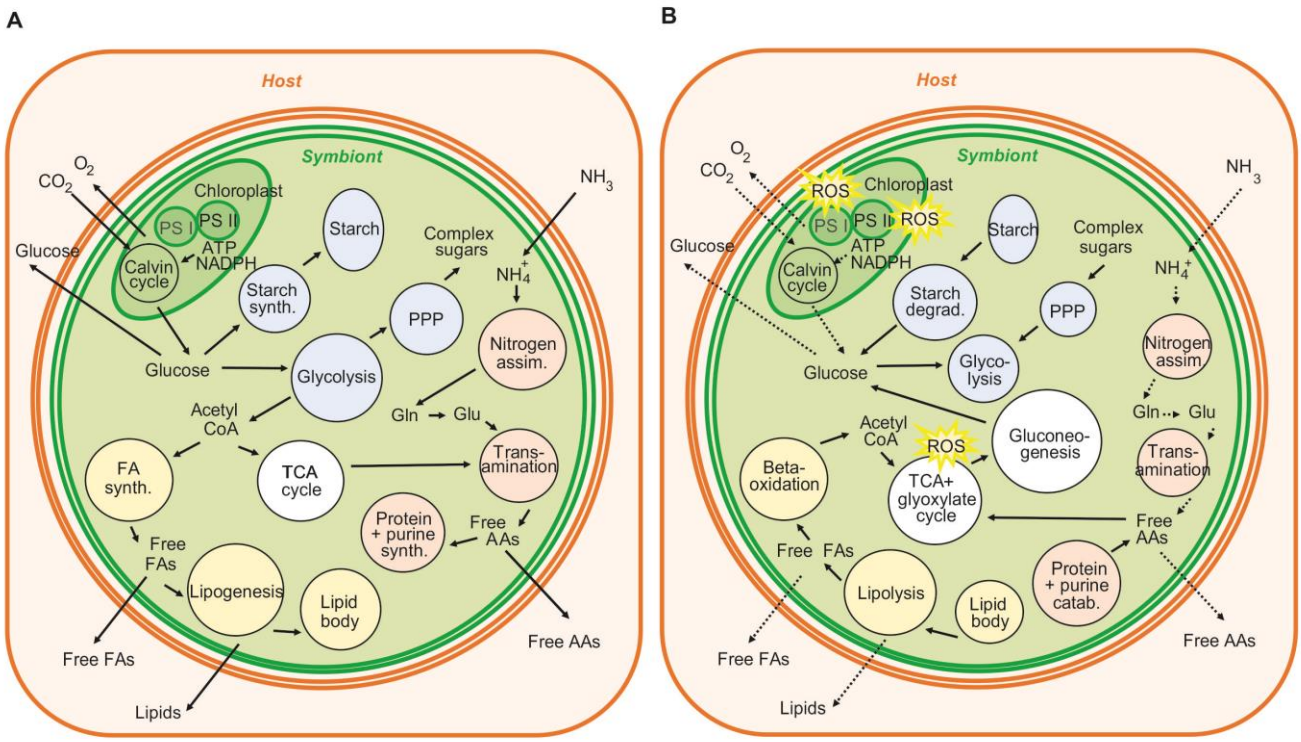

Fig. 2.10: Summary of major metabolic pathways in the dinoflagellate symbiont during photosynthetic conditions and functional symbiosis (A) and potential modifications during thermal stress and photoinhibition (B). Dotted lines denote a reduction in associated pathway activity. PPP Pentose phosphate pathway.

2.4.1 Changes to specific metabolite groups and pathways in response to heat stress

Fatty acids

Fatty acids and lipids are synthesised *de novo* by ligation of acetyl-CoA, *via* the action of elongase enzymes (Tumanov et al., 2015a). Synthesis pathways vary between species, and autotrophic and heterotrophic organisms have different abilities to produce specific fatty acid groups (Dunn et al., 2012; Leal et al., 2013). Fatty acids and lipids play major roles in the functional cnidarian-dinoflagellate symbiosis, acting directly in the primary metabolism of both partners and mobile compound exchange between partners (Patton et al., 1977; Kellogg and Patton, 1983; Imbs et al., 2014; Kopp et al., 2015). As major energy stores in the dinoflagellate symbiont, lipid and fatty acid pools are also indicative of carbon to nitrogen ratios (C:N), cell proliferation and the status of on-going nitrogen

assimilation (Wang et al., 2013; Jiang et al., 2014) (**Fig. 2.10**). Free fatty acid pools also function in cellular homeostasis, with highly conserved roles in membrane structure, function and cell signalling (Díaz-Almeyda et al., 2011; Dunn et al., 2012). Correspondingly, in the present study a high diversity and abundance of free SFAs, MUFAs and PUFAs were detected in the free fatty acid pools of both partners, in ambient and heat stressed conditions. Under ambient conditions, many of these compounds were found at relatively high abundance in both partners (C16_0, C18_0, C18_1), although the relative contributions of individual compounds differed in each partner (e.g. C22_2:C22_5 ratio). Multiple fatty acids (primarily DHA, C22_6n) were also detected in host pools that are characteristic of the mobile products of the dinoflagellate symbionts (Dunn et al., 2012; Kneeland et al., 2013), and *vice versa* (DPA, C22_5n) (Imbs et al., 2014).

A large reduction (ca. 25%) in the maximum quantum yield of PS II, suggests a significant degree of photoinactivation and/or photoinhibition in the dinoflagellate symbiont (Warner et al., 1999; Hill et al., 2004). Photoinhibition will likely result in a net reduction in the generation of cellular energy (ATP and NADPH) and an increase in ROS production in the dinoflagellate (Jones et al., 1998; Smith et al., 2005). This will impact the free fatty acid pools of both symbiont and host in a number of complex ways. Firstly, there will be a shift in metabolic modes from those which generate, rather than consume ATP. One such important mechanism for energy generation is gluconeogenesis, where energy stores are catabolised to produce ATP. Lipids are broken down *via* beta-oxidation to produce acetyl-CoA, which is in turn fed into the TCA cycle generating ATP (Grottoli and Rodrigues, 2011; Imbs and Yakovleva, 2012) (see organic acids below). Although total lipids, which comprise the entirety of lipid stores were not analysed, free pools of polar and semi-polar fatty acids comprise a major fraction (Imbs and Yakovleva, 2012; Jiang et al., 2014). Associated with photoinhibition and this energy deficit, a negative trend in pools of a number of SFAs was detected in the symbiont (C12_0 and C14_0). As both fatty acids are commonly associated with lipid stores of *Symbiodinium* (Patton et al., 1977; Kellogg and Patton, 1983), these relative reductions may be indicative of increased turnover and/or a decline in fatty acid elongation and lipogenesis in the heat stressed symbiont.

A decline in *de novo* lipogenesis pathways, which consume ATP and a reduction in downstream translocation of these mobile products to the host would also be expected under thermal stress and photoinhibition (Papina et al., 2007; Imbs and Yakovleva, 2012) (**Fig. 2.10**). Correspondingly, accumulations of multiple long-chain PUFA intermediates were detected in symbiont FA pools. Concomitantly, in host pools reductions of multiple long-chain PUFAs were detected, which are considered characteristic of symbiont-derived mobile products (such as DHA) (Papina et al., 2003; Kneeland et al., 2013). In the host a trend of increased activity of the TCA cycle and the production of acetyl-CoA was also estimated, consistent with a decline in mobile product translocation and an increase in the activity of this energy-generating network (Papina et al., 2007; Imbs and Yakovleva, 2012). An additional explanation for the observed accumulations in symbiont pools, is translocation of host-derived PUFAs (Imbs et al., 2014). Host-derived compounds include the long-chain PUFAs DPA (C22_5n) and linoleic acid (C18_2n) and the SFA arachidic acid (C20_0), all of which were also detected in symbiont pools in the present study. Interestingly, symbiont pools of DPA were also elevated with thermal stress, indicative of either a reduction in its metabolism and/or increased translocation of this compound during thermal stress.

A reduction in electron transport rate within the symbiont chloroplast as a result of photoinactivation and/or photoinhibition will also necessitate an alternative sink for electrons; a major mechanism in *Symbiodinium* is *via* the Mehler reaction (Reynolds et al., 2008; Roberty et al., 2014). This pathway in turn produces high levels of cellular ROS, in the form of relatively persistent hydrogen peroxide, which can result in damage to the lipid bilayer of cell membranes (Tchernov et al., 2004). PUFAs in particular are considered sensitive to both peroxidation and photo-oxidation (Tchernov et al., 2004; Papina et al., 2007). During prolonged oxidative stress, where antioxidant defences are overwhelmed, there will be increased oxidation of PUFAs to oxylipins, which are highly unstable and result in further damage (Gill and Tuteja, 2010). As a result, many oxylipins function as conserved messenger molecules in stress signalling, programmed cell death and defence responses (Savchenko et al., 2010). More specifically, the eicosanoid pathway (of which C20_4 is a major substrate) functions in this stress-signalling cascade, a process also recently described in the soft coral *Capnella imbricata* (Lõhelaid et al., 2015). The

observed reductions of C20 PUFAs in host pools can therefore be considered indicative of prolonged oxidative stress and highlight the possibility that oxylipin-based signalling cascades may also operate in *Aiptasia*.

Increased saturation of the cell lipid bilayer functions in thermal acclimation directly and indirectly, by increasing stability and protecting it against damage by ROS (Pearcy, 1978; Tchernov et al., 2004; Papina et al., 2007). A positive trend in the pools of the major SFAs C16_0 and C18_0 was detected, in addition to C18_1 in both partners. However, with the methods applied it was not possible to establish if these changes were associated with modifications to cell membranes, or simply a reflection of altered fatty acid metabolism, or a combination of the two. Increasing membrane saturation is energetically costly, however, consuming ATP to break and re-form lipid structures; it may also be dependent on cell-type (Díaz-Almeyda et al., 2011). In contrast, relatively thermally resistant *Symbiodinium* types may actively increase pools of PUFAs (Díaz-Almeyda et al., 2011). As the process of fatty acid desaturation is also in itself an aerobic reaction, desaturation, elongation and isomerisation may simultaneously reduce cellular oxidative stress and reduce peroxidation, thereby providing an additional mechanism for membrane stabilization (Guerzoni et al., 2001; Díaz-Almeyda et al., 2011). However, as PUFAs are in themselves susceptible to peroxidation by ROS, this response will only be effective as long as antioxidant responses are maintained. In agreement with Díaz-Almeyda et al. (2011), elevated pools of multiple PUFAs in the symbiont were detected following exposure to thermal stress. The homologous *Symbiodinium* type in the present study (B1) has previously been shown to be moderately robust to thermal and oxidative stress (Wietheger et al., 2015), and a similar mechanism may therefore operate in this symbiont. This process of PUFA accumulation is also common in dinoflagellates under nitrogen limitation, as C:N ratios become elevated, and may therefore also be indicative of reductions in nitrogen assimilation (see amino acids below) (Wang et al., 2015).

Amino acids

Amino acids pools not only function in biosynthesis, growth and respiration *via* gluconeogenesis, but their exchange as mobile compounds is also thought to play a role in maintaining the functional symbiosis (Livingstone, 1991; Wang and Douglas,

1999; Butterfield et al., 2013). Inorganic nitrogen is directly assimilated in both symbiont and host from ammonium and nitrate (Miller and Yellowlees, 1989; Pernice et al., 2012). Nitrate must first however be reduced by nitrate reductase, a process using reduced ferredoxins (Fd) from the photosynthetic transport chain, or NAD(P)H (in non-photosynthetic organisms) (Dagenais-Bellefeuille and Morse, 2013). Ammonium is then assimilated *via* the glutamine synthetase/glutamine:2-oxoglutarate aminotransferase (GS/GOGAT) cycle (Pernice et al., 2012). In this cycle, ammonium is added to glutamine (Gln) to produce glutamate (Glu), consuming ATP, Glu is then reduced back to Gln with either reduced-Fd, or NAD(P)H (Dagenais-Bellefeuille and Morse, 2013). The abundance of Glu and Gln can therefore serve as a sensitive indicator of nitrogen assimilation in the symbiosis (Pernice et al., 2012) (**Fig. 2.10**). The capacity to assimilate nitrogen in this way is present in both symbiont and the host, however the process is much more rapid in the dinoflagellate (Swanson and Hoegh-Guldberg, 1998; Pernice et al., 2012). Following assimilation by the symbiont, synthesised amino acids will therefore have a number of fates, where they may be: (1) used in the production of other amino acids and proteins; (2) directly metabolised *via* the TCA cycle (see organic acids below); (3) translocated to the host; or (4) metabolised in the purine pathway (Wang and Douglas, 1999; Pernice et al., 2012).

Thermal stress resulted in a number of changes to the amino acid pools of both symbiont and host, reflecting modifications to the activity of nitrogen assimilation and the downstream fate of assimilated compounds. Firstly, Glu accumulated in symbiont pools (and to a lesser extent in pools of the host). As nitrogen assimilation consumes ATP and requires reduced-Fd, photoinhibition is likely to result in a decline in the activity of this process, with the accumulation of the non-reduced intermediate Glu in symbiont pools as a result. Accumulations in symbiont pools of numerous other amino acid groups were also detected, these included isoleucine and valine, which under functional conditions are thought to be synthesised by the symbiont and translocated to the host (Wang and Douglas, 1999). Accumulations of these amino acids are therefore once again likely to be indicative of a reduction in the activity of ATP consuming biosynthesis pathways, such as transamination and protein synthesis and of declines in downstream mobile product translocation to the host,

coupled to increases in ATP generating pathways such as the breakdown of proteins during gluconeogenesis (Wang and Douglas, 1998; Whitehead and Douglas, 2003).

Of note was the accumulation of thiols, or the sulphur-containing amino acids, cysteine and methionine, in the symbiont pools with heat stress. This group has a number of highly conserved secondary functions, which include acting as ROS scavengers and redox sensors (Mayer et al., 1990), and may therefore perform a similar function in the symbiont under thermal and oxidative stress.

Organic acids, intermediates and antioxidants

Organic acids and pathway intermediates play essential roles in central metabolic pathways, including the TCA cycle, glycolysis, oxidative phosphorylation, the pentose phosphate pathway and gluconeogenesis (Livingstone, 1991; Ganot et al., 2011; Butterfield et al., 2013). They also have important functions in the production of co-enzymes, antioxidants, and as signalling molecules (Kruger et al., 2011). Heat treatment induced changes in these pools in both partners of the symbiosis. Most notably, increases of intermediates linked principally to glycolytic pathways and pyruvate metabolism were observed, in both symbiont and host. In glycolysis, glucose is broken down into pyruvate, which is eventually fed into the TCA cycle to generate energy (ATP) (Fernie et al., 2004). In the symbiont, reductions in pathway activities linked to modes of carbohydrate metabolism are likely to reflect the downstream results of photoinhibition (Lesser, 1997). Declines in the host would further imply that, under heat stress, carbohydrate pools were also diminished, most likely because of reduced translocation from the symbiont (Clark and Jensen, 1982; Loram et al., 2007) (**Fig. 2.10**).

However, in the host fraction reductions in pools of intermediates linked to other aspects of central metabolism were also detected, namely the TCA cycle and oxidative phosphorylation, suggesting increased turnover of these networks. These shifts are likely due to the ongoing energetic costs associated with maintaining homeostasis under elevated temperature, such as modifications to the structure of cell membranes, which in turn necessitate the generation of energy from alternate pathway modes (as discussed above) (Coles and Jokiel, 1977; Clark and Jensen, 1982), such as *via* gluconeogenesis and beta-oxidation, in the breakdown of proteins and lipids (Lehnert et al., 2014).

Also of note was the accumulation of nicotinamide in both partners (**Fig. 2.3**). This compound is the precursor to the essential coenzymes nicotinamide adenine dinucleotide (NAD) and nicotinamide adenine dinucleotide phosphate (NADP). These coenzymes facilitate many oxidation and reduction reactions in living cells, which include linking the TCA cycle and oxidative phosphorylation (Berglund and Ohlsson, 1995). In *Symbiodinium*, as in other primary producers, $NADP^+$ is a major acceptor of electrons in PS I (Takahashi and Murata, 2008). In higher plants, nicotinamide has been identified as a signal molecule of DNA damage and oxidative stress, which facilitates a number of defence-related metabolic reactions (Berglund, 1994; Berglund and Ohlsson, 1995). A similar defence and signalling mechanism may also function in the cnidarian-dinoflagellate symbiosis, though this awaits confirmation. In addition, pools of the antioxidant compound glutathione were elevated in both partners. Glutathione is a tripeptide antioxidant that serves as an important electron donor during oxidative stress in *Symbiodinium* (Lesser, 2006; Krueger et al., 2014) and in the cnidarian host (Downs et al., 2002; Desalvo et al., 2008; Sunagawa et al., 2008), consistent with the findings of this study.

2.5 Conclusions

Free metabolite pools and mobile compound exchange between symbiotic partners are essential to the functional cnidarian-dinoflagellate symbiosis. Primary metabolites function directly in central metabolism, and in cellular acclimation and homeostasis. Prolonged exposure to elevated temperatures above critical temperature thresholds results eventually in symbiont photoinhibition, bleaching and distinct changes in the metabolite profiles of both symbiont and host. These modifications are associated with declines in carbon fixation, altered metabolic mode, declines in mobile product translocation, and acclimation responses to thermal and oxidative stress. These data provide further insight into the differing cellular responses of symbiont and host to these abiotic stressors during bleaching in a model system for reef-building corals. The outputs of this study also generate a number of hypotheses that warrant further study. For instance, the roles of free metabolite pools in stress signalling cascades and signal transduction, within and between partners. This study also highlights the need for further investigation into

the primary metabolic networks of both partners in the symbiosis, where major gaps still remain.

2.6 The application of metabolomics to coral reef studies

Clearly a major strength of metabolomics-based techniques lies in the capacity to simultaneously detect subtle changes in a large variety of small compounds, with little *a priori* knowledge of the metabolite pools under investigation. As these pools have important and conserved roles in respiration, growth, cellular homeostasis and signalling, quantitative insight can be gained into the activity of these networks. However, in many cases direct evidence from the cnidarian-dinoflagellate symbiosis is still lacking and further targeted studies are therefore required to test the roles of many compounds in the cellular responses of both partners. For instance, a more in-depth understanding of the cell-signalling network is essential, if we are to better understand how the holobiont detects, communicates and responds to stress. These data may also prove useful in the development of metabolite markers of thermal and other abiotic stressors that can be used for monitoring of the symbiosis and of coral reef systems. Further studies that apply high-resolution visualisation of metabolite pools, such as nanoscale secondary ion mass spectrometry (NanoSIMS), coupled with stable isotope tracers will serve to provide further insight into the potential roles of free metabolites in differing compartments of the holobiont. These data, coupled with the ongoing outputs from rapidly developing ‘omics’ studies (genomics, transcriptomics, proteomics and metabolomics) will aid in further elucidating the metabolic cross-talk both within and between partners, which is essential for maintaining the functional holobiont.

Chapter 3 Metabolite profiling of symbiont and host during thermal stress and bleaching in the coral *Acropora aspera*

3.1 Introduction

Reef-building corals are formed by a complex intracellular symbiosis between dinoflagellate algae (genus *Symbiodinium*) and cnidarian host. In symbiosis, the algae are encapsulated in a host-derived membrane, the symbiosome, located within host gastrodermal cells (Wakefield and Kempf, 2001). The successful persistence of this complex partnership is based on the bi-directional exchange of nutrients, principally inorganic, from host to algae (dissolved inorganic carbon (DIC), dissolved inorganic nitrogen (DIN) and phosphorus) and organic from algae to host (carbohydrates, amino acids and lipids) (Muscatine and Hand, 1958; Yellowlees et al., 2008; Davy et al., 2012). Translocation mechanisms between partners are thought to include membrane-bound active transporters (such as ABC transporters), aided *via* enzymes (carbonic anhydrases and H^+ ATPase) and a proton gradient across the symbiosome membrane (Peng et al., 2010; Barott et al., 2015). In addition, a specific suite of associated microbes is also thought to contribute to these nutritional interactions, forming the coral 'holobiont' (Rohwer et al., 2002; Rosenberg et al., 2007). Under suitable conditions, this efficient exchange of mobile compounds within the coral holobiont drives photosynthesis and nitrogen assimilation in the symbiont, and fuels growth, calcification and successful reproduction in the host (Muscatine and Cernichiari, 1969; Yellowlees et al., 2008).

The coral symbiosis is, however, increasingly under the influence of thermal stress, associated with rising seawater temperatures (Hoegh-Guldberg, 1999; Hughes et al., 2003). Prolonged exposure to elevated temperature results in increased damage to the machinery of photosystem II (PS II) in the symbiont chloroplast, principally at the D1 protein and thylakoid membranes (Lesser, 1996; Warner et al., 1999; Takahashi and Murata, 2008). Eventually, repair mechanisms are inhibited and overwhelmed, leading to declines in carbon fixation (photoinhibition) (Murata et al., 2007; Takahashi and Murata, 2008). During photoinhibition, a variety of potentially damaging reactive oxygen species (ROS) are overproduced, principally at energy-generating sites, such as PS I and II, mitochondria, and the electron transport chain (Dat et al., 2000; Lesser, 2006). However, during thermal- and light-stress, the main

source of ROS production in the symbiont is associated with alternative electron transport flows, which divert excess energy away from the chloroplast during the Mehler reaction (Jones et al., 1998; Roberty et al., 2014). Additionally ROS are produced at a number of cell sites, such as the mitochondria and microbodies during cellular respiration (Lesser, 2006), turnover of which is enhanced in both partners during thermal stress (Jokiel and Coles, 1990). As charged molecules, most species of ROS are unable to permeate the lipid bilayer, and they therefore accumulate at sites of ROS production, causing lipid peroxidation, DNA damage and modifications to cellular proteins (Lesser, 2006; Gill and Tuteja, 2010). Eventually, increased cell death will occur *via* mechanisms such as necrosis and apoptosis (Dunn et al., 2004; Weis, 2008). In corals, this prolonged thermal stress will result eventually in dysfunction of the symbiotic relationship and the loss of algal cells *via* coral bleaching (Weis, 2008). Prolonged, severe and repeated bleaching episodes have major impacts on the resilience of coral reefs, and have principally driven major losses in live coral globally (Hoegh-Guldberg, 1999; Hughes et al., 2003).

Photoinhibition will also lead to modifications in central metabolism and mobile compound exchange between symbiotic partners (Clark and Jensen, 1982; Smith et al., 2005). Declines in carbon fixation will necessitate the generation of energy from alternative sources in the symbiont, leading to increases in the turnover of alternative networks and a net reduction in the biosynthesis of end products for translocation to the host (Clark and Jensen, 1982; Jokiel and Coles, 1990). Correspondingly, the host must meet the deficit of increased energetic costs associated with maintaining homeostasis, with an increase in heterotrophy, and the catabolism of lipid and protein stores (Grottoli et al., 2004; Grottoli et al., 2006). Free metabolite pools will also play an important role in maintaining cellular homeostasis in both symbiotic partners, primarily as antioxidants (sulphur-containing amino acids, organic acids and vitamins) and as compatible solutes (polyols, sugar alcohols) (Brown, 1997a; Lesser, 2006; Baird et al., 2009a). In addition, a number of compounds (oxylipins and oligosaccharins) are known to function in combination with ROS, as highly conserved cellular-damage signals in a range of systems (Field, 2009; Brosché et al., 2010; Lõhelaid et al., 2015). Similarly, free metabolite pools will also function as intermediates in the *de novo* production of secondary compounds central to cellular acclimation, such as heat shock proteins (HSPs), fluorescent proteins, hormones

and pigments (carotenoids and mycosporine-like amino acids) (Lesser, 2006; Baird et al., 2009a; Gill and Tuteja, 2010). However, major gaps remain in our understanding of this metabolic network in the coral holobiont. Insufficient data in the 'omics' fields (genomics, transcriptomics, proteomics and metabolomics) from the cnidarian-dinoflagellate symbiosis also impede the identification of pathways and small compounds, which likely play important roles in these metabolic responses. Greater knowledge of the cellular mechanisms invoked in each partner during acclimation, enhanced thermal resistance and therefore long-term resilience of the symbiosis are also essential, if we are to better understand how the symbiosis will persist into the future.

Comparative and quantitative GC-MS based metabolomics allow the rapid, repeatable and low-cost detection of multiple small compounds in a single sample (Villas-Bôas et al., 2005). The majority of these compounds are primary metabolites, which are readily identifiable by this method and have highly conserved roles in cellular metabolism and homeostatic networks (Wahid et al., 2007; Guy et al., 2008). As such, it is possible to rapidly detect, identify and quantify changes in these compounds and the activity of associated pathways in response to a given stressor (Viant, 2007). An additional strength of this untargeted process is the capacity to detect changes to compounds and networks, which may warrant further investigation in the coral holobiont. The focus of this study was to identify and quantify compounds in the free pools of the dinoflagellate symbiont (*Symbiodinium* ITS 2 type C3) and its host, the common reef-building coral *Acropora aspera*, that are responsive to thermal stress, and early- and late-phase coral bleaching. The outputs of this study therefore provide further insight into the cellular mechanisms invoked by each partner during exposure to these conditions and the associated energetic costs. These data also further our understanding of the roles of metabolic networks in a number of a key aspects, such as the maintenance of cellular homeostasis, damage signalling and signal transduction in the coral holobiont.

3.2 Materials and Methods

3.2.1 Collection and maintenance of specimens

Fragments (a maximum of 8 cm in length) of the coral *Acropora aspera* (light blue colour morph) were collected from Heron Island reef flat (Great Barrier Reef (GBR), Australia; 23°26'43"S, 151°54'53"E) at low tide under GBR Marine Permit G14/36933.2 between 27th-29th March 2015. Fragments (*n* = 9 per colony) were sampled from the unshaded upper branches of six replicate colonies (in total amounting to no more than 5% of the donor colony). Replicate colonies were separated by a minimum of 10 m to increase the likelihood of sampling different host genotypes.

Replicate fragments were mounted using light-diffusing egg-crate and acclimated for 10 days in four experimental aquaria (60 L). Continuous seawater flow-through (ca. 4 L min^{-1}) was provided from Heron Island reef flat. Aquaria were covered with shade cloth to reduce midday irradiance (ca. 500-1500 µmol photons m^{-2} s^{-1}). Additional water movement was provided in each aquarium by small submersible pumps.

Following acclimation, two aquaria were heated to 32°C ± 1°C, at a rate of 1°C *per* day. The treatment temperatures were maintained for a period of 8 days during daylight hours, but allowed to cool to 28°C ± 1°C overnight in order to more closely represent natural bleaching conditions of the reef flat (http://data.aims.gov.au/). Two aquaria were left at the ambient temperature of 27°C ± 3°C. Light and temperature data in each tank were recorded every 10 min by HOBO data loggers (Onset Computer Corporation, Bourne, MA, USA).

Daily measurements of maximum (dark-adapted) quantum yields of the efficiency of PS II were taken using pulse amplitude modulation fluorometry (Diving-PAM, Walz, Effeltrich, Germany). Maximum yields were taken 30 min after last light. Presented values are based on means of triplicate measurements taken from each colony representative (*n* = 6, one per colony, *per* treatment) designated for PAM sampling. PAM settings were maintained over the course of the experiment at: measuring light 4, saturation intensity 4, saturation width 0.6 s, gain 1 and damping 2, with the use of the measuring-light burst function. Measurements were taken at a standard distance of 5 mm from each sample.

3.2.2 Sampling for metabolite analysis

One fragment *per* colony was sampled from the ambient treatment at 0 d, after which one fragment *per* colony *per* treatment was sampled at two time-points, at 6 d and 8 d of exposure to treatment temperatures. Sampling was undertaken just before midday on each sampling day. Sampling involved the removal of individual nubbins from mounts and immediate immersion in liquid nitrogen This process was completed in less than 5 s. Samples were then immediately transferred for storage in a -80^{o}C freezer, until transport *via* dry shipper to the University of Melbourne for fragment processing.

3.2.3 Fragment processing

Tissue was removed from the coral fragments *via* airbrush into 50 mL of chilled MilliQ ultrapure water (MQ) at 4°C, in a 4°C environment. The tissue suspensions were then homogenised with a saw-tooth homogeniser (Ystral D-79282, Ballrechten-Dottingen, Germany) for 10 s at a mid-speed setting.

Three 1 mL aliquots were removed for *Symbiodinium* cell counts, photosynthetic pigment analysis and dominant *Symbiodinium* genotyping. The remaining tissue homogenate was centrifuged (2,500 x *g* for 5 min at 4°C) to separate *Symbiodinium* cells from the host material.

The supernatant comprising the host material was removed and re-centrifuged to pellet any remaining algal material (2,500 x *g* for 5 min at 4°C). The resulting supernatant, comprising the purified host material, was then immediately frozen at -80°C and freeze-dried (Alpha 1-4 LD Plus, Martin Christ, Osterode am Harz, Germany). The *Symbiodinium* pellet was washed twice with chilled MQ at 4°C, by repeated centrifugation (2,500 x *g* for 5 min at 4°C), to remove host material. The purified pellet was then frozen at -80°C and freeze-dried. Once fully dry, each fraction was weighed out (15 mg of symbiont fraction and 30 mg host fraction) into 1.5 mL microcentrifuge tubes, ready for metabolite extraction.

3.2.4 Intracellular metabolite extraction

For host samples, 750 µL of 100% cold MeOH (at -20°C) were added to extract the semi-polar metabolites. Methanol contained internal standards (IS) of 1% D-Sorbitol-1-^{13}C (Sigma-Aldrich, Auckland, New Zealand). Samples were then sonicated for 30

min at 4°C, vortexed to mix, and the semi-polar extract separated from the tissue debris *via* centrifugation (3,060 x *g* for 30 min at 4°C).

For algal samples, lysis of the *Symbiodinium* cell wall was achieved *via* bead-milling. Acid-washed glass beads (approximately 20 mg of 710–1,180 µm; Sigma-Aldrich, Auckland, New Zealand) and 200 µL of 100% cold MeOH (at -20°C) were added to each sample. Bead-milling (Tissuelyser II, Qiagen Inc., Hilden, Germany) was for 4 min at a frequency of 30 Hz. Visual counts (haemocytometer) of trial samples confirmed cellular disruption (over 90% of cells). A further 550 µL of 100% cold MeOH (plus IS at -20°C) were then added to each sample. The samples were then centrifuged (3,000 x *g* for 30 minutes at 4°C) to separate the semi-polar extract from the cell debris. The supernatants were collected and stored on ice.

For both host and symbiont samples, a second extraction of the cell debris was then undertaken with 750 µL 50% MeOH (at -20°C), in order to extract the polar fraction. The samples were vortexed to mix and re-centrifuged (3,000 x *g* for 30 minutes at 4°C). The supernatant, comprising the polar fraction, was removed and the polar and semi-polar extracts were combined and centrifuged at 21,200 x *g* for 5 min at 4°C to precipitate any particulates. Aliquots of each sample (200 µL of host and 150 µL of symbiont) were then concentrated *via* speedvac (Christ, RVC 2-33, John Morris Scientific, Melbourne, Australia) at 30°C until fully dry.

3.2.5 Calibration standard sample preparation

Calibration standards were prepared following the methods described in Dias et al. (2015). Twenty-eight sugars, sugar phosphates, sugar acids, and sugar alcohols, as well as twenty organic acids were purchased from Sigma–Aldrich (Australia). Stock solutions at 10 mM concentration were prepared for each individual standard except for 2-ketogluconic acid, for which a 2 mM stock solution was prepared. Aliquots (160 µL) of each sugar standard were subsequently pooled to reach a final volume of 4.48 mL. A 520 µL aliquot of 50% aqueous mixture of methanol was then added to the pooled sugar standards, resulting in a final volume of 5 mL and final concentration of 320 µM. For organic acids, 160 µL of each standard was subsequently pooled to reach a final volume of 4.16 mL, and a 840 µL aliquot of 50% aqueous mixture of methanol was then added, resulting in a final volume of 5 mL and a final concentration of 320 µM. The stock solutions were serially diluted with

50% aqueous mixture of methanol resulting in the following calibration series: 320,160, 80, 40, 20, 10, 5, 2.5, 1.25 and 0.625 µM calibration points for 2-oxoglutarate, aconitate, erlose, ferulic acid, fumarate, malate, maleate, malonate, melezitose, pipecolate, raffinose, salicylate, succinate and xylose; 160, 80, 40, 20, 10, 5, 2.5, 1.25 and 0.625 µM. Calibration points for 2-keto gluconic acid, arabinose, arabitol, β-gentiobiose, caffeic acid, citrate, erythritol, fructose, fructose-6-phosphate, fucose, galactitol, gluconate, glucose, glucuronate, itaconate, inositol, isocitrate, maltose, mannitol, mannose, melibiose, quinate, rhamnose, ribose, sucrose, syringic acid, trehalose, turanose, uric acid, xylitol; 80, 40, 20, 10,5, 2.5, 1.25 and 0.625 µM calibration points for galactose; and 160, 80, 40, 20, and 10 µM calibration points for nicotinic acid, shikimate and glucose-6-phosphate. Of each calibration stock, 40 µL were transferred into glass vial inserts, dried *in vacuo*, and stored at −20°C before subjecting to GC–*QqQ*–MS analysis.

3.2.6 Online derivatization

All samples were re-dissolved in 20 µL of 30 mg mL^{-1} methoxyamine hydrochloride in pyridine and derivatized at 37°C for 120 min with mixing at 500 rpm. 20 µL *N,O-bis*-(trimethylsilyl)trifluoroacetamide (BSTFA) and 1 µL retention-time standard mixture [0.029% (v/v) *n*-dodecane, *n*-pentadecane, *n*-nonadecane, *n*-docosane, *n*-octacosane, *n*-dotriacontane, *n*-hexatriacontane dissolved in pyridine] were then added and the samples incubated for a further 30 min with mixing at 500 rpm. Each derivatized sample was then allowed to rest for 60 min prior to injection into the GC-MS.

3.2.7 GC-MS analysis for the comparative data set

GC-MS analysis was performed on an Agilent 7890 gas chromatograph equipped with Gerstel MPS2 multipurpose sampler and coupled to an Agilent 5975C VL mass selective detector, run in splitless mode, with an injection volume of 1 µL of each sample and a technical replicate of two injections *per* sample. Instrument control was performed with Agilent G1701A Revision E.02.01 ChemStation software. The gas chromatograph was fitted with a Varian Factor 4 column (VF-5ms; 30 m × 0.25 mm × 0.25 um + 10m Ezi-guard). Helium (Ultra High Purity) was in constant flow mode at approximately 1 mL min^{-1} with retention-time locking (RTL) applied. The oven temperature was started at 70°C, held at this temperature for 1 min and then increased at 7°C min^{-1} to 325°C, and finally held at this temperature for 3.5 min.

The mass spectrometer quadrupole temperature was set at 150°C, with the source set at 250°C and the transfer line held at 280°C. Positive ion electron impact spectra at 70eV were recorded in scan mode with the following settings: a gain factor of 1.00, detector threshold of 150, mass to charge (*m/z*) range of 50-600 *m/z* and solvent delay of 6.0 min.

3.2.8 GC-MS analysis for the quantitative data set

Samples (1 µL) were injected into a GC–*QqQ*–MS system comprising of a Gerstel 2.5.2 Autosampler, a 7890A Agilent gas chromatograph and a 7000 Agilent triple-quadrupole MS (Agilent, Santa Clara, USA) with an electron impact (EI) ion source. The GC was operated in constant pressure mode (20 psi), with helium as the carrier gas and mannitol as a standard for RTL of the method. The MS was adjusted according to the manufacturer's recommendations using *tris*-(perfluorobutyl)-amine (CF43). A J & W Scientific VF-5MS column (30 m long with10 m guard column, 0.25 mm inner diameter, 0.25 µm film thickness) was used. The injection temperature was set at 250°C, the MS transfer line was set at 280°C, the ion source was adjusted to 250°C and the quadrupole was set at 150°C. Helium was used as the carrier gas at a flow rate of 1 mL min^{-1}. Nitrogen (UHP 5.0) was used as the collision-cell gas at a flow rate of 1.5 mL min^{-1}. Helium (UHP 5.0) was used as the quenching gas at a flow rate of 2.25 mL min^{-1}. The following temperature series program was used: injection at 70°C; hold for 1 min; 7°C min^{-1} oven temperature ramp to 325°C; final 6 min heating at 325°C.

3.2.9 Data analysis and validation

Metabolite data extraction and analysis were undertaken based on the protocol described in Dias et al. (2015), with the software package MetaboAnalyst 3.0 (Xia et al., 2015). Data were processed using the Agilent MassHunter Workstation Software, Quantitative Analysis, Version B.05.00/Build 5.0.291.0 for quantitation of all compounds. Compound identification was based on an in-house library of MS spectra, with retention indices based on n-alkane and fatty acid standards (Menhaden fish oil, Sigma-Aldrich, Auckland). Derivative peak areas were used to semi-quantify the concentrations of individual metabolites in the comparative data set. Data were then normalized to the final area of the internal standard and sample dry weight.

Data were tested for normality and homogeneity, and log transformed where appropriate. IBM SPSS Statistics (v22) was used for both repeated-measures ANOVA (RMANOVA) and ANOVA. RMANOVA was used to test for differences in maximum quantum yields between treatment groups and days (repeat measurements were from the same individuals, which were set aside in each treatment). ANOVA was used to test for differences in heat-stress indicators between treatments and sampling days. Statistical significance between the abundance of metabolite treatment means was determined by univariate tests (t-test, with false discovery rate, FDR) in MetaboAnalyst. Differences were considered significant at the $P < 0.05$ probability level. Fold change (FC) analysis was used to compare the absolute value change between group means, before data normalization was applied. Principal components analysis (PCA) using the normalised, log-transformed and auto-scaled metabolite data was undertaken with MetaboAnalyst. PCA analysis was used to summarize the multivariate metabolite data, capturing the variables that explained the greatest variation (principal components, PC) in each treatment group. The key-contributing metabolites, as determined by their contribution to the PCA plots, can be identified by their loadings values, as summarised in the corresponding loadings plots.

Pathway activity analysis using the Pathway Activity Profiling (PAPi) package was undertaken to compare activities using the normalized and transformed metabolite data following the methods described in Aggio et al. (2010). Briefly, using the normalized abundance data for each treatment at 6 d and 8 d as input, the PAPi package calculates activity scores of individual pathways from the Kyoto Encyclopedia of Gene and Genomes (KEGG) database. These activity scores are based on the relative changes in compounds (control *vs* treatment) associated with each pathway of interest. This algorithm is based on two main assumptions: 1) if a given pathway is active in a cell or organism, more intermediates associated with that pathway will be detected; and 2) there will be a lower abundance of associated pathway intermediates due to high turnover and *vice versa* during low activity (Aggio et al., 2010). The resulting activity score therefore serves as an indicator of the likelihood that a pathway is active within a cell, or organism under a given condition, without the requirement for absolute quantitation, such as during more detailed flux analysis. Resulting pathway activity scores were inverted to make interpretation in

plotted figures more intuitive, i.e. an increase in activity score representing an increase in the predicted pathway activity. Statistical significance between the abundance of metabolite treatment means was determined by univariate tests (t-test, with false discovery rate, FDR) in MetaboAnalyst.

3.2.10 Quantification of coral bleaching

Symbiodinium cell densities in corals were quantified using Improved Neubauer haemocytometer counts (Boeco, Germany), with a minimum of six replicate cell counts *per* sample (i.e. to a confidence interval below 10%). Cell density was normalised to coral fragment surface area, measured with the wax-dipping method (Stimson and Kinzie, 1991).

Symbiont chlorophyll *a* (chl *a*) content was quantified by N,N-dimethylformamide (DMF) extraction carried out in darkness over 48 h at 4°C. Extracts were centrifuged (16,000 x *g* for 5 min) and triplicate 200 µL aliquots were measured in 96-well plates (UVStar, Greiner Bio-One GmbH, Germany) at 646.8, 663.8, and 750 nm, using a microplate reader (Enspire_2300, Perkin-Elmer, Waltham, MA, USA). Chl *a* concentrations were determined after optical path length correction (0.555 cm) using the equations of Porra et al. (1989).

3.2.11 Identification of dominant Symbiodinium genotypes

For DNA extraction, a 200 µL aliquot of homogenate was centrifuged for 5 min at 16,100 × *g* to isolate the *Symbiodinium* cells. The supernatant was discarded and the algal cells resuspended in 200 µL guanidinium cell lysis/DNA extraction buffer (50% guanidinium isothiocyanate (w/v); 50 mM Tris (pH 7.6); 10 µM EDTA; 4.2% sarkosyl (w/v); 2.1% β-mercaptoethanol (v/v)). Following a one week incubation period at room temperature, the samples were centrifuged for 5 min at 16,100 × *g* to pellet the cellular debris, and 100 µL of supernatant were added to an equal volume of 2-propanol at 4 °C and left overnight for DNA precipitation. To collect the DNA, the samples were centrifuged for 30 min at 16,100 × *g* and the supernatant poured off. The DNA pellet was washed in 70% (v/v) ethanol, dried, and eluted in 50 µL TE buffer (10 mM Tris-HCl (pH 8.0); 1 mM EDTA).

For genetic analysis, the non-coding region of the psbA minicircle (*psbA*^{ncr}) was amplified and sequenced directly using the 7.4/7.8 primer pair (Moore et al., 2003). Since these primers preferentially amplify clade C *Symbiodinium* (LaJeunesse and

Thornhill 2011), the partial 18S/ITS region and a section of the 28S LSU rDNA were also amplified and sequenced using the generic dinoflagellate primers S-DINO and L0 (Pawlowski et al., 2000). Each end of the ~ 1600 nt amplicon was directly sequenced and compared to representative sequences from each *Symbiodinium* clade, to ensure that the dominant sequence in all samples belonged to clade C. The forward and reverse *psbA*^{ncr} sequences were manually aligned in Geneious v 7.0.6 (Biomatters Ltd) and the GenBank database was queried with the consensus sequences using the BLAST algorithm (Altschul et al., 1990).

3.3 Results

3.3.1 Symbiodinium DNA extraction and sequencing

Of the six colonies used in the study, four produced *psbA*^{ncr} sequences that were identical to a clade C3 variant found in *Acropora microclados* and *A. nasuta* at Heron Island, GBR (GenBank accession numbers JQ043641 and JQ043642; (LaJeunesse and Thornhill, 2011). The remaining two colonies hosted a *Symbiodinium* type with a *psbA*^{ncr} sequence that was 98.7% similar to the other four, but had no exact matches in the GenBank database. However, the ITS 2 region could be sequenced directly (without ambiguities) from these two colonies, and was identical to a *Symbiodinium* C3 variant previously isolated from *A. millepora* colonies at Heron Island (GenBank accession number HM031101; (Fisher et al., 2012). The dominant symbiont type of all six colonies is therefore referred to as *Symbiodinium* C3.

3.3.2 Thermal stress and bleaching indicators

Exposure to daily temperatures of 32°C ± 1°C (typical of summer maxima and ca. 5°C above ambient water temperatures of 27°C ± 3°C over the course of the study) for 6 d and 8 d, resulted in a decline in the maximum quantum yield of photosystem II (PS II), which differed with time and treatment group (RMANOVA time x treatment $F_{14,140}$ = 21.676, P < 0.001), loss of algal symbionts *per* unit area of coral, and a reduction of chl *a* symbiont cell^{-1}, consistent with photoinhibition and coral bleaching (**Fig. 3.1**). At 6 d there was a ca. 15% decline in the maximum quantum yield of PS II and a 49% reduction in *Symbiodinium* cell density (one-way ANOVA $F_{1,10}$ = 25.81 P < 0.001) (**Fig. 3.1**). At 8 d exposure to elevated temperature, there was a ca. 30% decline in the maximum quantum yield of PS II; this reduction was coupled to a 71%

reduction in *Symbiodinium* cell density relative to controls (one-way ANOVA $F_{1,10}$ = 89.86 P < 0.001). Coinciding with this decline at 8 d, there was a ca. 20% decline in symbiont chl *a* content cell^{-1} (one-way ANOVA $F_{1,10}$ = 6.44 P = 0.029) (**Fig. 3.1**). However, in terms of the progress of photoinhibition and bleaching between 6 d and 8 d, only symbiont cell density differed significantly between sampling days in the heat-treatment group (one-way ANOVA $F_{1, 10}$ = 10.166, P = 0.01).

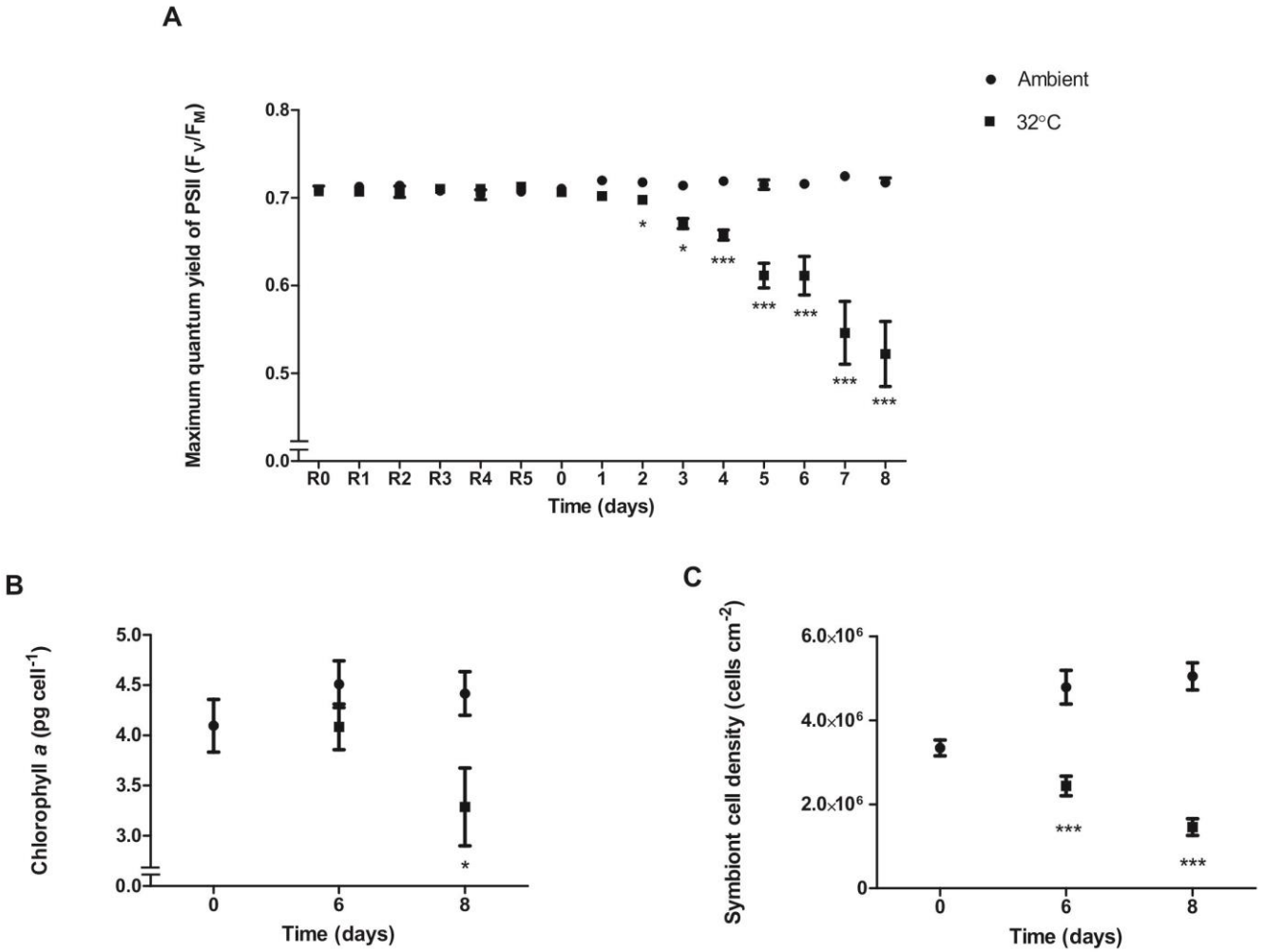

Fig. 3.1: Physiological effects of thermal stress in *Acropora aspera.* (A) Maximum quantum yields of PSII of *in hospite* symbionts versus time at ambient temperature (ca. 27°C) and elevated temperature (32°C); and (B) symbiont chlorophyll *a* content cell^{-1} and (C) symbiont cell density following 0, 6 and 8 days exposure to 32°C (n = 6). Error bars are mean ± S.E.M. R0 – R5 heat ramp for treatment group (1°C day^{-1}). * denotes $P < 0.05$, ** $P < 0.005$, *** $P < 0.001$.

3.3.3 Free metabolite pools of symbiont and host

The intracellular free metabolite pools of both the dinoflagellate symbiont and its coral host, were profiled under ambient conditions prior to the heat ramp at 0 d, and following exposure to thermal stress at 6 d and 8 d. A total of 73 and 67 compounds were identified *via* GC-MS analysis of the polar and semi-polar extracts of symbiont and host, respectively. These compounds consisted of a mixture of metabolite groups, primarily amino acids, intermediates, organic acids and amides, sugars, and fatty acids (**Table S3.1** and **Table S3.2**).

Due to the differing cell structure and composition of the symbiont and host fractions, extraction methodologies were optimized to target each fraction individually. As such, symbiont and host pools were not directly comparable. However, under ambient conditions, symbiont pools were characterised by a number of compounds that were not detectable (or present but in low abundance) in host pools and *vice versa* (**Table S3.1** and **Table S3.2**). In the symbiont, these included the saturated fatty acids (SFAs) C10:0, C12:0 and C22:0, in addition to the polyunsaturated fatty acid (PUFA) C18:3, and a number of sugar phosphates (glycerol-2-phosphate, glycerol-3-phosphate, inositol-2-phosphate), vitamins (threonate, phytol), intermediates (aspartate, glutarate) and amino acids (leucine, tyrosine). Compounds considered characteristic of host pools included a number of sugar alcohols (galactitol, threitol, myo-inositol), sugars (arabinose, iso-maltose) intermediates (tryptamine, thymidine, adenosine) and amino acids (beta-alanine, homoserine).

Although symbiont and host pools were not directly comparable, a number of fatty acids that were abundant in symbiont free metabolite pools and detected to a much lesser extent in host pools, may serve as mobile products exchanged from symbiont to host *in vivo*. Namely, the SFAs C14:0 and C16:0, and monounsaturated fatty acids (MUFAs) C16:1 and C18:1 (9-Z), and the PUFA docosahexaenoic acid (DHA) C22:6 (**Table S3.1**). In addition, a number of compounds were detected in the host extract, which may have originated *in vivo* from associated microorganisms within the host mucus, skeleton and tissues; specifically the disaccharides maltose, iso-maltose and the SFA C17:0.

3.3.4 Quantitation of key compounds

Absolute concentrations were calculated for a total of 29 key compounds (organic acids, carbohydrates and intermediates) that were detected in the free pools of symbiont and host samples at 8 d (**Table S3.3** and **Table S3.4**). The most abundant compounds in symbiont metabolite pools under ambient conditions were glucose (693.5 picomoles mg^{-1} dry weight ± 105.8 S.E.M.), galactose (533.9 picomoles mg^{-1} dry weight ± 44.1 S.E.M.) and succinate (109.1 picomoles mg^{-1} dry weight ± 13.8 S.E.M.). Similarly, in the host the most abundant compound was also glucose (2216.4 picomoles mg^{-1} dry weight ± 77.0 S.E.M.), followed by inositol (594.8 picomoles mg^{-1} dry weight ± 37.1 S.E.M.), galactose (470.7 picomoles mg^{-1} dry weight ± 46.9 S.E.M.), galactitol (420.0 picomoles mg^{-1} dry weight ± 71.7 S.E.M.) and maltose (410.9 picomoles mg^{-1} dry weight ± 34.5 S.E.M.).

3.3.5 Thermally-induced modifications to free metabolite pools

Marked modifications to free metabolite pools in response to thermal stress were observed in each symbiotic partner. These thermally-induced changes to pools of free metabolites were apparent in the spatial separation of treatment groups, relative to those at ambient water temperatures, in the PCA plots (**Fig. 3.2**). Ambient groups can be seen to cluster closely in space at each sampling point, whereas the treatment groups are separated along the axes of PC 2. This effect was greatest in both partners after 8 d of exposure to elevated temperature, and accounted for 19.4% and 14% of the data variability in symbiont and host, respectively. Compounds characteristic of this thermal stress can therefore be observed in the negative areas of loadings 2 for the symbiont and the positive areas of loadings 2 for the host (**Fig. 3.2**).

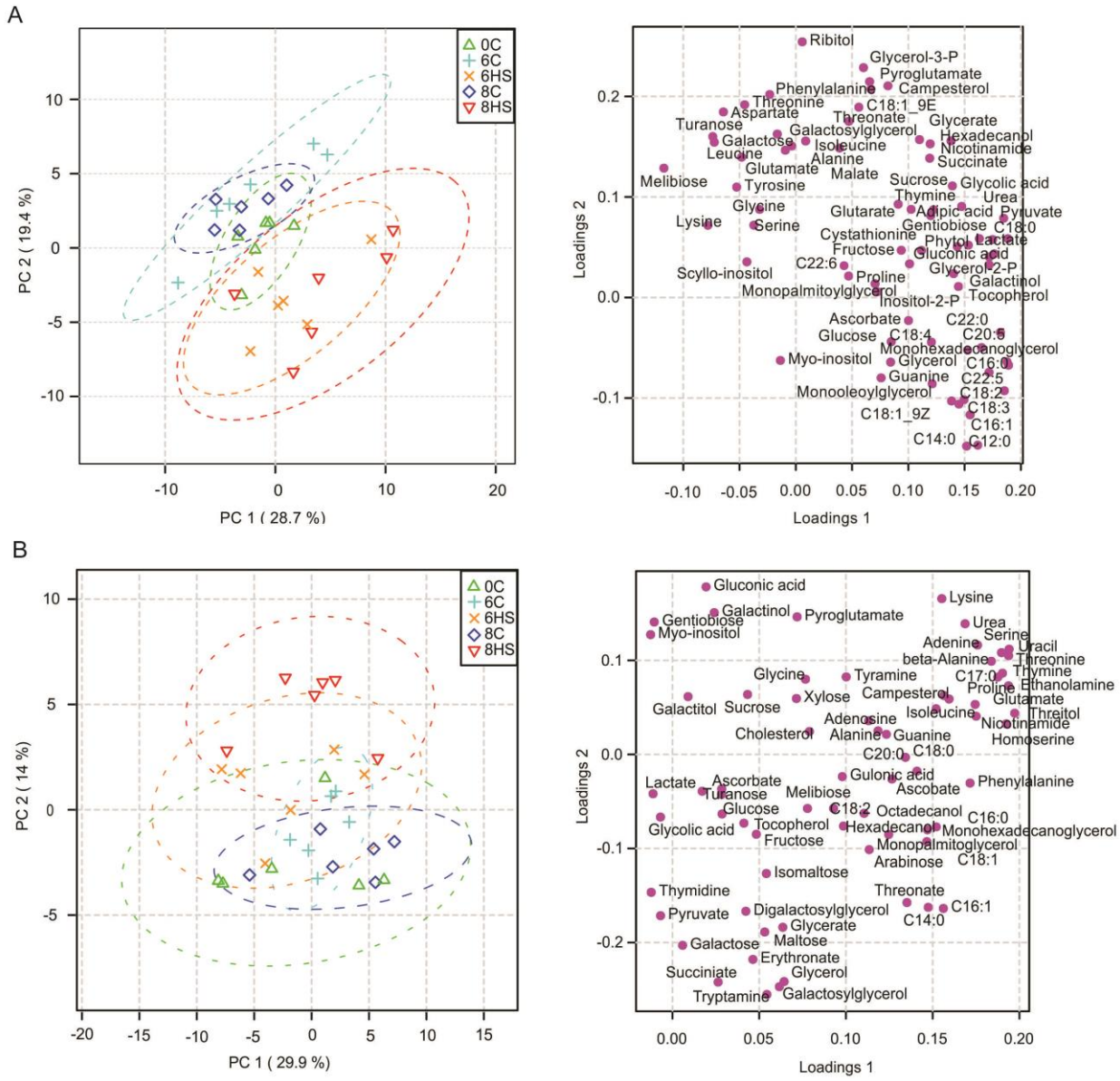

Fig. 3.2: PCA scores plot (left) and loads plot (right) of symbiont (A) and host (B) metabolite profile data. 0C: day 0 ambient; 6C: day 6 ambient; 6HS: day 6 heat stress; 8C: day 8 ambient; 8HS: day 8 heat stress (with 95% confidence regions) (*n* = 6).

At the level of individual metabolites, thermally-induced modifications to the relative abundance (ambient *versus* thermal stress) of multiple compounds were detected in both symbiont and host pools. In the symbiont, the greatest changes were associated with large accumulations (x5-10 fold changes) in the medium- and long-chain fatty acid pools, including a number of SFAs (C10:0, C12:0, C14:0, C16:0, C20:0), MUFAs (C18:1 (9Z) and C16:1) and PUFAs (C18:2, C18:3 and C22:5). In

contrast, relative reductions were observed for a number of carbohydrates, intermediates and amino acids, the greatest of which (x10 fold decline) were in pools of the disaccharides melibiose and turanose. These changes were fairly consistent between sampling points, although typically observed to a greater extent after more prolonged exposure to thermal stress at 8 d (**Fig. 3.3**).

In contrast, the greatest changes to host pools associated with thermal stress were predominantly negative and much greater in scale (up to x20 fold) (**Fig. 3.3**). These modifications in pool size were once again fairly consistent between sampling days, although more pronounced with longer exposure to elevated temperature at 8 d. The most notable reductions in terms of scale were observed for the intermediates tryptamine, ascorbate and threonate, and the lipogenesis intermediate galactosylglycerol. In contrast, smaller increases in pool sizes (up to x5 fold) of the amide urea, the purine guanine, the disaccharide gentiobiose, the organic acid gluconic acid and the sugar alcohol myo-inositol were also observed in response to heat treatment.

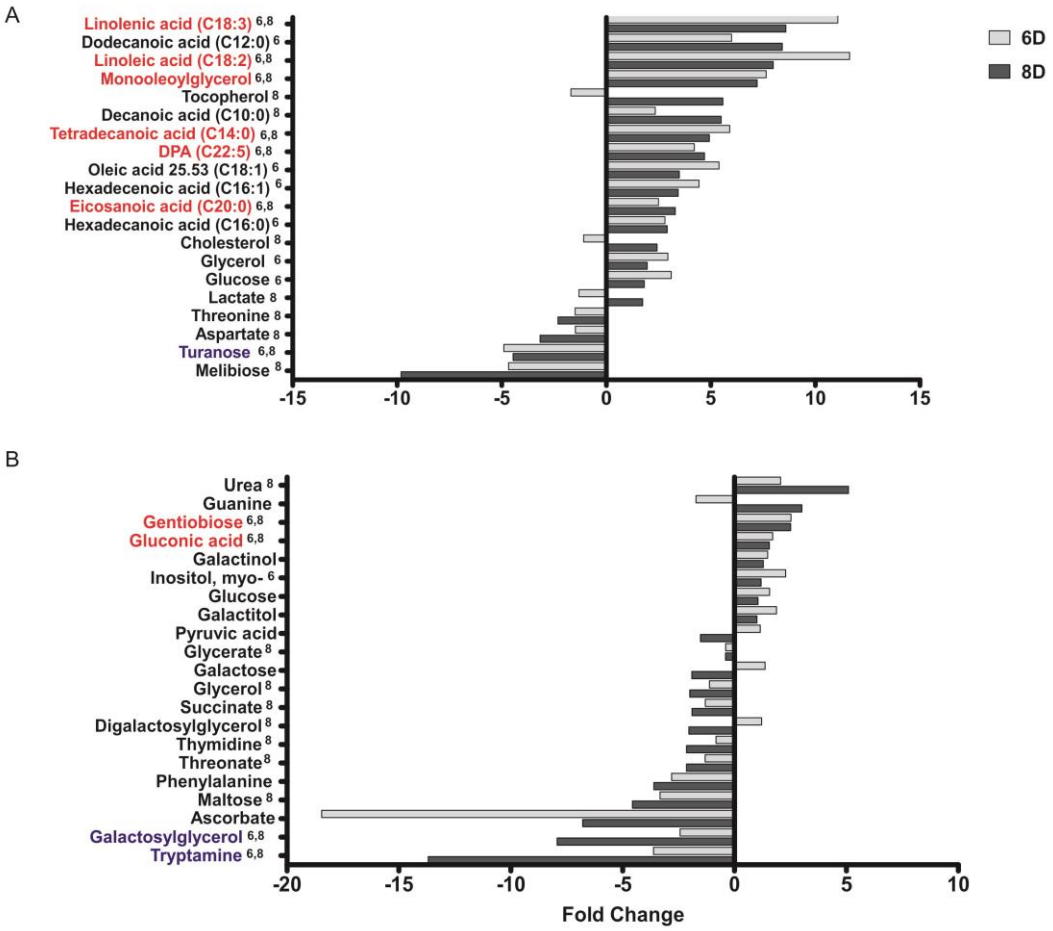

Fig. 3.3: (previous page): Relative fold changes between ambient and treatment groups of key compounds in symbiont (A) and host (B) pools at 6 d and 8 d (see over). [6 8] and colour text denote compounds that differed significantly between treatments at $P < 0.05$ (with FDR correction) for both time points, and 6 or 8 at one time-point only (red, increase in pool; blue decrease in pool with heat treatment at both time points).

3.3.6 Quantitation of key compounds during thermal stress

Thermally-induced modifications to intracellular pools of a total of 29 key organic acids, carbohydrates and intermediates, were quantified *via* targeted quantitative analysis for heat-treatment groups at 8 d (**Fig. 3.4**) (**Table S3.3** and **Table S3.4**). Supporting the outputs of the comparative data sets, in the symbiont significant declines were observed in pools of intermediates associated with central carbon metabolism, in addition to reductions in pool sizes of a number of hexose, monosaccharide and more complex carbohydrates, the greatest of which was for pools of galactose (ca. 50% decrease to 253.7 picomoles mg^{-1} dry weight ± 50.0 S.E.M.). In contrast, however, there was a non-significant trend of an increase in pools of the most abundant compound, glucose (ca. 50% increase to 1056.1 picomoles mg^{-1} dry weight ± 219.8 S.E.M.) (**Table S3.3**).

In the host, thermally-induced modifications included relatively large absolute increases in the concentration of the sugar alcohol xylitol (ca. 340% increase to 77.5 picomoles mg^{-1} dry weight ± 19.8 S.E.M.) and the disaccharide gentiobiose (ca. 50% decrease to 25.8 picomoles mg^{-1} dry weight ± 2.5 S.E.M.), coupled to reductions in pools of a number of central intermediates and monosaccharide and disaccharide sugars, including maltose (ca. 80% decrease to 72.7 picomoles mg^{-1} dry weight ± 13.9 S.E.M.) and xylose (ca. 80% decrease to 41.0 picomoles mg^{-1} dry weight ± 6.5 S.E.M.) (**Fig. 3.4**) (**Table S3.4**).

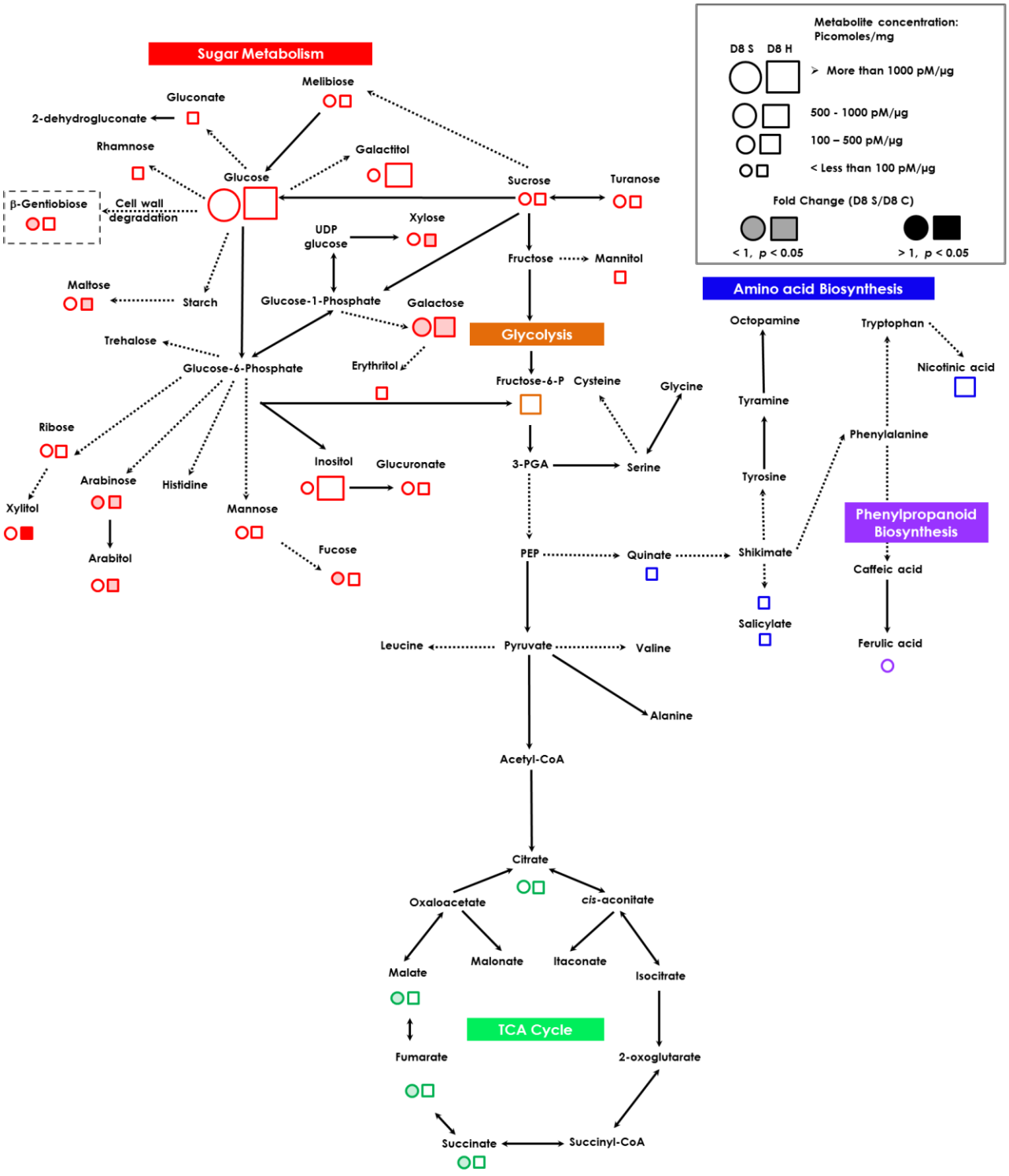

Fig. 3.4: Absolute concentrations of compounds detected in the free pools of the heat-stressed symbiont and host. Light shading denotes compounds that differed significantly ($P < 0.05$) with thermal stress relative to controls at 8 d with a fold-change below 1, whereas darker shading denotes compounds that differed significantly between treatments with a fold change above 1 (with FDR correction), symbiont (○) and host (□).

3.3.7 Thermally induced modifications to pathway activities of symbiont and host

Pathway activity analysis (PAPi) of the non-targeted metabolite profile data revealed pathway modes that showed altered turnover in response to heat treatment at 6 d and 8 d in symbiont and host (**Table S3.5** and **S3.6**). Exposure to elevated temperatures resulted in modifications to the activity of multiple pathways, which differed with symbiotic partner and treatment duration.

Notably, in the symbiont, reductions in pathway activity were estimated for networks associated with central carbon (glycolysis and pentose phosphate pathway), starch, galactose, glycerolipid and fatty acid metabolism. In contrast, increases were estimated for pathways associated with the metabolism of the vitamin riboflavin and the amino acid beta-alanine.

In host pools, reductions in activity were estimated for networks and intermediates associated with cell signalling (inositol derivatives) and antioxidant (ascorbate) pathways; these thermally induced alterations were coupled to increases in networks associated with central (TCA cycle, oxidative phosphorylation), galactose, glycerolipid and amino acid metabolism.

3.4 Discussion

In this study GC-MS based metabolite profiling was applied to detect change during thermal stress and on-going bleaching in the free pools (polar and semi-polar compounds) of remaining symbionts (*in hospite*) and the coral host. Characteristic thermally-induced modifications were detected in the metabolism of each symbiotic partner, which differed according to the duration of thermal stress exposure. These changes were most likely associated with symbiont photodamage and metabolic costs associated with thermal stress. Correspondingly, increases were observed in the activity of alternative energy modes (glyoxylate cycle), ROS-associated damage signalling and individual acclimation responses to thermal and oxidative stress in symbiont and host. These aspects are discussed in more detail in the sections that follow below.

3.4.1 Photoinhibition leads to alternative energy modes and the generation of excess ROS

Prolonged exposure to elevated temperature results in increased damage and inhibited repair to chloroplast structures, leading to photoinhibition, a reduction in carbon fixation and an increase in the production of ROS (Lesser, 1996; Warner et al., 1999; Takahashi and Murata, 2008). A decline in carbon fixation will affect the free metabolite pools of symbiont and host in a number of ways. Firstly, in the symbiont there will be a reduction in the production of cellular energy (ATP and NADPH), with corresponding declines in the *de novo* synthesis of glucose from the Calvin cycle (Jones et al., 1998; Smith et al., 2005). Under optimal photosynthetic conditions, the symbiont's free pools of glucose will turn over rapidly, fuelling downstream respiratory and biosynthesis pathways for symbiont growth, energy storage, and the production and translocation of mobile products to the host (Burriesci et al., 2012; Kopp et al., 2015). During thermal stress, an increase in the ratio of respiration to photosynthesis will necessitate a reduction in the activity of pathways which consume cellular energy, such as biosynthesis and growth, with an increase in those that produce ATP during respiration (Clark and Jensen, 1982; Jokiel and Coles, 1990). Correspondingly, as the severity of photodamage progressed from 6 d to 8 d in the current study, a reduction in the pool size of simple and complex carbohydrates (disaccharide, monosaccharide and hexose sugars) was detected in both partners. This decrease in carbon fixation and the production of complex carbohydrates coincided with downstream reductions in the turnover of central carbon metabolism pathways in the symbiont, namely glycolysis and the pentose phosphate pathway, in addition to the turnover of starch and galactose metabolism. Concurrently, in the host, the turnover of energy generating pathways was increased, with increased activity of the TCA cycle, oxidative phosphorylation and the metabolism of glycerolipids with thermal stress. Most likely these changes were in association with beta-oxidation of host lipid stores; which is a typical response during coral bleaching (Grottoli et al., 2004; Bachok et al., 2006; Imbs and Yakovleva, 2012).

Coupled to declines in the activity of carbon fixation, the availability of cellular energy and the activity of typical biosynthesis pathways, accumulation of multiple fatty acids (SFAs, PUFAs and MUFAs) was detected in symbiont pools. These accumulations

are likely to result from a number of interacting factors, primarily associated with symbiont ATP-limitation as discussed above. Namely, these are: 1) modifications to typical lipogenesis pathways (Sakamoto et al., 1994; Zhu et al., 1997; Papina et al., 2007); 2) a decline in the translocation of fatty acid mobile products to the host (Papina et al., 2003); 3) an increase in the catabolism of lipid stores (Grottoli et al., 2004); 4) modifications to lipid membrane structure (see below) (Tchernov et al., 2004; Papina et al., 2007); 5) a decline in nitrogen assimilation by the symbiont, leading to altered C:N ratios (Li et al., 2010; Kopp et al., 2015; Wang et al., 2015); and 6) translocation of host PUFAs from the host to symbiont (Imbs et al., 2014; Revel et al., 2016). Interestingly, the greatest changes to symbiont fatty acid pools were in two very differing groups of fatty acids, namely the PUFAs C18:3 and C18:2, and the mid-length SFA C12:0. In the case of the more abundant PUFAs, an increase in the production of C18:3 with elevated temperature has previously been detected in cultured microalgae (*Isochrysis galbana*) and cyanobacteria, owing to increased activity of ω3 desaturase, which catalyses its synthesis from C18:2 (Sakamoto et al.; Zhu et al., 1997). In contrast, C12:0 is typically found associated with lipid stores, such as triacylglycerol (TAG) and wax esters (Patton et al., 1977; Kellogg and Patton, 1983). A decline in typical lipogenesis activities coupled to an increase in catabolism of these stores, such as *via* the glyoxylate cycle present in the dinoflagellate (Butterfield et al., 2013), would likely result in greater abundances of this intermediate (amongst others) in the free pools of the dinoflagellate.

The wider holobiont will also be affected by elevated temperature, which can cause a shift in the associated microbiota (Forest et al., 2002; Rosenberg et al., 2007). Such thermally-induced modifications have been implicated in further symbiont photoinhibition, bleaching and disease (Rosenberg et al., 2007). Reductions of pools of maltose in the host fraction with exposure to thermal stress were detected, this disaccharide has not previously been reported as a translocated mobile compound in the symbiosis and is more commonly associated with microorganisms harboured within the host mucus, skeleton and tissues (Forest et al., 2002; Sharon and Rosenberg, 2008). Although with the methodology applied it was not possible to establish the direct source of this compound, a decline in its abundance in the host fraction may be indicative of a shift in the associated microbial consortium, for instance to one dominated by more pathogenic populations, such as *Vibrio* spp.

(Forest et al., 2002; Rosenberg et al., 2007; Lee et al., 2015; Tout et al., 2015). Of note, a reduction in maltose concentration has been reported as serving as a direct indicator for enhanced growth of the well-known coral pathogen, *Vibrio coralliilyticus*, when in culture under optimal conditions (temperatures above 27°C) (Brown and Bythell, 2005). Further to this, growth of *Vibrio* spp. are also enhanced in the tissues and mucus of bleached and thermally stressed corals (Bourne et al., 2008; Lee et al., 2015; Tout et al., 2015).

3.4.2 ROS accumulation initiates a signalling cascade

The increased turnover of central respiratory pathways during thermal stress, principally oxidative phosphorylation and the electron transport chain, will result in increased production of ROS in the mitochondria and microbodies of both symbiont and host (Downs et al., 2002; Lesser, 2006). In addition, photoinhibition and the increased activity of alternative electron flows will generate additional ROS in the symbiont at the chloroplast, *via* the Mehler reaction (Roberty et al., 2014; Roberty et al., 2015). Accumulation of ROS species at largely impermeable lipid membranes results in peroxidation of membrane PUFAs and the production of oxylipins (Gill and Tuteja, 2010) (**Fig. 3.5**). These unstable products may themselves be cytotoxic, reacting with proteins, other lipids and nucleic acids (Lesser, 2006; Gill and Tuteja, 2010). This damage can then result in the leakage of accumulated ROS and further cellular damage. The PUFAs C18:2 and C18:3, which are particularly abundant in the pools of both the symbiont and host, are highly susceptible to attack by singlet oxygen and hydroxyl radicals ($^1O_2$ and HO● respectively), producing a complex mixture of damaging lipid hydroperoxides (Gill and Tuteja, 2010). In association with ROS, these compounds may serve as damage signals, which are detected at the cellular membrane, initiating a cascade of signalling, feedback and modifications to fatty acid metabolism, the free fatty acid pool and eventually the composition of the lipid membrane (Lõhelaid et al., 2015) (**Fig. 3.5**). As total lipids were not analysed in the present study, it was not possible to establish thermally-induced modifications to the lipid membranes of symbiont and host, however the clear modifications to symbiont fatty acid pools seen here are indicative of altered fatty acid metabolism and lipogenesis as discussed above. Increased membrane saturation is one mechanism that may be employed in *Symbiodinium* to enhance membrane stability under elevated temperature, reducing lipid peroxidation and associated damage,

however this response is not uniform and may vary according to cell- and symbiont type (Tchernov et al., 2004; Papina et al., 2007). An alternative approach in thermally-resistant *Symbiodinium* types may include actively increasing pools of PUFAs (Díaz-Almeyda et al., 2011). As the process of fatty acid desaturation is an aerobic reaction, desaturation, elongation and isomerisation may simultaneously reduce cellular oxidative stress and reduce peroxidation, thereby providing an additional mechanism for membrane stabilization (Guerzoni et al., 2001; Díaz-Almeyda et al., 2011). However, as PUFAs are susceptible to peroxidation by ROS, this response will only be effective as long as antioxidant responses are maintained. As elevated pools of multiple PUFAs were detected in the symbiont following exposure to thermal stress, a similar mechanism may therefore operate in this symbiont-host combination.

The symbiont cellulose cell wall is also likely to be a site of attack and damage by ROS, leading in turn to the release of modified oligosaccharides (Wakefield et al., 2000; Field, 2009) (**Fig. 3.5**). In terrestrial plants, many of these compounds, termed oligosaccharins, have biological activity and roles in plant stress signalling (Dumville and Fry, 2003). One such compound is the rare disaccharide gentiobiose (Dumville and Fry, 2003; Takahashi et al., 2014). This compound functions in plant signalling, during periods of development associated with oxidative bursts and high ROS levels (Field, 2009; Aizat et al., 2014; Takahashi et al., 2014). As yet, the compound has no other described roles in central metabolism and is rapidly broken down (Dumville and Fry, 2003). Upon detection, increased levels of gentiobiose are thought to elicit antioxidant responses; namely the production of sulphur-containing amino acids (methionine and cysteine) and ascorbate (AsC), and the increased *de novo* synthesis of the antioxidant glutathione (GSH), with upregulation of associated genes (Takahashi et al., 2014). Elevated pools of gentiobiose were detected in both symbiont and host following exposure to thermal stress and associated ROS. In addition, large changes in pools of AsC and pathways linked to the metabolism of GSH were detected in both partners. The AsC-GSH pathway is highly conserved and known to function in both symbiont and host (Lesser, 2006; Baird et al., 2009a) (see below acclimation responses), however whether gentiobiose serves as a signal in the system will require further study (**Fig. 3.5**). Elevated pools of this compound in the host fraction may result from a number of sources: its active transport, damage

to symbiont cell membranes and increased leakiness (Barott et al., 2015), or from host autophagy and apoptosis of symbiont cells, which is increased during thermal stress and bleaching (Dunn et al., 2004; Dunn et al., 2007). Interestingly, pools of the unusual disaccharide turanose were reduced during thermal stress in the symbiont, suggesting increased turnover of this compound. In terrestrial plants this non-metabolized sugar is also thought to play a role in plant stress signalling and development (Sinha et al., 2002; Gonzali et al., 2005).

Coupled to these modifications to free pools in symbiont and host, accumulations of the sugar alcohol inositol were detected in host pools, and corresponding declines in the turnover of inositol phosphates and phosphatidylinositol were estimated in the heat-stressed host. Inositol derivatives are present in both dinoflagellate symbiont (Klueter et al., 2015) and cnidarian host (Burriesci et al., 2012). In addition to functions as compatible solutes, inositol derivatives have highly conserved roles in cellular recognition, signalling and development (Müller, 2004; Garrett et al., 2013; Philippon et al., 2015; Rosic et al., 2015). Interestingly, inositol phosphates are also thought to play a role in the activity of cell apoptosis and autophagy (Boehning et al., 2005; Chakraborty et al., 2008), both modes of cell death, which are elevated during thermal stress and play a role in coral bleaching (Dunn et al., 2004; Dunn et al., 2007). A previous study with multiple *Symbiodinium* types in culture has also shown that a number of inositol groups become elevated in the dinoflagellate under thermal stress (Klueter et al., 2015). Perhaps surprisingly, however, the potential role of this major inositol-based signalling network in the transduction of symbiosis dysfunction and cnidarian bleaching has, to date, been largely overlooked.

Temperature stress may also be communicated in the symbiosis *via* hormone networks, such as those derived from steroids and complex proteins (Tarrant, 2005; Tarrant et al., 2009). Two such stress-signalling pathways in terrestrial plants are brassinosteroids and glucosinolates (Ludwig-Müller et al., 2000; Bajguz and Hayat, 2009). In both symbiont and host, there was a trend of increased turnover of pathways closely resembling these terrestrial plant-signalling networks. Brassinosteroids are steroidal plant hormones, which play essential roles in plant development, and responses to abiotic stress and the generation of ROS (Bajguz and Hayat, 2009; Clouse, 2011). This large group of signalling hormones acts synergistically with other hormones, in order activate effective signal transduction

and stress responses, however the mechanisms involved are largely unresolved (Bajguz and Hayat, 2009). These hormones are synthesised from the steroid derivative camperstol (Clouse, 2011); both complex steroids and campestrol derivatives are abundant in dinoflagellate algae and their cnidarian hosts (Scheuer, 1978; Tarrant et al., 2009; Amo et al., 2010). In addition, steroids have signalling roles in cnidarians (Tarrant, 2005), so it is likely that both steroids and their derivatives could have a similar role within the symbiosis. Glucosinolates are amino acid derivatives that serve as important plant stress-signalling compounds, function in the production of HSPs, and may be involved in host/pathogen recognition (Ludwig-Müller et al., 2000; del Carmen Martínez-Ballesta et al., 2013). Gluconsinolates are formed *via* a portion of the Shikimate pathway, which is present in both partners (as discussed below) (Grubb and Abel, 2006; Rosic and Dove, 2011). As such, it is possible that a related signalling pathway could also function in the coral-dinoflagellate symbiosis.

3.4.3 Signal transduction results in an acclimation response

The detection of cellular damage leads to signal transduction between cells, eventuating in an acclimation response (Grüning et al., 2010). This response is highly complex and will include shifts in central pathway modes and associated metabolite pools (as discussed above). In addition, pools of secondary metabolites, such as hormones, vitamins and pigments will also play a pivotal role in the acclimation response of each partner. Chlorophyll *a* (chl *a*) is the primary phytopigment in *Symbiodinium*, however chlorophyll *c* (chl *c*) and accessory pigments, such as carotenoids, also function in light harvesting and have important roles in photoprotection (Venn et al., 2006; Strychar and Sammarco, 2011). Carotenoids primarily function in photoprotection *via* the dissipation of excess energy (dynamic photoinhibition), they may also act as antioxidants that are capable of scavenging ROS directly (Strychar and Sammarco, 2011). The carotenoids of *Symbiodinium* are relatively well characterised, being comprised principally of peridinin and fucoxanthin (Schever, 1983; Strychar and Sammarco, 2011). Eventually, however, phytopigments (chlorophylls and carotenoids) are themselves sensitive to degradation at elevated temperature (Venn et al., 2006; Strychar and Sammarco, 2011). In addition to the observed reductions in chlorophyll *a* content with prolonged thermal stress, there was a positive trend of increased biosynthesis

of chlorophyll and two carotenoid groups (phenylpropanoids and betalains). These carotenoid groups are typically found in terrestrial plants (Dixon and Paiva, 1995), however their identifications in the PAPi analysis (which is based on a predominately terrestrial KEGG database) serve to highlight potential increases in the turnover of closely related biosynthesis pathways with thermal stress. One alternative is the production of mycosporine-like amino acids (MAAs); as with the production of phenylpropanoids in terrestrial plants, the biosynthesis of MAAs is initially *via* the Shikimate pathway (Shick and Dunlap, 2002; Rosic and Dove, 2011). MAAs play essential photoprotective roles in many marine organisms (including *Symbiodinium*), and some MAAs may also act as antioxidants, with a capacity to quench ROS and scavenge free radicals (Rosic and Dove, 2011) (**Fig. 3.5**). Similarly in the host, there was also increased turnover of a related biosynthesis pathway at 8 d thermal stress, coupled to large increases in tryptophan, phenylalanine and tyrosine metabolism. Once again, these amino acids all function in the Shikimate pathway and the biosynthesis of MAAs (Shick and Dunlap, 2002; Rosic and Dove, 2011). Unusually for animals, some cnidarians are able to synthesise their own MAAs directly, in addition to those assimilated *via* diet (Shinzato et al., 2011). A diverse range of MAAs are found in the tissues of reef-building cnidarians, where they again function in important photoprotective roles (Shick and Dunlap, 2002; Rosic and Dove, 2011). Thermal stress has been widely documented to result in the increased biosynthesis of these protective compounds in corals (Rosic and Dove, 2011), so a similar response would therefore be expected in the current study.

Vitamins are ubiquitous in nature, playing essential roles in cellular function and homeostasis; in particular, AsC (vitamin C) and tocopherol (vitamin E) play complementary roles as ROS scavengers in plant cells (Gill and Tuteja, 2010). AsC is water-soluble and typically found throughout an organism, whereas tocopherols are lipid soluble and found exclusively associated with cellular membranes of the chloroplast (Gill and Tuteja, 2010). Tocopherols quench ROS and play an important role in limiting the production of lipid peroxidation *via* the production of tocopheroxyl radicals, and these may then be recycled back to tocopherol by AsC (Munné-Bosch, 2005). Tocopherols also play a role in the detoxification of nitric oxide (NO_x) (Gill and Tuteja, 2010). AsC is a powerful antioxidant and, in addition to its complimentary role with tocopherol, functions in the GSH-AsC cycle (as discussed above). In the

present study, large thermally induced modifications were observed to pools of both tocopherol and AsC. In the case of the symbiont, accumulations of both tocopherol and AsC at 8 d. These changes in symbiont antioxidant pools at 8 d coincided with the progression of photodamage and are likely indicative of responses to maintain oxidative state with increased ROS production (**Fig. 3.5**). In contrast, in the host, large declines in pools of AsC were observed at both sampling points, although interestingly these were to the greatest extent at 6 d. This reduction of intracellular pools of AsC at 6 d coincided unusually with a large reduction of AsC metabolism, indicative of an accumulation of pathway intermediates and a break down in the AsC-GSH cycle, which was prior to more severe bleaching observed at 8 d.

Exposure to increased temperatures, disruption to the electron transport chain and a decline in the exchange of osmotically active compounds will also lead to osmotic stress in the host (Mayfield and Gates, 2007). As such, non-reducing compounds such as complex sugars, polyols, sugar alcohols and certain amino acids may function as compatible solutes under these conditions (Bohnert et al., 1995; Mayfield and Gates, 2007). In the current study, elevated pools of glycerol were observed in the symbiont, coupled to large accumulations of xylitol, galactinol, myo-inositol and galactitol in the host. This accumulation of compatible solutes observed in the intracellular pools of the heat stressed host likely indicates exposure to osmotic stress and mechanisms to maintain both internal osmolality and a suitable osmotic environment for the remaining *in hospite* symbionts.

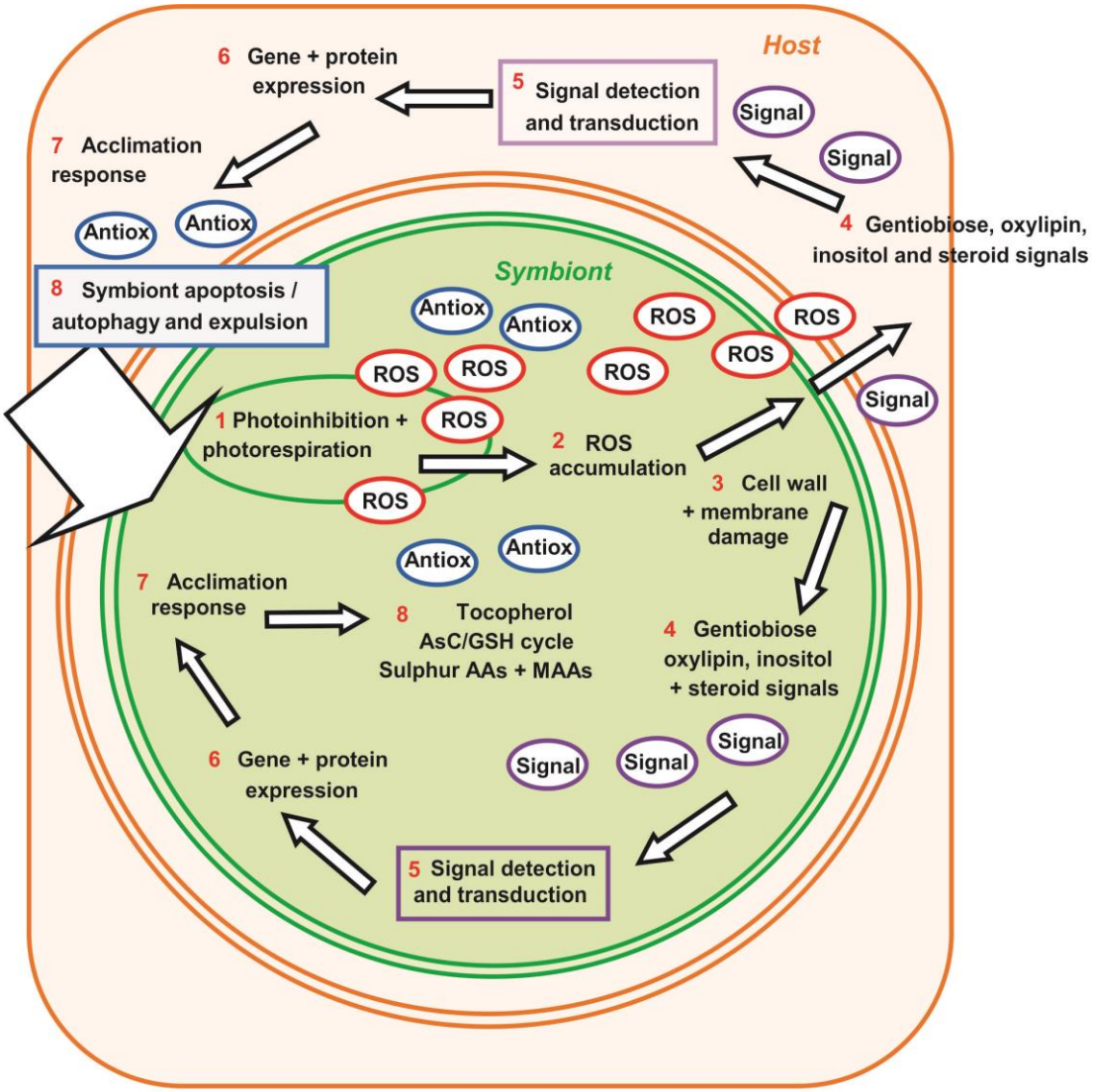

Fig. 3.5: A simplified schematic showing potential role of free metabolite pools in the detection of thermal and oxidative stress, signal transduction and responses of the symbiosis. 1) Photoinhibition and photorespiration result in the production of ROS at the chloroplast and mitochondria. 2) ROS overwhelm antioxidant responses and accumulate. 3) ROS result in damage to the cell wall and membranes. 4) Damage produces cell wall oligosaccharides and glycans, such as gentiobiose, while peroxidation of lipid membranes produces oxylipins. Other potential signals include the disaccharide turanose and inositol groups 5) Damage signals are detected in the symbiont and host, initiating signal transduction via mechanisms such as steroids and the phosphatidylinositol system. 6. Signal transduction results in altered gene and protein expression in symbiont and host. 7) Cellular acclimation in symbiont and host. 8) Antioxidant responses in the symbiont and host, such as the AsC/GSH cycle, tocopherol, sulphur-containing amino acids and MAAs. Host antioxidant responses, when overwhelmed, lead to enhanced apoptosis, autophagy and expulsion of symbiont cells (bleaching).

3.5 Conclusions

Thermal and oxidative stress during symbiont photodamage and bleaching resulted in clear modifications to the free metabolite pools of symbiont and host. These changes were associated with the energetic costs of maintaining cellular homeostasis, direct responses to maintain cell structure and function, the increased activity of ROS- and damage-associated signalling pathways and potentially changes to the associated microbial holobiont.

This study provides for the first time a holistic assessment of the complex changes elicited to the metabolism of the holobiont during exposure- and acclimation to elevated temperatures. In this instance, metabolic (non-enzymic) responses to maintain thermal, oxidative and osmotic state were more apparent in the host compared to the symbiont, suggesting that there may be a disparity in the level of these stressors between partners. For instance, although non-enzymic antioxidant pathways form only a portion of antioxidant responses, similar differences in enzymic antioxidant responses have also been observed between partners (Krueger et al., 2015), as have responses to maintain osmotic state (Mayfield and Gates, 2007) and expressed genes (Leggat et al., 2011). These data therefore highlight the complexity of cellular and metabolic change in each respective partner during thermal stress and bleaching and have implications for our understanding of the mechanisms responsible for symbiosis breakdown. Clearly further directed studies from a range of host-symbiont combinations, in a number of ‘omics fields (genomics, transcriptomics, proteomics and metabolomics) are required if we are to truly unravel the complex changes which occur in the holobiont during bleaching. These data are essential if we are to better understand the true capacity of corals for long-term acclimation and determine in what state reefs will persist under future climate change scenarios.

Chapter 4 The impact of thermal stress and bleaching on carbon fate in the cnidarian-dinoflagellate symbiosis

4.1 Introduction

Metabolic interactions between dinoflagellate symbionts and their cnidarian hosts underpin the success of the coral symbiosis in nutrient-poor tropical waters (Muscatine and Hand, 1958; Muscatine and Cernichiari, 1969; Yellowlees et al., 2008). In this relationship, inorganic nutrients (including carbon, nitrogen and phosphorus) are supplied by the host, facilitating symbiont carbon fixation *via* the C3 pathway and assimilation of nitrogen *via* the glutamine synthetase/glutamine:2-oxoglutarate aminotransferase (GS/GOGAT) cycle (Miller and Yellowlees, 1989; Streamer et al., 1993; Pernice et al., 2012). Studies with radio- and stable-isotope labelled carbon and nitrogen tracers have revealed that many of the resulting organic products are then translocated to the host, providing resources for host respiration, growth, calcification and reproduction (Muscatine and Hand, 1958; Tanaka et al., 2006; Bachar et al., 2007; Pernice et al., 2012; Kopp et al., 2015). This nutrient exchange is, however, likely to be affected by a range of factors, including the genotype and phenotype of each symbiotic partner, their respective environmental optima and exposure to associated environmental drivers (Loram et al., 2007; Stat and Gates, 2011). The holobiont in its entirety also comprises a specific suite of associated microbes, which are thought to contribute to these nutritional interactions (Rohwer et al., 2002; Rosenberg et al., 2007). A major threat to the persistence of the functional symbiosis is thermal stress, associated with elevated water temperatures (Hoegh-Guldberg, 1999; Carpenter et al., 2008; Lesser, 2011). This abiotic stress coupled to high light levels, can lead to photoinhibition in the symbiont, the overproduction of reactive oxygen species (ROS), dysfunction of the symbiosis and eventually the breakdown and loss of symbionts during bleaching (Lesser, 1996; Weis, 2008).

However, major gaps remain in our understanding of mobile compound exchange throughout the process of thermal stress and bleaching (Edmunds and Gates, 2003; Davy et al., 2012). Given the importance of this exchange in maintaining the

functional symbiosis, it is therefore essential that we better understand how elevated temperature affects the production of carbon- and nitrogen-rich mobile products, their translocation to the host, and the associated downstream pathways in both partners. During the early stages of thermal stress when the symbionts are still in the host (*in hospite*), they may remain photosynthetically viable (Ralph et al., 2001; Hill and Ralph, 2007), and a reduction of symbiont density may actually serve to increase the *per* cell productivity of the remaining symbionts, by increasing the availability of rate-limiting inorganic nutrients (principally dissolved inorganic carbon, DIC) and light (Tremblay et al., 2014; Hoadley et al., 2016). However, if the severity of photoinhibition increases with further exposure to elevated temperature, a reduction in carbon fixation and increased ROS production would be expected (Jones et al., 1998; Warner et al., 1999; Roberty et al., 2014). The associated reduction in energy availability, coupled to increased respiratory costs of maintaining cell homeostasis, will necessitate a number of changes to central metabolism in the symbiosis. Namely, these are: a decline in net biosynthesis and a reduction in mobile product translocation (Clark and Jensen, 1982; Smith et al., 2005); a requirement for the generation of energy from alternate sources (i.e. catabolism of stores); and also potentially an increase in host heterotrophy (Grottoli et al., 2004; Grottoli et al., 2006). However, detailed *in vivo* data elucidating the roles of individual compounds and pathways in the holobiont during thermal stress and symbiosis dysfunction remain to be fully elucidated.

The application of isotope tracers, such as ^{13}C-labelled substrates, enable active carbon pathway modes to be identified, and the fate of label in metabolite pools to be detected (**Fig. 4.1**). ^{13}C is a stable isotope that is naturally present in low abundance, typically 1-2% of a given compound (Klein and Heinzle, 2012). Exposure to a $^{13}CO_2$-enriched medium under photosynthetic conditions, will result in the incorporation of this label into organic products, and these compounds will in turn pass through metabolic pathways, redistributing into secondary intermediates and a number of metabolite end-points (Walter et al., 2009). In the cnidarian-dinoflagellate symbiosis, carbon is fixed by the symbiont from CO_2 within seconds, passing through the C3 pathway (Streamer et al., 1993; Whitehead and Douglas, 2003). Incubations with enriched seawater under photosynthetic conditions will therefore result in ^{13}C-label incorporation into Calvin cycle intermediates and end-products (e.g. glucose) within

minutes of exposure to the label (**Fig. 4.1**). Following fixation into carbohydrates, other labelled carbon-rich products such as fatty acids will be synthesised; these products may then be respired by the symbiont, incorporated into symbiont biosynthesis, or translocated to the host as mobile products (Patton et al., 1977; Whitehead and Douglas, 2003; Dunn et al., 2012). Eventually, labelled products will be synthesised into growth and storage bodies in both partners, such as starch/glycogen, proteins and lipids (von Holt and von Holt, 1968; Walter et al., 2009; Kopp et al., 2015). As a consequence, enriched compounds will be detected rapidly within the free-metabolite pools of the symbiont, and following translocation, those of the host and any associated microflora.

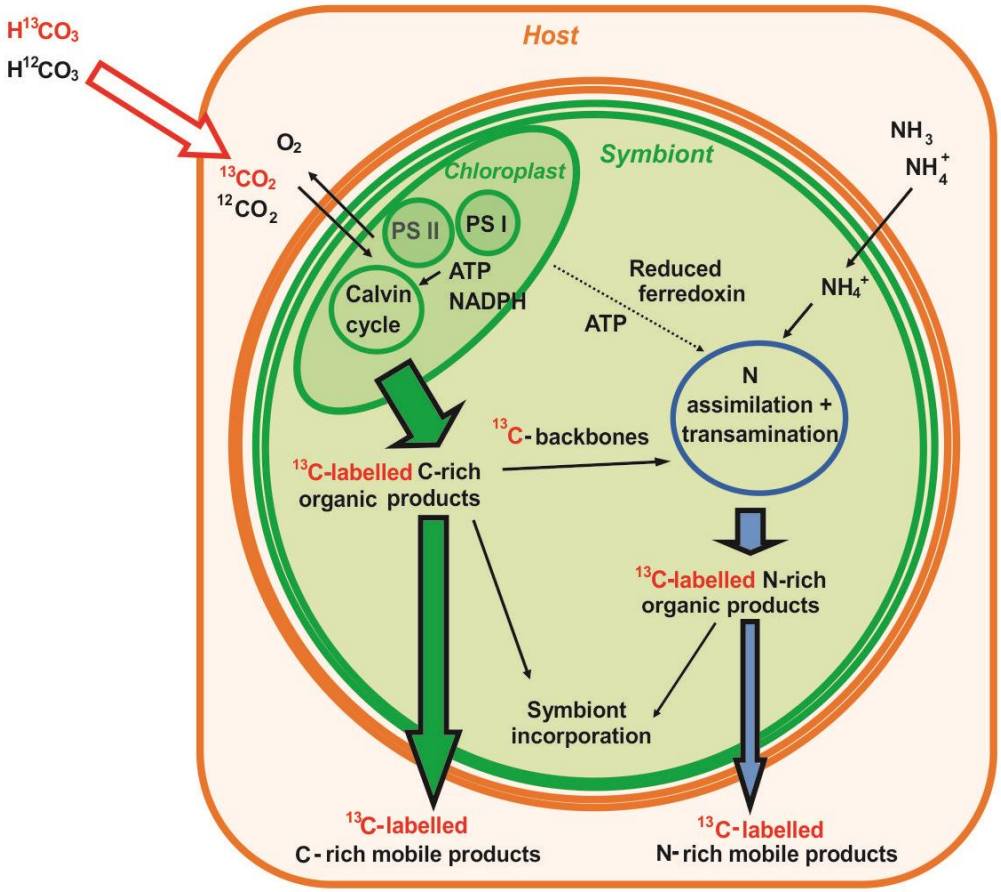

Fig. 4.1: Simplified schematic of the flow of a stable isotope tracer (^{13}C) from enriched bicarbonate ($H^{13}CO_3$), producing ^{13}C-labelled carbon-rich (C-rich) organic products (e.g. glucose). Products may be translocated to the host, incorporated in symbiont growth/respiration, or metabolised as ^{13}C-labelled carbon backbones in the transamination of nitrogen rich (N-rich) organic products (amino acids, proteins and purines). ^{13}C-labelled N-rich organic products may then be incorporated into the symbiont, or translocated to the host as ^{13}C-labelled N-rich mobile products.

The subsequent distribution of label (mass isotopomer distribution, MID) in a given compound reflects the characteristic labelling patterns associated with a given pathway and its turnover (Walter et al., 2009; Klein and Heinzle, 2012) (**Fig. 4.2**). Provided that the system remains saturated with label, the ratio of labelled products and intermediates will continue to increase with continued carbon fixation, becoming rapidly enriched above background levels, until eventually reaching an isotopic steady state (when all metabolites in the system have an equal distribution of this label) (Walter et al., 2009). In a non-isotopically stationary state, the isotope ratio and MID of a given compound will be dependent on the dynamic interplay of a number of variables, which determine the turnover (flux) of each compound (Young et al., 2011) (**Fig. 4.2**). Principally, these variables are the existing pool size of a given compound, its rate of turnover, the duration and enrichment level of label exposure, and the rate of carbon fixation. In the case of host pools, enrichment of a given compound will also be influenced by the quantity, composition and enrichment of the mobile products translocated *per* symbiont and the associated symbiont density (i.e. net translocation of labelled mobile compounds).

Stable isotope ^{13}C-tracers, coupled with detection and quantitation of MIDs *via* GC-MS, can therefore facilitate the investigation of carbon flow from fixation to metabolic intermediates and end-products, in the symbiont, host and wider holobiont. In this study, non-isotopically stationary ^{13}C-labelling was applied in order to detect thermally-induced modifications to symbiont carbon fixation and mobile product translocation in the anemone *Aiptasia* sp. (a model species for the symbiosis) (Weis et al., 2008) and subsequently a common reef-building coral, *Acropora aspera* and their *in hospite* dinoflagellates (*Symbiodinium* ITS 2 type B1 and C3 respectively). It was hypothesised that thermal stress and bleaching resulting in symbiont photoinhibition and a reduction in carbon fixation, would result firstly in alterations to the identity of labelled products and their corresponding MIDs in the free pools of the remaining *in hospite* symbionts, and subsequently modifications to the downstream pools of their respective hosts. Following more prolonged exposure to thermal stress and a breakdown in symbiosis function and mobile product translocation, it was anticipated that this enrichment in host pools would be minimal.

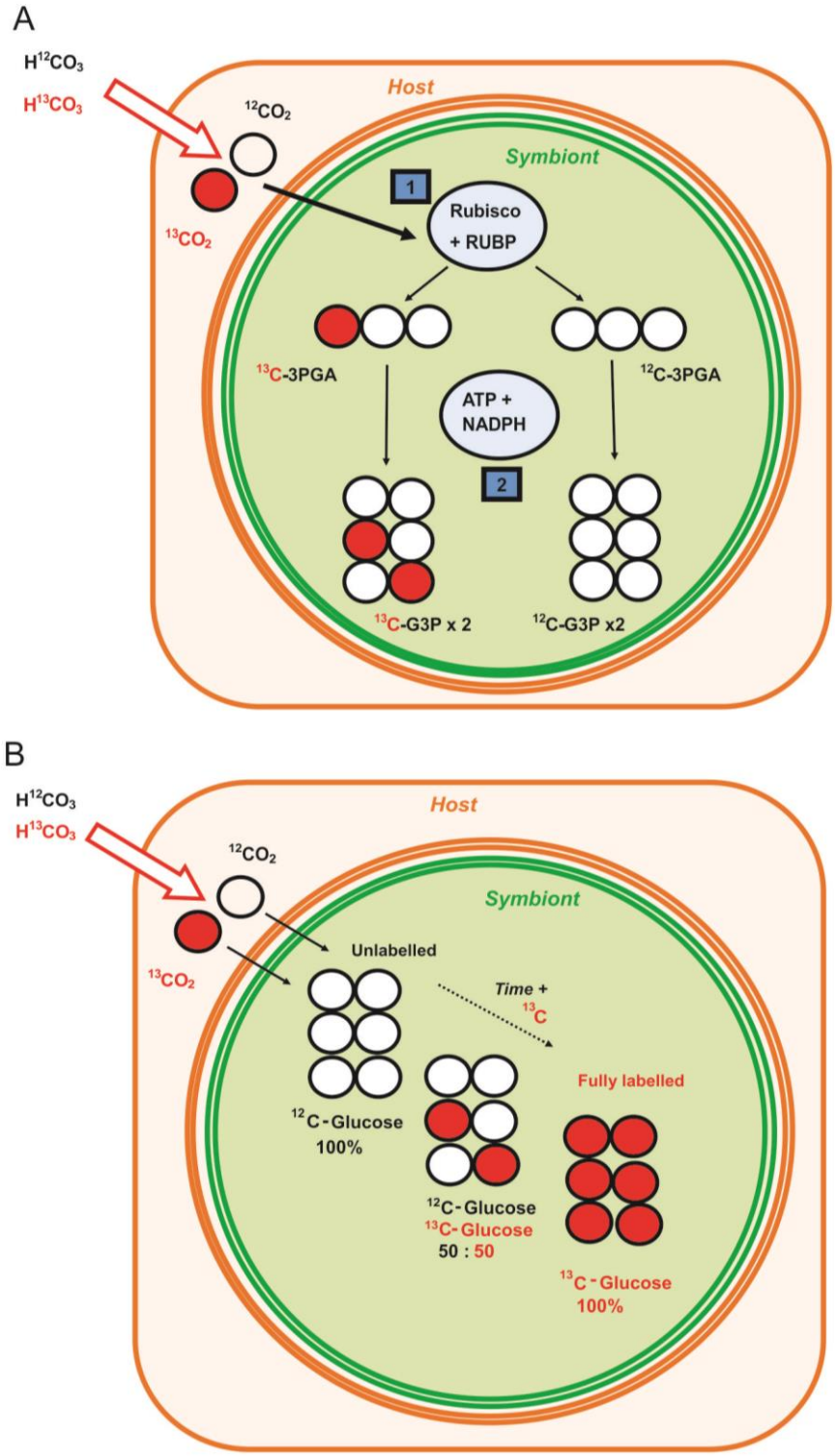

Fig. 4.2: **Simplified schematic showing the flow of a stable isotope tracer (^{13}C), from enriched bicarbonate ($H^{13}CO_3$) to glucose.** (A) In the Calvin cycle, $^{13}CO_2$ is fixed by Rubisco to ribulose-1,5-biphosphate (RUBP), producing the intermediate 3-phosphoglycerate (3PGA) (1); glyceraldehyde 3-phosphate (G3P) is then produced, with two molecules used to form one of glucose (2). (B) With continued input of ^{13}C alone, the ratio of labelled product to unlabelled product will continue to increase, until a steady state where all products are 100% labelled.

4.2 Materials and methods

4.2.1 Aiptasia *sp.*

A culture of *Aiptasia* sp. (of unknown Pacific origin) with its *in hospite* homologous symbiont (*Symbiodinium minutum*, ITS 2 type B1) (Starzak et al., 2014), was maintained in the lab in 1 µm filtered seawater (FSW) at 25 °C, with light provided by AQUA-GLO T8 fluorescent bulbs at ≈ 95 µmol quanta m^{-2} s^{-1} (light:dark = 12 h:12 h). Anemones were fed twice a week with freshly hatched *Artemia* sp. nauplii. Prior to the experiment, anemones were rinsed repeatedly with FSW to remove any external contaminants and transferred to 250 mL beakers (with 12 individuals *per* beaker). Individuals were acclimated to the experimental set-up for ten days, with the seawater in each beaker changed daily. Individuals were starved for five days prior to sampling, to ensure that any *Artemia* had been digested and expelled. Following acclimation, the treatment aquaria were ramped up to 32°C ± 0.5°C over a period of 48 hours (ca. 1°C 3 h^{-1} during the light period). This heat treatment was maintained for a period of seven days. Experimental controls were maintained at 25°C ± 0.5°C.

Daily measurements of maximum fluorescence yields of photosystem II (PS II) were taken using a DIVING-PAM Underwater Fluorometer (Walz, Effeltrich, Germany). In order to quantify maximum quantum yield (F_V/F_M), daily PAM measurements were taken from five individuals set aside in each treatment, following 30 min of dark adaptation, and mean ± standard error (S.E.M) calculated for each treatment on each respective day.

4.2.2 Acropora aspera

Fragments (a maximum of 8 cm in length) of the coral *Acropora aspera* (cream/light blue colour morph) (ITS 2 type C3, **Chapter 3.3.1**) were collected from Heron Island reef flat (Great Barrier Reef (GBR), Australia; 23°26’43”S, 151°54’53”E) at low tide under GBR Marine Permit G14/36933.2 between 27th-29th March 2015. Fragments (*n* = 11 per colony) were sampled from the unshaded upper branches of six replicate colonies (in total amounting to no more than 5% of the donor colony). Replicate colonies were separated by a minimum of 10 m to increase the likelihood of sampling different host genotypes.

Fragments were mounted using light-diffusing egg-crate and acclimated for 11 days in four experimental aquaria (60 L). Continuous seawater flow-through (ca. 4 L min^{-1})

was provided from Heron Island reef flat. Aquaria were covered with shade cloth to reduce midday irradiance (ca. 1500 to 500 µmol photons m^{-2} s^{-1}). Additional water movement was provided in each aquarium by small submersible pumps.

Following acclimation, two aquaria were heated to 32°C ± 1°C, at a rate of 1°C *per* day. Two control aquaria were left at ambient temperature, averaging 27°C ± 3°C. The treatment temperature was maintained for a period of nine days. Light and temperature data in each tank were recorded every 10 min by HOBO data loggers (Onset Computer Corporation, Bourne, MA, USA).

Daily measurements of maximum (dark-adapted) yields of PS II were taken using pulse amplitude modulation fluorometry (Diving-PAM, Walz, Effeltrich, Germany). Maximum yields were taken 30 min after last light. Presented values are based on means of triplicate measurements taken from each colony representative (*n* = 6, one per colony, *per* treatment) designated for PAM sampling. PAM settings were maintained over the course of the experiment at: measuring light 4, saturation intensity 4, saturation width 0.6 s, gain 1 and damping 2, with the use of the measuring light burst function. Measurements were taken at a standard distance of 5 mm from each sample.

4.2.3 Stable isotope (^{13}C) incubations

Aiptasia *sp.*

Sampling for metabolite stable isotope analysis was undertaken at 7 d (post heat-ramp). Prior to the start of the light cycle, for each sample FSW was exchanged for 200 mL of ^{13}C-labelled sodium bicarbonate ($H^{13}CO_3$) (4 mM) (Sigma-Aldrich, Auckland, New Zealand), or ^{12}C-sodium bicarbonate ($H^{12}CO_3$) (4 mM) in 0.22 µM FSW. Seawater pH was buffered to that of the FSW (pH 8.2), with the addition of NaOH solution (1 M).

Individuals were then incubated in the light (≈ 95 µmol quanta m^{-2} s^{-1}) for 5 h, under the relevant temperature treatment. At the end of this period, metabolism was immediately quenched by snap-freezing individuals in liquid nitrogen, with sampling taking less than 10 s. Individuals were then transferred to a -80°C freezer for storage. Six replicate samples were taken for each time-point, incubation type and

temperature; each replicate sample was comprised of 12 individuals, to ensure sufficient biomass for metabolite identification.

Acropora aspera

Incubations were initiated on 6 d and 9 d (post heat-ramp). At each sampling point, six coral fragments (one representative per colony) *per* treatment were incubated in the light in individual specimen jars placed in water baths at the relevant temperatures (either at a typical ambient temperature of 26°C ± 0.5°C, or 32°C ± 0.5°C).

Each jar contained 220 mL of 4 mM $H^{13}CO_3$- or $H^{12}CO_3$-enriched FSW (0.22 µM) representing a bicarbonate enrichment of approximately 66% (Tremblay et al., 2012). Seawater pH was buffered to that of the flow-through system (ca. 8.34 to 8.52, high water to low water). Incubations were for 4 h from the start of the natural light-cycle, with the beakers left open and regularly stirred (about every hour) to minimise reuse of respired $^{13}CO_2$. Following the incubation period, samples were immediately snap-frozen in liquid nitrogen and transferred to a -80°C freezer, until transport *via* dry shipper and analysis at the University of Melbourne. An additional 4-h incubation (*n* = 6, one fragment *per* colony) was carried out in the dark to confirm that label was not significantly incorporated by non-photosynthetic activities, such as heterotrophic feeding.

4.2.4 Sample processing of anemones and coral fragments

All sample processing was undertaken at 4°C in order to minimise any post-sampling metabolism. Anemones were homogenized with a saw-tooth homogeniser (IKA T10 BS5, ThermoFisher Scientific, Auckland, New Zealand) for 10 s at a mid-speed setting, and replicate anemones pooled (*n* = 12) to make each sample. The total sample volume was then topped up to 30 mL with chilled MilliQ water (MQ) at 4°C. Coral fragments were first defrosted on ice. Tissue was then removed from the skeleton *via* airbrush into 50 mL of chilled MQ at 4°C. The tissue suspensions were homogenised with a saw-tooth homogeniser (Ystral D-79282, Ballrechten-Dottingen, Germany) for 10 s at a mid-speed setting.

Following homogenization, anemone and coral samples were processed using the same methods. In each case, following a vortex for 30 s, three 1 mL aliquots were

removed from the whole homogenate for *Symbiodinium* cell counts, photosynthetic pigment analysis, host protein quantification and dominant *Symbiodinium* genotyping (corals only). The remaining tissue homogenate was centrifuged (2,500 x *g* for 5 min at 4°C) to separate *Symbiodinium* cells from host material. The supernatant comprising the host material was removed and re-centrifuged to pellet any contaminating algal material (4,500 x *g* for 5 min at 4°C). The resulting supernatant, comprising the purified host material, was then immediately frozen at -80°C and freeze-dried (Alpha 1-4 LD Plus, Martin Christ, Osterode am Harz, Germany). The *Symbiodinium* pellet was washed twice with 40 mL chilled MQ at 4°C, by repeated centrifugation (2,500 x *g* for 5 min at 4°C) to remove host material. The purified pellet was then frozen at -80°C and freeze-dried. Once fully dry, each fraction was weighed out (15 mg of symbiont fraction; 30 mg host fraction) into 1.5 mL microcentrifuge tubes, ready for metabolite extraction.

4.2.5 Intracellular metabolite extraction

For host samples, 750 µL of 100% cold MeOH (at -20°C) was added to each of the dry samples in order to extract the semi-polar metabolites. Methanol contained internal standards (IS) of D-Sorbitol-1-^{13}C (Sigma-Aldrich, Auckland, New Zealand) at 1%. Samples were then sonicated for 30 min at 4°C, vortexed to mix, and the non-polar fraction extracted and separated *via* centrifugation (3,060 x *g* for 30 min at 4°C).

For algal samples, lysis of the *Symbiodinium* cell wall was necessary, and achieved *via* bead-milling. Acid-washed glass beads (approximately 20 mg of 710–1,180 µm; Sigma-Aldrich, Auckland, New Zealand) and 200 µL of 100% cold MeOH (at -20°C) plus IS at 1% were added to each sample, and bead-milling (Tissuelyser II, Qiagen Inc., Hilden, Germany) conducted for 4 min at a frequency of 30 Hz. Visual counts (haemocytometer) of trial samples confirmed effective cellular disruption (over 90% of cells). A further 550 µL of 100% cold MeOH (at -20°C) were then added to each sample (including IS at 1%), and the samples centrifuged (3,000 x *g* for 30 min at 4°C).

The resulting supernatants containing the semi-polar extract were collected and stored on ice. Extraction of host cell debris or the algal cell pellet was then repeated with 750 µL 50% MeOH (at -20°C), and the samples vortexed to mix and re-centrifuged (3,000 x *g* for 30 minutes at 4°C) to extract the polar fraction. The

resulting semi-polar and polar extracts were then combined and centrifuged at 21,200 x *g* for 5 min at 4°C to precipitate any particulates. Aliquots of each fraction (200 µL host; 150 µL symbiont) were then concentrated *via* speedvac (Christ, RVC 2-33, John Morris Scientific, Melbourne, Australia) at 30°C, until dry.

4.2.6 Online derivatization and GC-MS analysis

All samples were re-dissolved in 20 µL of 30 mg mL^{-1} methoxyamine hydrochloride in pyridine and derivatized at 37°C for 120 min with mixing at 500 rpm. 20 µL *N,O-bis*-(trimethylsilyl)trifluoroacetamide (BSTFA) and 1 µL retention time standard mixture [0.029% (v/v) *n*-dodecane, *n*-pentadecane, *n*-nonadecane, *n*-docosane, *n*-octacosane, *n*-dotriacontane, *n*-hexatriacontane dissolved in pyridine] were then added and the samples incubated for 30 min with mixing at 500 rpm. Each derivatized sample then was allowed to rest for 60 min prior to injection into the GC-MS.

GC-MS analysis was performed on an Agilent 7890 gas chromatograph equipped with Gerstel MPS2 multipurpose sampler and coupled to an Agilent 5975C VL mass selective detector, run in splitless mode, with an injection volume of 1 µL of each sample and a technical replicate of two injections *per* sample. Instrument control was performed with Agilent G1701A Revision E.02.01 ChemStation software. The gas chromatograph was fitted with a Varian Factor 4 column (VF-5ms; 30 m × 0.25 mm × 0.25 µm + 10m Ezi-guard). Helium (Ultra High Purity) was in constant flow mode at approximately 1 mL min^{-1}, with retention time locking (RTL) applied. The oven temperature was started at 70°C, held at this temperature for 1 min, then increased by 7°C min^{-1} to 325°C, and finally held at this temperature for 3.5 min.

The mass spectrometer quadrupole temperature was set at 150°C, with the source set at 250°C and the transfer line held at 280°C. Positive ion electron impact spectra at 70 eV were recorded in scan mode with the following settings: gain factor 1.00; detector threshold 150; mass to charge (*m/z*) range 50-600 *m/z*; and solvent delay 6.0 min.

4.2.7 Data analysis and validation

Data were processed using the Agilent MassHunter Workstation Software, Quantitative Analysis, Version B.05.00/Build 5.0.291.0 for quantitation of all compounds. Metabolite data extraction and analysis were undertaken based on the

protocol described in Dias et al. (2015). Compound identification was based on an in-house library of MS spectra, with retention indices based on n-alkane standards and fatty acid standards (Menhaden fish oil, Sigma-Aldrich, Auckland). Where a metabolite could not be positively identified, putative identifications are presented where possible and noted with a question mark preceding the compound name. In the case of galactosylglycerol, multiple hits for this compound were detected at two retention times, indicative either of the existence of a structurally similar unknown compound (such as an intermediate), or isomers of the metabolite. In this instance the two compounds are reported as galactosylglycerol and differentiated by their respective retention times (i.e. galactosylglycerol_25.60 and galactosylglycerol_26.45). Derivative peak areas were used to semi-quantify the concentrations of individual metabolites. Data were then normalized to the final area of the internal standard and sample dry weight.

Samples were deconvoluted, peaks detected and labelled compounds identified with use of three software packages: Automated Mass spectral Deconvolution and Identification System (AMDIS), Metabolite Detector (MD) and Non-Targeted Tracer Fate Detection (NTFD) (Hiller et al., 2009; Hiller et al., 2013). Briefly, components in a given sample were separated, detected and identified during deconvolution using MD, with the application of retention indices from the alkane standard runs. Identifications were then manually cross-checked in AMDIS and MassHunter. The resulting data files were then imported directly in to NTFD for ^{13}C-enrichment analysis. The enriched (^{13}C-labelled) and non-enriched samples for each *Aiptasia* sample, or *Acropora* colony, at a given time-point and treatment were then loaded into NTFD. NTFD automatically pairs every compound detected in the labelled chromatogram to its counterpart in the unlabelled chromatogram, based on retention time and mass spectral identity (Hiller et al., 2013). The mass isotopomer distribution (MID) (i.e. M+0 – M+10) for every detected and labelled fragment ion was then calculated using the strictest detection settings in order to minimise the generation of false positives (Hiller et al., 2013; Weindl et al., 2015); required number of labelled fragments = 2, minimal isotopic enrichment = 5, R^2 = 0.98, and maximal fragment deviation = 0.02. A characteristic ion was then manually selected for each of the compounds identified as labelled. This ion was typically the most abundant and/or closest to the molecular ion. Mean values (n = 6) for each MID associated with this

ion were then calculated with standard error (S.E.M) for each compound, at a given time-point within each treatment.

In all instances, the MID is a fraction of the total ion distribution, amounting to 1, or 100% (**Fig.4.3**). Where there is no label incorporation, the non-enriched fraction (M+0) will amount to ca. 98.9%, with natural levels of ^{13}C at 1.1%. With ^{13}C enrichment, M+0 (non-labelled fraction) will decline, with corresponding increases in the labelled fraction (M+1 to M+10 etc). The sum of the total enriched fraction can therefore be represented as 1 – M+0, or M+X.

In order to account for differences in symbiont densities and relative pool sizes of each compound between treatments and time-points, in each case relative amounts of the labelled (M+X) and non-labelled (M+0) fraction were calculated for each compound, for symbiont ($_S$M+0 and $_S$M+X) and host ($_H$M+0 and $_H$M+X), based on the calculations below (**Equations 1-4)** and as illustrated in **Fig. 4.3**. It should be noted that, in the case of the host, relative amounts of each compound were first normalised to symbiont density to account for differences between treatments (i.e. bleaching) and hence translocation of labelled product (fewer symbionts, therefore less net translocated and labelled product in total).

$_S$M+0 = $M + 0 \times Normalised\ compound\ area$ [Eq. 1]

$_S$M+X = $(1 - M + 0) \times Normalised\ compound\ area$ [Eq. 2]

$_H$M+0 = $\left(\frac{Normalised\ compound\ area}{Normalised\ symbiont\ density}\right) \times M + 0$ [Eq. 3]

$_H$M+X = $\left(\frac{Normalised\ compound\ area}{Normalised\ symbiont\ density}\right) \times (1 - M + 0)$ [Eq. 4]

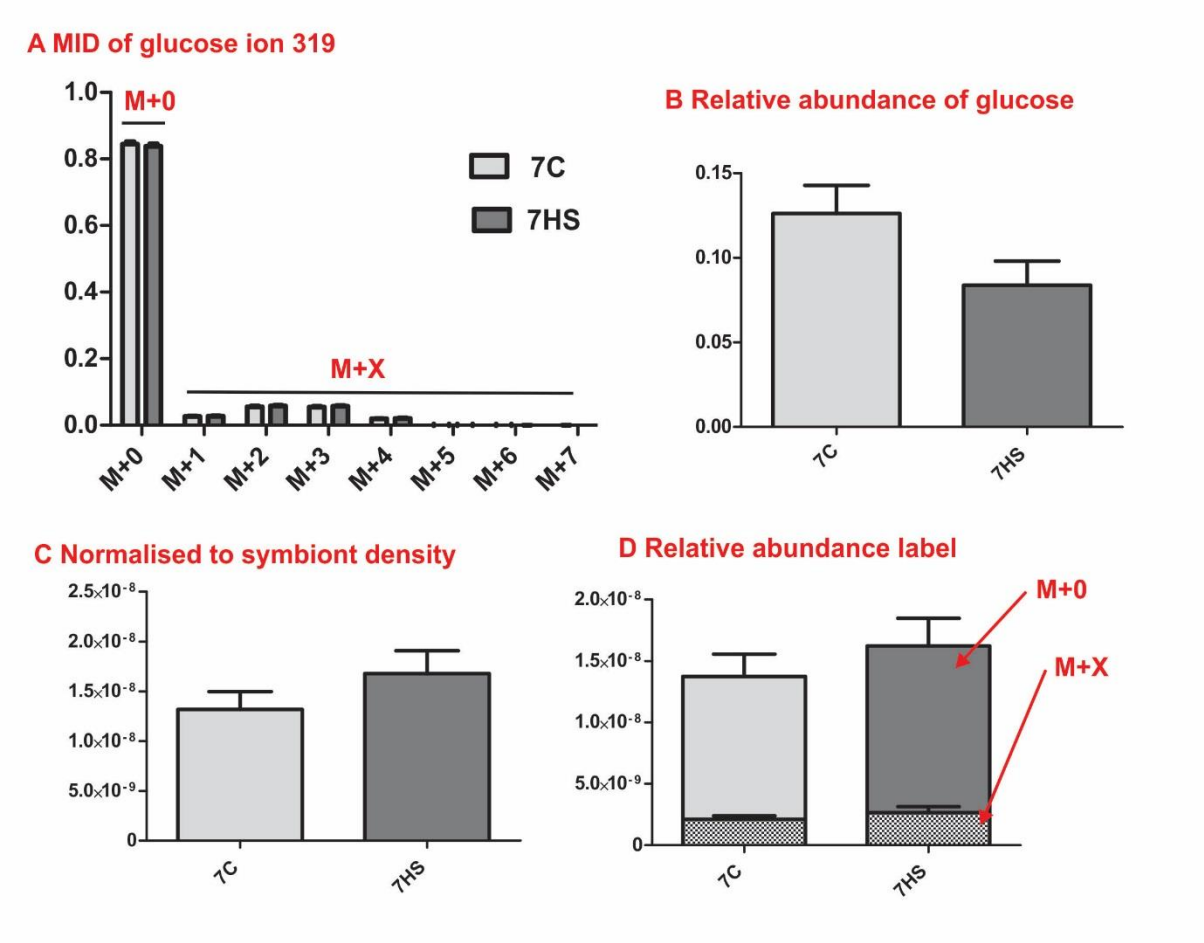

Fig. 4.3: Summary of the process of calculation for relative label amount in each compound in the host fraction. In the case of glucose: (A) Unlabelled glucose was detected in host pools at a retention time of 21.06 min. The ion 319 was used to calculate the MID (M+0 – M+10) of the compound with NTFD, in terms of label incorporation M+1 - M+10 (M+X) and the remaining unlabelled fraction (M+0), under control (7C; 7 days control temperature) and treatment (7HS; 7 days heat-stress) temperatures; (B and C) The relative abundance of glucose in each sample (B), was then normalised to respective symbiont density, producing a relative abundance normalised to symbiont cell number (C); (D) The normalised and relative amounts (y-axis) of labelled (M+X in grey hatching) and un-labelled fractions (M+0 shaded) could then be determined, by multiplying enrichment (M+X) by normalised amount of glucose. Data are means of each treatment group (*n* = 6), plus S.E.M.

As the transformed enrichment data failed the assumptions of parametric tests (normality), a non-parametric equivalent (independent samples Mann-Whitney U test) was used to compare both relative enrichment values, and relative amounts of each compound between treatments and time-points, in IBM SPSS Statistics (v22). In all other data sets, RMANOVA or one-way ANOVA were applied, as the

untransformed data met test assumptions of normality and variance. Differences were considered significant at the $P < 0.05$ probability level.

4.2.8 Quantification of bleaching in Aiptasia *and corals*

Symbiodinium cell densities were quantified in the un-enriched samples using Improved Neubauer haemocytometer counts (Boeco, Germany), with a minimum of six replicate cell counts *per* sample to a confidence interval of below 10%. Cell density was normalised to soluble protein content (*Aiptasia* sp. only), which was assessed by the Bradford assay (Bradford, 1976) carried out on the supernatant of centrifuged (16,000 x *g* for 10 min) host fraction, or to coral fragment surface area measured with the wax-dipping method (Stimson and Kinzie, 1991).

Symbiont chlorophyll *a* (Chl *a*) content was quantified in the un-enriched samples after N,N dimethylformamide (DMF) extraction in darkness over 48 h at 4°C. Extracts were centrifuged (16,000 x *g* for 5 min) and triplicate 200-µL aliquots were measured in 96-well plates (UVStar, Greiner Bio-One GmbH, Germany) at 646.8, 663.8 and 750 nm, using a microplate reader (Enspire_2300, Perkin-Elmer, Waltham, MA, USA). Chl *a* concentrations were determined after optical path-length correction (0.555 cm) using the equations of Porra et al. (1989).

4.3 Results

4.3.1 Aiptasia *thermal stress indicators*

Exposure of *Aiptasia* to 32°C for 7 days resulted in a significant decline in the maximum quantum yields of PS II (F_v/F_m; **Fig. 4.4**), which differed with time and treatment (RMANOVA, time x temperature $F_{9,72} = 10.49$, $P < 0.001$, with Bonferroni correction). After 7 days, F_v/F_m within the treatment group declined ca. 8% to 0.59 ± 0.01 *versus* 0.64 ± 0.01 in the control. However, this relatively small decline in maximum quantum yields coincided with a 49% reduction in symbiont density relative to controls at 7 d (4.89 $x10^6$ cells mg^{-1} protein ± 0.38 $x10^6$ S.E. *versus* 9.62 $x10^6$ cells mg^{-1} protein ± 0.51 $x10^6$ S.E.M, respectively; one-way ANOVA, $F_{1,12} = 35.02$, $P < 0.001$). Chlorophyll *a* concentration *per* remaining cell, however, was not significantly affected by temperature, with values ranging from approximately 2.03 to 3.07 pg chl *a* $cell^{-1}$ (one-way ANOVA, $F_{1,10} = 3.27$, $P = 0.101$).

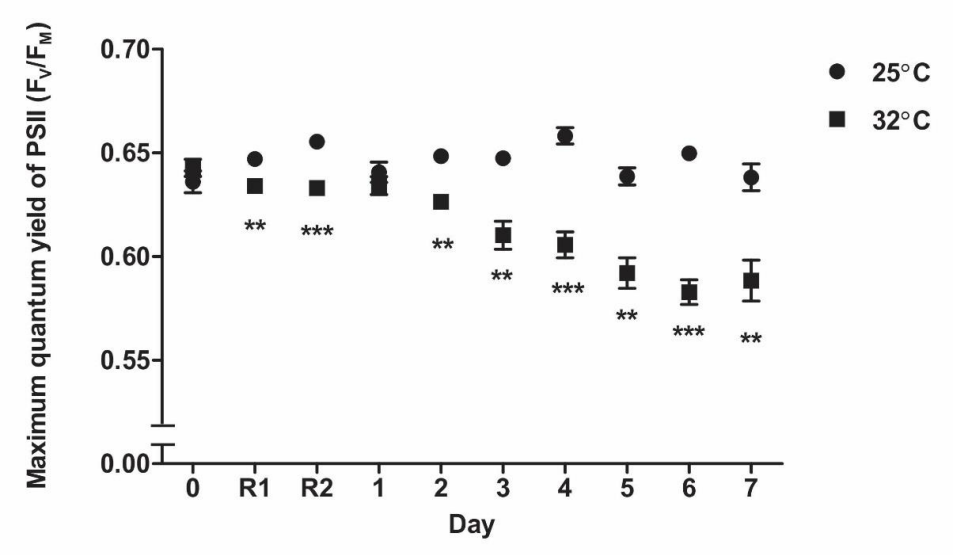

Fig. 4.4: Daily measurements of maximum quantum yields of PSII of *in hospite Symbiodinium* in *Aiptasia* at 25°C and 32°C. R1 – R2: heat ramp for treatment group (ca. 1°C 3 h^{-1} during the light). Asterisks denote statistically significant test results, * $P < 0.05$, ** $P < 0.005$, *** $P < 0.001$. ($n = 5$; values are means ± S.E.M).

4.3.2 Acropora aspera *thermal stress indicators*

Exposure to 32°C for both 6 and 9 days resulted in significant declines in the maximum quantum yields of PS II (F_v/F_m; **Fig. 4.5**), which differed with time and treatment (RMANOVA, time x temperature $F_{15,150} = 21.13$, $P < 0.001$, with Bonferroni correction). After 6 days, F_v/F_m within the treatment group declined ca. 15% to 0.61 ± 0.05, compared to 0.72 ± 0.01 in the control. After 9 days, photoinhibition was more severe in the treatment group, with a decline of ca. 36% to 0.46 ± 0.13, compared to 0.72 ± 0.01 in the control.

Symbiodinium cell density also declined significantly in the heat-treatment group at both 6 d (one-way ANOVA, $F_{1,10} = 42.49$, $P < 0.001$) and 9 d (one-way ANOVA, $F_{1,10} = 65.78$, $P < 0.001$). Elevated temperature caused a reduction of ca. 39% and 69% in symbiont density relative to controls after 6 and 9 days, respectively (**Fig. 4.5**). Chlorophyll *a* concentration *per* cell, however, remained unaffected by temperature, with values ranging from approximately 4.9 to 4.4 pg chl *a* $cell^{-1}$ (one-way ANOVA, 6 d $F_{1,10} = 1.339$, $P = 0.274$, 9 d $F_{1,10} = 1.609$, $P = 0.233$).

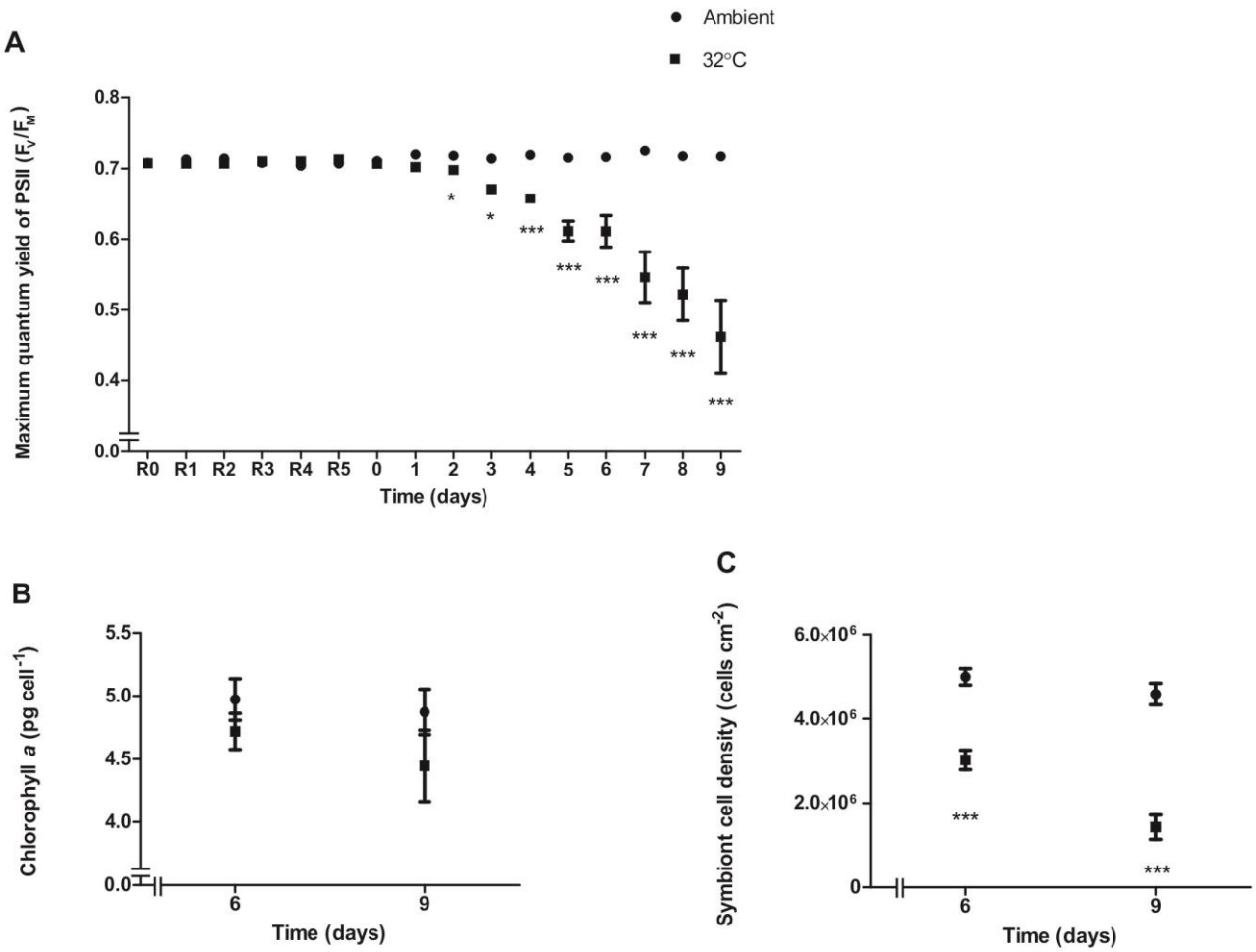

Fig. 4.5: Bleaching response of *Acropora aspera* to elevated temperature. (A) Maximum quantum yield of PSII of *in hospite Symbiodinium* in *A. aspera* fragments versus time at ambient temperature (ca. 27°C) and elevated temperature 32°C (n = 6). R0 – R5: heat ramp for treatment group (ca. 1°C day^{-1}). (B) Symbiont chlorophyll a content cell^{-1} and (C) symbiont cell density following 6 and 9 days exposure to 32°C (n = 6). In each case, asterisks denote statistically significant test results, * $P < 0.05$, ** $P < 0.005$, *** $P < 0.001$. (n = 6; values are means ± S.E.M.)

4.3.3 *^{13}C labelling in* Aiptasia

A total of 32 compounds were consistently labelled from symbiont (26 in total) and host (13 in total) free pools in the *Aiptasia* model (**Table S4.1** and **S4.2**). In the symbiont fraction, almost half of these compounds were comprised of saturated, monounsaturated and polyunsaturated fatty acids, in addition to a number of lipogenesis intermediates. In contrast, in the host fraction the majority of labelled compounds were comprised of a range of carbohydrate groups, namely sugar alcohols, and mono- and disaccharides. Thermal stress resulted in altered relative pool size (abundance) and label amount (M+X) in metabolite pools of both symbiont and host; changes to each partner are discussed in more detail in the sections below.

Aiptasia- *associated symbiont*

Fatty acids comprised the major group (in terms of number of compounds) that were labelled in the dinoflagellate, though the highest degree of enrichment was detected in monosaccharide sugars (glucose and galactose), central pathway- (citrate) and lipogenesis intermediates (galactosylglycerol_25.60, monopalmitoylgylcerol and monohexadecanoylglycerol). Under ambient conditions, total enrichment (M+X) of these compounds was ca. 35%. In contrast, label incorporation into the fatty acid pool was around ca. 15%-20%. Label was detected in a number of compounds under control conditions, where no tracer was detectable under thermal stress; these included glycerol, threonate, C22:0 and melibiose (**Table S4.1**).

Interestingly, in the case of glucose, citrate and the major fatty acids C16:0 and C18:0, there was no effect of thermal stress on either compound pool size or enrichment (**Fig. 4.6**). In contrast, thermal stress resulted in a number of complex changes to both pool size and enrichment in a number of downstream metabolites. Primarily, this involved increased enrichment of the monosaccharide galactose and increased pool size of the sugar alcohol scyllo-inositol; notably, for scyllo-inositol, this increase in pool size was ca. 620% relative to controls. In contrast, a reduction in label incorporation was observed for the disaccharide turanose and the fatty acid C16:1, coupled to declines in the pools of adenosine, maltose, turanose, galactosylglycerol_25.60, C12:0, C14:0, C16:1 and an unidentified fatty acid.

A. Carbohydrates

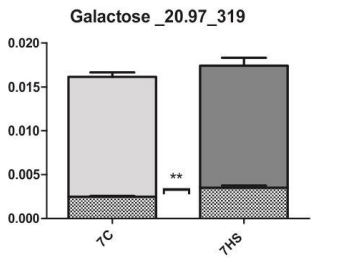

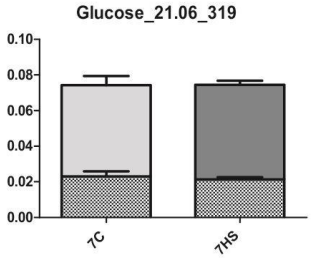

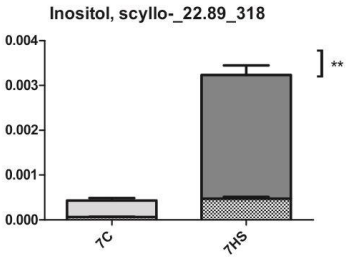

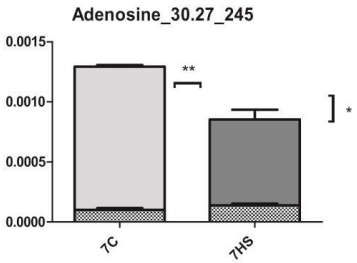

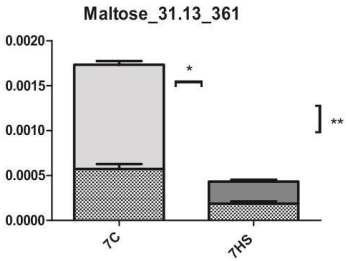

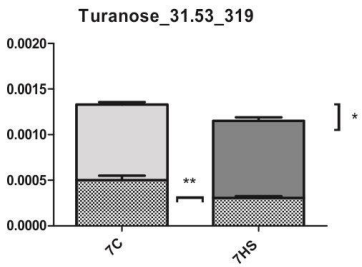

B. Intermediates

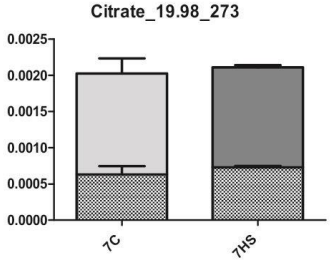

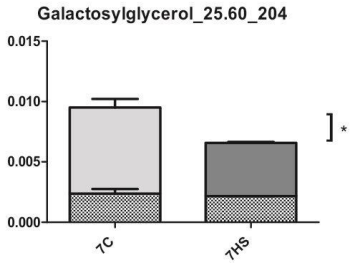

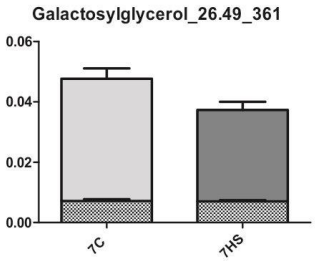

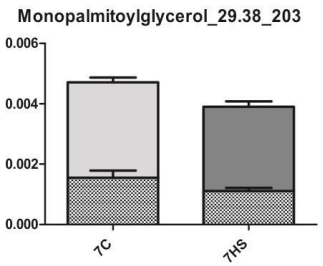

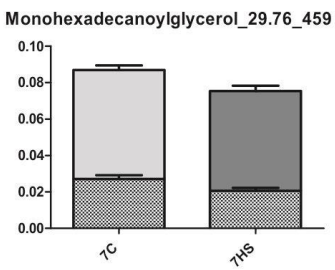

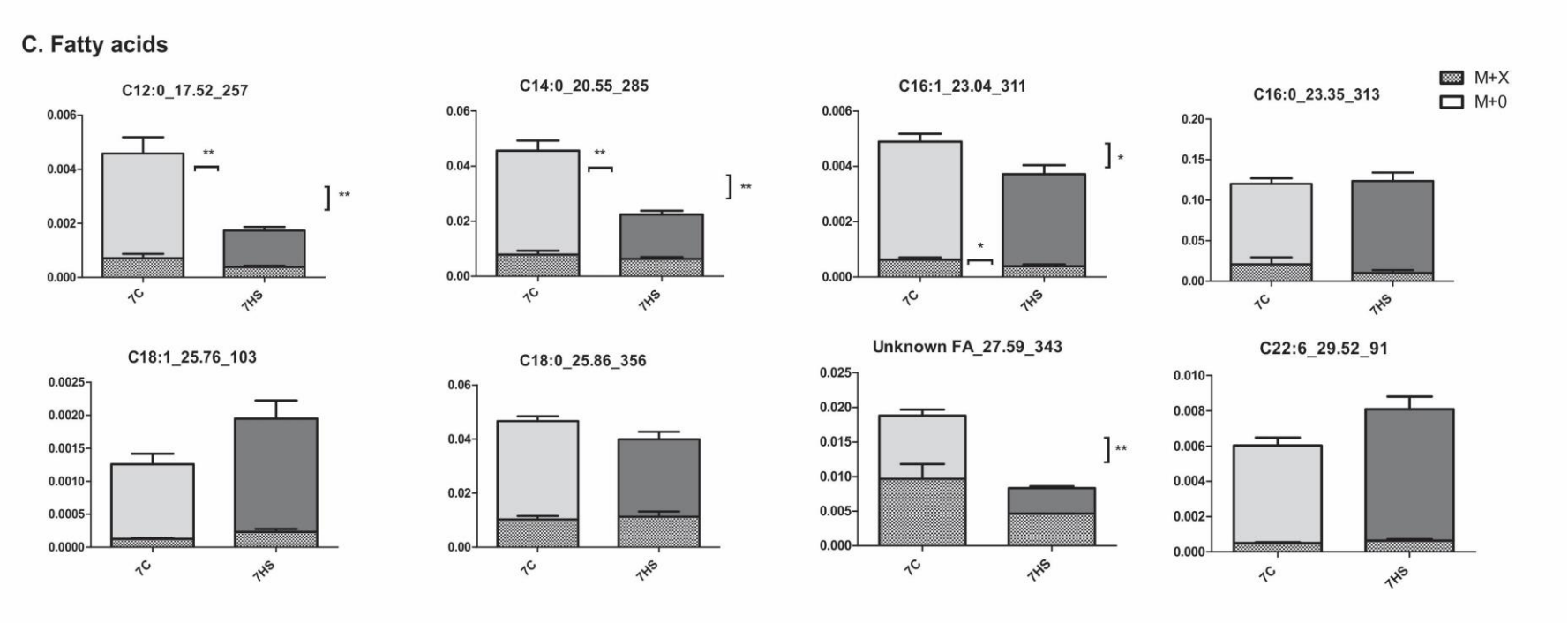

Fig. 4.6 (above and previous page): Enrichment (M+X) and abundance of key compounds in symbiont pools at the control temperature (C) and under heat stress (HS) at 7 d, with un-labelled retention time and quantification ion. Grey hatching represents the labelled (M+X) fraction of the total pool (total bar height) and the remaining shaded fraction represents the unlabelled (M+0) fraction. Data are normalised relative mean abundances plus S.E.M. (n = 6). Horizontal brackets represent significant differences between treatments of either M+0 or M+X. Vertical brackets represent significant differences between treatments in normalised relative abundance of a given compound (Mann Whitney U test). Asterisks denote significance at * P < 0.05, ** P < 0.01, *** P < 0.001.

Aiptasia *host*

Interestingly, under control conditions, the major labelled compound in the *Aiptasia* host fraction was the sugar alcohol myo-inositol, which was ca. 48% labelled. This was followed by the lipogenesis intermediate galactosylglycerol_25.60 and the monosaccharide galactose, ranging from ca. 20 – 28% enriched (**Fig. 4.7**).

When the abundance of individual compounds in host pools were normalised to symbiont number, there was no effect of thermal stress on pool size of a number of metabolites, including the mono- and disaccharide sugars fructose, galactose and glucose. Similarly there was also no difference in enrichment of these compounds between treatments. In contrast, a large increase in both enrichment and pool size was detected for the sugar alcohol scyllo-inositol. Once again, the scale of increase in scyllo-inositol with thermal stress was notable, at ca. 1300% compared to controls. In addition, there was also increased enrichment of the lipogenesis intermediate galactosylglycerol_25.60 with thermal stress. This was coupled to increased pools of glycerol and myo-inositol in the heat-stressed group.

Label was detected in a number of compounds under control conditions for which no detectable labelling was observed under thermal stress, and *vice versa*. Compounds that were enriched under control conditions only included sucrose and turanose, whilst those only labelled during thermal stress included the antioxidant precursors glutamate and pyroglutamate, in addition to the glycolysis intermediate glycerate (**Table S4.2**).

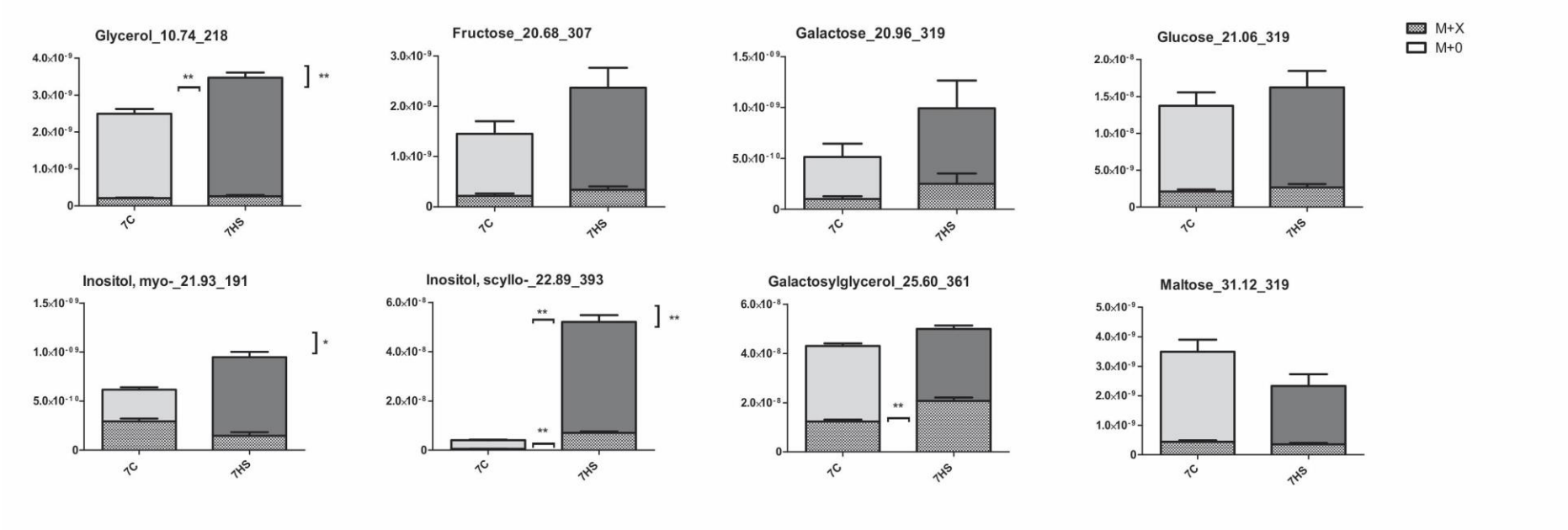

Fig. 4.7: Enrichment (M+X) and abundance of compounds in host pools under control (C) and heat stress (HS) at 7 d, with un-labelled retention time and quantification ion. Grey hatching represents the labelled (M+X) fraction of the total pool (total bar height) and the remaining shaded fraction represents the unlabelled (M+0) fraction. Data are normalised relative mean abundances plus S.E.M. (n = 6). Horizontal brackets represent significant differences between treatments of either M+0 or M+X. Vertical brackets represent significant differences between treatments in normalised relative abundance of a given compound (Mann Whitney U test). Asterisks denote significance at * $P < 0.05$, ** $P < 0.01$, *** $P < 0.001$.

4.3.4 ^{13}C *labelling in* Acropora aspera

A total of 47 compounds were consistently labelled from symbiont (21 in total) and host (34 in total) fractions of the coral *A. aspera* (**Table S4.3** to **S4.6**). As for *Aiptasia*, in the symbiont the majority of labelled compounds consisted of fatty acids and lipogenesis intermediates. In the coral host, a greater number and diversity of labelled compounds were detected compared both to the coral symbiont and the *Aiptasia* model (both host and symbiont), including a number of amino acids, intermediates, carbohydrates, fatty acids and lipogenesis intermediates. Thermal stress for 6 d and 9 d resulted in a number of complex changes, both with respect to the relative abundance and enrichment (M+X) of the free metabolite pools of symbiont and host; changes to each fraction are discussed in more detail in the sections below.

No significant enrichment of either symbiont, or host pools was detected in the dark incubations, suggesting that label incorporation was *via* symbiont photosynthesis and translocation of organic products.

Acropora-*associated symbiont*

Under ambient conditions, high enrichment (between 32-69%) was detected in a number of metabolite groups, including glycerol, C14:0, glucose, C16:0, and monopalmitoyl- and monohexadecanoylglycerol. However the greatest labelling was detected in an unidentified sugar detected at a retention time of 38.70 (73% enriched) (**Fig.4.8**).

Thermal stress resulted in a number of complex modifications to both relative pool size and enrichment of a number of compounds, which varied with stress duration. Pools of a number of central carbon metabolites were elevated with thermal stress, including glucose (ca. 190% at 9 d) and glycerol (ca. 200% at 6 d and 80% at 9 d). In the case of glycerol at 6 d, this increase in pool size was also reflected in the enrichment of the pool, corresponding to an increase of M+X by 200% at ca. 32% enriched.

Similarly, there was also increased labelling of the galactose pool at 6 d thermal stress (100% increase and ca. 15% enriched). In addition, pools of early phase lipogenesis intermediates were also elevated at both 6 d and 9 d relative to controls,

including pools of monopalmitolylglycerol, monohexadecanoylglycerol, C12:0, C14:0 and C16:0. For C12:0 and C14:0, the scale of change was notable at both 6 d and 9 d, with increased pools of C12:0 (480% and 530%, respectively) and C14:0 (290% and 277%, respectively). Coupled to these large accumulations of C12:0 and C14:0 with thermal stress, overall enrichment was reduced (ca. 50% control to ca. 30% heat stress), though at 6 d relative pool size of the M+X fraction had increased. At 9 d thermal stress, however, enrichment of the total pool was further reduced to ca. 20%.

Coinciding with these accumulations of early-stage lipogenesis intermediates and fatty acids in the symbiont pools, there was a decline in the enrichment of the longer-chain fatty acids at 9 d (and in some cases no label was detected); namely C20:5, C20:0 and C22:6, in addition to the lipogenesis intermediate galactosylglycerol_26.45.

A. Carbohydrates

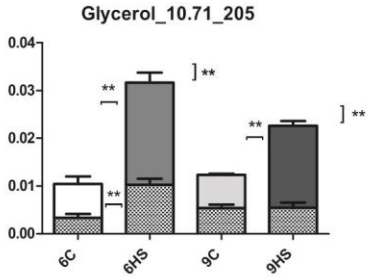

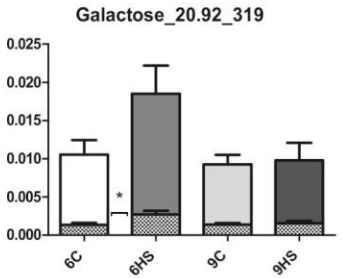

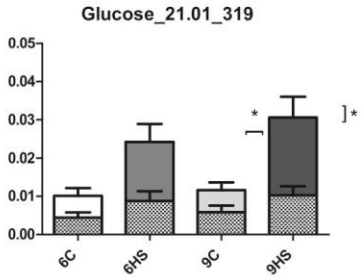

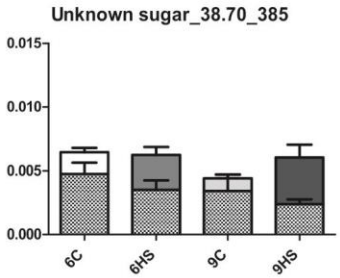

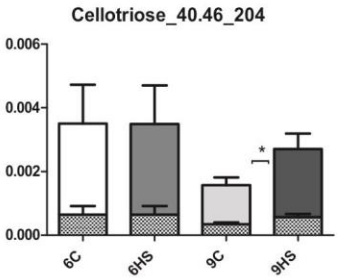

B. Intermediates

M+0
M+X

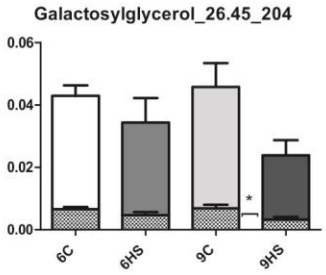

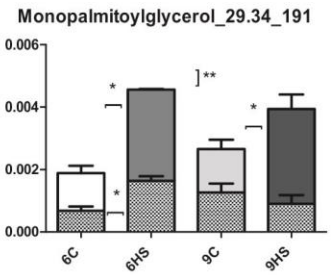

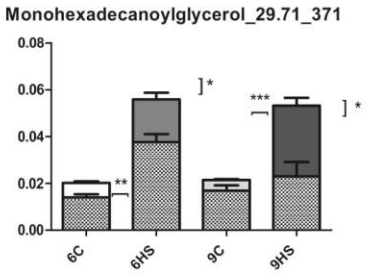

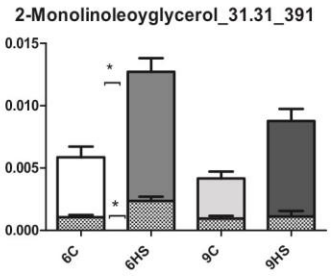

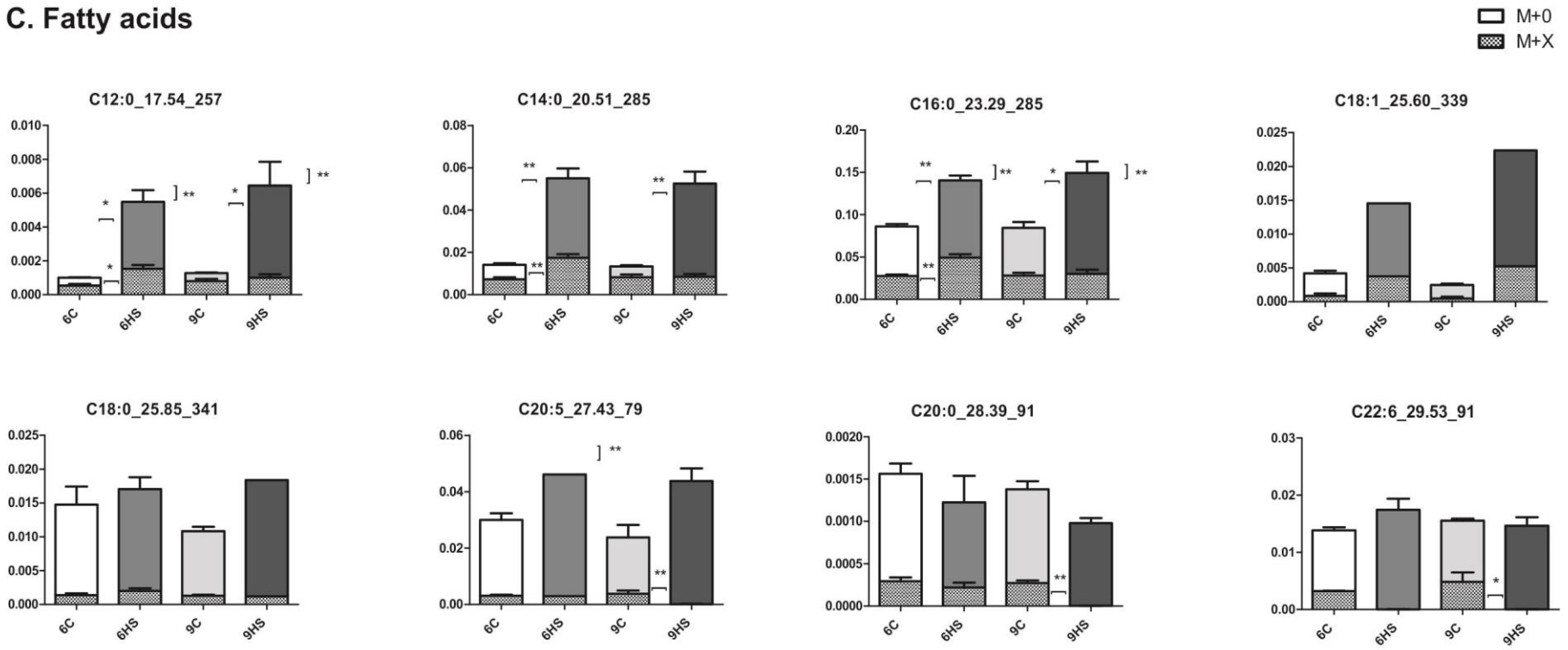

Fig. 4.8 (above and previous page): Enrichment (M+X) and abundance of compounds in symbiont pools under control (C) and heat stress (HS) at 6 d and 9 d, with un-labelled retention time and quantification ion. Grey hatching represents the labelled (M+X) fraction of the total pool (total bar height) and the remaining shaded fraction represents the unlabelled (M+0) fraction. Data are normalised relative mean abundances plus S.E.M. (n = 6); where no error bar is present label was detected in only a single replicate. Horizontal brackets represent significant differences between treatments of either M+0 or M+X. Vertical brackets represent significant differences between treatments in normalised relative abundance of a given compound (Mann Whitney U test). Asterisks denote significance at * $P < 0.05$, ** $P < 0.01$, *** $P < 0.001$.

Acropora *host*

As for the symbiont, relatively high levels of enrichment (31-73%) were detected in the coral host for a number of compounds under ambient conditions, including glycerol, glycerate, galactose, scyllo-inositol and monopalmitoylglycerol, with the highest enrichment in the lipogenesis intermediate galactosylglycerol_25.60 (ca. 75% enriched). Following normalisation to account for differences in symbiont density, thermal stress resulted in a number of complex modifications to both relative abundance and enrichment of multiple compounds, which varied with stress duration. Most notably, there was a large increase (above 200%) in the abundance of a number of compounds at 9 d; for instance glycerol (ca. 270%), serine (ca. 1000%) and proline (ca. 200%) (**Fig. 4.9**).

In contrast, the abundance of some compounds, when normalised to symbiont density, closely mirrored dinoflagellate number (i.e. they appeared unchanged according to treatment after normalisation); for instance maltose, erythronate, glycerate, glutamate and galactosylglycerol_26.45.

Additional modifications after thermal stress were observed for a number of compounds in terms of enrichment and abundance, at both 6 d and 9 d. Interestingly, there were notably large increases of the labelled galactose pool with thermal stress at both sampling points (ca. 80% and 160%, respectively) and glucose at 9 d only (ca. 1200%). In contrast, there was reduced enrichment after 9 d of thermal stress for a number of compounds, including turanose, proline, C16:0, galactinol and galactosylglycerol_25.60. In addition, no label was detected in a number of compounds at 9 d, including myo-inositol, C14:0, or the lipogenesis intermediates monopalmitolyglycerol, monohexadecanoylglycerol and digalactosylglycerol. The lack of labelling after 9 d of thermal stress in myo-insitol is notable given that relative pool size was elevated by ca. 1300%. In contrast, pools of scyllo-inositol were both elevated (ca. 370%) and increasingly labelled (ca. 1110% increase, 20% enriched) after 9 d of elevated temperature.

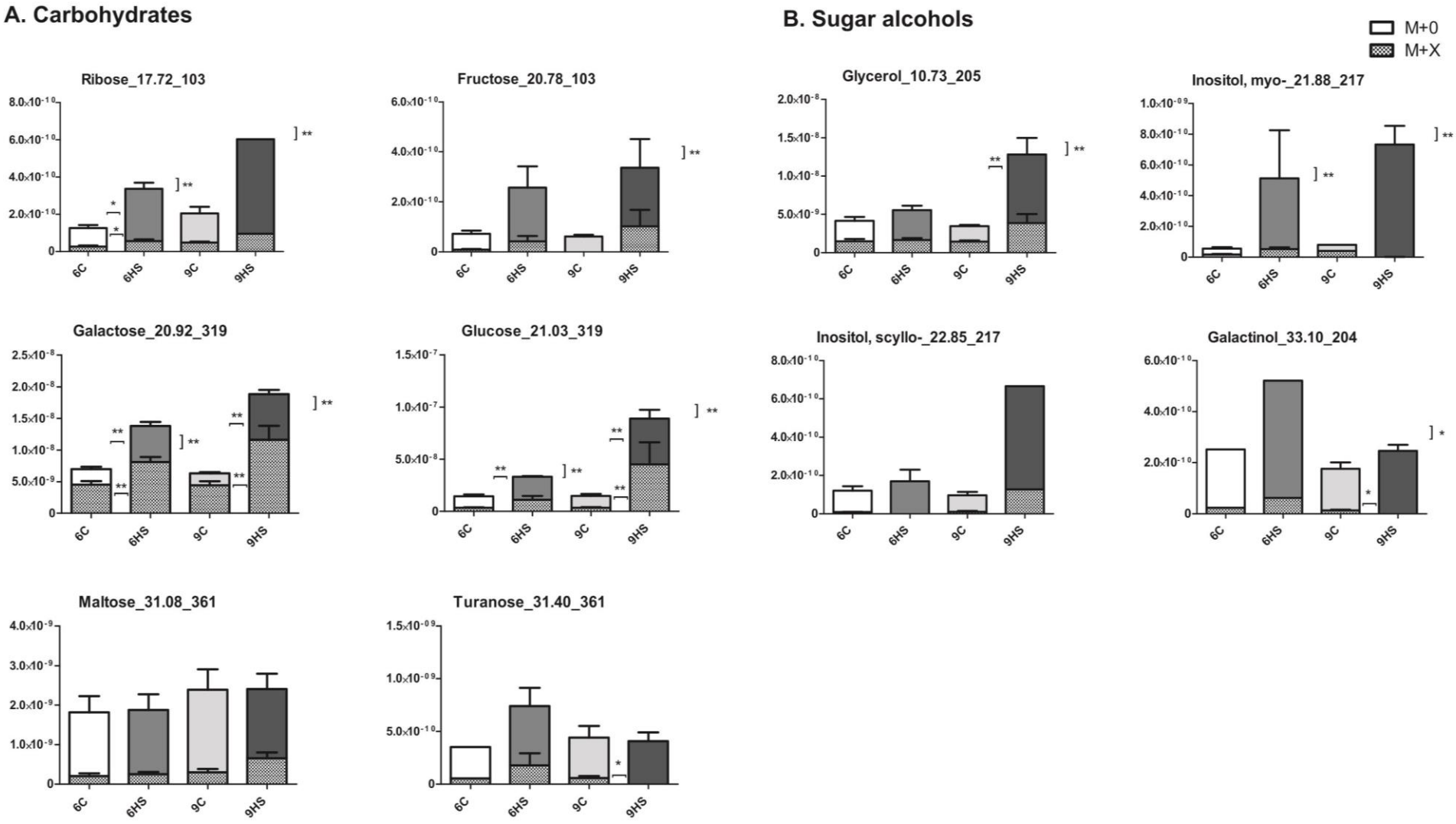
A. Carbohydrates
B. Sugar alcohols
M+0
M+X
Ribose_17.72_103
Fructose_20.78_103
Glycerol_10.73_205
Inositol, myo-_21.88_217
Galactose_20.92_319
Glucose_21.03_319
Inositol, scyllo-_22.85_217
Galactinol_33.10_204
Maltose_31.08_361
Turanose_31.40_361
6C
6HS
9C
9HS

C. Amino acids and intermediates

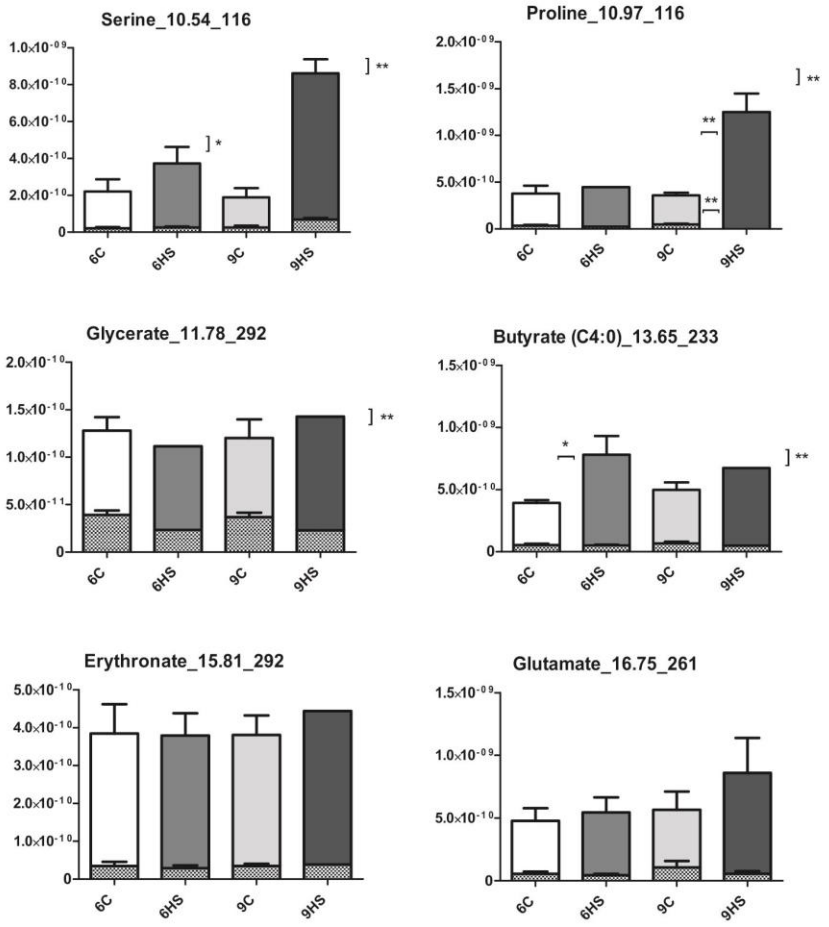

D. Lipogenesis intermediates

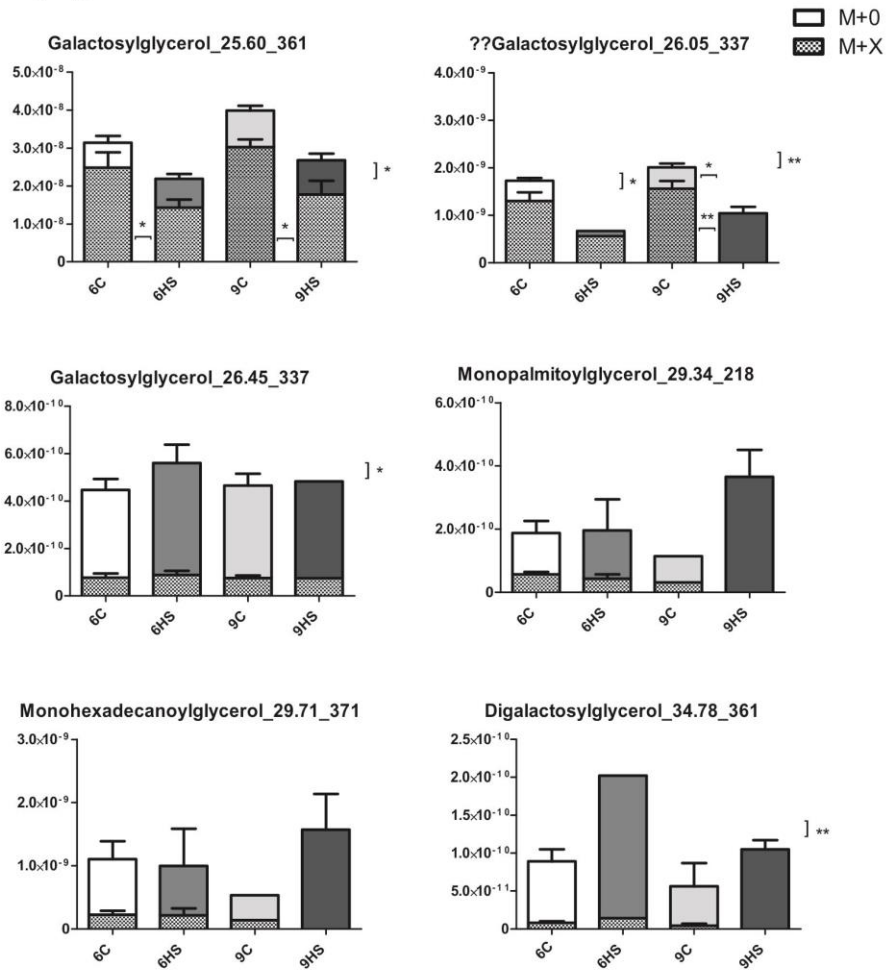

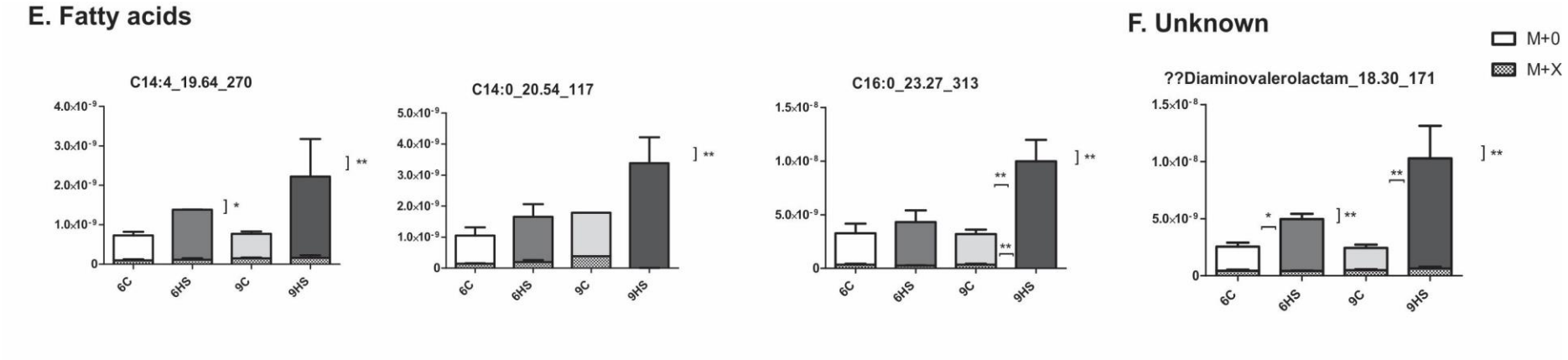

Fig. 4.9 (Above and previous pages): Enrichment (M+X) and abundance of compounds in host pools under control (C) and heat stress (HS) at 6 d and 9 d, with un-labelled retention time and quantification ion. Grey hatching represents the labelled (M+X) fraction of the total pool (total bar height) and the remaining shaded fraction represents the unlabelled (M+0) fraction. Data are normalised relative mean abundances plus S.E.M. (n = 6); where no error bar is present label was detected in only a single replicate. Horizontal brackets represent significant differences between treatments of either M+0 or M+X. Vertical brackets represent significant differences between treatments in normalised relative abundance of a given compound (Mann Whitney U test). Asterisks denote significance at * $P < 0.05$, ** $P < 0.01$, *** $P < 0.001$.

4.4 Discussion

Exposure to elevated temperatures (32°C for 6 d, 7 d and 9 d) resulted in declines in maximum quantum yields of PS II relative to control or ambient conditions, in the *in hospite* dinoflagellate symbionts of *Aiptasia* sp. and the coral *Acropora aspera* (harbouring *Symbiodinium* ITS 2 types B1 and C3, respectively). Changes in the efficiency of PS II in *Aiptasia* were relatively minimal across the experiment (ca. 8% decline in maximum yields of PS II relative to controls at 7 d) and appeared to stabilise prior to metabolite sampling at 7 d. Continuing declines in maximum quantum yields of PS II were more apparent in *A. aspera,* perhaps due to the greater irradiance to which it was subjected (maximum mid-day irradiance of around 500 µmol quanta m^{-2} s^{-1} compared to 95 µmol quanta m^{-2} s^{-1}). Reductions in maximum quantum yields of PS II are considered indicative of photoinactivation and photoinhibition in the dinoflagellate symbiont (Warner et al., 1996; Jones et al., 1998; Warner et al., 1999) and here coincided with large declines in symbiont density (up to ca. 70% in *A. aspera* at 9 d), characteristic of bleaching during thermal stress (Hoegh-Guldberg and Smith, 1989; Jokiel and Coles, 1990).

This thermal stress resulted in clear changes to the free metabolite pools of symbiont and host in both symbioses. These modifications were principally associated with alterations to central metabolism, biosynthesis pathways, the breakdown of energy stores and the maintenance of oxidative and osmotic state. However, perhaps surprisingly given the degree of thermal stress and photodamage observed, in all instances there was continued fixation and translocation of labelled organic products, suggesting that remaining symbionts were, at least in part, metabolically functional in terms of continued provision of mobile products towards host metabolism.

4.4.1 Continued carbon fixation and mobile product translocation during thermal stress

Interestingly, in all treatments and at all sampling time-points, there was significant labelling (above 30%) of organic compounds detected in symbiont and host free-metabolite pools. As no enrichment was detected in either the pools of the symbiont or host dark controls (*A. aspera* only was tested in this

respect), this would imply that even during the pronounced stages of thermal stress seen after nine days of elevated temperature in *A. aspera*, the remaining symbionts continued to fix carbon, synthesise organic compounds *de novo* and translocate mobile products to the host. Given that glucose is a major output of carbon fixation in the dinoflagellate (Streamer et al., 1993; Whitehead and Douglas, 2003; Burriesci et al., 2012), it would be expected that, under optimal conditions (i.e. non-photoinhibited) with high rates of carbon fixation and energy generation, glucose pools would turnover at a rapid rate with a high degree of label incorporation. In contrast, during thermal stress and photoinhibition, the rate of carbon fixation, and therefore the production of glucose *de novo* (and therefore labelled glucose) would decline (Smith et al., 2005; Hoogenboom et al., 2006).

In *Aiptasia* after seven days of elevated temperature treatment, there was no difference in either the relative abundance or the degree enrichment of glucose, in either the symbiont (ca. 30% enriched) or host (at ca. 15% enriched) intracellular pools. This was likely as a result of the minimal photodamage observed to the *Aiptasia*-associated symbiont and the stabilisation of maximum quantum yields prior to metabolite sampling. It may be that in this instance the symbiosis was, following a degree of bleaching, able to acclimate to the new conditions and establish a new steady state density, such as previously shown following bleaching (Jones and Yellowlees, 1997; Jones et al., 2008). However, in the coral-associated dinoflagellate after both six and nine days of thermal stress, there was also no change in the enrichment of the glucose pool, which remained high (ca. 50-30% enriched). These findings are surprising, particularly in the more advanced stages of photodamage observed at day nine. As photoinhibition leads to a reduction in carbon fixation and turnover of the Calvin cycle (Jones et al., 1998; Smith et al., 2005), a decline in the production and enrichment of associated downstream products would be expected under these conditions. Therefore it may be that in this instance the rate of repair to photosystems was able to keep pace with the rate of damage, with photosystems under a state of photoinactivation, rather than photoinhibition. Additionally given the central role of glucose in metabolism, it is likely that the turnover of this compound is

tightly regulated (Geiger and Servaites, 1994; Smeekens et al., 2010). It is therefore conceivable that, where carbon fixation is still on-going, but under conditions of ATP limitation (such as associated with conditions of photoinactivation), energy requirements for the *de novo* production of glucose in the dinoflagellate (and therefore continued high enrichment) are sourced from alternate sources, such as the breakdown of energy stores (lipid and starch) (see glyoxylate cycle below).

Further to this, in the pools of the coral host there was a massive increase (*per* symbiont cell) in the amount of enriched and non-enriched glucose under thermal stress, which corresponded to a 500% and 1200% increase in the labelled fraction at 6 d and 9 d, respectively. The scale of this increase in glucose abundance *per* symbiont in the host may reflect, in part, an artefact of the normalisation process. That is, as glucose is a central metabolite, total pools (M+0 and M+X) are unlikely to be entirely symbiont-derived; as a result, normalisation to symbiont number in the bleached fragments would potentially result in a large relative increase *per* symbiont. However, this accumulation of glucose was also coupled to an increase in enrichment of the compound in host pools. Taken together these data indicate continued glucose synthesis *de novo*, translocation of the enriched compound, input from non-labelled sources (such as associated with gluconeogenesis) and increased metabolism (turnover) of this compound under thermal stress in free pools of the *A. aspera* host.

These data therefore support previous work from the *in hospite* symbiosis, showing glucose to be the major translocated mobile compound in the symbiosis (Ishikura et al., 1999; Whitehead and Douglas, 2003; Burriesci et al., 2012), as opposed to the traditionally held view of glycerol as the dominant component of translocated photosynthate (Muscatine, 1967; Muscatine and Cernichiari, 1969; Trench, 1971). Further to this, the degree of labelling of glucose pools in the heat-stressed coral host also suggests that, under thermal stress and photodamage, translocation is not only still ongoing, but may actually increase *per* symbiont. As such remaining *in hospite* symbionts may still play a role in the maintenance of host energy budgets (primarily respiration) (Muscatine et al., 1984; Bachar et al., 2007) during

ongoing bleaching. This increase in *per* symbiont translocation of carbon at lower symbiont densities, may be due to increases in the availability of light and inorganic compounds, such as DIC and DIN (Tremblay et al., 2014; Hoadley et al., 2016). Nevertheless, the drastic reductions in symbiont density seen here, coupled to increased respiration in the heat-stressed hosts (Coles and Jokiel, 1977; Clark and Jensen, 1982), would still likely necessitate additional energy generation from alternate sources, such as the breakdown of energy stores (lipid and protein) (Grottoli et al., 2004; Imbs and Yakovleva, 2012) and where possible an increase in heterotrophy (Grottoli et al., 2006).

Further to the continued translocation of glucose in the heat-stressed coral, a number of other compounds were also detected in the anemone and coral that may function as mobile (i.e. translocated) compounds under both ambient conditions and those associated with elevated temperature; these include maltose, glycerate, erythronate, glutamate and galactosylglycerol_26.45. In all cases, following normalisation to symbiont number, relative pool size and label incorporation closely matched symbiont number between sampling days (and therefore appeared unchanged). The presence of organic acids is unsurprising, as a number have been previously recorded as mobile compounds in the symbiosis (including glutamate and glycerate) (Muscatine and Cernichiari, 1969; Trench, 1971; Burriesci et al., 2012). Similarly. lipids have also been reported as translocated compounds (Patton et al., 1977; Kellogg and Patton, 1983; Papina et al., 2003), however the detection of maltose was surprising as this has not been reported previously in the translocate of this symbiosis (though it is well known in the hydra-*Chlorella* symbiosis) (Cernichiari et al., 1969; Mews, 1980). Maltose is a product of starch breakdown, and as the symbiont has major starch stores its exchange is plausible, yet its lack of detection in previous studies of translocation in symbiotic anthozoans suggests the possibility of another origin, as discussed further in **Section 4.4.5**.

4.4.2 Enhanced galactose metabolism during thermal stress

Also of note were thermally-induced modifications to both the enrichment and abundance of pools of a number of carbohydrates, particularly galactose. These alterations to the galactose pool were to a lesser extent in the

anemone, where in the symbiont fraction only, there was an increase in the enriched pool of ca. 40%. Similarly in the heat stressed symbionts of *A. aspera* at 6 d only, there was an increase in the abundance of the labelled compound of ca. 100%. These increases were not coupled to significant changes in the total pool size of the compound, suggesting instead increased turnover of the labelled pool only (*de novo* synthesis) during the initial phases of thermal stress, which was not observed in the later stage of thermal stress at 9 d. In the pools of the heat-stressed anemone host, a trend of increase was observed in the abundance of both the labelled and non-labelled fraction (i.e. an increase in the total galactose pool size). Further to this, in the coral host, abundances of the labelled and non-labelled compound were significantly increased with thermal stress at both sampling points. At 9 d this increase in the total pool size was to the greatest extent, at around 200%. Interestingly however, in all treatments enrichment of the coral host's galactose pool was high (ca. 60-70% labelled). As galactose forms a major portion of the coral host's free metabolite pool under ambient and heat-stress conditions (**Chapter 3**), this high degree of enrichment is most likely associated with rapid incorporation and turnover of this pool. It is therefore likely that this monosaccharide plays a central role in some aspect of the metabolism of the coral symbiosis, and that turnover of symbiont pools and input into host pools is enhanced during thermal stress from both photosynthetic and non-photosynthetic sources.

Few data are available on the metabolism of galactose in the cnidarian-dinoflagellate symbiosis, and it has not previously been reported as a mobile compound in the symbiosis. Excluding symbiont translocation, host galactose pools may be sourced *via* a number of central biosynthesis pathways, and based on analysis of Kyoto Encyclopedia of Genes and Genomes (KEGG) data for the anemone *Nematostella vectensis* (http://www.genome.jp), synthesised from glucose, the hydrolysis of glycerolipids such as galactosylglycerol, or from heterotrophic sources associated with the breakdown of lactose. Galactose may then be used in central metabolic processes, such as glycolysis, and in biosynthesis pathways, such as the production of glycerolipids, glycoproteins and other complex polymers, like

those associated with the organic matrix of the coral skeleton (Cuif et al., 1999; Ramos-Silva et al., 2014). Galactose-binding lectins also play an essential role in cellular recognition, and the establishment and maintenance of symbiosis (Fenton-Navarro et al., 2003; Wood-Charlson et al., 2006). The role of this compound in the coral-symbiosis clearly requires further study, however it is of interest that the turnover of this pool (i.e. the degree of labelling) is so much greater in the coral host than in *Aiptasia*. This may, in part, be due to differences in the physiologies of the anemone and reef-building coral, including skeleton formation and the production of skeletal organic matrix-associated compounds.

4.4.3 Modifications to lipogenesis and energy stores during thermal stress

Another major change detected in symbiont pools of both *Aiptasia* and the coral (and to a lesser extent the coral host), were thermally-induced modifications to pools of a number of fatty acids, primarily the usually rare mid-length fatty acids, C12:0 and C14:0; in both cases, large alterations to the relative size of these fatty acid pools were seen. Interestingly, however, these changes were not consistent between symbioses. In the case of the *Aiptasia* symbiont (*Symbiodinium* ITS 2 type B1), there was a decline in pool size of both C12:0 and C14:0 (ca. 60% and 50%, respectively) with exposure to elevated temperature. This decline accompanied an increase in the overall enrichment of the total pool (M+0 and M+X), from ca. 15% to 25% enriched. A similar decline in abundance in the symbiont of *Aiptasia* was also observed with respect to the lipogenesis intermediate galactosylglycerol_25.60 and the fatty acid C16:1; this was accompanied by increased enrichment of the galactosylglycerol_25.60 pool in the *Aiptasia* host tissues.

In contrast, in the coral symbiont (*Symbiodinium* ITS 2 type C3) subjected to thermal stress, there was a large increase in pool size of these same fatty acids, at both 6 d and 9 d (ca. 530% for C12:0 and 280% for C14:0 at 9 d). For both C12:0 and C14:0, the increased pool size coincided with a reduction in labelling of the total pool (ca. 50% to 30% enriched). A similar trend in the coral-associated dinoflagellate was also observed for glycerol (a precursor to fatty acid synthesis), C16:0 and multiple lipogenesis intermediates. These changes were also reflected in modifications to multiple lipogenesis

intermediates in the coral host pool (primarily galactosylglycerol_25.60, C14:0 and C16:0).

These differences in fatty acid biosynthesis and early phase lipogenesis in the symbioses may be attributed to a number of interacting factors owing to their differing physiologies (see below), however the different light intensities and consequently the degrees of symbiont photodamage (Iglesias-Prieto and Trench, 1997; Ferrier-Pagès et al., 2007) are likely to be major drivers. It would be expected that, under optimal conditions (i.e. non-photoinhibited) with high rates of carbon fixation and energy generation, early-phase fatty acid biosynthesis and lipogenesis would turn over at the highest rates, with the highest degree of label incorporation and a relatively small pool of fatty acid intermediates such as C12:0 and C14:0 (Patton et al., 1977; Smith et al., 2005; Leal et al., 2013). In contrast, during thermal stress, carbon fixation, biosynthesis and therefore label incorporation into the fatty acid pool should decline, with corresponding accumulations of intermediates in the fatty acid pool as a result (Smith et al., 2005; Papina et al., 2007). Similarly, the breakdown of these lipid stores (such as triglycerides, TAG) during the glyoxylate cycle, will also lead to the accumulation of un-enriched fatty acid intermediates in the free pool.

Unusually, the glyoxylate cycle is present in both partners of the symbiosis and serves as a clear indicator of the importance of lipid metabolism in symbiotic cnidarians (Tytler and Trench, 1986; Butterfield et al., 2013). More typically, the cycle is associated with developing seeds of terrestrial plants, which similar to the dinoflagellates (and their hosts), produce a high abundance and diversity of fatty acids and large lipid stores, which include TAG (Eastmond and Graham, 2001; Rawsthorne, 2002). Under sub-optimal conditions for seed development, turnover of the glyoxylate cycle is enhanced, leading to modifications of pools of a number of fatty acids, but most notably accumulations of the unusual mid-length C12:0 and C14:0 (as observed in the coral-symbiosis) (Eccleston and Ohlrogge, 1998; Poirier et al., 1999). It is therefore not unreasonable to suggest that a similar mechanism may also operate under sub-optimal conditions in both symbiont and host of the cnidarian-dinoflagellate symbiosis. Indeed, increased expression of the

enzymes involved in this pathway have been detected in thermally-stressed corals (Kenkel et al., 2013; Shinzato et al., 2014). Further to this, there was minimal labelling of long-chain fatty acids at 9 d in both coral symbiont and host, suggesting minimal *de novo* biosynthesis of these later stage lipid precursors with prolonged thermal stress.

In contrast, photodamage in *Aiptasia*, which was exposed to much lower light intensities than the coral, was minimal (ca. 7% decline in maximum quantum yields of PS II), though a degree of damage to the photosynthetic machinery was still apparent. Rather than accumulations of C12:0 and C14:0, thermal stress resulted in increased turnover and much reduced abundance of these pools. In this instance it may be that input into lipogenesis (and the synthesis of TAG stores) was still ongoing; this was evident in the continued labelling of the long-chain fatty acids C16:0, C18:1, C18:0 and C22:6, and in the labelling in host pools of galactosylglycerol_25.60. In contrast, there was also a large reduction in the *Aiptasia* symbiont pools of maltose, a product of starch breakdown (Grant et al., 2006; Li et al., 2010). It may be that, during the early phases of photoinhibition and associated ATP limitation, this store is preferentially broken down in favour of the less efficient beta-oxidation of lipid stores.

Differences between *Aiptasia* and the coral symbiosis may, however, also be attributed to a number of other factors including the differing physiology of *Symbiodinium* types (Tchernov et al., 2004; Díaz-Almeyda et al., 2011) and the composition of free metabolite pools in the symbiont (Díaz-Almeyda et al., 2011; Klueter et al., 2015), in addition to their rates and modes of carbon fixation (Brading et al., 2013; Oakley et al., 2014), and their responses to light, photoinhibition and thermal stress (Warner et al., 1996; Ferrier-Pagès et al., 2007; Takahashi et al., 2009; Hill et al., 2012). In addition, both cell metabolism and responses to light and thermal stress will differ over the course of the day (Brown et al., 1999; Jones and Hoegh-Guldberg, 2001) (although sampling was mid-light cycle in each case) and in response to the *in hospite* environment of the host (Bhagooli and Hidaka, 2003; Abrego et al., 2008; Baird et al., 2009a).

4.4.4 Accumulations of inositol and compatible solutes with thermal stress

Thermally-induced modifications were also detected to both pool size and the degree of enrichment of a number of compatible solutes, including sugar alcohols inositol (both scyllo- and myo-), glycerol and galactinol. The scale of change was most notable for inositol (both scyllo- and myo-), within both partners of *Aiptasia* and also in pools of the coral host. These thermally induced changes included a large increase in abundance of this compound, by about 435% and 1200% in the *Aiptasia*-associated symbiont and host, respectively. Similarly, pools of the stereoisomer myo-inositol were also drastically increased in the heat-stressed coral host, by up to 1350%, with no label detected in this pool at the final time-point; this change was therefore indicative of largely a host-mediated response.

Exposure to increased temperatures, disruption to the electron transport chain and a decline in the exchange of osmotically active compounds will also lead to osmotic stress in the host (Mayfield and Gates, 2007). As such, non-reducing compounds such as complex sugars, polyols, sugar alcohols and certain amino acids may function as compatible solutes under these conditions (Bohnert et al., 1995; Mayfield and Gates, 2007). The accumulation of compatible solutes observed in the intracellular pools of the heat stressed host (and to a lesser extent in those of the dinoflagellate symbionts) likely indicate exposure to osmotic stress and mechanisms to maintain both internal osmolality and also in the case of the host, the necessity to provide a suitable osmotic environment for the remaining *in hospite* symbionts.

In addition to their functions as compatible solutes, the roles of inositol derivatives in the cnidarian-dinoflagellate symbiosis are currently receiving increased attention (Bertucci et al., 2013; Rosic et al., 2015), in part because of their highly conserved functions in cellular recognition, signalling and cell development (Boehning et al., 2005; Chakraborty et al., 2008). Interestingly, inositol phosphates and the phosphatidylinositol network are also thought to function in calcium signalling, carbon concentration, the activity of heat shock proteins, cell apoptosis and autophagy (Boehning et al., 2005; Patterson et al., 2005; Chakraborty et al., 2008). Both autophagy and apoptosis are modes of cell death that are elevated during thermal stress and function in coral

bleaching (Dunn et al., 2004; Dunn et al., 2007). These data also support a previous study with *Symbiodinium* in culture, which reported significant increases in pools of several inositol types (not identified) with elevated temperature in multiple *Symbiodinium* genotypes, suggesting that the accumulation of these groups may be a conserved response between *Symbiodinium* genotypes (Klueter et al., 2015). Once again, the cellular roles of inositol derivatives and that of the wider signalling network within the cnidarian-dinoflagellate symbiosis warrant more in-depth study; in particular, the potential roles of inositol in signal transduction in the holobiont during the breakdown of symbiosis (e.g. thermal bleaching) requires elucidation.

4.4.5 Alterations to the holobiont with thermal stress

In addition to the changes to the symbiont and host discussed above, thermal stress is also likely to result to changes to the combined coral holobiont (Rosenberg et al., 2007; Bourne et al., 2008; Thurber et al., 2009). A number of compounds were detected in the coral host extract which may have originated *in vivo* from the microbiota found associated with coral mucus, tissues and skeleton (Rohwer et al., 2002). These compounds included the short-chain fatty acid butyrate (C4:0) and the disaccharide maltose. In the case of C4:0, this compound's abundance was elevated in the coral host pools after both 6 d and 9 d thermal stress. C4:0 is commonly found associated with the metabolism of sulphur reducing bacteria (Parkes et al., 1993; Struchtemeyer et al., 2011) and, given that these microorganisms are widespread in the associated coral holobiont (Raina et al., 2009; Raina et al., 2010), these changes may be indicative of alterations their abundance and the composition of the combined holobiont.

4.5 Conclusions

Central carbon metabolism and carbon fate were traced in two cnidarian-dinoflagellate symbioses *via* the application of a stable isotope (^{13}C), in a dynamic labelling study, during functional conditions and those associated with thermal stress. Clear thermally induced changes were apparent in both

free metabolite pool composition and photosynthetically fixed carbon fate. These changes varied with symbiotic partner and with the extent of exposure to thermal stress and associated symbiont photodamage. Modifications were associated with changes to both pool size and turnover of multiple compounds, coupled principally to increases in cell respiration, the necessity for the generation of ATP from alternate sources and the maintenance of cell homeostasis. However, perhaps surprisingly given the degree of thermal stress and photodamage observed, in all instances there was continued fixation and translocation of labelled organic product (glucose), suggesting that remaining symbionts were, at least in part, metabolically functional in terms of some continued provision towards host metabolism. These data also suggest that if may be possible for a new steady state to be established, if following a degree of bleaching, the extent of photodamage is limited and symbionts remain metabolically functional.

The outputs of this study provide valuable insight into the complex metabolic interactions between symbiont and host in the cnidarian-dinoflagellate symbiosis, both during functional symbiosis and thermal stress. Although some differences between host-symbiont combinations were apparent, there was also a high degree of commonality between symbioses, highlighting a number of conserved responses to thermal stress. A better understanding of these networks and change elicited during exposure- and acclimation to abiotic stress is essential if we are to more accurately evaluate the threats facing coral reefs and to interpret their potential for long-term acclimation and persistence.

Chapter 5 General discussion

5.1 Summary

Currently, major gaps remain in our understanding of central and secondary metabolic networks in the cnidarian-dinoflagellate symbiosis, yet more in-depth knowledge of these systems is essential if we are to better understand how coral reefs will persist in the face of environmental change. This thesis furthers our knowledge of a number of aspects of metabolism in both partners of the symbiosis, under functional conditions and those associated with thermal and oxidative stress, namely: central metabolic pathways and alternate modes of metabolism; metabolic networks associated with cellular homeostasis and acclimation; the interaction of metabolism and ROS in cell signalling and signal transduction during bleaching; and carbon fate and symbiont function during thermal stress. Presented below is a summary of the major findings from this research (**Chapters 2-4**), which forms the basis of this thesis. After which, these data, their limitations and opportunities for further study are discussed in the broader context of thermal stress and bleaching in the cnidarian-dinoflagellate symbiosis.

The main overarching aim of this research was to develop the application of metabolomics techniques, to furthering our understanding of cellular and metabolic changes, during thermal stress in the cnidarian-dinoflagellate symbiosis. To this end, the principal techniques applied included untargeted and targeted metabolite profiling of polar and semi-polar extracts *via* GC-MS, of the intracellular metabolite pools of each symbiotic partner (symbiont and host) in a both a model symbiosis (*Aiptasia* sp.) and a coral (*Acropora aspera*). These methods were subsequently combined with stable isotope labelling (^{13}C) and pathway activity analysis.

In **Chapter 2**, these techniques were developed and applied to the model symbiotic cnidarian *Aiptasia* sp., and its homologous symbiont (*Symbiodinium* ITS 2 type B1), to characterise both ambient and thermally-induced metabolite profiles (amino and non-amino organic acids) in both partners. Thermal stress (32°C for 6 d), symbiont photodamage and associated bleaching, resulted in

characteristic modifications to the free metabolite pools of both partners. In the symbiont, primarily accumulations of multiple fatty acids, coupled to a reduction in the activity of symbiont carbohydrate metabolism and downstream biosynthesis pathways (such as lipogenesis), with an increase in the catabolism of lipid stores. In host pools, thermally induced changes were associated with declines in mobile product translocation, the requirement for ATP generation *via* alternate modes (catabolism of stores) and exposure to oxidative stress. These data generate a number of questions which warranted further investigation, namely:

1. What are the principal drivers of change to the symbiont fatty acid pool during thermal stress? Are modifications associated primarily with lipogenesis, store catabolism (such as beta-oxidation *via* the glyoxylate cycle), membrane structure, nitrogen assimilation, or derived from host translocation?
2. Similarly, how do thermal stress and symbiont photodamage affect carbon fixation, and the production and translocation of mobile products?
3. Do thermal sensitivities differ between partners?
4. How is symbiosis dysfunction communicated within and between partners, and do free metabolite pools play a role?

These outputs and the questions raised informed the subsequent data chapters (**Chapter 3** and **4**). In **Chapter 3** metabolite profiling techniques (focussing this time on carbohydrate pools) were once again applied to the study of thermally-induced changes to the free pools of the coral *A. aspera* and its symbionts (dominant *Symbiodinium* ITS 2 type C3) at differing stages of symbiont photodamage and thermal stress (6 d and 8 d at 32°C). Additionally, targeted analysis was applied to quantify changes to these pools in terms of absolute amounts at 8 d, in both symbiont and host. Once again symbiont and host pools displayed highly characteristic responses to thermal stress, which were observed to a greater extent with more prolonged exposure to these conditions at 8 d. In the symbiont, large accumulations of a range of fatty acid groups were once again observed, coupled to reductions in

pools of multiple carbohydrates. In contrast, in the host, reductions in pool size were detected for a number of fatty acids, carbohydrates, organic acids and intermediates. These changes in host pools corresponded to increased turnover of a number of networks with thermal stress including: energy-generating pathways, antioxidant networks, ROS-associated damage and damage signalling, and were potentially indicative of change to the associated microbial holobiont. A number of questions were generated which warrant further investigation:

1. Are the symbionts that remain *in hospite* metabolically functional (fixing carbon and translocating mobile products) during thermal stress and bleaching?
2. If functional, how does thermal stress affect the turnover and downstream products of carbon metabolism in both partners?
3. What roles do metabolic networks play in the damage signalling cascade and the cellular mechanisms of bleaching?

Finally in **Chapter 4**, metabolite profiling techniques optimized in **Chapter 2** and **3** were applied with ^{13}C labelling in both *Aiptasia* sp. and *Acropora aspera*, in order to further investigate the questions raised in these preceding studies. Once again, clear thermally-induced changes were observed to central carbon metabolism, biosynthesis pathways and alternative energy-generation modes in symbiont and host, in both symbioses. These responses, however, differed according to partner and to the degree of exposure to photodamage and thermal stress. Interestingly however, in all cases there was continued fixation of carbon, production of mobile products and translocation to the host. This suggests that even during the later stages of bleaching and photodamage, the remaining *in hospite* symbionts are metabolically functional as symbionts, at least in part.

Taken together, these outputs generate a number of questions that warrant further study:

1. What role does host-symbiont combination play in symbiont function during thermal stress? What roles do other abiotic stressors and environmental variables (e.g. light, nutrient input) play in symbiont function during thermal stress?
2. How do metabolic networks contribute to damage signalling pathways and signal transduction within individual partners and the holobiont as a whole?
3. How do these responses differ over the course of the day, or year?

Overall, these data generate a number of important findings with regard to the metabolic and cellular function of the cnidarian-dinoflagellate symbiosis and that of each respective partner during thermal stress and bleaching (summarised in **Figure 5.1**). Namely, these are:

- Metabolic costs associated with photodamage and acclimation to elevated temperatures, in terms of modifications to central metabolism, biosynthesis and catabolism of energy stores;
- Potential sites of thermal and oxidative stress in each partner;
- Functions of primary metabolites and metabolic networks in cellular homeostatic and acclimatory responses to thermal and oxidative stress;
- Modifications to carbon fixation, mobile product translocation and carbon fate (symbiont functionality) during thermal stress and bleaching; and
- The interplay of free metabolite pools, ROS-associated cellular damage, damage signalling and signal transduction in the coral holobiont during bleaching.

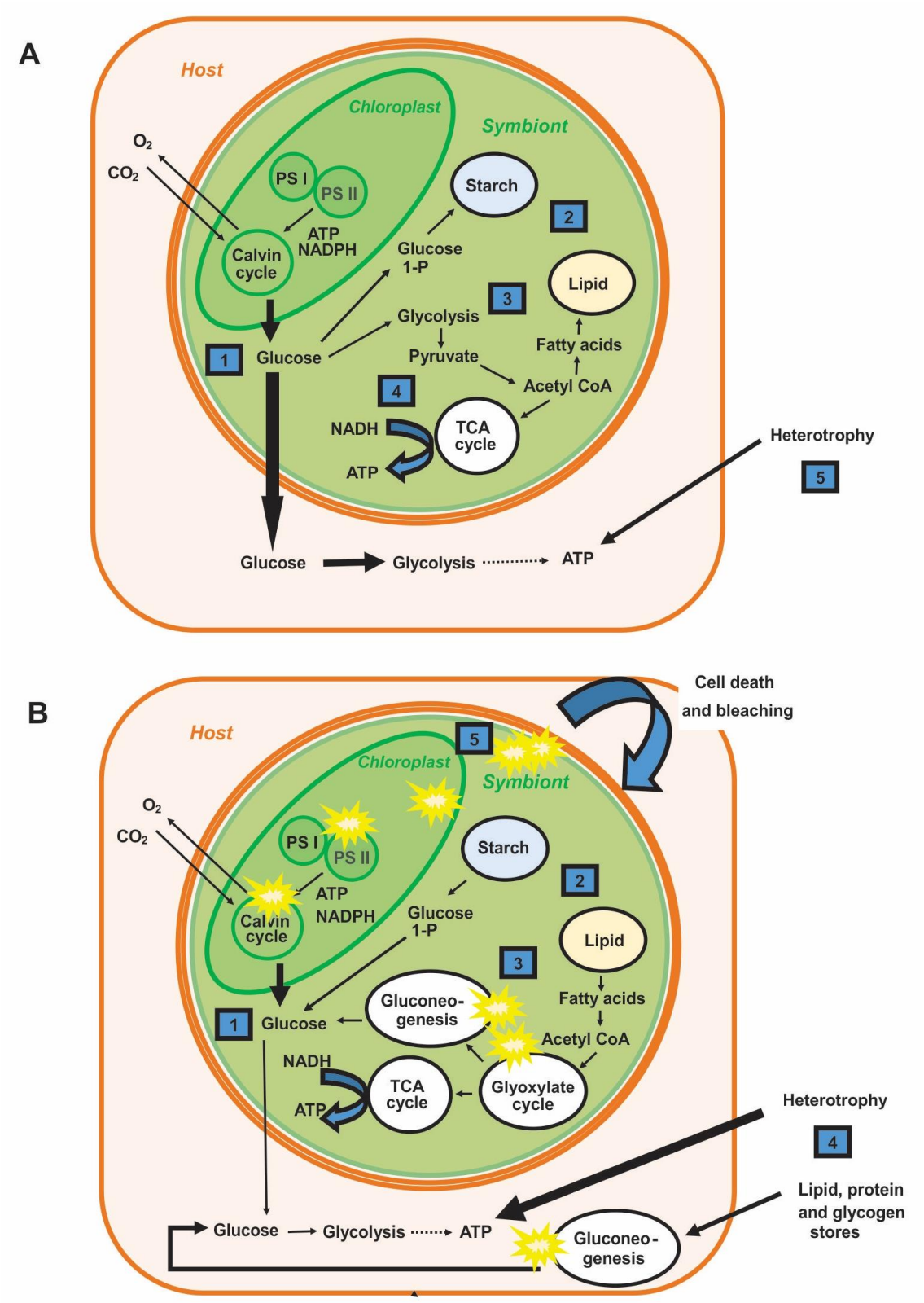

Fig. 5.1: Summary schematic of central carbon metabolism and metabolic interactions in the cnidarian-dinoflagellate symbiosis, during functional conditions (A), and during thermal stress and bleaching (B). See over for full legend.

Fig. 5.1 (Previous page): A1. Carbon is fixed *via* the Calvin cycle, producing glucose as the primary end-product; this is then translocated to the host as a major mobile product. A2. Excess energy is used in biosynthesis pathways and the production of a number of major storage products in the dinoflagellate, primarily starch and lipids. A3. The major mode of energy generation in symbiont and host under these photosynthetic conditions is *via* glycolysis and the TCA cycle, A4. Succinate and NADH generated during the TCA cycle are finally oxidised during oxidative phosphorylation, *via* the electron transport chain, in turn producing additional cellular energy (ATP). A5. In the host, central metabolism is supplemented by the energy gained from heterotrophic feeding. B1. Damage to the machinery of photosynthesis, PS II, the Calvin cycle and the thylakoid membranes of the chloroplast is on-going, resulting in increased production of ROS at these sites. Carbon continues to be fixed *via* the Calvin cycle, producing glucose as the primary end-product. This is then translocated to the host as a major mobile product, however symbiont densities are drastically reduced, and therefore total net translocation is reduced relative to (A). B2. Thermal stress leads to increased respiratory rates, and in order to meet increased energy requirements storage bodies, lipid and starch are broken down to produce cellular energy. B3. Lipid stores are broken down *via* beta-oxidation in the glyoxylate cycle, the products of which in turn feed into gluconeogenesis, the TCA cycle and oxidative phosphorylation in order to generate cellular energy. However, these processes also result in the generation of further ROS at multiple sites. B4. Host heterotrophy and the catabolism of stores (lipid, glycogen and protein) are also increased in order to meet increased energy requirements associated with the maintenance of cell homeostasis. This in turn leads to the production of further cellular ROS at multiple sites. B5. ROS eventually overwhelm symbiont and host antioxidant responses, leading to cellular damage and initiating a signalling cascade, which results eventually in the breakdown and loss of further symbiont cells and more advanced stages of bleaching.

5.2 Value and limitations of metabolomics to the study of the cnidarian-dinoflagellate symbiosis, and its potential application to future studies

Clearly, a major strength of metabolomics-based techniques is the capacity to simultaneously detect and quantify fine-scale and ecologically-relevant changes, with little *a priori* knowledge of the system under investigation (Fiehn, 2002; Lankadurai et al., 2013). Additionally, as many of the compounds detected *via* GC-MS-based techniques are primary metabolites, owing often to their highly-conserved central roles in metabolism, unknown compounds are readily detected and identifiable (Wahid et al., 2007; Guy et al., 2008). Similarly, the large resulting data sets are also useful for generating multiple

hypotheses regarding the mechanisms responsible for any uncovered differences between samples, or treatment groups, based often on these central and conserved roles (Lankadurai et al., 2013).

However, without in-depth knowledge of the basis of these changes in the system under study, i.e. central metabolism and secondary metabolism, these hypotheses will remain unresolved. This is a major issue for the cnidarian-dinoflagellate symbiosis, as to date major gaps still exist in our understanding, even of the central metabolism of this complex and dynamic symbiosis (Edmunds and Gates, 2003; Davy et al., 2012). In order to further our understanding in this respect, focussed studies with clear research objectives are required to uncover key aspects of the symbiosis, which are as yet unanswered (Edmunds and Gates, 2003). Once these fundamentals of metabolism have been further elucidated, more complex, multi-platform studies that couple the 'omics fields (genomics, transcriptomics, proteomics and metabolomics) and methods such as fluxomics (see below), will serve to uncover more complex alterations in the holobiont, such as responses to abiotic stress. However, without the basics to inform these complex studies, they will serve only to generate yet more unanswered hypotheses.

These targeted studies may include metabolomics- and non-metabolomics-based techniques such as:

1) Quantitative studies under defined conditions to elucidate metabolic networks in the holobiont, rates of change and the enzymes involved (stoichiometry). These data will inform methods such as the quantitative analysis of pathway turnover (fluxomics) and enable the effects of a given variable, to be better established (see for instance Yang et al., 2002; Duckwall et al., 2013; Heise et al., 2014);
2) Development and application of standard methods and reporting to enable better comparisons between studies, as outlined by the Metabolomics Standards Initiative presented in Sansone (2007);
3) Identification of small molecules (primary and secondary metabolites) specific to the symbiosis, coupled to open-source metabolomics libraries to facilitate putative identifications of unknown compounds by

collaborating groups (Schauer et al., 2005; Sansone, 2007; Sogin et al., 2014);

4) More in depth understanding of the metabolic changes associated with daily and annual cycles (Brown et al., 1999; Jones and Hoegh-Guldberg, 2001); and
5) Characterisation of signalling systems and networks in individuals and the holobiont as a whole (Müller, 2004; Burman and Ktistakis, 2010; Grüning et al., 2010).

These gaps in current knowledge in turn highlight some of the limitations of the current study and the challenges of applying metabolomics to this complex symbiotic system. These are summarised below:

1) Data snapshots with limited sample replication: In all cases the data presented in this thesis are snapshots at a single point in time. Samples were consistently taken at a given time (i.e. mid-light cycle) to ensure consistency and to enable comparison between groups. However, as the metabolome is highly variable over time, a snapshot of a single time-point has limitations in terms of the conclusions that can be drawn from the data set (Villas-Bôas et al., 2006; Kim and Verpoorte, 2010). Similarly, carbon fixation and associated translocation of photosynthate will also alter with time (Muscatine et al., 1984). In addition to sampling over the course of a day and at different times of year (Brown et al., 1999; Fitt et al., 2000; Jones and Hoegh-Guldberg, 2001; Warner et al., 2002), more sampling points over the course of the study would have provided much greater insight into the changes under examination. Further to this, owing to the natural variability of the metabolome, (Villas-Bôas et al., 2006; Tredwell et al., 2011), higher sampling replication at each time-point would also enable more fine-scale changes to be confidently detected.
2) Data based on single coral-symbiont and anemone-symbiont combinations: A huge amount of variation also exists in the cnidarian-dinoflagellate symbiosis, in terms of both the physiology and the responses of each partner to thermal stress (Baker, 2003; Tchernov et

al., 2004; Oakley et al., 2014; Wooldridge, 2014). As such, it is expected that the associated metabolic responses of these partnerships would differ greatly to those applied in the current study (Loram et al., 2007; Papina et al., 2007; Klueter et al., 2015). Some differences were apparent in the responses of the symbioses applied (e.g. symbiont C12:0 and C14:0 levels), however most of the patterns observed were common between the two symbiotic partnerships. Nevertheless, caution should still be exercised when generalising across different symbioses.

3) Many abundant compounds in both partners were not identifiable with the libraries and standards available: Similarly, in many cases where compounds were identified, few data were available to elucidate their roles in symbiosis metabolism.
4) The data presented in each chapter are also based on the application of a single extraction and derivatization method, which targets a specific suite of compounds. As a result, any compounds not targeted by these methods would not be extracted or analysed (Roessner et al., 2006; Villas-Bôas et al., 2006). A major aspect, therefore, which was excluded by the methods applied, was the lipid fraction. Lipids are known to serve a major role in the functional symbiosis (Patton et al., 1977; Kellogg and Patton, 1983; Dunn et al., 2012) and during thermal stress (Grottoli et al., 2004; Tchernov et al., 2004; Tolosa et al., 2011; Imbs and Yakovleva, 2012).
5) In order for symbiont and host pools to be analysed separately, owing to the structure of the symbiosis, the dinoflagellate had first to be isolated and both fractions purified. This separation process was optimized taking into account a number of factors:
   (i) Metabolism was fully quenched in both partners (immersion in liquid nitrogen);
   (ii) Processing was undertaken rapidly at the lowest temperatures possible (4°C) to reduce any exposure to post-sampling change;
   (iii) Samples were fully homogenised, fractions purified (symbiont in host fraction and *vice versa*) and cells lysed;

(iv) Samples were not contaminated by compounds that would result in reduced final data quality (such as matrix effects associated with the precipitation of salts from buffers, antifreezes or those associated with detergents); and

(v) Biomass was sufficient to enable detection of compounds present in low abundance, particularly when associated with much reduced symbiont biomass during bleaching.

However, some degree of change from the respective profiles of symbiont and host *in vivo* is still possible, owing to the necessity of working at 4°C rather than below -20°C and working with MilliQ water to separate each fraction, rather than with osmotically-compatible buffers (see Villas-Bôas et al., 2006 for a review of sample preparation for metabolomics studies).

5.3 Current advances in the metabolomics of the cnidarian-dinoflagellate symbiosis and future challenges

Notwithstanding the limitations of this research, the outputs of this study offer valuable insight into the broader issues of cellular and metabolic change during thermal stress and bleaching in the cnidarian-dinoflagellate symbiosis. Each of the major aspects are discussed in more detail below.

5.3.1 How do thermal stress and bleaching affect central metabolism in the symbiosis and what is its capacity for acclimation to change?

As nutrient exchange in the cnidarian-dinoflagellate symbiosis underpins its success, it is perhaps surprising how little we still know of central metabolism in the partnership, even under functional conditions (Edmunds and Gates, 2003; Davy et al., 2012). Only by understanding function, can we begin to unpick the complex changes that occur during dysfunction (Edmunds and Gates, 2003). Studies to date have largely centred on certain aspects of metabolism, such as lipogenesis (Patton et al., 1977; Kellogg and Patton, 1983; Grottoli et al., 2004; Dunn et al., 2012), nitrogen assimilation (Cook et al., 1988; Wang and Douglas, 1998; Grover et al., 2002; Pernice et al., 2012; Rädecker et al., 2015), carbon fixation (Yellowlees et al., 1993; Allemand et

al., 1998; Leggat et al., 1999; Kopp et al., 2015), or mobile product translocation (Muscatine and Cernichiari, 1969; Trench, 1971; Whitehead and Douglas, 2003; Burriesci et al., 2012), and/or how these central aspects are affected by a certain stressor (Papina et al., 2007; Buxton et al., 2009; Díaz-Almeyda et al., 2011; Imbs and Yakovleva, 2012; Béraud et al., 2013; Oakley et al., 2014). More holistic studies of central metabolism within the symbiosis were therefore lacking, with only one other study applying metabolic profiling techniques to the *in hospite* symbiosis (Burriesci et al., 2012). The outputs of this thesis therefore further our understanding of the interaction of central metabolic networks within the symbiosis under functional conditions, and identify a number of changes to these networks associated with thermal stress.

This thesis supports and builds upon the outputs of Burriesci et al. (2012), finding glucose and downstream glycolysis to be central to the functional symbiosis. However, it is also clear that there is high functional redundancy in the metabolism of both partners, which during sub-optimal conditions were able to supplement this primary energy source with alternate modes of ATP production (**Figure 5.1**). A key alternate mode observed in the current study was a shift from biosynthesis to the breakdown of stores, primarily the beta-oxidation of lipids during the glyoxylate cycle. This is not surprising given the importance of lipids in the function of this symbiosis (Patton et al., 1977; Kellogg and Patton, 1983; Dunn et al., 2012) and given that this response has been reported as operating during thermal stress and bleaching (Grottoli et al., 2004; Grottoli and Rodrigues, 2011; Imbs and Yakovleva, 2012). The activity of the glyoxylate cycle and alterations to fatty acid pools were apparent in both partners, however interestingly thermally-induced changes to fatty acid metabolism (and most likely also to lipogenesis) were most apparent in the dinoflagellate symbiont.

Large accumulations of both lipids and fatty acids have also been detected in the dinoflagellate during nitrogen stress, and may therefore also indicate a decline in nitrogen assimilation (Dagenais Bellefeuille et al., 2014; Jiang et al., 2014; Wang et al., 2015) during thermal stress and photoinhibition. Similarly, lipids also accumulate in the dinoflagellate during cell senescence, as a result

of reduced rates of cell division (Miller and Yellowlees, 1989; Smith and Muscatine, 1999). As such, stress-induced changes to lipogenesis and the fatty acid pool therefore serve as a conserved stress response in the dinoflagellate during sub-optimal conditions.

Interestingly, even during the advanced stages of bleaching, it was evident that mobile product translocation to the host was maintained by the remaining *in hospite* symbionts (**Figure 5.1**). This output was surprising as it does not fit with the model of reduced carbon fixation and translocation during photoinhibition (Jones et al., 1998; Smith et al., 2005). This suggests that in the current study that symbionts were either not significantly photodamaged, or that both production and supply were somehow maintained under conditions of energy limitation. Further targeted studies *via* a range of 'omics' techniques would be useful to determine the mechanisms at play here. If indeed the *in hospite* symbionts are photodamaged, yet continued in their *de novo* production and translocation of glucose, this translocation maybe somehow manipulated and maintained *via* some form of host control. One potential mechanism is *via* proteins associated with the symbiosome membrane, such as the proton pump, the V-type H^+-ATPase (Barott et al., 2015). Alternatively, ongoing translocation during symbiont photoinhibition may also operate simply as a sink for excess electrons and hence removal of excess carbon.

Similarly, it would be interesting to determine at what point (if any) this translocation breaks down and to quantify the compounds and absolute amounts of translocate exchanged. This would be simply resolved with further metabolomics-based studies coupled with the application of stable isotope tracers. If indeed *in hospite* symbionts continue to fix carbon, but are unable to reproduce due to nitrogen limitation, this limitation will have implications for post-bleaching recovery of symbiont densities, necessitating either an increase in supply of these limiting resources from host to symbiont, or re-colonisation of symbiont populations from the environment. Host heterotrophy may serve in a number of coral species as an important additional supply of nitrogen, aiding in symbiont re-population following bleaching (Grottoli et al., 2004; Grottoli et al., 2006; Hughes and Grottoli, 2013), particularly in

vertically-transmitting species, where symbiont uptake from the environment is uncommon (Grottoli et al., 2014).

5.3.2 What roles do free metabolite pools play in cellular homeostasis and acclimation to thermal stress?

Similarly, the direct roles of free metabolite pools in the maintenance of cellular homeostasis have received little interest in the cnidarian-dinoflagellate symbiosis to date. However, certain aspects of metabolism, which are associated with the maintenance of cell structure and function have been of more focus, primarily membrane composition (Tchernov et al., 2004; Papina et al., 2007; Díaz-Almeyda et al., 2011), enzymatic and non-enzymatic antioxidants (Hawkridge et al., 2000; Császár et al., 2009; Krueger et al., 2014; Roberty et al., 2015), photoprotective pigments including MAAs (Shick and Dunlap, 2002; Banaszak et al., 2006; Rosic and Dove, 2011), fluorescent proteins (Salih et al., 2000; Roth et al., 2010), photopigments (Ambarsari et al., 1997; Dove, 2004; Venn et al., 2006; Strychar and Sammarco, 2011; Krämer et al., 2013) and compatible solutes (Mayfield and Gates, 2007).

With the methods applied here, it was possible to simultaneously detect changes to the turnover of these secondary acclimatory responses, providing further insight into the interplay and relative importance of each mechanism in a given partner, at a certain level of thermal stress. It was apparent that, relative to the symbiont, stress was manifest in the host with increased turnover of antioxidant precursors (glutamate and pyroglutamate) and the accumulation of low molecular weight non-enzymatic antioxidants (most notably relating to the AsC and GSH cycle), the production of MAAs and the accumulation of compatible solutes. Increasing evidence from both cellular and molecular studies suggests that the cnidarian may in some instances be the first site of thermal and oxidative stress in the symbiosis (Leggat et al., 2011; Wooldridge, 2014; Krueger et al., 2015). This may have implications for how we perceive the mechanisms responsible for coral bleaching, which is typically based on the symbiont as the first site of ROS damage and oxidative stress (Lesser, 1996; Weis, 2008).

Further to this, if indeed in many instance the host is the most sensitive partner, improving resilience *via* uptake of more thermally resistant symbiont types *via* mechanisms such as switching and shuffling (Baker, 2003) are unlikely to be of much benefit, particularly if under typical conditions these novel types are sub-optimal in terms of mobile product translocation (Loram et al., 2007; Jones and Berkelmans, 2011; Stat and Gates, 2011). Indeed it has been shown that cnidarian hosts are capable of acclimation without any change in symbiont type (Bellantuono et al., 2012a; Bellantuono et al., 2012b). However, further studies from a range of host-symbiont combinations would provide more insight into these differing sensitivities and responses to thermal and oxidative stress. Moreover, studies in a range of 'omics' fields that subject these symbioses to prolonged periods of thermal stress will be useful for elucidating further capacity for long-term acclimation in both partners and identifying the key mechanisms employed (see for instance van Oppen et al., 2015).

5.3.3 How do metabolic networks function in cell signalling, cell death and bleaching mechanisms?

To date, major gaps remain in our understanding of cellular communication in the holobiont, however increasing evidence suggests that, in the cnidarian at least, highly conserved systems operate in signalling networks associated with thermal stress and ROS (Lesser, 2006; Weis, 2008), inositol and inositol derivatives (Müller, 2004; Lehnert et al., 2014; Rosic et al., 2015), oxylipins (Lõhelaid et al., 2015), steroid derivatives and hormones (Tarrant, 2005; Tarrant et al., 2009), and that symbiosis increases the expression of a number of these networks (Yuyama et al., 2011; Lehnert et al., 2014). It was apparent in the present study that thermal stress also resulted in increased activity of a number of these metabolic networks in the symbiosis. As such, it is likely that metabolic signals in combination with ROS, play a role in the crosstalk between networks, signal transduction, acclimation, and/or cell death and bleaching (**Figure 5.1**). Similar networks and their crosstalk in signal transduction and cellular acclimation have been more widely investigated in terrestrial plants, *via* the application of a combination of 'omics' fields (for detailed reviews see Gibson, 2004; Field, 2009; Smeekens et al., 2010).

Interestingly, given the importance of understanding how the symbiosis as a whole detects, communicates and responds to abiotic stress, the interaction of these signalling systems (with the exception of ROS) has received little research focus to date in the cnidarian-dinoflagellate symbiosis. This thesis therefore serves to highlight the potential significance of these systems, which warrant detailed study.

5.4 A future for coral reefs – what has metabolomics taught us?

Mean water temperatures on the central Great Barrier Reef (GBR) are currently about 27°C, with summer maxima of about 30°C (Hoegh-Guldberg, 1999). Under current emissions scenarios, which aim to limit temperature rises to below 2°C (Frieler et al., 2013; Kwiatkowski et al., 2015), summer maxima on the central GBR would reach 32°C by the end of this century. In this thesis, it has been shown that exposure of both a model symbiosis and a common acroporid-dinoflagellate symbiosis to this water temperature, even for relatively short periods of time and with little cumulative stress, results in thermal and oxidative stress, and breakdown and loss of dinoflagellate symbionts during bleaching. More specifically it is apparent that thermal and oxidative stress necessitate energetically costly responses to maintain cellular homeostasis in both symbiotic partners. These responses included a range of compounds with described roles as antioxidants, compatible solutes and cell signals, in addition to the *de novo* synthesis of secondary protective compounds central to cellular acclimation, such as carotenoids and MAAs.

However, it was also apparent in the current study that oxidative stress was more manifest in the host, relative to remaining *in hospite* symbionts. This disparity suggests that in this instance ROS and oxidative stress were not generated in the symbiont, but rather as a result of enhanced host respiratory needs. A likely source under these conditions is the breakdown of lipid stores, *via* beta oxidation (Grottoli et al., 2004; Grottoli and Rodrigues, 2011). This process generates ROS (specifically hydrogen peroxide) at cell microbodies such as the peroxisomes and glyoxysomes (Lesser, 2006). The enzymic

response to detoxify hydrogen peroxide is catalase, levels of which have been shown to be elevated in host tissue under bleaching conditions, independent of such responses in the symbiont, or of host superoxide dismutase (Krueger et al., 2014). Further to this, branching species such as the acroporids, which have high metabolic rates, would most likely be more at risk from the excess generation of ROS *via* this source, fitting with well-known bleaching sensitives between differing host species and growth forms (Wooldridge, 2014).

Short-term acclimation in the host without any change in symbiont type has been shown (Bellantuono et al., 2012a; Bellantuono et al., 2012b). This was apparent to a certain degree in *Aiptasia* sp. in **Chapter 4**, with the establishment of a new steady state in the symbiont population following bleaching. Indeed phenotypic variability associated with differing exposure to environmental conditions at a given site, or even within a single colony is widely documented (reviewed in Brown, 1997a). If, however, phenotypic plasticity and cellular acclimation do not enable cnidarian species and their symbionts to keep pace with the current rate of change (Bellantuono et al., 2012b; Frieler et al., 2013; Grottoli et al., 2014), this will lead to large-scale losses of thermally-sensitive species. For instance, as a genus, the acroporids are considered sensitive to thermal stress (Baird et al., 2009a; Wooldridge, 2014); however they are also a major component of reef systems globally, in terms of species diversity, cover and habitat complexity (Goreau, 1959; Veron, 2000). The loss of these major ecosystem engineers would have disastrous implications for coral reef ecosystems as we know them, in terms of their structure and function (Hughes, 1994; Pandolfi et al., 2011). Clearly therefore, we must take direct action to further limit projected temperature increases, if we are to ensure that functional coral reefs are preserved (Frieler et al., 2013; Kwiatkowski et al., 2015).

If in many instances the host is indeed the site of symbiosis breakdown, this offers a degree of hope for minimising cumulative stress and downstream impacts to the symbiosis as a whole, with any activity that minimises symbiont photoinhibition and the production of additional ROS (Takahashi and Murata, 2008) likely aiding the preservation of symbiont metabolic function *in hospite*. Similarly, past efforts for increasing holobiont fitness typically focussed on

enhancing symbiont resistance to thermal and oxidative stress (Baker, 2001; Berkelmans and van Oppen, 2006; Jones et al., 2008), though clearly this would offer little benefit if the host is more typically the site of symbiosis breakdown. Further to this, assisted evolution is one drastic option that may be applied to enhance natural coral resistance to abiotic stress (van Oppen et al., 2015). However, in order for direct intervention to be a success, these programs must be based on sound understanding of the cellular changes (at a range of 'omics' levels) that are desired. In the first instance, this study serves to highlight the central metabolic mechanisms and sites associated with this thermal stress and acclimation in the cnidarian-dinoflagellate symbiosis, and furthers our understanding of the metabolic pathways involved in enhanced thermal resistance and cellular acclimation. In this regard, there is a clear need for future work to elucidate a number of central aspects further, namely; quantitative *in hospite* metabolomics data to determine the absolute metabolic costs of thermal stress in a range of host-symbiont combinations; proteomics data to characterise translocation mechanisms and their control, in addition to the modes- and receptors of cell signalling and signal transduction; coupled to genomics and transcriptomics studies to determine capacity for- and mechanisms of long-term acclimation.

5.5 Concluding comments

This thesis serves as an important first step in developing metabolomics as a tool for elucidating the complex and highly dynamic changes in the coral symbiosis during thermal stress. The power of these techniques lies in the capacity to simultaneously assess rapid and often post-translational change in a highly repeatable and quantitative manner with little *a priori* knowledge of the system under study.

With the application of metabolite profiling techniques coupled to stable isotope tracers, this study has shown, for the first time, the interaction of a number of complex changes within the metabolic networks of individual partners of multiple cnidarian-dinoflagellate symbioses during thermal stress.

These changes varied according to partner, highlighting the importance of the methods employed here to analyse each fraction individually. Thermally-induced modifications were associated with alterations to: central metabolism, biosynthesis, catabolism, cell signalling, the maintenance of cellular homeostasis and longer-term acclimation mechanisms. This study therefore highlights the interaction and relative importance of central pathways and complex secondary mechanisms invoked during cellular acclimation to thermal, oxidative stress and symbiosis dysfunction during coral bleaching.

The outputs from this research therefore further our understanding of the capacity of the cnidarian-dinoflagellate symbiosis for long-term acclimation to thermal stress under future climate scenarios. Further research to elucidate these changes in a range of 'omics' fields is necessary if we are to have a better understanding of the threats facing coral reefs and their true capacity for not only survival, but for the long-term global recovery and persistence of these incredibly complex and important systems.

References

Abrego, D., Ulstrup, K. E., Willis, B. L. and van Oppen, M. J. H. (2008). Species–specific interactions between algal endosymbionts and coral hosts define their bleaching response to heat and light stress. *Proceedings of the Royal Society B: Biological Sciences* **275**, 2273-2282.

Aggio, R. B. M., Ruggiero, K. and Villas-Bôas, S. G. (2010). Pathway Activity Profiling (PAPi): from the metabolite profile to the metabolic pathway activity. *Bioinformatics* **26**, 2969-2976.

Aizat, W. M., Dias, D. A., Stangoulis, J. C. R., Able, J. A., Roessner, U. and Able, A. J. (2014). Metabolomics of capsicum ripening reveals modification of the ethylene related-pathway and carbon metabolism. *Postharvest Biology and Technology* **89**, 19-31.

Allemand, D., Furla, P. and Bénazet-Tambutté, S. (1998). Mechanisms of carbon acquisition for endosymbiont photosynthesis in Anthozoa. *Canadian Journal of Botany* **76**, 925-941.

Altschul, S. F., Gish, W., Miller, W., Myers, E. W. and Lipman, D. J. (1990). Basic local alignment search tool. *Journal of molecular biology* **215**, 403-410.

Ambarsari, I., Brown, B. E., Barlow, R. G., Britton, G. and Cummings, D. (1997). Fluctuations in algal chlorophyll and carotenoid pigments during solar bleaching in the coral *Goniastrea aspera* at Phuket, Thailand. *Marine Ecology Progress Series* **159**, 303-307.

Amo, M., Suzuki, N., Kawamura, H., Yamaguchi, A., Takano, Y. and Horiguchi, T. (2010). Sterol composition of dinoflagellates: Different abundance and composition in heterotrophic species and resting cysts. *Geochemical Journal* **44**, 225-231.

Arif, C., Daniels, C., Bayer, T., Banguera-Hinestroza, E., Barbrook, A., Howe, C. J., LaJeunesse, T. C. and Voolstra, C. R. (2014). Assessing *Symbiodinium* diversity in scleractinian corals via next-generation sequencing-based genotyping of the ITS2 rDNA region. *Molecular Ecology* **23**, 4418-4433.

Bachar, A., Achituv, Y., Pasternak, Z. and Dubinsky, Z. (2007). Autotrophy versus heterotrophy: The origin of carbon determines its fate in a

symbiotic sea anemone. *Journal of Experimental Marine Biology and Ecology* **349**, 295-298.

Bachok, Z., Mfilinge, P. and Tsuchiya, M. (2006). Characterization of fatty acid composition in healthy and bleached corals from Okinawa, Japan. *Coral Reefs* **25**, 545-554.

Baghdasarian, G. and Muscatine, L. (2000). Preferential expulsion of dividing algal cells as a mechanism for regulating algal-cnidarian symbiosis. *The Biological Bulletin* **199**, 278-286.

Baird, A. H., Bhagooli, R., Ralph, P. J. and Takahashi, S. (2009a). Coral bleaching: the role of the host. *Trends in Ecology & Evolution* **24**, 16-20.

Baird, A. H., Guest, J. R. and Willis, B. L. (2009b). Systematic and Biogeographical Patterns in the Reproductive Biology of Scleractinian Corals. *Annual Review of Ecology, Evolution, and Systematics* **40**, 551-571.

Bajguz, A. and Hayat, S. (2009). Effects of brassinosteroids on the plant responses to environmental stresses. *Plant Physiology and Biochemistry* **47**, 1-8.

Baker, A. C. (2001). Ecosystems: Reef corals bleach to survive change. *Nature* **411**, 765-766.

Baker, A. C. (2003). Flexibility and Specificity in Coral-Algal Symbiosis: Diversity, Ecology, and Biogeography of *Symbiodinium*. *Annual Review of Ecology, Evolution, and Systematics* **34**, 661-689.

Baker, A. C., Glynn, P. W. and Riegl, B. (2008). Climate change and coral reef bleaching: An ecological assessment of long-term impacts, recovery trends and future outlook. *Estuarine, Coastal and Shelf Science* **80**, 435-471.

Banaszak, A. T., Barba Santos, M. G., LaJeunesse, T. C. and Lesser, M. P. (2006). The distribution of mycosporine-like amino acids (MAAs) and the phylogenetic identity of symbiotic dinoflagellates in cnidarian hosts from the Mexican Caribbean. *Journal of Experimental Marine Biology and Ecology* **337**, 131-146.

Barott, K. L., Venn, A. A., Perez, S. O., Tambutté, S. and Tresguerres, M. (2015). Coral host cells acidify symbiotic algal microenvironment to promote photosynthesis. *Proceedings of the National Academy of Sciences* **112**, 607-612.

Bellantuono, A. J., Granados-Cifuentes, C., Miller, D. J., Hoegh-Guldberg, O. and Rodriguez-Lanetty, M. (2012a). Coral thermal tolerance: tuning gene expression to resist thermal stress. *PLoS One* **7**, e50685.

Bellantuono, A. J., Hoegh-Guldberg, O. and Rodriguez-Lanetty, M. (2012b). Resistance to thermal stress in corals without changes in symbiont composition. *Proceedings of the Royal Society of London B: Biological Sciences* **279**, 1100-1107.

Béraud, E., Gevaert, F., Rottier, C. and Ferrier-Pagès, C. (2013). The response of the scleractinian coral *Turbinaria reniformis* to thermal stress depends on the nitrogen status of the coral holobiont. *Journal of Experimental Biology* **216**, 2665-2674.

Berglund, T. (1994). Nicotinamide, a missing link in the early stress response in eukaryotic cells: A hypothesis with special reference to oxidative stress in plants. *FEBS Letters* **351**, 145-149.

Berglund, T. and Ohlsson, A. (1995). Defensive and secondary metabolism in plant tissue cultures, with special reference to nicotinamide, glutathione and oxidative stress. *Plant Cell, Tissue and Organ Culture* **43**, 137-145.

Berkelmans, R. and van Oppen, M. J. H. (2006). The role of zooxanthellae in the thermal tolerance of corals: a 'nugget of hope' for coral reefs in an era of climate change. *Proceedings of the Royal Society B: Biological Sciences* **273**, 2305-2312.

Bertucci, A., Moya, A., Tambutté, S., Allemand, D., Supuran, C. T. and Zoccola, D. (2013). Carbonic anhydrases in anthozoan corals—A review. *Bioorganic & medicinal chemistry* **21**, 1437-1450.

Bertucci, A., Tambutté, É., Tambutté, S., Allemand, D. and Zoccola, D. (2010). Symbiosis-dependent gene expression in coral–dinoflagellate association: cloning and characterization of a P-type H^+-ATPase gene. *Proceedings of the Royal Society B: Biological Sciences* **277**, 87-95.

Bhagooli, R. (2013). Inhibition of Calvin–Benson cycle suppresses the repair of photosystem II in *Symbiodinium*: implications for coral bleaching. *Hydrobiologia* **714**, 183-190.

Bhagooli, R. and Hidaka, M. (2003). Comparison of stress susceptibility of in hospite and isolated zooxanthellae among five coral species. *Journal of Experimental Marine Biology and Ecology* **291**, 181-197.

Boehning, D., van Rossum, D. B., Patterson, R. L. and Snyder, S. H. (2005). A peptide inhibitor of cytochrome c/inositol 1,4,5-trisphosphate receptor binding blocks intrinsic and extrinsic cell death pathways. *Proceedings of the National Academy of Sciences of the United States of America* **102**, 1466-1471.

Bohnert, H. J., Nelson, D. E. and Jensen, R. G. (1995). Adaptations to environmental stresses. *The Plant Cell* **7**, 1099.

Bourne, D., Iida, Y., Uthicke, S. and Smith-Keune, C. (2008). Changes in coral-associated microbial communities during a bleaching event. *ISME J* **2**, 350-363.

Bradford, M. M. (1976). A rapid and sensitive method for the quantitation of microgram quantities of protein utilizing the principle of protein-dye binding. *Analytical biochemistry* **72**, 248-254.

Brading, P., Warner, M. E., Smith, D. J. and Suggett, D. J. (2013). Contrasting modes of inorganic carbon acquisition amongst *Symbiodinium* (Dinophyceae) phylotypes. *New Phytologist* **200**, 432-442.

Brosché, M., Overmyer, K., Wrzaczek, M., Kangasjärvi, J. and Kangasjärvi, S. (2010). Stress Signaling III: Reactive Oxygen Species (ROS). In *Abiotic Stress Adaptation in Plants*, eds. A. Pareek S. K. Sopory and H. J. Bohnert), pp. 91-102: Springer Netherlands.

Brown, B. E. (1997a). Adaptations of reef corals to physical environmental stress. *Advances in Marine Biology* **31**, 221-299.

Brown, B. E. (1997b). Coral bleaching: causes and consequences. *Coral Reefs* **16**, S129-S138.

Brown, B. E., Ambarsari, I., Warner, M. E., Fitt, W. K., Dunne, R. P., Gibb, S. W. and Cummings, D. G. (1999). Diurnal changes in photochemical efficiency and xanthophyll concentrations in shallow water reef corals : evidence for photoinhibition and photoprotection. *Coral Reefs* **18**, 99-105.

Brown, B. E. and Bythell, J. C. (2005). Perspectives on mucus secretion in reef corals. *Marine Ecology Progress Series* **296**, 291-309.

Burke, L. M., Reytar, K., Spalding, M. and Perry, A. (2011). Reefs at risk revisited: World Resources Institute Washington, DC.

Burman, C. and Ktistakis, N. T. (2010). Regulation of autophagy by phosphatidylinositol 3-phosphate. *FEBS Lett* **584**, 1302–1312.

Burriesci, M. S., Raab, T. K. and Pringle, J. R. (2012). Evidence that glucose is the major transferred metabolite in dinoflagellate–cnidarian symbiosis. *J Exp Biol* **215**, 3467-3477.

Butterfield, E. R., Howe, C. J. and Nisbet, R. E. R. (2013). An analysis of dinoflagellate metabolism using EST data. *Protist* **164**, 218-236.

Buxton, L., Badger, M. and Ralph, P. (2009). Effects Of Moderate Heat Stress And Dissolved Inorganic Carbon Concentration On Photosynthesis And Respiration Of *Symbiodinium* Sp (Dinophyceae) In Culture And In Symbiosis. *Journal of Phycology* **45**, 357-365.

Byler, K. A., Carmi-Veal, M., Fine, M. and Goulet, T. L. (2013). Multiple Symbiont Acquisition Strategies as an Adaptive Mechanism in the Coral *Stylophora pistillata*. *PLoS One* **8**, e59596.

Cantin, N. E., van Oppen, M. J., Willis, B. L., Mieog, J. C. and Negri, A. P. (2009). Juvenile corals can acquire more carbon from high-performance algal symbionts. *Coral Reefs* **28**, 405-414.

Carpenter, K. E., Abrar, M., Aeby, G., Aronson, R. B., Banks, S., Bruckner, A., Chiriboga, A., Cortés, J., Delbeek, J. C., DeVantier, L. et al. (2008). One-Third of Reef-Building Corals Face Elevated Extinction Risk from Climate Change and Local Impacts. *Science* **321**, 560-563.

Cernichiari, E., Muscatine, L. and Smith, D. C. (1969). Maltose Excretion by the Symbiotic Algae of *Hydra viridis*. *Proceedings of the Royal Society of London B: Biological Sciences* **173**, 557-576.

Chakraborty, A., Koldobskiy, M. A., Sixt, K. M., Juluri, K. R., Mustafa, A. K., Snowman, A. M., van Rossum, D. B., Patterson, R. L. and Snyder, S. H. (2008). HSP90 regulates cell survival via inositol hexakisphosphate kinase-2. *Proceedings of the National Academy of Sciences* **105**, 1134-1139.

Chappell, J. (1980). Coral morphology, diversity and reef growth. *Nature* **286**, 249-252.

Clark, K. B. and Jensen, K. R. (1982). Effects of temperature on carbon fixation and carbon budget partitioning in the zooxanthellal symbiosis of *Aiptasia pallida* (Verrill). *Journal of Experimental Marine Biology and Ecology* **64**, 215-230.

Clouse, S. D. (2011). Brassinosteroids. *The Arabidopsis Book / American Society of Plant Biologists* **9**, e0151.

Coffroth, M. A. and Santos, S. R. (2005). Genetic Diversity of Symbiotic Dinoflagellates in the Genus *Symbiodinium*. *Protist* **156**, 19-34.

Coles, S. L. and Jokiel, P. L. (1977). Effects of temperature on photosynthesis and respiration in hermatypic corals. *Marine Biology* **43**, 209-216.

Connell, J. H. (1978). Diversity in tropical rain forests and coral reefs. *Science* **199**, 1302-1310.

Cook, C., D'Elia, C. and Muller-Parker, G. (1988). Host feeding and nutrient sufficiency for zooxanthellae in the sea anemone *Aiptasia pallida*. *Marine Biology* **98**, 253-262.

Cook, C. B. and Davy, S. K. (2001). Are free amino acids responsible for the `host factor' effects on symbiotic zooxanthellae in extracts of host tissue? *Hydrobiologia* **461**, 71-78.

Crossland, C., Hatcher, B. and Smith, S. (1991). Role of coral reefs in global ocean production. *Coral Reefs* **10**, 55-64.

Császár, N. B. M., Seneca, F. O. and van Oppen, M. J. H. (2009). Variation in antioxidant gene expression in the scleractinian coral *Acropora millepora* under laboratory thermal stress. *Marine Ecology Progress Series* **392**, 93-102.

Cuif, J. P., Dauphin, Y., Freiwald, A., Gautret, P. and Zibrowius, H. (1999). Biochemical markers of zooxanthellae symbiosis in soluble matrices of skeleton of 24 Scleractinia species. *Comparative Biochemistry and Physiology Part A: Molecular & Integrative Physiology* **123**, 269-278.

D'Autreaux, B. and Toledano, M. B. (2007). ROS as signalling molecules: mechanisms that generate specificity in ROS homeostasis. *Nat Rev Mol Cell Biol* **8**, 813-824.

D'Elia, C. F., Domotor, S. L. and Webb, K. L. (1983). Nutrient uptake kinetics of freshly isolated zooxanthellae. *Marine Biology* **75**, 157-167.

Dagenais-Bellefeuille, S. and Morse, D. (2013). Putting the N in dinoflagellates. *Frontiers in Microbiology* **4**, 369.

Dagenais Bellefeuille, S., Dorion, S., Rivoal, J. and Morse, D. (2014). The Dinoflagellate *Lingulodinium polyedrum* Responds to N Depletion by a Polarized Deposition of Starch and Lipid Bodies. *PLoS One* **9**, e111067.

Dat, J., Vandenabeele, S., Vranová, E., Van Montagu, M., Inzé*, D. and Van Breusegem, F. (2000). Dual action of the active oxygen species during plant stress responses. *Cellular and Molecular Life Sciences* **57**, 779-95.

Davy, S. K., Allemand, D. and Weis, V. M. (2012). Cell biology of cnidarian-dinoflagellate symbiosis. *Microbiology and Molecular Biology Reviews* **76**, 229-261.

Davy, S. K., Withers, K. J. T. and Hinde, R. (2006). Effects of host nutritional status and seasonality on the nitrogen status of zooxanthellae in the temperate coral *Plesiastrea versipora* (Lamarck). *Journal of Experimental Marine Biology and Ecology* **335**, 256-265.

De Bary, A. (1879). Die erscheinung der symbiose. Strassburg, Germany: Verlag von Karl J. Trubner.

De Groot, R. S., Wilson, M. A. and Boumans, R. M. (2002). A typology for the classification, description and valuation of ecosystem functions, goods and services. *Ecological Economics* **41**, 393-408.

del Carmen Martínez-Ballesta, M., Moreno, D. A. and Carvajal, M. (2013). The Physiological Importance of Glucosinolates on Plant Response to Abiotic Stress in *Brassica*. *International Journal of Molecular Sciences* **14**, 11607-11625.

Desalvo, M., Voolstra, C., Sunagawa, S., Schwarz, J., Stillman, J., Coffroth, M. A., Szmant, A. and Medina, M. (2008). Differential gene expression during thermal stress and bleaching in the Caribbean coral *Montastraea faveolata*. *Molecular Ecology* **17**, 3952-3971.

Dettmer, K., Aronov, P. A. and Hammock, B. D. (2007). Mass spectrometry-based metabolomics. *Mass Spectrometry Reviews* **26**, 51-78.

Dias, D. A., Hill, C. B., Jayasinghe, N. S., Atieno, J., Sutton, T. and Roessner, U. (2015). Quantitative profiling of polar primary metabolites of two

chickpea cultivars with contrasting responses to salinity. *Journal of Chromatography B* **1000**, 1-13.

Díaz-Almeyda, E., Thomé, P. E., El Hafidi, M. and Iglesias-Prieto, R. (2011). Differential stability of photosynthetic membranes and fatty acid composition at elevated temperature in *Symbiodinium*. *Coral Reefs* **30**, 217-225.

Dixon, R. A. and Paiva, N. L. (1995). Stress-Induced Phenylpropanoid Metabolism. *The Plant Cell* **7**, 1085-1097.

Doebeli, M. and Knowlton, N. (1998). The evolution of interspecific mutualisms. *Proceedings of the National Academy of Sciences* **95**, 8676-8680.

Donner, S. D., Skirving, W. J., Little, C. M., Oppenheimer, M. and Hoegh-Guldberg, O. (2005). Global assessment of coral bleaching and required rates of adaptation under climate change. *Global Change Biology* **11**, 2251-2265.

Dove, S. (2004). Scleractinian corals with photoprotective host pigments are hypersensitive to thermal bleaching. *Marine Ecology Progress Series* **272**, 99-116.

Downs, C. A., Fauth, J. E., Halas, J. C., Dustan, P., Bemiss, J. and Woodley, C. M. (2002). Oxidative stress and seasonal coral bleaching. *Free Radical Biology and Medicine* **33**, 533-543.

Du, H., Wang, Z., Yu, W., Liu, Y. and Huang, B. (2011). Differential metabolic responses of perennial grass *Cynodon transvaalensis*×*Cynodon dactylon* (C4) and *Poa Pratensis* (C3) to heat stress. *Physiologia Plantarum* **141**, 251-264.

Duckwall, C. S., Murphy, T. A. and Young, J. D. (2013). Mapping cancer cell metabolism with ^{13}C flux analysis: Recent progress and future challenges. *Journal of Carcinogenesis* **12**, 13.

Dumville, J. C. and Fry, S. C. (2003). Gentiobiose: a novel oligosaccharin in ripening tomato fruit. *Planta* **216**, 484-495.

Dunn, S. R., Bythell, J. C., Le Tissier, M. D. A., Burnett, W. J. and Thomason, J. C. (2002). Programmed cell death and cell necrosis activity during hyperthermic stress-induced bleaching of the symbiotic sea anemone *Aiptasia* sp. *Journal of Experimental Marine Biology and Ecology* **272**, 29-53.

Dunn, S. R., Schnitzler, C. E. and Weis, V. M. (2007). Apoptosis and autophagy as mechanisms of dinoflagellate symbiont release during cnidarian bleaching: every which way you lose. *Proceedings of the Royal Society of London B: Biological Sciences* **274**, 3079-3085.

Dunn, S. R., Thomas, M. C., Nette, G. W. and Dove, S. G. (2012). A lipidomic approach to understanding free fatty acid lipogenesis derived from dissolved inorganic carbon within cnidarian-dinoflagellate symbiosis. *PLoS One* **7**, e46801.

Dunn, S. R., Thomason, J. C., Le Tissier, M. D. and Bythell, J. C. (2004). Heat stress induces different forms of cell death in sea anemones and their endosymbiotic algae depending on temperature and duration. *Cell Death Differ* **11**, 1213-22.

Eakin, C. M., Lough, J. M. and Heron, S. F. (2009). Climate Variability and Change: Monitoring Data and Evidence for Increased Coral Bleaching Stress. In *Coral Bleaching*, vol. 205 eds. M. H. van Oppen and J. Lough), pp. 41-67: Springer Berlin Heidelberg.

Eastmond, P. J. and Graham, I. A. (2001). Re-examining the role of the glyoxylate cycle in oilseeds. *Trends in Plant Science* **6**, 72-78.

Eccleston, V. S. and Ohlrogge, J. B. (1998). Expression of Lauroyl-Acyl Carrier Protein Thioesterase in *Brassica napus* Seeds Induces Pathways for Both Fatty Acid Oxidation and Biosynthesis and Implies a Set Point for Triacylglycerol Accumulation. *The Plant Cell* **10**, 613-621.

Edmunds, P. J. and Gates, R. D. (2003). Has coral bleaching delayed our understanding of fundamental aspects of coral–dinoflagellate symbioses? *Bioscience* **53**, 976-980.

Ezzat, L., Towle, E., Irisson, J.-O., Langdon, C. and Ferrier-Pagès, C. (2016). The relationship between heterotrophic feeding and inorganic nutrient availability in the scleractinian coral *T. reniformis* under a short-term temperature increase. *Limnology and oceanography* **61**, 89-102.

Fadlallah, Y. H. (1983). Sexual reproduction, development and larval biology in scleractinian corals. *Coral Reefs* **2**, 129-150.

Falkowski, P. G., Dubinsky, Z., Muscatine, L. and McCloskey, L. (1993). Population control in symbiotic corals. *Bioscience* **43**, 606-611.

Fancy, S.-A. and Rumpel, K. (2008). GC-MS-Based Metabolomics. In *Biomarker Methods in Drug Discovery and Development*, (ed. F. Wang), pp. 317-340: Humana Press.

Fenton-Navarro, B., Arreguín-L, B. n., García-Hernández, E., Heimer, E., B. Aguilar, M., Rodríguez-A, C. and Arreguín-Espinosa, R. (2003). Purification and structural characterization of lectins from the cnidarian *Bunodeopsis antillienis*. *Toxicon* **42**, 525-532.

Fernie, A. R., Carrari, F. and Sweetlove, L. J. (2004). Respiratory metabolism: glycolysis, the TCA cycle and mitochondrial electron transport. *Current Opinion in Plant Biology* **7**, 254-261.

Ferrier-Pagès, C., Richard, C., Forcioli, D., Allemand, D., Pichon, M. and Shick, J. M. (2007). Effects of temperature and UV radiation increases on the photosynthetic efficiency in four scleractinian coral species. *The Biological Bulletin* **213**, 76-87.

Fiehn, O. (2002). Metabolomics--the link between genotypes and phenotypes. *Plant Molecular Biology* **48**, 155-171.

Fiehn, O., Kopka, J., Dörmann, P., Altmann, T., Trethewey, R. N. and Willmitzer, L. (2000). Metabolite profiling for plant functional genomics. *Nature biotechnology* **18**, 1157-1161.

Field, R. (2009). Oligosaccharide Signalling Molecules. In *Plant-derived Natural Products*, eds. A. E. Osbourn and V. Lanzotti), pp. 349-359: Springer US.

Fisher, P. L., Malme, M. K. and Dove, S. (2012). The effect of temperature stress on coral–*Symbiodinium* associations containing distinct symbiont types. *Coral Reefs* **31**, 473-485.

Fitt, W., McFarland, F., Warner, M. and Chilcoat, G. (2000). Seasonal patterns of tissue biomass and densities of symbiotic dinoflagellates in reef corals and relation to coral bleaching. *Limnology and oceanography* **45**, 677-685.

Fleury, B. G., Coll, J. C., Tentori, E., Duquesne, S. and Figueiredo, L. (2000). Effect of nutrient enrichment on the complementary (secondary) metabolite composition of the soft coral *Sarcophyton ehrenbergi* (Cnidaria: Octocorallia: Alcyonaceae) of the Great Barrier Reef. *Marine Biology* **136**, 63-68.

Forest, R., Victor, S., Farooq, A. and Nancy, K. (2002). Diversity and distribution of coral-associated bacteria. *Marine Ecology Progress Series* **243**, 1-10.

Freudenthal, H. D. (1962). *Symbiodinium* gen. nov. and *Symbiodinium microadriaticum* sp. nov., a Zooxanthella: Taxonomy, Life Cycle, and Morphology. *The Journal of Protozoology* **9**, 45-52.

Frieler, K., Meinshausen, M., Golly, A., Mengel, M., Lebek, K., Donner, S. D. and Hoegh-Guldberg, O. (2013). Limiting global warming to 2°C is unlikely to save most coral reefs. *Nature Clim. Change* **3**, 165-170.

Ganot, P., Moya, A., Magnone, V., Allemand, D., Furla, P. and Sabourault, C. (2011). Adaptations to Endosymbiosis in a Cnidarian-Dinoflagellate Association: Differential Gene Expression and Specific Gene Duplications. *PLoS Genetics* **7**, e1002187.

Garrett, T. A., Schmeitzel, J. L., Klein, J. A., Hwang, J. J. and Schwarz, J. A. (2013). Comparative Lipid Profiling of the Cnidarian *Aiptasia pallida* and Its Dinoflagellate Symbiont. *PLoS One* **8**, e57975.

Gates, R. D., Hoegh-Guldberg, O., McFall-Ngai, M. J., Bil, K. Y. and Muscatine, L. (1995). Free amino acids exhibit anthozoan "host factor" activity: they induce the release of photosynthate from symbiotic dinoflagellates *in vitro*. *Proceedings of the National Academy of Sciences* **92**, 7430-7434.

Geiger, D. R. and Servaites, J. C. (1994). Diurnal regulation of photosynthetic carbon metabolism in C3 plants. *Annual Review of Plant Biology* **45**, 235-256.

Gibson, S. I. (2004). Sugar and phytohormone response pathways: navigating a signalling network. *Journal of Experimental Botany* **55**, 253-264.

Gill, S. S. and Tuteja, N. (2010). Reactive oxygen species and antioxidant machinery in abiotic stress tolerance in crop plants. *Plant Physiology and Biochemistry* **48**, 909-930.

Glynn, P. W. (1996). Coral reef bleaching: facts, hypotheses and implications. *Global Change Biology* **2**, 495-509.

Godinot, C., Ferrier-Pagés, C. and Grover, R. (2009). Control of phosphate uptake by zooxanthellae and host cells in the scleractinian coral *Stylophora pistillata*. *Limnology and oceanography* **54**, 1627-1633.

Godinot, C., Grover, R., Allemand, D. and Ferrier-Pagès, C. (2011). High phosphate uptake requirements of the scleractinian coral *Stylophora pistillata*. *Journal of Experimental Biology* **214**, 2749-2754.

Gómez-Cabrera, M. C., Ortiz, J. C., Loh, W. K. W., Ward, S. and Hoegh-Guldberg, O. (2008). Acquisition of symbiotic dinoflagellates (*Symbiodinium*) by juveniles of the coral *Acropora longicyathus*. *Coral Reefs* **27**, 219-226.

Gonzali, S., Novi, G., Loreti, E., Paolicchi, F., Poggi, A., Alpi, A. and Perata, P. (2005). A turanose-insensitive mutant suggests a role for WOX5 in auxin homeostasis in *Arabidopsis thaliana*. *The Plant Journal* **44**, 633-645.

Gordon, B., Leggat, W. and Motti, C. (2013). Extraction Protocol for Nontargeted NMR and LC-MS Metabolomics-Based Analysis of Hard Coral and Their Algal Symbionts. In *Metabolomics Tools for Natural Product Discovery*, vol. 1055 eds. U. Roessner and D. A. Dias), pp. 129-147: Humana Press.

Gordon, B. R. and Leggat, W. (2010). *Symbiodinium*—Invertebrate symbioses and the role of metabolomics. *Marine drugs* **8**, 2546-2568.

Goreau, T. F. (1959). The Ecology of Jamaican Coral Reefs I. Species Composition and Zonation. *Ecology* **40**, 67-90.

Grant, A., Rémond, M., People, J. and Hinde, R. (1997). Effects of host-tissue homogenate of the scleractinian coral *Plesiastrea versipora* on glycerol metabolism in isolated symbiotic dinoflagellates. *Marine Biology* **128**, 665-670.

Grant, A. J., Rémond, M., Starke-Peterkovic, T. and Hinde, R. (2006). A cell signal from the coral *Plesiastrea versipora* reduces starch synthesis in its symbiotic alga, *Symbiodinium* sp. *Comparative Biochemistry and Physiology Part A: Molecular & Integrative Physiology* **144**, 458-463.

Griffin, J. L. and Shockcor, J. P. (2004). Metabolic profiles of cancer cells. *Nat Rev Cancer* **4**, 551-561.

Grottoli, A. and Rodrigues, L. (2011). Bleached *Porites compressa* and *Montipora capitata* corals catabolize δ^{13}C-enriched lipids. *Coral Reefs* **30**, 687-692.

Grottoli, A. G., Rodrigues, L. J. and Juarez, C. (2004). Lipids and stable carbon isotopes in two species of Hawaiian corals, *Porites compressa* and *Montipora verrucosa*, following a bleaching event. *Marine Biology* **145**, 621-631.

Grottoli, A. G., Rodrigues, L. J. and Palardy, J. E. (2006). Heterotrophic plasticity and resilience in bleached corals. *Nature* **440**, 1186-1189.

Grottoli, A. G., Warner, M. E., Levas, S. J., Aschaffenburg, M. D., Schoepf, V., McGinley, M., Baumann, J. and Matsui, Y. (2014). The cumulative impact of annual coral bleaching can turn some coral species winners into losers. *Global Change Biology* **20**, 3823-3833.

Grover, R., Maguer, J.-F., Reynaud-Vaganay, S. and Ferrier-Pages, C. (2002). Uptake of ammonium by the scleractinian coral *Stylophora pistillata*: effect of feeding, light, and ammonium concentrations. *Limnology and oceanography* **47**, 782-790.

Grubb, C. D. and Abel, S. (2006). Glucosinolate metabolism and its control. *Trends in Plant Science* **11**, 89-100.

Grüning, N.-M., Lehrach, H. and Ralser, M. (2010). Regulatory crosstalk of the metabolic network. *Trends in Biochemical Sciences* **35**, 220-227.

Gu, J., Weber, K., Klemp, E., Winters, G., Franssen, S. U., Wienpahl, I., Huylmans, A.-K., Zecher, K., Reusch, T. B. H., Bornberg-Bauer, E. et al. (2012). Identifying core features of adaptive metabolic mechanisms for chronic heat stress attenuation contributing to systems robustness. *Integrative biology : quantitative biosciences from nano to macro* **4**, 480-493.

Guerzoni, M. E., Lanciotti, R. and Cocconcelli, P. S. (2001). Alteration in cellular fatty acid composition as a response to salt, acid, oxidative and thermal stresses in *Lactobacillus helveticus*. *Microbiology* **147**, 2255-2264.

Guy, C., Kaplan, F., Kopka, J., Selbig, J. and Hincha, D. K. (2008). Metabolomics of temperature stress. *Physiologia Plantarum* **132**, 220-235.

Hall, V. and Hughes, T. (1996). Reproductive strategies of modular organisms: comparative studies of reef-building corals. *Ecology* **77**, 950-963.

Harii, S., Yasuda, N., Rodriguez-Lanetty, M., Irie, T. and Hidaka, M. (2009). Onset of symbiosis and distribution patterns of symbiotic dinoflagellates in the larvae of scleractinian corals. *Marine Biology* **156**, 1203-1212.

Harrison, P. (2011). Sexual Reproduction of Scleractinian Corals. In *Coral Reefs: An Ecosystem in Transition*, eds. Z. Dubinsky and N. Stambler), pp. 59-85: Springer Netherlands.

Hawkridge, J. M., Pipe, R. K. and Brown, B. E. (2000). Localisation of antioxidant enzymes in the cnidarians *Anemonia viridis* and *Goniopora stokesi*. *Marine Biology* **137**, 1-9.

Heise, R., Arrivault, S., Szecowka, M., Tohge, T., Nunes-Nesi, A., Stitt, M., Nikoloski, Z. and Fernie, A. R. (2014). Flux profiling of photosynthetic carbon metabolism in intact plants. *Nat. Protocols* **9**, 1803-1824.

Herre, E. A., Knowlton, N., Mueller, U. G. and Rehner, S. A. (1999). The evolution of mutualisms: exploring the paths between conflict and cooperation. *Trends in Ecology & Evolution* **14**, 49-53.

Hill, R., Larkum, A., Prášil, O., Kramer, D., Szabó, M., Kumar, V. and Ralph, P. (2012). Light-induced dissociation of antenna complexes in the symbionts of scleractinian corals correlates with sensitivity to coral bleaching. *Coral Reefs* **31**, 963-975.

Hill, R., Larkum, A. W. D., Frankart, C., Kühl, M. and Ralph, P. J. (2004). Loss of Functional Photosystem II Reaction Centres in Zooxanthellae of Corals Exposed to Bleaching Conditions: Using Fluorescence Rise Kinetics. *Photosynthesis Research* **82**, 59-72.

Hill, R. and Ralph, P. (2008). Impact of bleaching stress on the function of the oxygen evolving complex of zooxanthellae from scleractinian corals. *Journal of Phycology* **44**, 299-310.

Hill, R. and Ralph, P. J. (2007). Post-bleaching viability of expelled zooxanthellae from the scleractinian coral *Pocillopora damicornis*. *Mar Ecol Prog Ser* **352**, 137-144.

Hill, R., Szabó, M., ur Rehman, A., Vass, I., Ralph, P. J. and Larkum, A. W. (2014). Inhibition of photosynthetic CO_2 fixation in the coral *Pocillopora*

damicornis and its relationship to thermal bleaching. *J Exp Biol* **217**, 2150-2162.

Hill, R., Ulstrup, K. E. and Ralph, P. J. (2009). Temperature induced changes in thylakoid membrane thermostability of cultured, freshly isolated, and expelled zooxanthellae from scleractinian corals. *Bulletin of Marine Science* **85**, 223-244.

Hiller, K., Hangebrauk, J., Jäger, C., Spura, J., Schreiber, K. and Schomburg, D. (2009). MetaboliteDetector: Comprehensive Analysis Tool for Targeted and Nontargeted GC/MS Based Metabolome Analysis. *Analytical Chemistry* **81**, 3429-3439.

Hiller, K., Wegner, A., Weindl, D., Cordes, T., Metallo, C. M., Kelleher, J. K. and Stephanopoulos, G. (2013). NTFD—a stand-alone application for the non-targeted detection of stable isotope-labeled compounds in GC/MS data. *Bioinformatics* **29**, 1226-1228.

Hoadley, K. D., Pettay, D. T., Dodge, D. and Warner, M. E. (2016). Contrasting physiological plasticity in response to environmental stress within different cnidarians and their respective symbionts. *Coral Reefs* **35**, 529-542.

Hoegh-Guldberg, O. (1999). Climate change, coral bleaching and the future of the world's coral reefs. *Marine and Freshwater Research* **50**, 839-866.

Hoegh-Guldberg, O. and Jones, R. J. (1999). Photoinhibition and photoprotection in symbiotic dinoflagellates from reef-building corals. *Marine Ecology Progress Series* **183**, 73-86.

Hoegh-Guldberg, O., Mumby, P. J., Hooten, A. J., Steneck, R. S., Greenfield, P., Gomez, E., Harvell, C. D., Sale, P. F., Edwards, A. J., Caldeira, K. et al. (2007). Coral Reefs Under Rapid Climate Change and Ocean Acidification. *Science* **318**, 1737-1742.

Hoegh-Guldberg, O. and Smith, G. J. (1989). The effect of sudden changes in temperature, light and salinity on the population density and export of zooxanthellae from the reef corals *Stylophora pistillata* Esper and *Seriatopora hystrix* Dana. *Journal of Experimental Marine Biology and Ecology* **129**, 279-303.

Holling, C. S. (1973). Resilience and Stability of Ecological Systems. *Annual Review of Ecology and Systematics* **4**, 1-23.

Hoogenboom, M. O., Anthony, K. R. N. and Connolly, S. R. (2006). Energetic cost of photoinhibition in corals. *Marine Ecology Progress Series* **313**, 1-12.

Hoogenboom, M. O., Campbell, D. A., Beraud, E., DeZeeuw, K. and Ferrier-Pagès, C. (2012). Effects of light, food availability and temperature stress on the function of photosystem II and photosystem I of coral symbionts. *PLoS One* **7**, e30167-e30167.

Hughes, A. D. and Grottoli, A. G. (2013). Heterotrophic compensation: a possible mechanism for resilience of coral reefs to global warming or a sign of prolonged stress? *PLoS One* **8**, e81172.

Hughes, T. P. (1994). Catastrophes, phase shifts, and large-scale degradation of a Caribbean coral reef. *Science-AAAS-Weekly Paper Edition* **265**, 1547-1551.

Hughes, T. P., Baird, A. H., Bellwood, D. R., Card, M., Connolly, S. R., Folke, C., Grosberg, R., Hoegh-Guldberg, O., Jackson, J. and Kleypas, J. (2003). Climate change, human impacts, and the resilience of coral reefs. *Science* **301**, 929-933.

Hughes, T. P., Graham, N. A., Jackson, J. B., Mumby, P. J. and Steneck, R. S. (2010). Rising to the challenge of sustaining coral reef resilience. *Trends in Ecology & Evolution* **25**, 633-642.

Hughes, T. P., Rodrigues, M. J., Bellwood, D. R., Ceccarelli, D., Hoegh-Guldberg, O., McCook, L., Moltschaniwskyj, N., Pratchett, M. S., Steneck, R. S. and Willis, B. (2007). Phase shifts, herbivory, and the resilience of coral reefs to climate change. *Current Biology* **17**, 360-365.

Iglesias-Prieto, R., Govind, N. S. and Trench, R. K. (1991). Apoprotein Composition and Spectroscopic Characterization of the Water-Soluble Peridinin--Chlorophyll a--Proteins from Three Symbiotic Dinoflagellates. *Proceedings of the Royal Society of London B: Biological Sciences* **246**, 275-283.

Iglesias-Prieto, R. and Trench, R. (1997). Acclimation and adaptation to irradiance in symbiotic dinoflagellates. II. Response of chlorophyll–protein complexes to different photon-flux densities. *Marine Biology* **130**, 23-33.

Imbs, A. B. and Yakovleva, I. M. (2012). Dynamics of lipid and fatty acid composition of shallow-water corals under thermal stress: an experimental approach. *Coral Reefs* **31**, 41-53.

Imbs, A. B., Yakovleva, I. M., Dautova, T. N., Bui, L. H. and Jones, P. (2014). Diversity of fatty acid composition of symbiotic dinoflagellates in corals: Evidence for the transfer of host PUFAs to the symbionts. *Phytochemistry* **101**, 76-82.

Ishikura, M., Adachi, K. and Maruyama, T. (1999). Zooxanthellae release glucose in the tissue of a giant clam, *Tridacna crocea*. *Marine Biology* **133**, 665-673.

Jiang, P.-L., Pasaribu, B. and Chen, C.-S. (2014). Nitrogen-Deprivation Elevates Lipid Levels in *Symbiodinium* spp. by Lipid Droplet Accumulation: Morphological and Compositional Analyses. *PLoS One* **9**, e87416.

Johannes, R., Wiebe, W., Crossland, C., Rimmer, D. and Smith, S. (1983). Latitudinal limits of coral reef growth. *Marine ecology progress series. Oldendorf* **11**, 105-111.

Jokiel, P. L. and Coles, S. L. (1990). Response of Hawaiian and other Indo-Pacific reef corals to elevated temperature. *Coral Reefs* **8**, 155-162.

Jones, A. M. and Berkelmans, R. (2011). Tradeoffs to Thermal Acclimation: Energetics and Reproduction of a Reef Coral with Heat Tolerant *Symbiodinium* Type-D. *Journal of Marine Biology* **2011**, 12 pages.

Jones, A. M., Berkelmans, R., van Oppen, M. J. H., Mieog, J. C. and Sinclair, W. (2008). A community change in the algal endosymbionts of a scleractinian coral following a natural bleaching event: field evidence of acclimatization. *Proceedings of the Royal Society of London B: Biological Sciences* **275**, 1359-1365.

Jones, R. and Hoegh-Guldberg, O. (2001). Diurnal changes in the photochemical efficiency of the symbiotic dinoflagellates (Dinophyceae) of corals: photoprotection, photoinactivation and the relationship to coral bleaching. *Plant, Cell & Environment* **24**, 89-99.

Jones, R., Hoegh-Guldberg, O., Larkum, A. and Schreiber, U. (1998). Temperature-induced bleaching of corals begins with impairment of

the CO_2 fixation mechanism in zooxanthellae. *Plant, Cell & Environment* **21**, 1219-1230.

Jones, R. J. and Yellowlees, D. (1997). Regulation and control of intracellular algae (= zooxanthellae) in hard corals. *Philosophical Transactions of the Royal Society of London B: Biological Sciences* **352**, 457-468.

Kanani, H., Chrysanthopoulos, P. K. and Klapa, M. I. (2008). Standardizing GC-MS metabolomics. *Journal of chromatography.B, Analytical technologies in the biomedical and life sciences* **871**, 191-201.

Kaplan, F., Kopka, J., Haskell, D. W., Zhao, W., Schiller, K. C., Gatzke, N., Sung, D. Y. and Guy, C. L. (2004). Exploring the temperature-stress metabolome of *Arabidopsis*. *Plant Physiol* **136**, 4159-68.

Kellogg, R. B. and Patton, J. S. (1983). Lipid droplets, medium of energy exchange in the symbiotic anemone *Condylactis gigantea*: a model coral polyp. *Marine Biology* **75**, 137-149.

Kenkel, C. D., Meyer, E. and Matz, M. V. (2013). Gene expression under chronic heat stress in populations of the mustard hill coral (*Porites astreoides*) from different thermal environments. *Molecular Ecology* **22**, 4322-4334.

Kim, H. K. and Verpoorte, R. (2010). Sample preparation for plant metabolomics. *Phytochemical Analysis* **21**, 4-13.

Klein, S. and Heinzle, E. (2012). Isotope labeling experiments in metabolomics and fluxomics. *Wiley Interdisciplinary Reviews: Systems Biology and Medicine* **4**, 261-272.

Klueter, A., Crandall, J., Archer, F., Teece, M. and Coffroth, M. (2015). Taxonomic and Environmental Variation of Metabolite Profiles in Marine Dinoflagellates of the Genus *Symbiodinium*. *Metabolites* **5**, 74-99.

Kneeland, J., Hughen, K., Cervino, J., Hauff, B. and Eglinton, T. (2013). Lipid biomarkers in *Symbiodinium* dinoflagellates: new indicators of thermal stress. *Coral Reefs* **32**, 923-934.

Kopp, C., Domart-Coulon, I., Escrig, S., Humbel, B. M., Hignette, M. and Meibom, A. (2015). Subcellular Investigation of Photosynthesis-Driven Carbon Assimilation in the Symbiotic Reef Coral *Pocillopora damicornis*. *mBio* **6**.

Kopp, C., Pernice, M., Domart-Coulon, I., Djediat, C., Spangenberg, J. E., Alexander, D. T. L., Hignette, M., Meziane, T. and Meibom, A. (2013). Highly Dynamic Cellular-Level Response of Symbiotic Coral to a Sudden Increase in Environmental Nitrogen. *mBio* **4**, e00052-13.

Krämer, W. E., Schrameyer, V., Hill, R., Ralph, P. J. and Bischof, K. (2013). PSII activity and pigment dynamics of *Symbiodinium* in two Indo-Pacific corals exposed to short-term high-light stress. *Marine Biology* **160**, 563-577.

Krueger, T., Becker, S., Pontasch, S., Dove, S., Hoegh-Guldberg, O., Leggat, W., Fisher, P. L. and Davy, S. K. (2014). Antioxidant plasticity and thermal sensitivity in four types of *Symbiodinium* sp. *Journal of Phycology* **50**, 1035-1047.

Krueger, T., Hawkins, T. D., Becker, S., Pontasch, S., Dove, S., Hoegh-Guldberg, O., Leggat, W., Fisher, P. L. and Davy, S. K. (2015). Differential coral bleaching—Contrasting the activity and response of enzymatic antioxidants in symbiotic partners under thermal stress. *Comparative Biochemistry and Physiology Part A: Molecular & Integrative Physiology* **190**, 15-25.

Kruger, A., Gruning, N. M., Wamelink, M. M., Kerick, M., Kirpy, A., Parkhomchuk, D., Bluemlein, K., Schweiger, M. R., Soldatov, A., Lehrach, H. et al. (2011). The pentose phosphate pathway is a metabolic redox sensor and regulates transcription during the antioxidant response. *Antioxid Redox Signal* **15**, 311-24.

Kwiatkowski, L., Cox, P., Halloran, P. R., Mumby, P. J. and Wiltshire, A. J. (2015). Coral bleaching under unconventional scenarios of climate warming and ocean acidification. *Nature Clim. Change* **5**, 777-781.

LaJeunesse, T. C. (2001). Investigating the biodiversity, ecology, and phylogeny of endosymbiotic dinoflagellates in the genus *Symbiodinium* using the ITS region: in search of a “species” level marker. *Journal of Phycology* **37**, 866-880.

LaJeunesse, T. C., Bhagooli, R., Hidaka, M., deVantier, L., Done, T., Schmidt, G. W., Fitt, W. K. and Hoegh-Guldberg, O. (2004). Closely related *Symbiodinium* spp. differ in relative dominance in coral reef host communities

across environmental, latitudinal and biogeographic gradients. *Marine Ecology Progress Series* **284**, 147-161.

LaJeunesse, T. C., Lee, S. Y., Gil-Agudelo, D. L., Knowlton, N. and Jeong, H. J. (2015). *Symbiodinium necroappetens* sp. nov. (Dinophyceae): an opportunist 'zooxanthella' found in bleached and diseased tissues of Caribbean reef corals. *European Journal of Phycology* **50**, 223-238.

LaJeunesse, T. C., Loh, W. K. W., van Woesik, R., Hoegh-Guldberg, O., Schmidt, G. W. and Fitt, W. K. (2003). Low symbiont diversity in southern Great Barrier Reef corals relative to those of the Caribbean. *Limnology and oceanography* **48**, 2046-2054.

LaJeunesse, T. C., Smith, R., Walther, M., Pinzón, J., Pettay, D. T., McGinley, M., Aschaffenburg, M., Medina-Rosas, P., Cupul-Magaña, A. L. and Pérez, A. L. (2010). Host–symbiont recombination versus natural selection in the response of coral–dinoflagellate symbioses to environmental disturbance. *Proceedings of the Royal Society B: Biological Sciences* **283**, rspb20100385.

LaJeunesse, T. C. and Thornhill, D. J. (2011). Improved Resolution of Reef-Coral Endosymbiont *Symbiodinium* Species Diversity, Ecology, and Evolution through *psbA* Non-Coding Region Genotyping. *PLoS One* **6**, e29013.

Lankadurai, B. P., Nagato, E. G. and Simpson, M. J. (2013). Environmental metabolomics: an emerging approach to study organism responses to environmental stressors. *Environmental Reviews* **21**, 180-205.

Leal, M. C., Nunes, C., Kempf, S., Reis, A., da Silva, T. L., Serôdio, J., Cleary, D. F. R. and Calado, R. (2013). Effect of light, temperature and diet on the fatty acid profile of the tropical sea anemone *Aiptasia pallida*. *Aquaculture Nutrition* **19**, 818-826.

Lee, S. T. M., Davy, S. K., Tang, S.-L., Fan, T.-Y. and Kench, P. S. (2015). Successive shifts in the microbial community of the surface mucus layer and tissues of the coral *Acropora muricata* under thermal stress. *FEMS microbiology ecology* **91**.

Leggat, W., Badger, M. R. and Yellowlees, D. (1999). Evidence for an Inorganic Carbon-Concentrating Mechanism in the Symbiotic Dinoflagellate *Symbiodinium* sp. *Plant Physiol* **121**, 1247-1255.

Leggat, W., Hoegh-Guldberg, O., Dove, S. and Yellowlees, D. (2007). Analysis of an EST library from the dinoflagellate (*Symbiodinium* sp.) symbiont of reef-building corals. *Journal of Phycology* **43**, 1010-1021.

Leggat, W., Seneca, F., Wasmund, K., Ukani, L., Yellowlees, D. and Ainsworth, T. D. (2011). Differential responses of the coral host and their algal symbiont to thermal stress. *PLoS One* **6**, e26687.

Lehnert, E. M., Mouchka, M. E., Burriesci, M. S., Gallo, N. D., Schwarz, J. A. and Pringle, J. R. (2014). Extensive Differences in Gene Expression Between Symbiotic and Aposymbiotic Cnidarians. *G3: Genes|Genomes|Genetics* **4**, 277-295.

Lesser, M. (1997). Oxidative stress causes coral bleaching during exposure to elevated temperatures. *Coral Reefs* **16**, 187-192.

Lesser, M. P. (1996). Elevated temperatures and ultraviolet radiation cause oxidative stress and inhibit photosynthesis in symbiotic dinoflagellates. *Limnology and oceanography* **41**, 271-283.

Lesser, M. P. (2006). Oxidative stress in marine environments: biochemistry and physiological ecology. *Annual Review of Physiology* **68**, 253-278.

Lesser, M. P. (2011). Coral bleaching: causes and mechanisms. In *Coral reefs: An ecosystem in transition*, pp. 405-419: Springer.

Lewis, C. L. and Coffroth, M. A. (2004). The Acquisition of Exogenous Algal Symbionts by an Octocoral After Bleaching. *Science* **304**, 1490-1492.

Li, Y., Han, D., Hu, G., Sommerfeld, M. and Hu, Q. (2010). Inhibition of starch synthesis results in overproduction of lipids in *Chlamydomonas reinhardtii*. *Biotechnology and Bioengineering* **107**, 258-268.

Lilley, R., Ralph, P. J. and Larkum, A. W. (2010). The determination of activity of the enzyme Rubisco in cell extracts of the dinoflagellate alga *Symbiodinium* sp. by manganese chemiluminescence and its response to short-term thermal stress of the alga. *Plant, Cell & Environment* **33**, 995-1004.

Little, A. F., Van Oppen, M. J. and Willis, B. L. (2004). Flexibility in algal endosymbioses shapes growth in reef corals. *Science* **304**, 1492-1494.

Livingstone, D. R. (1991). Origins and Evolution of Pathways of Anaerobic Metabolism in the Animal Kingdom. *American Zoologist* **31**, 522-534.

Lõhelaid, H., Teder, T. and Samel, N. (2015). Lipoxygenase-allene oxide synthase pathway in octocoral thermal stress response. *Coral Reefs* **34**, 143-154.

Loram, J. E., Trapido-Rosenthal, H. G. and Douglas, A. E. (2007). Functional significance of genetically different symbiotic algae *Symbiodinium* in a coral reef symbiosis. *Molecular Ecology* **16**, 4849-4857.

Ludwig-Müller, J., Krishna, P. and Forreiter, C. (2000). A Glucosinolate Mutant of *Arabidopsis* Is Thermosensitive and Defective in Cytosolic Hsp90 Expression after Heat Stress. *Plant Physiol* **123**, 949-958.

Malmendal, A., Overgaard, J., Bundy, J. G., Sørensen, J. G., Nielsen, N. C., Loeschcke, V. and Holmstrup, M. (2006). Metabolomic profiling of heat stress: hardening and recovery of homeostasis in *Drosophila*. *American Journal of Physiology - Regulatory, Integrative and Comparative Physiology* **291**, R205-R212.

Mayer, R. R., Cherry, J. H. and Rhodes, D. (1990). Effects of Heat Shock on Amino Acid Metabolism of Cowpea Cells. *Plant Physiol* **94**, 796-810.

Mayfield, A. B. and Gates, R. D. (2007). Osmoregulation in anthozoan–dinoflagellate symbiosis. *Comparative Biochemistry and Physiology Part A: Molecular & Integrative Physiology* **147**, 1-10.

Mews, L. K. (1980). The Green Hydra Symbiosis. III. The Biotrophic transport of Carbohydrate from Alga to Animal. *Proceedings of the Royal Society of London B: Biological Sciences* **209**, 377-401.

Michaud, M. R., Benoit, J. B., Lopez-Martinez, G., Elnitsky, M. A., Lee, R. E. and Denlinger, D. L. (2008). Metabolomics reveals unique and shared metabolic changes in response to heat shock, freezing and desiccation in the Antarctic midge, *Belgica antarctica*. *Journal of Insect Physiology* **54**, 645-655.

Miller, D. J. and Yellowlees, D. (1989). Inorganic Nitrogen Uptake by Symbiotic Marine Cnidarians: A Critical Review. *Proceedings of the Royal Society of London. Series B, Biological Sciences* **237**, 109-125.

Moberg, F. and Folke, C. (1999). Ecological goods and services of coral reef ecosystems. *Ecological Economics* **29**, 215-233.

Moore, R. B., Ferguson, K. M., Loh, W. K., Hoegh-Guldberg, O. and Carter, D. A. (2003). Highly organized structure in the non-coding region of the *psbA* minicircle from clade C *Symbiodinium*. *International Journal of Systematic and Evolutionary Microbiology* **53**, 1725-1734.

Moran, R. (1982). Formulae for Determination of Chlorophyllous Pigments Extracted with N,N-Dimethylformamide. *Plant Physiol* **69**, 1376-1381.

Müller, W. (2004). Signalling systems in Cnidaria. In *Cell Signalling in Prokaryotes and Lower Metazoa*, pp. 91-114: Springer.

Mumby, P. J., Dahlgren, C. P., Harborne, A. R., Kappel, C. V., Micheli, F., Brumbaugh, D. R., Holmes, K. E., Mendes, J. M., Broad, K. and Sanchirico, J. N. (2006). Fishing, trophic cascades, and the process of grazing on coral reefs. *Science* **311**, 98-101.

Munné-Bosch, S. (2005). The role of -tocopherol in plant stress tolerance. *Journal of Plant Physiology* **162**, 743-748.

Murata, N., Takahashi, S., Nishiyama, Y. and Allakhverdiev, S. I. (2007). Photoinhibition of photosystem II under environmental stress. *Biochimica et Biophysica Acta (BBA)-Bioenergetics* **1767**, 414-421.

Muscatine, L. (1967). Glycerol excretion by symbiotic algae from corals and Tridacna and its control by the host. *Science* **156**, 516-519.

Muscatine, L. and Cernichiari, E. (1969). Assimilation of photosynthetic products of zooxanthellae by a reef coral. *The Biological Bulletin* **137**, 506-523.

Muscatine, L., Falkowski, P. G., Dubinsky, Z., Cook, P. A. and McCloskey, L. R. (1989). The Effect of External Nutrient Resources on the Population Dynamics of Zooxanthellae in a Reef Coral. *Proceedings of the Royal Society of London B: Biological Sciences* **236**, 311-324.

Muscatine, L., Falkowski, P. G., Porter, J. W. and Dubinsky, Z. (1984). Fate of Photosynthetic Fixed Carbon in Light- and Shade-Adapted Colonies of the Symbiotic Coral *Stylophora pistillata*. *Proceedings of the Royal Society of London B: Biological Sciences* **222**, 181-202.

Muscatine, L., Ferrier-Pagès, C., Blackburn, A., Gates, R. D., Baghdasarian, G. and Allemand, D. (1998). Cell-specific density of symbiotic dinoflagellates in tropical anthozoans. *Coral Reefs* **17**, 329-337.

Muscatine, L. and Hand, C. (1958). Direct evidence for the transfer of materials from symbiotic algae to the tissues of a coelenterate. *Proceedings of the National Academy of Sciences of the United States of America* **44**, 1259-1263.

Muscatine, L. and Porter, J. W. (1977). Reef corals: mutualistic symbioses adapted to nutrient-poor environments. *Bioscience* **27**, 454-460.

Nielsen, J., Villas-Bôas, S. G., Roessner, U., Hansen, M. A. E., Smedsgaard, J. and Nielsen, J. (2006). Metabolomics in Functional Genomics and Systems Biology. In *Metabolome Analysis*, pp. 1-14: John Wiley & Sons, Inc.

Nyström, M., Graham, N. A. J., Lokrantz, J., Norström, A. V., Stockholm Resilience, C., Systemekologiska, i., Stockholms, u. and Naturvetenskapliga, f. (2008). Capturing the cornerstones of coral reef resilience: linking theory to practice. *Coral Reefs* **27**, 795-809.

Oakley, C. A., Schmidt, G. W. and Hopkinson, B. M. (2014). Thermal responses of *Symbiodinium* photosynthetic carbon assimilation. *Coral Reefs* **33**, 501-512.

Oliver, S. G., Winson, M. K., Kell, D. B. and Baganz, F. (1998). Systematic functional analysis of the yeast genome. *Trends in biotechnology* **16**, 373-378.

Pandolfi, J. M. (2011). The Paleoecology of Coral Reefs, pp. 13-24. Dordrecht: Springer Netherlands.

Pandolfi, J. M., Bradbury, R. H., Sala, E., Hughes, T. P., Bjorndal, K. A., Cooke, R. G., McArdle, D., McClenachan, L., Newman, M. J. H., Paredes, G. et al. (2003). Global Trajectories of the Long-Term Decline of Coral Reef Ecosystems. *Science* **301**, 955-958.

Pandolfi, J. M., Connolly, S. R., Marshall, D. J. and Cohen, A. L. (2011). Projecting Coral Reef Futures Under Global Warming and Ocean Acidification. *Science* **333**, 418-422.

Papina, M., Meziane, T. and van Woesik, R. (2003). Symbiotic zooxanthellae provide the host-coral *Montipora digitata* with polyunsaturated

fatty acids. *Comparative Biochemistry and Physiology Part B: Biochemistry and Molecular Biology* **135**, 533-537.

Papina, M., Meziane, T. and van Woesik, R. (2007). Acclimation effect on fatty acids of the coral *Montipora digitata* and its symbiotic algae. *Comparative Biochemistry and Physiology Part B: Biochemistry and Molecular Biology* **147**, 583-589.

Parkes, R. J., Dowling, N., White, D., Herbert, R. and Gibson, G. (1993). Characterization of sulphate-reducing bacterial populations within marine and estuarine sediments with different rates of sulphate reduction. *FEMS Microbiology Letters* **102**, 235-250.

Patterson, R. L., van Rossum, D. B., Kaplin, A. I., Barrow, R. K. and Snyder, S. H. (2005). Inositol 1,4,5-trisphosphate receptor/GAPDH complex augments Ca^{2+} release via locally derived NADH. *Proceedings of the National Academy of Sciences of the United States of America* **102**, 1357-1359.

Patton, J. S., Abraham, S. and Benson, A. A. (1977). Lipogenesis in the intact coral *Pocillopora capitata* and its isolated zooxanthellae: Evidence for a light-driven carbon cycle between symbiont and host. *Marine Biology* **44**, 235-247.

Pawlowski, J., Holzmann, M., Fahrni, J., Pochon, X. and Lee, J. (2000). Molecular identification of algal endosymbionts in large miliolid Foraminifera: 2. Dinoflagellates. *The Journal of eukaryotic microbiology* **48**, 368-373.

Pearcy, R. W. (1978). Effect of Growth Temperature on the Fatty Acid Composition of the Leaf Lipids in *Atriplex lentiformis* (Torr.) Wats. *Plant Physiol* **61**, 484-486.

Peng, S.-E., Wang, Y.-B., Wang, L.-H., Chen, W.-N. U., Lu, C.-Y., Fang, L.-S. and Chen, C.-S. (2010). Proteomic analysis of symbiosome membranes in Cnidaria–dinoflagellate endosymbiosis. *PROTEOMICS* **10**, 1002-1016.

Pernice, M., Meibom, A., Van Den Heuvel, A., Kopp, C., Domart-Coulon, I., Hoegh-Guldberg, O. and Dove, S. (2012). A single-cell view of ammonium assimilation in coral-dinoflagellate symbiosis. *ISME J* **6**, 1314-1324.

Pettay, D. T., Wham, D. C., Pinzon, J. H. and Lajeunesse, T. C. (2011). Genotypic diversity and spatial–temporal distribution of *Symbiodinium* clones in an abundant reef coral. *Molecular Ecology* **20**, 5197-5212.

Philippon, H., Brochier-Armanet, C. and Perrière, G. (2015). Evolutionary history of phosphatidylinositol- 3-kinases: ancestral origin in eukaryotes and complex duplication patterns. *BMC evolutionary biology* **15**, 1-16.

Pochon, X. and Gates, R. D. (2010). A new *Symbiodinium* clade (Dinophyceae) from soritid foraminifera in Hawai'i. *Molecular Phylogenetics and Evolution* **56**, 492-497.

Pochon, X., Montoya-Burgos, J. I., Stadelmann, B. and Pawlowski, J. (2006). Molecular phylogeny, evolutionary rates, and divergence timing of the symbiotic dinoflagellate genus *Symbiodinium*. *Molecular Phylogenetics and Evolution* **38**, 20-30.

Poirier, Y., Ventre, G. and Caldelari, D. (1999). Increased Flow of Fatty Acids toward β-Oxidation in Developing Seeds of *Arabidopsis* Deficient in Diacylglycerol Acyltransferase Activity or Synthesizing Medium-Chain-Length Fatty Acids. *Plant Physiol* **121**, 1359-1366.

Porra, R., Thompson, W. and Kriedemann, P. (1989). Determination of accurate extinction coefficients and simultaneous equations for assaying chlorophylls a and b extracted with four different solvents: verification of the concentration of chlorophyll standards by atomic absorption spectroscopy. *Biochimica et Biophysica Acta (BBA)-Bioenergetics* **975**, 384-394.

Porter, J. W. (1976). Autotrophy, Heterotrophy, and Resource Partitioning in Caribbean Reef-Building Corals. *The American Naturalist* **110**, 731-742.

Rädecker, N., Pogoreutz, C., Voolstra, C. R., Wiedenmann, J. and Wild, C. (2015). Nitrogen cycling in corals: the key to understanding holobiont functioning? *Trends in Microbiology* **23**, 490-497.

Raina, J.-B., Dinsdale, E. A., Willis, B. L. and Bourne, D. G. (2010). Do the organic sulfur compounds DMSP and DMS drive coral microbial associations? *Trends in Microbiology* **18**, 101-108.

Raina, J.-B., Tapiolas, D., Willis, B. L. and Bourne, D. G. (2009). Coral-associated bacteria and their role in the biogeochemical cycling of sulfur. *Applied and Environmental Microbiology* **75**, 3492-3501.

Ralph, P. J., Gademann, R. and Larkum, A. W. (2001). Zooxanthellae expelled from bleached corals at 33ºC are photosynthetically competent. *Marine Ecology Progress Series* **220**, 163-168.

Ramos-Silva, P., Kaandorp, J., Herbst, F., Plasseraud, L., Alcaraz, G., Stern, C., Corneillat, M., Guichard, N., Durlet, C., Luquet, G. et al. (2014). The Skeleton of the Staghorn Coral *Acropora millepora*: Molecular and Structural Characterization. *PLoS One* **9**, e97454.

Rawsthorne, S. (2002). Carbon flux and fatty acid synthesis in plants. *Progress in Lipid Research* **41**, 182-196.

Revel, J., Massi, L., Mehiri, M., Boutoute, M., Mayzaud, P., Capron, L. and Sabourault, C. (2016). Differential distribution of lipids in epidermis, gastrodermis and hosted *Symbiodinium* in the sea anemone *Anemonia viridis*. *Comparative Biochemistry and Physiology Part A: Molecular & Integrative Physiology* **191**, 140-151.

Reynolds, J. M., Bruns, B. U., Fitt, W. K. and Schmidt, G. W. (2008). Enhanced photoprotection pathways in symbiotic dinoflagellates of shallow-water corals and other cnidarians. *Proceedings of the National Academy of Sciences* **105**, 13674-13678.

Richmond, R. H. and Hunter, C. L. (1990). Reproduction and recruitment of corals: comparisons among the Caribbean, the Tropical Pacific, and the Red Sea. *Marine ecology progress series. Oldendorf* **60**, 185-203.

Roberty, S., Bailleul, B., Berne, N., Franck, F. and Cardol, P. (2014). PSI Mehler reaction is the main alternative photosynthetic electron pathway in *Symbiodinium* sp., symbiotic dinoflagellates of cnidarians. *New Phytologist* **204**, 81-91.

Roberty, S., Fransolet, D., Cardol, P., Plumier, J. C. and Franck, F. (2015). Imbalance between oxygen photoreduction and antioxidant capacities in *Symbiodinium* cells exposed to combined heat and high light stress. *Coral Reefs* **34**, 1063-1073.

Roessner, U., Villas-Bôas, S. G., Roessner, U., Hansen, M. A. E., Smedsgaard, J. and Nielsen, J. (2006). The Chemical Challenge of the Metabolome. In *Metabolome Analysis*, pp. 15-38: John Wiley & Sons, Inc.

Rohwer, F., Seguritan, V., Azam, F. and Knowlton, N. (2002). Diversity and distribution of coral-associated bacteria. *Marine Ecology Progress Series* **243**, 1-10.

Rosenberg, E., Koren, O., Reshef, L., Efrony, R. and Zilber-Rosenberg, I. (2007). The role of microorganisms in coral health, disease and evolution. *Nat Rev Micro* **5**, 355-362.

Rosenblum, E., Viant, M., Braid, B., Moore, J., Friedman, C. and Tjeerdema, R. (2005). Characterizing the metabolic actions of natural stresses in the California red abalone, *Haliotis rufescens* using ^{1}H NMR metabolomics. *Metabolomics* **1**, 199-209.

Rosic, N., Ling, E. Y. S., Chan, C.-K. K., Lee, H. C., Kaniewska, P., Edwards, D., Dove, S. and Hoegh-Guldberg, O. (2015). Unfolding the secrets of coral-algal symbiosis. *ISME J* **9**, 844-856.

Rosic, N. N. and Dove, S. (2011). Mycosporine-Like Amino Acids from Coral Dinoflagellates. *Applied and Environmental Microbiology* **77**, 8478-8486.

Roth, M. S. (2014). The engine of the reef: photobiology of the coral–algal symbiosis. *Frontiers in Microbiology* **5**, 422.

Roth, M. S., Latz, M. I., Goericke, R. and Deheyn, D. D. (2010). Green fluorescent protein regulation in the coral *Acropora yongei* during photoacclimation. *J Exp Biol* **213**, 3644-3655.

Rowan, R., Whitney, S. M., Fowler, A. and Yellowlees, D. (1996). Rubisco in marine symbiotic dinoflagellates: form II enzymes in eukaryotic oxygenic phototrophs encoded by a nuclear multigene family. *The Plant Cell* **8**, 539-53.

Sakamoto, T., Los, D. A., Higashi, S., Wada, H., Nishida, I., Ohmori, M. and Murata, N. (1994). Cloning of ω3 desaturase from cyanobacteria and its use in altering the degree of membrane-lipid unsaturation. *Plant Molecular Biology* **26**, 249-263.

Salih, A., Larkum, A., Cox, G., Kuhl, M. and Hoegh-Guldberg, O. (2000). Fluorescent pigments in corals are photoprotective. *Nature* **408**, 850-853.

Sansone, S. A., Fan, T., Goodacre R, Griffin JL, Hardy NW, Kaddurah-Daouk R, Kristal BS, Lindon J, Mendes P, Morrison N, Nikolau B, Robertson D, Sumner LW, Taylor C, van der Werf M, van Ommen B, Fiehn O. (2007). The Metabolomics Standards Initiative. *Nat Biotech* **25**, 846-848.

Savchenko, T., Walley, J. W., Chehab, E. W., Xiao, Y., Kaspi, R., Pye, M. F., Mohamed, M. E., Lazarus, C. M., Bostock, R. M. and Dehesh, K. (2010). Arachidonic acid: an evolutionarily conserved signaling molecule modulates plant stress signaling networks. *The Plant Cell Online* **22**, 3193-3205.

Schauer, N., Steinhauser, D., Strelkov, S., Schomburg, D., Allison, G., Moritz, T., Lundgren, K., Roessner-Tunali, U., Forbes, M. G., Willmitzer, L. et al. (2005). GC–MS libraries for the rapid identification of metabolites in complex biological samples. *FEBS Letters* **579**, 1332-1337.

Scheuer, P. (1978). Marine natural products: Chemical and biological perspectives. New York Academic Press

Schever, P. (1983). Marine Natural Products V2: Chemical And Biological Perspectives: Elsevier.

Schmitz, K. and Kremer, B. P. (1977). Carbon fixation and analysis of assimilates in a coral-dinoflagellate symbiosis. *Marine Biology* **42**, 305-313.

Schoenberg, D. and Trench, R. (1980). Genetic variation in *Symbiodinium* (= *Gymnodinium*) *microadriaticum* Freudenthal, and specificity in its symbiosis with marine invertebrates. I. Isoenzyme and soluble protein patterns of axenic cultures of *Symbiodinium microadriaticum*. *Proceedings of the Royal Society of London B: Biological Sciences* **207**, 405-427.

Sharon, G. and Rosenberg, E. (2008). Bacterial Growth on Coral Mucus. *Current Microbiology* **56**, 481-488.

Shick, J. M. and Dunlap, W. C. (2002). Mycosporine-like amino acids and related gadusols: Biosynthesis, Accumulation, and UV-Protective Functions in Aquatic Organisms. *Annual Review of Physiology* **64**, 223-262.

Shinzato, C., Satoh, N. and Shoguchi, E. (2014). A genomic approach to coral-dinoflagellate symbiosis: Studies of *Acropora digitifera* and *Symbiodinium minutum*. *Frontiers in Microbiology* **5**.

Shinzato, C., Shoguchi, E., Kawashima, T., Hamada, M., Hisata, K., Tanaka, M., Fujie, M., Fujiwara, M., Koyanagi, R., Ikuta, T. et al. (2011). Using the *Acropora digitifera* genome to understand coral responses to environmental change. *Nature* **476**, 320-323.

Silverstein, R. N., Correa, A. M. and Baker, A. C. (2012). Specificity is rarely absolute in coral–algal symbiosis: implications for coral response to climate change. *Proceedings of the Royal Society B: Biological Sciences* **279**, 2609-2618.

Sinha, A. K., Hofmann, M. G., Römer, U., Köckenberger, W., Elling, L. and Roitsch, T. (2002). Metabolizable and Non-Metabolizable Sugars Activate Different Signal Transduction Pathways in Tomato. *Plant Physiol* **128**, 1480-1489.

Smart, K. F., Aggio, R. B. M., Van Houtte, J. R. and Villas-Boas, S. G. (2010). Analytical platform for metabolome analysis of microbial cells using methyl chloroformate derivatization followed by gas chromatography-mass spectrometry. *Nat. Protocols* **5**, 1709-1729.

Smedsgaard, J., Villas-Bôas, S. G., Roessner, U., Hansen, M. A. E., Smedsgaard, J. and Nielsen, J. (2006). Analytical Tools. In *Metabolome Analysis*, pp. 83-145: John Wiley & Sons, Inc.

Smeekens, S., Ma, J., Hanson, J. and Rolland, F. (2010). Sugar signals and molecular networks controlling plant growth. *Current Opinion in Plant Biology* **13**, 273-278.

Smith, C. A., Want, E. J., O'Maille, G., Abagyan, R. and Siuzdak, G. (2006). XCMS: Processing Mass Spectrometry Data for Metabolite Profiling Using Nonlinear Peak Alignment, Matching, and Identification. *Analytical Chemistry* **78**, 779-787.

Smith, D. J., Suggett, D. J. and Baker, N. R. (2005). Is photoinhibition of zooxanthellae photosynthesis the primary cause of thermal bleaching in corals? *Global Change Biology* **11**, 1-11.

Smith, G. J. and Muscatine, L. (1999). Cell cycle of symbiotic dinoflagellates: variation in G1 phase-duration with anemone nutritional status and macronutrient supply in the *Aiptasia pulchella–Symbiodinium pulchrorum* symbiosis. *Marine Biology* **134**, 405-418.

Sogin, E. M., Anderson, P., Williams, P., Chen, C.-S. and Gates, R. D. (2014). Application of ^{1}H-NMR Metabolomic Profiling for Reef-Building Corals. *PLoS One* **9**, e111274.

Spann, N., Aldridge, D. C., Griffin, J. L. and Jones, O. A. H. (2011). Size-dependent effects of low level cadmium and zinc exposure on the metabolome of the Asian clam, *Corbicula fluminea*. *Aquatic Toxicology* **105**, 589-599.

Spurgeon, J. P. G. (1992). The economic valuation of coral reefs. *Marine Pollution Bulletin* **24**, 529-536.

Starzak, D., Quinnell, R., Nitschke, M. and Davy, S. (2014). The influence of symbiont type on photosynthetic carbon flux in a model cnidarian–dinoflagellate symbiosis. *Marine Biology* **161**, 711-724.

Stat, M. and Gates, R. D. (2011). Clade D *Symbiodinium* in Scleractinian Corals: A "Nugget" of Hope, a Selfish Opportunist, an Ominous Sign, or All of the Above? *Journal of Marine Biology* **2011**, 9.

Stimson, J. and Kinzie, R. A. (1991). The temporal pattern and rate of release of zooxanthellae from the reef coral *Pocillopora damicornis* (Linnaeus) under nitrogen-enrichment and control conditions. *Journal of Experimental Marine Biology and Ecology* **153**, 63-74.

Streamer, M., McNeil, Y. R. and Yellowlees, D. (1993). Photosynthetic carbon dioxide fixation in zooxanthellae. *Marine Biology* **115**, 195-198.

Struchtemeyer, C. G., Duncan, K. E. and McInerney, M. J. (2011). Evidence for syntrophic butyrate metabolism under sulfate-reducing conditions in a hydrocarbon-contaminated aquifer. *FEMS microbiology ecology* **76**, 289-300.

Strychar, K. B. and Sammarco, P. W. (2011). Effects of heat stress on phytopigments of zooxanthellae (*Symbiodinium* spp.) symbiotic with the corals *Acropora hyacinthus, Porites solida,* and *Favites complanata*. *International Journal of Biology* **4**, p3.

Suescún-Bolívar, L. P., Iglesias-Prieto, R. and Thomé, P. E. (2012). Induction of Glycerol Synthesis and Release in Cultured *Symbiodinium*. *PLoS One* **7**, e47182.

Suggett, D. J., Goyen, S., Evenhuis, C., Szabó, M., Pettay, D. T., Warner, M. E. and Ralph, P. J. (2015). Functional diversity of photobiological traits within the genus *Symbiodinium* appears to be governed by the interaction of cell size with cladal designation. *New Phytologist* **208**, 370-381.

Sunagawa, S., Choi, J., Forman, H. J. and Medina, M. (2008). Hyperthermic stress-induced increase in the expression of glutamate-cysteine ligase and glutathione levels in the symbiotic sea anemone *Aiptasia pallida*. *Comparative Biochemistry and Physiology Part B: Biochemistry and Molecular Biology* **151**, 133-138.

Sutton, D. C. and Hoegh-Guldberg, O. (1990). Host-Zooxanthella Interactions in Four Temperate Marine Invertebrate Symbioses: Assessment of Effect of Host Extracts on Symbionts. *The Biological Bulletin* **178**, 175-186.

Suzuki, N., Koussevitzky, S., Mittler, R. O. N. and Miller, G. A. D. (2012). ROS and redox signalling in the response of plants to abiotic stress. *Plant, Cell & Environment* **35**, 259-270.

Swanson, R. and Hoegh-Guldberg, O. (1998). Amino acid synthesis in the symbiotic sea anemone *Aiptasia pulchella*. *Marine Biology* **131**, 83-93.

Takahashi, H., Imamura, T., Konno, N., Takeda, T., Fujita, K., Konishi, T., Nishihara, M. and Uchimiya, H. (2014). The Gentio-Oligosaccharide Gentiobiose Functions in the Modulation of Bud Dormancy in the Herbaceous Perennial *Gentiana*. *The Plant Cell* **26**, 3949-3963.

Takahashi, S. and Murata, N. (2008). How do environmental stresses accelerate photoinhibition? *Trends in Plant Science* **13**, 178-182.

Takahashi, S., Nakamura, T., Sakamizu, M., Woesik, R. v. and Yamasaki, H. (2004). Repair Machinery of Symbiotic Photosynthesis as the Primary Target of Heat Stress for Reef-Building Corals. *Plant and Cell Physiology* **45**, 251-255.

Takahashi, S., Whitney, S. M. and Badger, M. R. (2009). Different thermal sensitivity of the repair of photodamaged photosynthetic machinery in cultured *Symbiodinium* species. *Proceedings of the National Academy of Sciences* **106**, 3237-3242.

Tanaka, Y., Miyajima, T., Koike, I., Hayashibara, T. and Ogawa, H. (2006). Translocation and conservation of organic nitrogen within the coral-zooxanthella symbiotic system of *Acropora pulchra*, as demonstrated by dual

isotope-labeling techniques. *Journal of Experimental Marine Biology and Ecology* **336**, 110-119.

Tarrant, A. M. (2005). Endocrine-like Signaling in Cnidarians: Current Understanding and Implications for Ecophysiology. *Integrative and Comparative Biology* **45**, 201-214.

Tarrant, A. M., Reitzel, A. M., Blomquist, C. H., Haller, F., Tokarz, J. and Adamski, J. (2009). Steroid metabolism in cnidarians: Insights from *Nematostella vectensis*. *Molecular and Cellular Endocrinology* **301**, 27-36.

Tchernov, D., Gorbunov, M. Y., de Vargas, C., Narayan Yadav, S., Milligan, A. J., Häggblom, M. and Falkowski, P. G. (2004). Membrane lipids of symbiotic algae are diagnostic of sensitivity to thermal bleaching in corals. *Proceedings of the National Academy of Sciences of the United States of America* **101**, 13531-13535.

Thompson, J. R., Rivera, H. E., Closek, C. J. and Medina, M. (2015). Microbes in the coral holobiont: partners through evolution, development, and ecological interactions. *Frontiers in Cellular and Infection Microbiology* **4**.

Thornhill, D., Fitt, W. and Schmidt, G. (2006). Highly stable symbioses among western Atlantic brooding corals. *Coral Reefs* **25**, 515-519.

Thornhill, D. J., Xiang, Y., Fitt, W. K. and Santos, S. R. (2009). Reef Endemism, Host Specificity and Temporal Stability in Populations of Symbiotic Dinoflagellates from Two Ecologically Dominant Caribbean Corals. *PLoS One* **4**, e6262.

Thurber, R. V., Willner-Hall, D., Rodriguez-Mueller, B., Desnues, C., Edwards, R. A., Angly, F., Dinsdale, E., Kelly, L. and Rohwer, F. (2009). Metagenomic analysis of stressed coral holobionts. *Environmental microbiology* **11**, 2148-2163.

Toller, W. W., Rowan, R. and Knowlton, N. (2001). Repopulation of Zooxanthellae in the Caribbean Corals *Montastraea annularis* and *M. faveolata* following Experimental and Disease-Associated Bleaching. *The Biological Bulletin* **201**, 360-373.

Tolosa, I., Treignier, C., Grover, R. and Ferrier-Pagès, C. (2011). Impact of feeding and short-term temperature stress on the content and isotopic signature of fatty acids, sterols, and alcohols in the scleractinian coral *Turbinaria reniformis*. *Coral Reefs* **30**, 763-774.

Tout, J., Siboni, N., Messer, L. F., Garren, M., Stocker, R., Webster, N. S., Ralph, P. J. and Seymour, J. R. (2015). Increased seawater temperature increases the abundance and alters the structure of natural *Vibrio* populations associated with the coral *Pocillopora damicornis*. *Frontiers in Microbiology* **6**.

Tredwell, G. D., Edwards-Jones, B., Leak, D. J. and Bundy, J. G. (2011). The Development of Metabolomic Sampling Procedures for *Pichia pastoris*, and Baseline Metabolome Data. *PLoS One* **6**, e16286.

Tremblay, P., Grover, R., Maguer, J. F., Hoogenboom, M. and Ferrier-Pagès, C. (2014). Carbon translocation from symbiont to host depends on irradiance and food availability in the tropical coral *Stylophora pistillata*. *Coral Reefs* **33**, 1-13.

Tremblay, P., Grover, R., Maguer, J. F., Legendre, L. and Ferrier-Pagès, C. (2012). Autotrophic carbon budget in coral tissue: a new ^{13}C-based model of photosynthate translocation. *J Exp Biol* **215**, 1384-1393.

Trench, R. (1971). The physiology and biochemistry of zooxanthellae symbiotic with marine coelenterates. I. The assimilation of photosynthetic products of zooxanthellae by two marine coelenterates. *Proceedings of the Royal Society of London. Series B. Biological Sciences* **177**, 225-235.

Trench, R. (1993). Microalgal-invertebrate symbioses- a review. *Endocytobiosis and Cell Research* **9**, 135-175.

Tumanov, S., Bulusu, V. and Kamphorst, J. J. (2015a). Chapter Six - Analysis of Fatty Acid Metabolism Using Stable Isotope Tracers and Mass Spectrometry. In *Methods in Enzymology*, vol. Volume 561 (ed. M. M. Christian), pp. 197-217: Academic Press.

Tumanov, S., Zubenko, Y., Greven, M., Greenwood, D. R., Shmanai, V. and Villas-Boas, S. G. (2015b). Comprehensive lipidome profiling of Sauvignon blanc grape juice. *Food Chemistry* **180**, 249-256.

Tytler, E. M. and Trench, R. K. (1986). Activities of Enzymes in beta-carboxylation Reactions and of Catalase in Cell-Free Preparations from the Symbiotic Dinoflagellates *Symbiodinium* Spp. from a Coral, a Clam, a Zoanthid and Two Sea Anemones. *Proceedings of the Royal Society of London B: Biological Sciences* **228**, 483-492.

van Oppen, M. J. H., Oliver, J. K., Putnam, H. M. and Gates, R. D. (2015). Building coral reef resilience through assisted evolution. *Proceedings of the National Academy of Sciences* **112**, 2307-2313.

Venn, A. A., Loram, J. E. and Douglas, A. E. (2008). Photosynthetic symbioses in animals. *Journal of Experimental Botany* **59**, 1069-1080.

Venn, A. A., Wilson, M. A., Trapido-Rosenthal, H. G., Keely, B. J. and Douglas, A. E. (2006). The impact of coral bleaching on the pigment profile of the symbiotic alga, *Symbiodinium*. *Plant, Cell & Environment* **29**, 2133-2142.

Veron, J. (2000). Corals of the World, vol. 1–3. *Australian Institute of Marine Science, Townsville*.

Viant, M. R. (2007). Metabolomics of aquatic organisms: the new omics; on the block. *Marine Ecology Progress Series* **332**, 301-306.

Viant, M. R. (2008). Recent developments in environmental metabolomics. *Molecular BioSystems* **4**, 980-986.

Viant, M. R., Werner, I., Rosenblum, E. S., Gantner, A. S., Tjeerdema, R. S. and Johnson, M. L. (2003). Correlation between heat-shock protein induction and reduced metabolic condition in juvenile steelhead trout (*Oncorhynchus mykiss*) chronically exposed to elevated temperature. *Fish Physiology and Biochemistry* **29**, 159-171.

Villas-Bôas, S. G., Mas, S., Åkesson, M., Smedsgaard, J. and Nielsen, J. (2005). Mass spectrometry in metabolome analysis. *Mass Spectrometry Reviews* **24**, 613-646.

Villas-Bôas, S. G., Villas-Bôas, S. G., Roessner, U., Hansen, M. A. E., Smedsgaard, J. and Nielsen, J. (2006). Sampling and Sample Preparation. In *Metabolome Analysis*, pp. 39-82: John Wiley & Sons, Inc.

von Holt, C. and von Holt, M. (1968). Transfer of photosynthetic products from zooxanthellae to coelenterate hosts. *Comparative Biochemistry and Physiology* **24**, 73-81.

Wahid, A., Gelani, S., Ashraf, M. and Foolad, M. R. (2007). Heat tolerance in plants: An overview. *Environmental and Experimental Botany* **61**, 199-223.

Wakefield, T., Farmer, M. and Kempf, S. (2000). Revised description of the fine structure of *in situ* "zooxanthellae" genus *Symbiodinium*. *The Biological Bulletin* **199**, 76-84.

Wakefield, T. S. and Kempf, S. C. (2001). Development of Host- and Symbiont-Specific Monoclonal Antibodies and Confirmation of the Origin of the Symbiosome Membrane in a Cnidarian–Dinoflagellate Symbiosis. *The Biological Bulletin* **200**, 127-143.

Walter, M. v. G., Wouter, A. v. W., Joseph, J. H. and Roelco, J. K. (2009). Use Of AEX-HPLC-ESI-MS For ^{13}C-Labeling Based Metabolic Flux Analysis In *Saccharomyces Cerevisiae* And *Penicillium Chrysogenum*. In *The Metabolic Pathway Engineering Handbook*, pp. 20-1-20-14: CRC Press.

Wang, J. and Douglas, A. (1998). Nitrogen recycling or nitrogen conservation in an alga-invertebrate symbiosis? *Journal of Experimental Biology* **201**, 2445-53.

Wang, J. T. and Douglas, A. E. (1997). Nutrients, Signals, and Photosynthate Release by Symbiotic Algae (The Impact of Taurine on the Dinoflagellate Alga *Symbiodinium* from the Sea Anemone *Aiptasia pulchella*). *Plant Physiol* **114**, 631-636.

Wang, J. T. and Douglas, A. E. (1999). Essential amino acid synthesis and nitrogen recycling in an alga–invertebrate symbiosis. *Marine Biology* **135**, 219-222.

Wang, L.-H., Chen, H.-K., Jhu, C.-S., Cheng, J.-O., Fang, L.-S. and Chen, C.-S. (2015). Different strategies of energy storage in cultured and freshly isolated *Symbiodinium* sp. *Journal of Phycology* **51**, 1127-1136.

Wang, L.-H., Lee, H.-H., Fang, L.-S., Mayfield, A. B. and Chen, C.-S. (2013). Fatty Acid and Phospholipid Syntheses Are Prerequisites for the Cell Cycle of *Symbiodinium* and Their Endosymbiosis within Sea Anemones. *PLoS One* **8**, e72486.

Warner, M. and Berry-Lowe, S. (2006). Differential xanthophyll cycling and photochemical activity in symbiotic dinoflagellates in multiple locations of three species of Caribbean coral. *Journal of Experimental Marine Biology and Ecology* **339**, 86-95.

Warner, M., Chilcoat, G., McFarland, F. and Fitt, W. (2002). Seasonal fluctuations in the photosynthetic capacity of photosystem II in

symbiotic dinoflagellates in the Caribbean reef-building coral *Montastraea*. *Marine Biology* **141**, 31-38.

Warner, M. E., Fitt, W. K. and Schmidt, G. W. (1996). The effects of elevated temperature on the photosynthetic efficiency of zooxanthellae *in hospite* from four different species of reef coral: a novel approach. *Plant, Cell & Environment* **19**, 291-299.

Warner, M. E., Fitt, W. K. and Schmidt, G. W. (1999). Damage to photosystem II in symbiotic dinoflagellates: A determinant of coral bleaching. *Proceedings of the National Academy of Sciences* **96**, 8007-8012.

Weindl, D., Wegner, A. and Hiller, K. (2015). Chapter Eight - Non-targeted Tracer Fate Detection. In *Methods in Enzymology*, vol. Volume 561 (ed. M. M. Christian), pp. 277-302: Academic Press.

Weis, V. M. (2008). Cellular mechanisms of Cnidarian bleaching: stress causes the collapse of symbiosis. *Journal of Experimental Biology* **211**, 3059-3066.

Weis, V. M. (2010). The susceptibility and resilience of corals to thermal stress: adaptation, acclimatization or both? *Molecular Ecology* **19**, 1515-1517.

Weis, V. M., Davy, S. K., Hoegh-Guldberg, O., Rodriguez-Lanetty, M. and Pringle, J. R. (2008). Cell biology in model systems as the key to understanding corals. *Trends in Ecology & Evolution* **23**, 369-376.

Weis, V. M., Reynolds, W. S. and Krupp, D. A. (2001). Host-symbiont specificity during onset of symbiosis between the dinoflagellates *Symbiodinium* spp. and planula larvae of the scleractinian coral *Fungia scutaria*. *Coral Reefs* **20**, 301-308.

Whitehead, L. and Douglas, A. (2003). Metabolite comparisons and the identity of nutrients translocated from symbiotic algae to an animal host. *Journal of Experimental Biology* **206**, 3149-3157.

Wiechert, W. (2001). ^{13}C Metabolic Flux Analysis. *Metabolic Engineering* **3**, 195-206.

Wietheger, A., Fisher, P., Gould, K. and Davy, S. (2015). Sensitivity to oxidative stress is not a definite predictor of thermal sensitivity in symbiotic dinoflagellates. *Marine Biology* **162**, 2067-2077.

Withers, K. J. T., Grant, A. J. and Hinde, R. (1998). Effects of free amino acids on the isolated symbiotic algae of the coral *Plesiastrea versipora* (Lamarck): absence of a host release factor response. *Comparative Biochemistry and Physiology - Part A: Molecular & Integrative Physiology* **120**, 599-607.

Wood-Charlson, E. M., Hollingsworth, L. L., Krupp, D. A. and Weis, V. M. (2006). Lectin/glycan interactions play a role in recognition in a coral/dinoflagellate symbiosis. *Cellular Microbiology* **8**, 1985-1993.

Wooldridge, S. (2014). Differential thermal bleaching susceptibilities amongst coral taxa: re-posing the role of the host. *Coral Reefs* **33**, 15-27.

Xia, J., Mandal, R., Sinelnikov, I. V., Broadhurst, D. and Wishart, D. S. (2012). MetaboAnalyst 2.0—a comprehensive server for metabolomic data analysis. *Nucleic Acids Research*.

Xia, J., Psychogios, N., Young, N. and Wishart, D. S. (2009). MetaboAnalyst: a web server for metabolomic data analysis and interpretation. *Nucleic Acids Research* **37**, W652-W660.

Xia, J., Sinelnikov, I. V., Han, B. and Wishart, D. S. (2015). MetaboAnalyst 3.0—making metabolomics more meaningful. *Nucleic Acids Research*.

Xu, Y., Du, H. and Huang, B. (2013). Identification of Metabolites Associated with Superior Heat Tolerance in Thermal Bentgrass through Metabolic Profiling. *Crop Sci.* **53**, 1626-1635.

Yancey, P., H, Marina Heppenstall, Steven Ly, Raymond M. Andrell, Ruth D. Gates, Virginia L. Carter and Mary Hagedorn. (2010). Betaines and Dimethylsulfoniopropionate as Major Osmolytes in Cnidaria with Endosymbiotic Dinoflagellates. *Physiological and Biochemical Zoology* **83**, 167-173.

Yang, C., Hua, Q. and Shimizu, K. (2002). Metabolic Flux Analysis in *Synechocystis* Using Isotope Distribution from ^{13}C-Labeled Glucose. *Metabolic Engineering* **4**, 202-216.

Ye, Y., Zhang, L., Hao, F., Zhang, J., Wang, Y. and Tang, H. (2012). Global Metabolomic Responses of *Escherichia coli* to Heat Stress. *Journal of Proteome Research* **11**, 2559-2566.

Yellowlees, D., Dionisio-Sese, M. L., Masuda, K., Maruyama, T., Abe, T., Baillie, B., Tsuzuki, M. and Miyachi, S. (1993). Role of carbonic anhydrase in the supply of inorganic carbon to the giant clam—zooxanthellate symbiosis. *Marine Biology* **115**, 605-611.

Yellowlees, D., Rees, T. A. V. and Leggat, W. (2008). Metabolic interactions between algal symbionts and invertebrate hosts. *Plant, Cell & Environment* **31**, 679-694.

Young, J. D., Shastri, A. A., Stephanopoulos, G. and Morgan, J. A. (2011). Mapping photoautotrophic metabolism with isotopically nonstationary ^{13}C flux analysis. *Metabolic Engineering* **13**, 656-665.

Yuyama, I., Watanabe, T. and Takei, Y. (2011). Profiling Differential Gene Expression of Symbiotic and Aposymbiotic Corals Using a High Coverage Gene Expression Profiling (HiCEP) Analysis. *Marine Biotechnology* **13**, 32-40.

Zamboni, N., Fendt, S.-M., Ruhl, M. and Sauer, U. (2009). ^{13}C-based metabolic flux analysis. *Nat. Protocols* **4**, 878-892.

Zhu, C., Lee, Y. and Chao, T. (1997). Effects of temperature and growth phase on lipid and biochemical composition of *Isochrysis galbana* TK1. *Journal of Applied Phycology* **9**, 451-457.

Appendices

Table S2.1 Polar and semi-polar compounds identified from symbiont and host free metabolite pools of *Aiptasia* sp. under ambient conditions and thermal stress, with reference ion and retention time

Compound	Reference ion	Retention time/ min
Amino acids and peptides		
Alanine	102	10.975
Asparagine	127	16.639
beta-Alanine	88	12.652
Creatinine	202	16.661
Cysteine	192	19.873
Glutamic acid	174	17.995
Glutathione	142	19.566
Glycine	88	11.386
Isoleucine	115	13.98
Leucine	144	14.044
Methionine	147	18.087
Norvaline	130	13.336
Phenylalanine	162	19.8
Proline	128	14.89
Serine	100	17.256
Threonine	115	15.554
Tyrosine	236	28.558
Valine	130	12.69
Organic acids and amides		
Aspartic acid	160	16.215
cis-Aconitic acid	153	15.392
Citraconic acid	127	10.131
Citric acid	143	16.229
Fumaric acid	113	9.104
Itaconic acid	127	10.069
Lactic acid	103	9.103
Nicotinamide	57	6.026
Malonic acid	101	7.362
Quinic acid	191	16.315
Succinic acid	115	8.955
Monounsaturated fatty acids		
cis-Vaccenic acid (C18_1n-7c)	55	23.821
Oleic acid (C18_1n-9c)	55	23.798
Palmitoleic acid (C16_1n-7c)	55	20.744
Polyunsaturated fatty acids		
11,14,17-Eicosatrienoic acid (C20_3n-3,6,9c)	79	26.878
11,14-Eicosadienoic (C20_2n-6,9c)	67	26.597
13,16-Docosadienoic acid (C22_2n-6,9c)	67	29.68
Adrenic acid (C22_4n-6,9,12,15c)	79	29.362
alpha-Linolenic acid (C18_3n-3,6,9c)	79	23.723
Arachidonic acid (C20_4n-6,9,12,15c)	79	26.206
bishomo-gamma-Linolenic acid (C20_3n-6,9,12c)	79	26.429
DHA (C22_6n-3,6,9,12,15,18c)	79	29.436
DPA (C22_5n-3,6,9,12,15c)	79	29.597
EPA (C20_5n-3,6,9,12,15c)	79	26.496
gamma-Linolenic acid (C18_3n-6,9,12c)	79	24.018
Linoleic acid (C18_2n-6,9c)	67	23.848
Saturated fatty acids		
Arachidic acid (C20_0)	74	26.807
Dodecanoic acid (C12_0)	74	14.935
Myristic acid (C14_0)	74	17.458

Compound	Reference ion	Retention time/ min
Palmitic acid (C16_0)	74	21.093
Stearic acid (C18_0)	74	24.004

Table S2.2. **Symbiont (A) and host (H) quantitative MCF data summary at 6 d for control (C) and heat-treatment samples (HS). Individual compound concentration (ρg μg^{-1} dry weight). Mean ± S.E.M, *n* = 3 (comprising 6 individuals *per* sample)**

	Concentration (ρg μg^{-1} dry weight)			
Compound	A6C	A6HS	H6C	H6HS
11,14,17-Eicosatrienoic acid (C20_3n-3,6,9c)	207.322 ± 38.12	397.274 ± 46.92	196.311 ± 41.76	290.064 ± 130.74
11,14-Eicosadienoic (C20_2n-6,9c)	193.073 ± 49.39	379.374 ± 75.81	215.255 ± 34.17	242.235 ± 70.25
13,16-Docosadienoic acid (C22_2n-6,9c)	291.097 ± 62.12	586.304 ± 133.86	302.949 ± 48.09	341.664 ± 99.62
Adipic acid	0.537 ± 0.08	7.061 ± 6.03	5.871 ± 0.92	12.645 ± 3.07
Adrenic acid (C22_4n-6,9,12,15c)	173.313 ± 45.63	357.673 ± 26.99	372.559 ± 29.51	272.682 ± 151.46
Alanine	3.799 ± 1.03	6.845 ± 1.53	108.256 ± 24.39	311.390 ± 71.17
alpha-Linolenic acid (C18_3n-3,6,9c)	72.055 ± 18.40	150.300 ± 9.02	160.003 ± 12.19	113.765 ± 61.30
Arachidic acid (C20_0)	13.742 ± 4.42	24.537 ± 6.44	15.030 ± 2.02	21.12 7 ± 8.61
Arachidonic acid (C20_4n-6,9,12,15c)	90.653 ± 24.00	191.262 ± 21.46	230.993 ± 23.73	175.390 ± 103.59
Aspartic acid	0.127 ± 0.03	0.446 ± 0.09	133.977 ± 17.04	263.280 ± 54.30
beta-Alanine	0.311 ± 0.03	0.925 ± 0.22	371.597 ± 71.01	341.407 ± 20.21
bishomo-gamma-Linolenic acid (C20_3n-6,9,12c)	61.583 ± 15.77	107.895 ± 28.74	85.807 ± 20.72	66.769 ± 49.29
cis-Aconitic acid	0.925 ± 0.17	3.036 ± 1.13	362.531 ± 121.05	381.470 ± 52.52
Citric acid	4.974 ± 0.98	13.283 ± 2.32	2620.966 ± 338.74	2264.430 ± 254.17
Creatinine	0.399 ± 0.05	0.644 ± 0.15	16.265 ± 6.15	19.955 ± 6.86
Cysteine	0.220 ± 0.04	0.904 ± 0.28	136.212 ± 18.44	196.637 ± 67.36
DHA (C22_6n-3,6,9,12,15,18c)	144.072 ± 38.14	297.947 ± 38.79	356.277 ± 35.05	277.710 ± 165.08
Dodecanoic acid (C12_0)	12.258 ± 3.76	7.975 ± 1.84	7.838 ± 0.50	17.363 ± 3.43
DPA (C22_5n-3,6,9,12,15c)	162.190 ± 42.95	342.193 ± 38.40	413.275 ± 42.46	313.795 ± 185.34
EPA (C20_5n-3,6,9,12,15c)	85.097 ± 22.89	179.002 ± 19.54	217.762 ± 22.37	165.344 ± 97.66
Fumaric acid	0.365 ± 0.03	1.035 ± 0.24	1.723 ± 0.30	5.246 ± 0.78
gamma-Linolenic acid (C18_3n-6,9,12c)	134.211 ± 24.68	257.177 ± 30.38	127.083 ± 27.04	187.774 ± 84.64
Glutamic acid	0.382 ± 0.02	1.277 ± 0.37	1727.299 ± 403.88	3800.340 ± 796.19
Glutathione	1.579 ± 0.30	5.170 ± 1.82	815.381 ± 184.87	1968.489 ± 428.28
Glycine	0.673 ± 0.10	2.003 ± 0.26	226.544 ± 19.47	294.700 ± 55.29
Isoleucine	1.277 ± 0.14	3.281 ± 0.51	30.754 ± 3.92	35.860 ± 8.24
Itaconic acid	3.168 ± 0.79	8.112 ± 1.36	248.923 ± 58.42	266.668 ± 35.54
Lactic acid	78.988 ± 13.57	198.179 ± 24.66	223.116 ± 29.89	597.862 ± 161.96
Leucine	0.100 ± 0.02	0.263 ± 0.08	50.848 ± 9.31	63.713 ± 15.711

Compound	Concentration (ρg μg^{-1} dry weight) A6C	A6HS	H6C	H6HS
Linoleic acid (C18_2n-6,9c)	105.548 ± 27.01	207.393 ± 41.44	117.674 ± 18.68	132.423 ± 38.41
Methionine	0.284 ± 0.04	0.871 ± 0.20	33.922 ± 4.40	55.388 ± 9.74
Myristic acid (C14_0)	202.190 ± 69.77	100.206 ± 26.52	50.633 ± 8.71	52.564 ± 11.54
Nicotinamide	3.132 ± 0.56	9.581 ± 2.10	7.403 ± 0.75	15.320 ± 3.06
Norvaline	0.062 ± 0.01	0.145 ± 0.02	117.869 ± 14.05	156.369 ± 17.11
Oleic acid (C18_1n-9c)	559.457 ± 150.71	1069.883 ± 266.52	647.429 ± 112.99	766.758 ± 230.85
Palmitic acid (C16_0)	672.062 ± 180.22	1185.424 ± 165.77	1033.564 ± 127.11	1265.585 ± 281.44
Palmitoleic acid (C16_1n-7c)	47.715 ± 17.03	109.967 ± 20.85	79.278 ± 17.15	106.159 ± 32.82
Phenylalanine	0.526 ± 0.12	0.449 ± 0.05	108.746 ± 13.81	123.563 ± 24.41
Proline	0.186 ± 0.09	0.160 ± 0.03	198.188 ± 36.21	135.627 ± 21.31
Serine	0.796 ± 0.04	2.229 ± 0.70	63.522 ± 16.57	103.430 ± 22.74
Stearic acid (C18_0)	325.926 ± 92.26	637.585 ± 112.57	375.651 ± 28.45	558.445 ± 142.17
Succinic acid	19.544 ± 4.21	50.798 ± 8.54	134.309 ± 14.93	189.181 ± 36.02
Threonine	1.480 ± 0.20	4.062 ± 0.76	34.993 ± 11.84	47.498 ± 12.87
Tyrosine	0.066 ± 0.01	0.978 ± 0.76	7.085 ± 6.04	6.374 ± 5.78
Valine	0.056 ± 0.01	0.129 ± 0.02	105.043 ± 12.52	139.354 ± 15.24

Table S2.3 Symbiont heat-responsive compounds at day 6 from quantitative MCF data (fold change and t-test, metabolite x treatment, *P* < 0.05)

Compound	Fold change	log2(FC)	*P* value
Amino acids and peptides			
Aspartic acid	3.516	1.814	0.017
beta-Alanine	2.975	1.573	0.014
Cysteine	4.102	2.036	0.032
Glutamic acid	3.340	1.740	0.037
Glutathione	3.274	1.711	0.061
Glycine	2.977	1.574	0.006
Isoleucine	2.570	1.362	0.010
Methionine	3.061	1.614	0.026
Norvaline	2.325	1.217	0.024
Threonine	2.745	1.457	0.019
Valine	2.325	1.217	0.024
Organic acids and amides			
Citric acid	2.671	1.417	0.027
Fumaric acid	2.839	1.505	0.017
Itaconic acid	2.561	1.357	0.045
Lactic acid	2.509	1.327	0.010
Nicotinamide	3.059	1.613	0.028
Succinic acid	2.599	1.378	0.034
Fatty acids			
Adrenic acid (C22_4n-6,9,12,15c)	2.064	1.045	0.044
alpha-Linolenic acid (C18_3n-3,6,9c)	2.086	1.061	0.036
Arachidonic acid (C20_4n-6,9,12,15c)	2.110	1.077	0.049
DHA (C22_6n-3,6,9,12,15,18c)	2.068	1.048	0.058
DPA (C22_5n-3,6,9,12,15c)	2.110	1.077	0.049
EPA (C20_5n-3,6,9,12,15c)	2.104	1.073	0.050
Palmitoleic acid (C16_1n-7c)	2.305	1.205	0.087

Table S2.4. Host heat-responsive compounds at day 6 from quantitative MCF data (fold change and t-test, metabolite x treatment, *P* < 0.05)

Compound	Fold change	log2(FC)	*P* value
Amino acids and peptides			
Alanine	2.876	1.524	0.035
Glutamic acid	2.200	1.138	0.078
Glutathione	2.414	1.272	0.047
Organic acids and amides			
Adipic acid	2.154	1.107	0.096
Fumaric acid	3.044	1.606	0.007
Lactic acid	2.680	1.422	0.057
Nicotinamide	2.070	1.049	0.030
Fatty acids			
Dodecanoic acid (C12_0)	2.215	1.148	0.019

Table S3.1 Summary of mean comparative data (n = 6) for symbiont samples at Days 0, 6 and 8, under ambient conditions (C) and thermal stress (HS)

	0C	S.E.M	6C	S.E.M	6HS	S.E.M	8C	S.E.M	8HS	S.E.M
1-Monohexadecanoglycerol	27.720	7.599	11.888	1.381	30.909	7.483	13.528	3.053	39.260	7.600
1-Monooctodecanoglycerol	0.761	0.157	0.445	0.083	0.613	0.131	0.438	0.086	0.826	0.096
Adipic acid	0.065	0.011	0.099	0.026	0.073	0.022	0.082	0.016	0.099	0.026
Alanine	0.130	0.015	0.132	0.018	0.093	0.011	0.140	0.017	0.115	0.035
Ascorbate	0.192	0.029	0.154	0.031	0.228	0.062	0.149	0.022	0.256	0.055
Aspartate	0.456	0.065	0.342	0.065	0.231	0.050	0.365	0.043	0.115	0.023
Campesterol	4.263	0.582	6.737	1.734	3.257	0.631	5.452	0.609	4.337	0.880
Cholesterol	0.105	0.021	0.127	0.037	0.117	0.015	0.092	0.012	0.223	0.041
Cystathionine	1.198	0.367	0.263	0.049	0.872	0.376	0.315	0.094	0.657	0.328
Decanoic acid (C10:0)	0.173	0.023	0.211	0.052	0.493	0.174	0.144	0.014	0.794	0.195
DHA (C22:6)	1.854	0.216	1.095	0.238	1.666	0.304	1.274	0.199	1.237	0.340
Diethylene glycol	0.530	0.090	1.086	0.291	0.337	0.092	0.581	0.116	0.561	0.151
Docosanoic acid (C22:0)	0.698	0.095	0.861	0.215	1.459	0.313	0.688	0.112	1.839	0.469
Dodecanoic acid (C12:0)	3.403	0.373	1.876	0.425	11.244	3.019	1.615	0.139	13.592	4.025
DPA (C22:5)	0.671	0.125	0.451	0.071	1.902	0.484	0.487	0.036	2.288	0.751
Eicosanoic acid (C20:0)	0.423	0.066	0.386	0.086	0.962	0.146	0.362	0.034	1.195	0.357
Eicosapentaenoic acid (C20:5)	2.772	0.461	2.230	0.336	5.898	1.295	2.403	0.314	5.548	1.458
Fructose	0.120	0.042	0.201	0.123	0.167	0.040	0.091	0.007	0.119	0.016
Galactinol	0.726	0.059	1.393	0.462	1.014	0.154	0.808	0.101	1.495	0.258
Galactose	14.648	3.184	13.675	2.416	10.957	1.862	14.268	1.415	6.878	1.434
Galactosylglycerol	39.889	9.531	53.199	12.328	25.196	6.222	47.557	14.079	15.125	5.456
Gentiobiose	6.892	2.604	7.370	2.408	1.435	0.403	14.225	4.100	1.213	0.478
Gluconic acid	0.388	0.061	0.670	0.185	0.509	0.116	0.504	0.065	0.796	0.200
Glucose	6.115	0.654	4.525	0.474	14.057	3.016	4.803	0.599	8.715	1.924
Glutamate	0.116	0.025	0.130	0.012	0.088	0.016	0.167	0.034	0.092	0.025
Glutaric acid	0.101	0.022	0.168	0.044	0.127	0.039	0.152	0.029	0.177	0.052
Glycerate	0.055	0.006	0.085	0.014	0.053	0.009	0.072	0.008	0.066	0.014

	0C	S.E.M	6C	S.E.M	6HS	S.E.M	8C	S.E.M	8HS	S.E.M
Glycerol	191.425	30.112	100.824	10.342	297.045	45.226	109.411	12.111	214.180	70.621
Glycerol-2-P	0.130	0.006	0.184	0.048	0.170	0.033	0.158	0.020	0.241	0.048
Glycerol-3-P	1.426	0.159	1.997	0.333	1.185	0.215	1.865	0.078	1.273	0.255
Glycine	0.044	0.004	0.057	0.009	0.043	0.003	0.120	0.049	0.057	0.013
Glycolic acid	0.596	0.069	0.992	0.226	0.664	0.148	0.822	0.150	0.892	0.171
Guanine	2.567	0.621	2.612	0.557	3.918	1.641	1.227	0.114	4.876	2.048
Hexadecanoic acid (C16:0)	233.946	20.640	147.190	15.147	412.834	99.158	146.348	14.025	426.033	137.207
Hexadecanol	1.551	0.167	1.889	0.342	1.545	0.386	2.092	0.106	2.211	0.476
Hexadecenoic acid (C16:1)	31.172	5.459	16.385	1.893	72.622	19.385	19.970	3.205	68.734	20.237
Inositol, myo-	0.502	0.069	0.451	0.111	0.539	0.073	0.483	0.071	0.727	0.192
Inositol, scyllo-	0.615	0.169	0.452	0.070	0.549	0.154	0.589	0.119	0.358	0.108
Inositol-2-P	0.145	0.033	0.154	0.036	0.165	0.027	0.189	0.016	0.405	0.124
Isoleucine	0.518	0.083	0.395	0.110	0.318	0.046	0.364	0.087	0.176	0.034
Lactate	0.616	0.053	0.642	0.130	0.490	0.068	0.535	0.031	0.933	0.113
Leucine	1.930	0.351	1.390	0.366	1.185	0.181	1.419	0.323	0.774	0.152
Linoleic acid (C18:2)	13.313	3.132	1.923	0.270	21.296	7.823	2.616	0.572	22.457	9.410
Linolenic acid (C18:3)	12.206	2.858	1.573	0.199	18.316	6.005	2.333	0.544	18.621	7.203
Lysine	0.150	0.028	0.143	0.028	0.115	0.010	0.150	0.045	0.123	0.049
Malate	0.052	0.013	0.119	0.051	0.070	0.020	0.059	0.004	0.043	0.004
Melibiose	1.878	0.680	2.003	0.669	0.429	0.121	4.027	1.164	0.410	0.114
Monolinoleylglycerol	0.698	0.339	0.119	0.041	0.372	0.165	0.180	0.081	0.492	0.159
Monooleoylglycerol	0.421	0.147	0.052	0.011	0.397	0.114	0.085	0.026	0.613	0.155
Monopalmitoglycerol	2.367	0.778	1.258	0.272	1.928	0.574	1.783	0.450	2.825	0.632
Nicotinamide	0.076	0.012	0.110	0.014	0.080	0.016	0.096	0.011	0.103	0.015
Octadecanoic acid (C18:0)	14.928	1.626	12.836	1.877	16.105	2.447	11.349	1.029	18.252	4.251
Octadecanol	0.576	0.052	0.808	0.116	0.683	0.137	0.769	0.092	1.248	0.235
Oleic acid_25.53 (C18:1) (9Z)	18.324	2.835	4.841	0.530	26.101	4.918	6.790	1.391	23.697	7.453
Oleic acid_25.612 (C18:1) (9E)	0.372	0.065	0.462	0.067	0.230	0.050	0.460	0.051	0.320	0.052
Phenylalanine	0.257	0.041	0.246	0.037	0.150	0.022	0.218	0.044	0.106	0.015

	0C	S.E.M	6C	S.E.M	6HS	S.E.M	8C	S.E.M	8HS	S.E.M
Phytol	3.904	0.796	6.460	1.977	5.696	1.674	5.905	0.688	14.518	4.332
Proline	0.634	0.151	0.648	0.475	0.666	0.155	0.268	0.087	0.308	0.059
Pyroglutamate	64.725	9.558	104.783	20.925	47.815	11.867	72.030	15.387	65.777	17.933
Pyruvic acid	1.147	0.086	1.707	0.390	1.229	0.223	1.097	0.107	1.876	0.274
Ribitol	0.272	0.030	0.525	0.110	0.173	0.037	0.410	0.036	0.186	0.042
Serine	0.680	0.124	0.480	0.147	0.483	0.058	0.612	0.186	0.305	0.065
Stearidonic acid (C18:4)	1.964	0.219	1.242	0.186	2.817	0.661	1.207	0.152	2.118	0.557
Succinate	0.131	0.018	0.253	0.064	0.150	0.030	0.199	0.037	0.187	0.042
Sucrose	0.856	0.124	1.561	0.427	1.088	0.135	0.928	0.112	1.040	0.107
Tetradecanoic acid (C14:0)	46.660	5.245	21.424	2.147	126.376	28.923	23.482	2.734	115.720	28.737
Threonate	0.120	0.009	0.126	0.017	0.088	0.011	0.114	0.009	0.080	0.014
Threonine	0.329	0.048	0.290	0.055	0.194	0.023	0.311	0.061	0.135	0.022
Thymine	0.107	0.022	0.194	0.035	0.130	0.038	0.167	0.025	0.204	0.055
Tocopherol	0.714	0.152	1.221	0.525	0.721	0.111	0.601	0.127	3.349	1.592
Turanose	0.429	0.086	0.241	0.032	0.049	0.012	0.193	0.030	0.043	0.007
Tyrosine	0.562	0.082	0.467	0.081	0.447	0.128	0.428	0.122	0.251	0.053
Urea	0.195	0.022	0.311	0.102	0.212	0.020	0.185	0.018	0.296	0.046

Table S3.2 Summary of mean comparative data (*n* = 6) for host samples at Days 0, 6 and 8, under ambient conditions (C) and thermal stress (HS)

	0C	S.E.M	6C	S.E.M	6HS	S.E.M	8C	S.E.M	8HS	S.E.M
1-Monohexadecanoglycerol	0.431369	0.080682	0.332118	0.043246	0.396992	0.083268	0.486776	0.069592	0.521997	0.260422
Adenine	39.4492	16.18969	25.04666	5.483669	18.80187	6.837621	27.91988	5.489185	41.61764	7.911027
Adenosine	0.038097	0.006432	0.062865	0.012665	0.03442	0.007259	0.043758	0.01054	0.046276	0.016888
Alanine	0.060866	0.021177	0.083462	0.022689	0.045606	0.021109	0.226092	0.125881	0.121572	0.04311
Arabinose	0.582385	0.079692	0.645173	0.088709	0.546723	0.036558	0.631983	0.076438	0.498809	0.043715
Ascorbate	2.071844	1.321119	1.6422	1.03596	0.089007	0.0362	0.710848	0.434863	0.124083	0.075292

	0C	S.E.M	6C	S.E.M	6HS	S.E.M	8C	S.E.M	8HS	S.E.M
beta_Alanine	0.016596	0.006571	0.026274	0.004121	0.026292	0.013398	0.037309	0.010767	0.034392	0.008436
Campesterol	1.50435	0.180083	1.674018	0.120948	1.591606	0.075472	1.645803	0.219035	1.727491	0.215319
Cellobiose	0.619143	0.278179	0.261785	0.067285	0.225091	0.136205	0.558465	0.219964	0.918681	0.759093
Cholesterol	0.050905	0.003871	0.062073	0.009798	0.061738	0.005927	0.058928	0.006426	0.060884	0.006669
Diethylene glycol	0.365857	0.022158	0.570956	0.078215	0.395153	0.024387	0.483845	0.113792	0.386082	0.035707
Digalactosylglycerol	0.166155	0.029527	0.237151	0.043147	0.28663	0.047879	0.25202	0.039485	0.103762	0.016141
Eicosanoic acid (C20:0)	0.106162	0.026238	0.081818	0.003581	0.092499	0.017786	0.110976	0.014048	0.112286	0.00835
Erythronate	2.293181	0.393573	2.07646	0.417127	1.416067	0.137731	2.46243	0.327309	0.944529	0.072703
Ethanolamine	0.284162	0.136328	0.414422	0.153961	0.507149	0.339577	0.759899	0.193083	0.677466	0.266359
Fructose	0.385901	0.053784	0.42078	0.042083	0.582807	0.240188	0.570256	0.180133	0.301754	0.054972
Galactinol	0.031724	0.0029	0.03178	0.002398	0.047186	0.004263	0.037698	0.002799	0.049547	0.004313
Galactitol	7.182725	1.473217	6.086866	1.460977	11.40478	1.727717	7.371189	2.066096	7.93775	0.647312
Galactose	24.83825	1.247635	20.80661	1.422647	28.48372	2.383205	22.81095	3.189515	11.95283	1.701144
Galactosylglycerol	142.8784	26.4283	91.37297	10.71849	37.53099	5.581038	127.0193	26.7708	17.89149	2.095142
Gentiobiose	0.084629	0.013461	0.0615	0.015143	0.155253	0.016618	0.065564	0.014388	0.134584	0.019318
Gluconic acid	1.047349	0.075473	0.839624	0.063774	1.429495	0.085871	0.986736	0.106064	1.544255	0.093324
Glucose	69.90295	7.708507	57.68582	5.881093	90.25238	11.86752	58.56382	3.613706	59.16389	8.62066
Glutamate	1.69342	0.643539	1.34586	0.545493	0.57847	0.374895	2.19423	1.065662	0.91591	0.219045
Glyceric acid	0.52522	0.091561	0.503399	0.088669	0.384708	0.032966	0.651058	0.120061	0.288952	0.029329
Glycerol	24.59473	3.705151	17.75128	2.593014	15.787	2.057689	19.88347	2.6667	10.20005	1.986556
Glycine	63.27843	12.95646	75.84173	10.59746	70.07464	5.080642	66.67032	3.882555	72.07451	3.794372
Glycolic acid	0.291654	0.070934	0.192752	0.031857	0.162649	0.03603	0.251191	0.037593	0.179426	0.040386
Guanine	1.347335	0.229048	0.417439	0.173582	0.242366	0.159213	0.453437	0.173817	1.141701	0.372361
Gulonic acid	0.033142	0.001667	0.039533	0.007437	0.026266	0.002175	0.046323	0.004742	0.036942	0.004752
Hexadecanoic acid (C16:0)	8.627514	2.045812	7.198602	0.28528	7.700059	1.440837	9.563273	1.23542	8.247188	1.440968
Hexadecanol	11.42006	1.585083	10.79539	0.650125	11.48032	0.909218	11.58852	1.11337	10.64401	2.323984
Hexadecenoic acid (C16:1)	0.720965	0.16894	0.58271	0.044975	0.502219	0.106801	0.832877	0.073588	0.519033	0.141742
Homoserine	0.097875	0.035799	0.18235	0.062583	0.062652	0.02794	0.267036	0.096164	0.076495	0.015375
Inositol, myo	12.26325	0.45548	16.13745	1.016891	36.79334	3.186349	19.87482	2.283924	24.57553	2.962208
Isoleucine	0.21519	0.083819	0.516905	0.191288	0.249191	0.172731	1.004173	0.417465	0.392971	0.181454
Isomaltose	0.131423	0.031934	0.101044	0.0301	0.096089	0.020465	0.140812	0.05529	0.049973	0.007208

	0C	S.E.M	6C	S.E.M	6HS	S.E.M	8C	S.E.M	8HS	S.E.M
Lactate	0.602542	0.099359	0.572204	0.144934	0.559413	0.119626	0.823178	0.135855	0.739619	0.189736
Linoleic acid (C18:2)	0.108453	0.026218	0.046781	0.003501	0.075361	0.018208	0.06773	0.005684	0.080664	0.021354
Lysine	1.645628	0.705284	1.397503	0.38209	2.063397	1.03272	1.524621	0.315995	3.205463	0.789699
Maltose	6.623683	1.283987	10.41744	3.619627	3.130655	0.631535	10.01536	1.711845	1.890304	0.617972
Melibiose	0.072185	0.014063	0.077832	0.012828	0.118792	0.023727	0.102544	0.019591	0.062651	0.007219
Monopalmitoglycerol	0.130433	0.031184	0.08386	0.008407	0.123427	0.020615	0.131619	0.016481	0.134373	0.055545
Nicotinamide	6.476109	1.732351	6.606637	0.603985	6.678558	0.902976	9.332339	1.45481	7.673835	0.561457
Octadecanoic acid (C18:0)	3.726172	0.843249	3.151695	0.102777	3.452375	0.631877	4.270755	0.613049	4.13355	0.323331
Octadecanol	1.788856	0.302061	2.902722	0.555892	2.418367	0.221969	4.008957	1.027617	2.139962	0.333525
Oleic acid (C18:1) (9Z)	0.477235	0.114028	0.341628	0.007772	0.381357	0.087189	0.488058	0.048124	0.424372	0.094025
Phenylalanine	0.146069	0.060912	0.15552	0.052463	0.055315	0.017609	0.233633	0.063006	0.062248	0.015384
Proline	0.649257	0.311871	1.154635	0.455721	0.973364	0.804818	2.390983	1.111711	1.131416	0.437134
Pyroglutamic acid	8.056648	2.388984	6.920184	1.393791	6.54786	0.632413	8.763392	2.670523	11.00797	1.48461
Pyruvate	0.209587	0.027376	0.16391	0.010931	0.188226	0.03867	0.237555	0.028027	0.142572	0.023096
Serine	1.482155	0.65409	2.530701	0.875933	2.356952	1.565328	4.450221	1.524541	4.712645	1.592371
Succinate	1.586254	0.166677	1.417884	0.13911	0.970095	0.064422	1.70836	0.118609	0.84131	0.071133
Sucrose	1.013433	0.187753	1.080575	0.352859	1.130872	0.318625	2.475688	1.35357	1.7749	0.43555
Tetradecanoic acid (C14:0)	1.987947	0.369402	1.77271	0.166382	1.727855	0.237336	2.291166	0.262597	1.533292	0.265673
Threitol	0.067521	0.01497	0.103326	0.009553	0.068846	0.016125	0.108196	0.01628	0.081695	0.009753
Threonate-1,4-lactone	0.097237	0.021872	0.095659	0.020131	0.061388	0.009811	0.149062	0.019235	0.061959	0.007518
Threonine	0.975911	0.43445	1.722579	0.512378	1.118539	0.718385	2.585949	0.725536	2.581485	0.730256
Thymidine	0.861803	0.136825	0.984875	0.199564	0.751262	0.121652	0.922758	0.185849	0.50549	0.047948
Thymine	8.481598	3.867548	9.733234	1.702218	5.210333	3.038886	11.95358	2.721209	11.64775	2.431764
Tocopherol	0.432716	0.051816	0.582033	0.13754	0.346193	0.029698	0.497643	0.086848	0.342521	0.045969
Tryptamine	10.93651	1.535359	6.399536	1.13201	1.766677	0.364731	10.50857	2.659553	0.873216	0.152368
Tyramine	8.461174	2.084254	12.1555	2.156054	13.04689	2.242306	14.35625	2.853908	14.64793	3.251184
Uracil	0.736169	0.313395	0.862134	0.13473	0.581735	0.334511	1.004431	0.276864	1.448566	0.277993
Urea	0.030189	0.012915	0.060558	0.012853	0.12452	0.075568	0.098633	0.040816	0.317049	0.082002
Xylose	1.11979	0.440805	0.883941	0.399132	2.439149	0.742706	1.545418	0.607745	2.025016	0.866403

Table S3.3 Mean quantitative data (*n* = 6) for the symbiont fraction at Day 8; concentrations in picomoles *per* mg dry weight, with fold change and student-t-test outputs.

	Mean conc.	S.E.M.	x-fold	S.E.M.	Mean conc.	S.E.M.	x-fold	S.E.M.	t-Test
	D8 C				D8 HS				
Succinate	109.098	13.830	1.000	0.127	31.145	5.776	***0.285***	***0.185***	***0.000***
Fumarate	66.153	9.440	1.000	0.143	28.211	1.799	**0.426**	**0.064**	**0.003**
Malate	53.969	5.032	1.000	0.093	33.067	2.085	**0.613**	**0.063**	**0.003**
Xylose	15.348	0.636	1.000	0.041	15.943	1.150	1.039	0.072	0.661
Ribose	13.589	0.937	1.000	0.069	15.605	0.976	1.148	0.063	0.167
Arabinose	40.075	3.139	1.000	0.078	21.797	1.721	***0.544***	***0.079***	***0.000***
Xylitol	10.212	1.550	1.000	0.152	13.871	1.631	1.358	0.118	0.135
arabitol	8.965	1.000	1.000	0.112	14.302	2.221	1.595	0.155	0.053
Fucose	29.873	1.636	1.000	0.055	23.414	1.304	**0.784**	**0.056**	**0.012**
Citrate	47.327	4.168	1.000	0.088	50.579	2.294	1.069	0.045	0.510
Mannose	19.230	1.610	1.000	0.084	18.278	1.303	0.950	0.071	0.656
Galactose	533.919	44.124	1.000	0.083	253.671	50.004	***0.475***	***0.197***	***0.002***
Glucose	693.531	105.800	1.000	0.153	1056.117	219.789	1.523	0.208	0.168
Glucuronate	22.210	1.078	1.000	0.049	25.382	1.683	1.143	0.066	0.144
Galactitol	8.834	0.789	1.000	0.089	10.555	0.513	1.195	0.049	0.097
Inositol	32.512	5.509	1.000	0.169	43.151	9.744	1.327	0.226	0.364
Ferulic Acid	53.809	5.448	1.000	0.101	58.997	3.579	1.096	0.061	0.445
Sucrose	44.279	6.661	1.000	0.150	53.805	8.683	1.215	0.161	0.404
Maltose	48.939	4.964	1.000	0.101	53.478	8.759	1.093	0.164	0.662
Turanose	24.900	1.350	1.000	0.054	18.842	3.988	0.757	0.212	0.181
beta-Gentibiose	47.096	2.044	1.000	0.043	59.491	3.866	**1.263**	**0.065**	**0.018**
Melibiose	57.247	6.292	1.000	0.110	65.197	5.634	1.139	0.086	0.369

Table S3.4 Mean quantitative data (*n* = 6) for the host fraction at Day 8; concentrations in picomoles *per* mg dry weight, with fold change and student-t-test outputs.

	Mean conc.	S.E.M.	x-fold	S.E.M.	Mean conc.	S.E.M.	x-fold	S.E.M.	t-Test
	D8 C				D8 HS				
Nicotinic Acid	406.866	58.431	1.000	0.144	376.964	54.174	0.927	0.144	0.715
Succinate	26.174	6.771	1.000	0.259	12.735	4.568	0.487	0.359	0.131
Fumarate	9.403	0.677	1.000	0.072	11.608	1.421	1.235	0.122	0.192
Malate	16.300	2.544	1.000	0.156	17.428	2.997	1.069	0.172	0.780
Erythritol	5.306	0.305	1.000	0.058	4.211	0.419	0.794	0.100	0.061
Salicylate	1.727	0.419	1.000	0.243	2.166	1.017	1.255	0.470	0.698
Xylose	211.047	22.514	1.000	0.107	40.988	6.468	***0.194***	***0.158***	***0.000***
Ribose	93.657	8.711	1.000	0.093	98.410	6.217	1.051	0.063	0.666
Arabinose	87.536	11.109	1.000	0.127	54.691	8.002	**0.625**	**0.146**	**0.037**
Xylitol	17.469	1.877	1.000	0.107	77.531	19.836	**4.438**	**0.256**	**0.013**
Rhamnose	11.941	1.490	1.000	0.125	9.260	1.064	0.775	0.115	0.174
arabitol	49.790	2.596	1.000	0.052	40.589	1.264	**0.815**	**0.031**	**0.010**
Fucose	13.536	0.797	1.000	0.059	13.999	1.148	1.034	0.082	0.747
Shikimate	53.739	5.308	1.000	0.099	65.975	25.152	1.228	0.381	0.644
Citrate	46.228	4.760	1.000	0.103	65.917	11.477	1.426	0.174	0.144
Quinate	6.679	0.642	1.000	0.096	6.837	1.011	1.024	0.148	0.898
Mannose	27.983	1.679	1.000	0.060	18.491	1.361	***0.661***	***0.074***	***0.001***
Galactose	470.677	46.889	1.000	0.100	325.794	43.259	**0.692**	**0.133**	**0.046**
Glucose	2216.367	77.014	1.000	0.035	2169.945	198.120	0.979	0.091	0.832
Mannitol	22.251	5.346	1.000	0.240	28.943	7.500	1.301	0.259	0.484
Glucuronate	14.337	0.758	1.000	0.053	15.979	1.050	1.115	0.066	0.234
Galactitol	419.989	71.748	1.000	0.171	458.941	30.210	1.093	0.066	0.628
Gluconate	37.385	6.387	1.000	0.171	27.658	1.554	0.740	0.056	0.170
Inositol	594.793	37.145	1.000	0.062	675.396	48.213	1.136	0.071	0.215
Fructose-6-P	166.137	37.440	1.000	0.225	118.430	46.586	0.713	0.393	0.443
Sucrose	56.729	27.628	1.000	0.487	34.200	12.951	0.603	0.379	0.477
Maltose	410.871	34.501	1.000	0.084	72.665	13.870	***0.177***	***0.191***	***0.000***
Turanose	29.049	2.239	1.000	0.077	23.411	1.496	0.806	0.064	0.063
beta-Gentibiose	17.420	1.684	1.000	0.097	25.829	2.457	**1.483**	**0.095**	**0.018**
Melibiose	14.865	1.514	1.000	0.102	19.602	2.947	1.319	0.150	0.183

Table S3.5 Relative change in key symbiont metabolite pathway activities following 6 and 8 days of heat stress at 32 °C (* *P* < 0.05, t-test activity score x treatment, with FDR correction).

Pathway	6 d	8 d
Linoleic acid metabolism	-7.012*	-4.908
Vitamin digestion and absorption	1.406	-4.194*
Ubiquinone and other terpenoid-quinone biosynthesis	1.447	-3.499
Purine metabolism	-1.400	-3.415
Fatty acid biosynthesis	-3.256*	-3.187
Biosynthesis of unsaturated fatty acids	-2.927*	-2.966
Cutin, suberine and wax biosynthesis	-2.888	-2.947
Fatty acid metabolism	-2.805*	-2.911
Fatty acid elongation	-2.805*	-2.911
Fatty acid degradation	-2.777*	-2.883
Biosynthesis of plant secondary metabolites	-2.693	-2.825
Fat digestion and absorption	1.082	-2.428*
Steroid degradation	1.082	-2.428*
Steroid hormone biosynthesis	1.082	-2.428*
ABC transporters	-2.778*	-1.838
Indole alkaloid biosynthesis	-3.106	-1.814
Glycolysis / Gluconeogenesis	-2.295*	-1.791
Pentose phosphate pathway	-2.268*	-1.769
Terpenoid backbone biosynthesis	1.388	-1.710
Vitamin B6 metabolism	1.388	-1.710
Phosphatidylinositol signalling system	-1.165	-1.686
Inositol phosphate metabolism	-1.165	-1.686
Pyruvate metabolism	1.379	-1.686
Starch and sucrose metabolism	-2.353*	-1.648
D-Alanine metabolism	1.391	-1.609
Ascorbate and aldarate metabolism	1.169	-1.595*
Citrate cycle (TCA cycle)	1.434	-1.554
Taurine and hypotaurine metabolism	1.397	-1.484
Glycerolipid metabolism	-2.091*	-1.461
Biosynthesis of phenylpropanoids	1.453	-1.406
Pentose and glucuronate interconversions	1.592	-1.368
Galactose metabolism	-1.971*	-1.364
Pantothenate and CoA biosynthesis	1.402	-1.362
Nicotinate and nicotinamide metabolism	1.401	-1.344
Tyrosine metabolism	1.329	-1.342
Thiamine metabolism	1.298	-1.328
Fructose and mannose metabolism	1.198	-1.302
Carbon fixation in photosynthetic organisms	1.416	-1.294
Arginine and proline metabolism	1.293	-1.292
Phenylalanine metabolism	1.352	-1.246

Table S3.5 (cont.)

Pathway (cont.)	6 d	8 d
Alanine aspartate and glutamate metabolism	1.432	-1.212
Glyoxylate and dicarboxylate metabolism	1.375	-1.118
Cysteine and methionine metabolism	1.306	-1.089
Glycine, serine and threonine metabolism	1.325	1.008
Valine, leucine and isoleucine biosynthesis	1.298	1.015
Biosynthesis of terpenoids and steroids	1.873	1.056
Oxidative phosphorylation	1.687	1.063
Glutathione metabolism	2.182	1.095
Biosynthesis of plant hormones	1.848	1.109
2-Oxocarboxylic acid metabolism	1.284	1.152
Lysine degradation	1.293	1.180
Carbohydrate digestion and absorption	-1.316	1.199
Steroid biosynthesis	2.035	1.216
Selenocompound metabolism	1.428	1.219
Amino sugar and nucleotide sugar metabolism	-1.374	1.223
Brassinosteroid biosynthesis	2.069	1.257
Betalain biosynthesis	1.046	1.708
Isoquinoline alkaloid biosynthesis	1.046	1.708
D-Glutamine and D-glutamate metabolism	1.485	1.806
Nitrogen metabolism	1.485	1.806
Phenylpropanoid biosynthesis	1.195	1.813
Phenylalanine, tyrosine and tryptophan biosynthesis	1.195	1.813
Glucosinolate biosynthesis	1.180	1.827
Valine, leucine and isoleucine degradation	1.173	1.833
Sphingolipid metabolism	-1.008	2.005
Cyanoamino acid metabolism	1.175	2.089
Porphyrin and chlorophyll metabolism	1.471	2.100
Lysine biosynthesis	1.402	2.160
Riboflavin metabolism	3.043*	2.204
Histidine metabolism	1.480	2.563*
beta-Alanine metabolism	1.479	3.170*

Table S3.6 Relative change in key host metabolite pathway activities following 6 and 8 days of heat stress at 32 °C (* *P* < 0.05, t-test activity score x treatment, with FDR correction).

Pathway	D6	D8
Biotin metabolism	-1.501	-2.170
Lysine biosynthesis	-1.346	-1.832
beta-Alanine metabolism	1.461	-1.424
Pantothenate and CoA biosynthesis	1.322	-1.271
Inositol phosphate metabolism	-2.280*	-1.237
Phosphatidylinositol signalling system	-2.280*	-1.237
Purine metabolism	1.136	-1.210
Linoleic acid metabolism	-1.611	-1.191
Ascorbate and aldarate metabolism	-2.055*	-1.187
Lysine degradation	1.071	-1.104
Thiamine metabolism	1.082	-1.079
Cyanoamino acid metabolism	1.083	-1.077
Glutathione metabolism	1.109	-1.074
Glycine, serine and threonine metabolism	1.091	-1.067
Sphingolipid metabolism	1.074	-1.059
Biosynthesis of amino acids	1.091	-1.053
Brassinosteroid biosynthesis	1.052	-1.050
Steroid biosynthesis	1.050	-1.049
Glyoxylate and dicarboxylate metabolism	1.097	-1.039
Fat digestion and absorption	1.005	-1.033
Steroid degradation	1.005	-1.033
Steroid hormone biosynthesis	1.005	-1.033
Pentose phosphate pathway	-1.559	-1.012
Glycolysis / Gluconeogenesis	-1.558	-1.007
ABC transporters	-1.198	1.046
Biosynthesis of unsaturated fatty acids	-1.081	1.116
Fatty acid degradation	-1.066	1.120
Glycerophospholipid metabolism	-1.224	1.122
Starch and sucrose metabolism	-1.364	1.128
Amino sugar and nucleotide sugar metabolism	-1.513	1.144
Fatty acid metabolism	-1.070	1.160
Fatty acid elongation	-1.070	1.160
Fatty acid biosynthesis	-1.055	1.174
Pyruvate metabolism	-1.016	1.202
Phosphonate and phosphinate metabolism	-1.202	1.216
Nicotinate and nicotinamide metabolism	-1.014	1.224
Carbohydrate digestion and absorption	-1.367	1.258
Biosynthesis of terpenoids and steroids	1.184	1.325
Pentose and glucuronate interconversions	-1.054	1.581
Propanoate metabolism	1.296	1.590*

Table S3.6 (cont).

Pathway (cont.)	D6	D8
D-Alanine metabolism	1.058	1.755
Selenocompound metabolism	1.830	1.860
Fructose and mannose metabolism	-1.385	1.890
Galactose metabolism	-1.051	1.932*
Phenylalanine metabolism	1.377	1.951*
Arginine and proline metabolism	1.461	1.963
Citrate cycle (TCA cycle)	1.366	1.978*
Oxidative phosphorylation	1.462	2.031*
Biosynthesis of phenylpropanoids	1.431	2.083*
Alanine, aspartate and glutamate metabolism	1.689	2.160
Taurine and hypotaurine metabolism	1.961	2.252
Histidine metabolism	2.327	2.396
Nitrogen metabolism	2.327	2.396
D-Glutamine and D-glutamate metabolism	2.327	2.396
Phenylalanine, tyrosine and tryptophan biosynthesis	2.812	3.753
Glucosinolate biosynthesis	2.812	3.753
Glycerolipid metabolism	2.035*	5.189*
Tryptophan metabolism	3.622*	12.034*

Table S4.1 Summarised NTFD output (M+0) data for *Aiptasia* symbiont under control (C) and thermal stress (HS) conditions at 7 d

													Mean 7C		Mean 7HS	
Group	M+0 7C						M+0 7HS						M+0	M+X	M+0	M+X
Glycerol	0.820	0.704	0.910	0.936									0.843	**0.157**		
Threonate	0.889												0.889	**0.111**		
C12:0	0.833	0.766	0.826	0.906	0.890	0.875	0.753	0.732	0.759	0.781	0.779	0.857	0.849	**0.151**	0.777	**0.223**
Citrate	0.658	0.649	0.648	0.738	0.729	0.727	0.665	0.645					0.691	**0.309**	0.655	**0.345**
C14:0	0.795	0.764	0.806	0.892	0.877	0.860	0.688	0.673	0.707	0.717	0.728	0.804	0.832	**0.168**	0.720	**0.280**
Glucose	0.640	0.644	0.765	0.696			0.678	0.689	0.753	0.734			0.686	**0.314**	0.713	**0.287**
Hexadecanoic methyl ester	0.914						0.928	0.910	0.895	0.897	0.896	0.922	0.914	**0.086**	0.908	**0.092**
C16:1	0.869	0.843	0.857	0.897	0.881	0.891	0.894	0.870	0.881	0.920	0.877	0.933	0.873	**0.127**	0.896	**0.104**
Inositol_scyllo	0.856	0.850					0.849	0.851	0.850	0.843	0.867	0.858	0.853	**0.147**	0.853	**0.147**
C16:0	0.943	0.716	0.827				0.882	0.947					0.829	**0.171**	0.915	**0.085**
Galactosylglycerol _25.59	0.754	0.722	0.738	0.798			0.675	0.666					0.753	**0.247**	0.671	**0.329**
C18:1	0.887	0.908	0.905				0.883	0.888	0.891	0.874			0.900	**0.100**	0.884	**0.116**
C18:0	0.743	0.748	0.746	0.844	0.820	0.799	0.702	0.701	0.762				0.783	**0.217**	0.721	**0.279**
Galactosylglycerol_26 .48	0.844	0.848	0.843	0.850	0.848	0.861	0.810	0.826	0.813	0.786	0.819	0.807	0.849	**0.151**	0.810	**0.190**
Unknown FA_27.22	0.672	0.651					0.664	0.685					0.662	**0.338**	0.675	**0.325**
Unknown FA_27.6	0.442	0.405	0.603	0.549			0.428	0.459					0.500	**0.500**	0.443	**0.557**
Monopalmitolyglycerol	0.615	0.567	0.676	0.766	0.713	0.725	0.671	0.681	0.706	0.726	0.738	0.784	0.677	**0.323**	0.718	**0.282**
Mono-hexadecenoylglycerol	0.911	0.917	0.905	0.926	0.926		0.919	0.917	0.920	0.920	0.941		0.917	**0.083**	0.923	**0.077**
Mono-hexadecanoylglycerol	0.676	0.632	0.690	0.757	0.682	0.698	0.693	0.686	0.732	0.764	0.737	0.756	0.689	**0.311**	0.728	**0.272**
Adenosine	0.896	0.912	0.943	0.936			0.841	0.839	0.859	0.822	0.834	0.827	0.922	**0.078**	0.837	**0.163**
Maltose	0.827	0.815	0.830	0.877	0.771		0.815	0.677	0.764				0.824	**0.176**	0.752	**0.248**
Turanose	0.621	0.585	0.585	0.647	0.685		0.730	0.701	0.757	0.764	0.722		0.625	**0.375**	0.735	**0.265**

Table S4.2 Summarised NTFD output (M+0) data for *Aiptasia* host under control (C) and thermal stress (HS) conditions at 7 d

Group	M+0 7C						M+0 7HS						Mean 7C		Mean 7HS	
													M+0	M+X	M+0	M+X
Glycerol	0.934	0.903	0.901	0.914	0.925		0.934	0.898	0.921	0.931	0.942		0.915	**0.085**	0.914	**0.086**
Glycerate							0.937	0.907							0.922	**0.078**
Pyroglutamate							0.840	0.847							0.844	**0.156**
Glutamate							0.812	0.881							0.847	**0.153**
Fructose MX1	0.862	0.837	0.840	0.865	0.875	0.846	0.847	0.828	0.858	0.869	0.872	0.862	0.854	**0.146**	0.850	**0.150**
Galactose	0.770	0.794	0.785	0.818	0.837		0.733	0.824	0.731	0.758	0.740		0.801	**0.199**	0.800	**0.200**
Glucose	0.851	0.821	0.835	0.864	0.853		0.836	0.816	0.829	0.860	0.848		0.845	**0.155**	0.841	**0.159**
Inositol, scyllo-	0.859	0.856	0.896	0.873	0.899		0.863	0.861	0.856	0.860	0.879	0.874	0.876	**0.124**	0.878	**0.122**
Inositol, myo-	0.509	0.507	0.527	0.553			0.802	0.858	0.882				0.524	**0.476**	0.685	**0.315**
Galactosylglycerol_25.58	0.701	0.673	0.686	0.734	0.733	0.747	0.615	0.588	0.554	0.579	0.577	0.607	0.712	**0.288**	0.684	**0.316**
Galactosylglycerol_26.47	0.861	0.872					0.838	0.831	0.834	0.831			0.866	**0.134**	0.834	**0.166**
Sucrose	0.255	0.292											0.274	**0.726**		
Maltose	0.855	0.857	0.864	0.884	0.884	0.879	0.839	0.819	0.881	0.847	0.827		0.870	**0.130**	0.861	**0.139**
Unknown sugar_31.39	0.883	0.867	0.843	0.877									0.867	**0.133**	0.860	**0.140**

Table S4.3 Summarised NTFD output (M+0) data for *A. aspera* symbiont under control (C) and thermal stress (HS) conditions at 6 d

													6C		6HS	
Group	M+0 6C						M+0 6HS						M+0	M+X	M+0	M+X
Glycerol	0.664	0.647	0.555	0.682	0.695	0.733	0.577	0.733	0.742	0.644	0.703	0.663	0.663	**0.337**	0.677	**0.323**
C12:0		0.454		0.381	0.498	0.583	0.480	0.790	0.799	0.680	0.753	0.742	0.479	**0.521**	0.707	**0.293**
C14:0	0.506	0.511	0.411	0.369	0.562	0.569	0.518	0.778	0.755	0.632	0.708	0.653	0.488	**0.512**	0.674	**0.326**
Galactose	0.908	0.850	0.853	0.845	0.879	0.880	0.876	0.823	0.817	0.852	0.859	0.849	0.869	**0.131**	0.846	**0.154**
Glucose	0.587	0.534	0.498	0.546	0.617		0.631	0.510	0.596	0.706	0.657		0.556	**0.444**	0.620	**0.380**
C16:0	0.685	0.702	0.647	0.633	0.687	0.724	0.585	0.723	0.689	0.572	0.685	0.640	0.680	**0.320**	0.649	**0.351**
C18:1	0.888	0.702					0.742						0.795	**0.205**	0.742	**0.258**
C18:0	0.915	0.894	0.892	0.909	0.917		0.862	0.909	0.886	0.913	0.873		0.905	**0.095**	0.889	**0.111**
Galactosylglycerol	0.872	0.822	0.803	0.823	0.869	0.881	0.876	0.841	0.836	0.851	0.889	0.859	0.845	**0.155**	0.859	**0.141**
Monopalmitoylglycerol	0.596	0.666	0.612	0.685			0.605	0.653	0.674				0.640	**0.360**	0.644	**0.356**
Monohexadecanoylglycerol	0.287	0.356	0.273	0.258	0.307	0.367	0.204	0.449	0.471	0.243	0.305	0.278	0.308	**0.692**	0.325	**0.675**
2-Monolinoleoylglycerol	0.823	0.797	0.766	0.836	0.846	0.844	0.735	0.847	0.826	0.838	0.822		0.819	**0.181**	0.814	**0.186**
Gentiobiose	0.876	0.871	0.900	0.901			0.914						0.887	**0.113**	0.914	**0.086**
Campesterol	0.889	0.886	0.860	0.856	0.862								0.871	**0.129**		
C20:5	0.870	0.906	0.830	0.898	0.935	0.922	0.937						0.893	**0.107**	0.937	**0.063**
C20:0	0.825	0.803	0.764	0.837	0.851	0.819	0.826	0.813					0.816	**0.184**	0.819	**0.181**
C22:6	0.760	0.750	0.792										0.767	**0.233**		
Maltotriose	0.836	0.830	0.773	0.851	0.830								0.824	**0.176**		
Unknown sugar_38.7	0.270	0.228	0.298				0.321	0.498	0.407	0.504	0.473		0.265	**0.735**	0.441	**0.559**
Cellotriose	0.817	0.774	0.744	0.778	0.847	0.847	0.808	0.776	0.819	0.815			0.801	**0.199**	0.804	**0.196**

Table S4.4 Summarised NTFD output (M+0) data for *A. aspera* symbiont under control (C) and thermal stress (HS) conditions at 9 d

													9C		9HS	
Group	M+0 9C						M+0 9HS						M+0	M+X	M+0	M+X
Glycerol	0.555	0.509	0.477	0.653	0.631	0.625	0.617	0.818	0.817	0.756	0.786	0.811	0.575	**0.425**	0.767	**0.233**
C12:0	0.329	0.316				0.485	0.614	0.884	0.900	0.840	0.843	0.854	0.376	**0.624**	0.823	**0.177**
C14:0	0.443	0.256	0.365	0.439	0.473		0.678	0.885	0.900	0.845	0.825	0.845	0.395	**0.605**	0.830	**0.170**
Galactose	0.879	0.844	0.815	0.850	0.866	0.849	0.880	0.838	0.846	0.799	0.806	0.831	0.851	**0.149**	0.833	**0.167**
Glucose	0.520	0.486	0.416	0.498	0.509		0.596	0.550	0.596	0.634	0.724	0.736	0.486	**0.514**	0.639	**0.361**
C16:0	0.666	0.666	0.664	0.673			0.631	0.829	0.884	0.781	0.822	0.828	0.667	**0.333**	0.796	**0.204**
C18:1	0.937	0.855	0.907	0.612			0.765						0.828	**0.172**	0.765	**0.235**
C18:0	0.831	0.864	0.899	0.925			0.935						0.880	**0.120**	0.935	**0.065**
Galactosylglycerol	0.855	0.803	0.812	0.839	0.860	0.892	0.850	0.860	0.894	0.875	0.858	0.881	0.843	**0.157**	0.870	**0.130**
Monopalmitoylglycerol	0.556	0.499	0.525				0.661	0.886	0.772	0.812			0.527	**0.473**	0.783	**0.217**
Mono-hexadecanoylglycerol	0.241	0.158	0.243	0.247	0.201		0.318	0.863	0.902	0.481	0.505	0.557	0.218	**0.782**	0.604	**0.396**
2-Monolinoleoylglycerol	0.703	0.836	0.788	0.791			0.783	0.934	0.884	0.913			0.779	**0.221**	0.879	**0.121**
Gentiobiose	0.872	0.849	0.901	0.904			0.831	0.891					0.882	**0.118**	0.861	**0.139**
Campesterol																
C20:5	0.841	0.803	0.803	0.908									0.839	**0.161**		
C20:0	0.816	0.734	0.825	0.831	0.810								0.803	**0.197**		
C22:6	0.629	0.765											0.697	**0.303**		
Maltotriose	0.745	0.763	0.822	0.823			0.819						0.788	**0.212**	0.819	**0.181**
Unknown sugar_38.7	0.250	0.216					0.441	0.633	0.604	0.658			0.233	**0.767**	0.584	**0.416**
Cellotriose	0.782	0.702	0.773	0.805	0.785		0.790	0.777	0.802				0.769	**0.231**	0.790	**0.210**

Table S4.5. Summarised NTFD output (M+0) data for *A. aspera* host under control (C) and thermal stress (HS) conditions at 6 d

													6C		6HS	
Group	M+0 6C						M+0 6HS						M+0	M+X	M+0	M+X
Glycerol	0.615	0.633	0.636	0.606	0.694	0.695	0.660	0.632	0.693	0.706	0.775	0.754	0.646	**0.354**	0.703	**0.297**
Serine	0.876	0.874	0.934				0.913	0.936	0.943	0.933			0.895	**0.105**	0.931	**0.069**
Proline	0.925	0.884	0.901				0.945						0.903	**0.097**	0.945	**0.055**
Glyceric acid	0.687	0.703					0.792						0.695	**0.305**	0.792	**0.208**
Butyric acid	0.859	0.802	0.782	0.933	0.927		0.899	0.934	0.929	0.949	0.937		0.860	**0.140**	0.929	**0.071**
Erythronic acid	0.921	0.890	0.895	0.938			0.914	0.920	0.945				0.911	**0.089**	0.926	**0.074**
Unknown sugar_16.18	0.901	0.853	0.831	0.903			0.926	0.934					0.872	**0.128**	0.930	**0.070**
Unknown sugar_16.49	0.817	0.792					0.939	0.950					0.805	**0.195**	0.944	**0.056**
Glutarate_16.66	0.866	0.816	0.935				0.897						0.872	**0.128**	0.897	**0.103**
Glutamate	0.870	0.823	0.859	0.938	0.932		0.904	0.925	0.920	0.924	0.944	0.927	0.884	**0.116**	0.924	**0.076**
Glutarate_17.20	0.855	0.800	0.774	0.869	0.930	0.922	0.894	0.902	0.921	0.925	0.932	0.934	0.858	**0.142**	0.918	**0.082**
Arabinose	0.891						0.945	0.939					0.891	**0.109**	0.942	**0.058**
Ribose	0.787	0.756	0.841				0.814	0.841	0.834	0.859	0.840		0.795	**0.205**	0.838	**0.162**
??Diaminovalerolactam	0.762	0.749	0.833	0.916	0.907		0.904	0.915	0.918	0.932	0.909		0.833	**0.167**	0.916	**0.084**
Arabitol	0.897	0.942					0.896	0.920	0.924				0.920	**0.080**	0.914	**0.086**
C14:4	0.873	0.792	0.849	0.932	0.921		0.891	0.942					0.873	**0.127**	0.917	**0.083**
C14:0	0.800	0.899					0.895	0.875	0.883				0.850	**0.150**	0.884	**0.116**
Fructose	0.826	0.898	0.904	0.898			0.900	0.843	0.818				0.882	**0.118**	0.854	**0.146**
Galactose	0.436	0.344	0.259	0.351	0.361	0.333	0.470	0.389	0.427	0.402	0.394	0.392	0.347	**0.653**	0.413	**0.587**
Glucose	0.766	0.734	0.680	0.738	0.858	0.850	0.810	0.459	0.550	0.777	0.837	0.827	0.771	**0.229**	0.710	**0.290**
Inositol, scyllo_21.89	0.699	0.575	0.778				0.924	0.789					0.684	**0.316**	0.856	**0.144**
Inositol, scyllo_22.85	0.902	0.944											0.923	**0.077**		
C16:0	0.879	0.884	0.898	0.903			0.858	0.949	0.950	0.947			0.891	**0.109**	0.926	**0.074**
Inositol, myo-	0.920	0.945											0.933	**0.067**		
Galactosylglycerol_25.60	0.215	0.280	0.254	0.235	0.324		0.210	0.397	0.350	0.319	0.390	0.397	0.261	**0.739**	0.344	**0.656**
Galactosylglycerol_26.05	0.237	0.239	0.251	0.244	0.271		0.168						0.248	**0.752**	0.168	**0.832**
Galactosylglycerol_26.45	0.869	0.790	0.817	0.796	0.881	0.871	0.851	0.815	0.848	0.849	0.861		0.838	**0.162**	0.845	**0.155**
Monopalmitoylglycerol	0.657	0.722					0.651	0.815					0.690	**0.310**	0.733	**0.267**

Group	M+0 6C						M+0 6HS						6C		6HS	
													M+0	M+X	M+0	M+X
Mono-hexadecanoylglycerol	0.641	0.714	0.940	0.751			0.652	0.808					0.762	**0.238**	0.730	**0.270**
Sucrose	0.920						0.861	0.834					0.920	**0.080**	0.847	**0.153**
Maltose	0.880	0.871	0.851	0.865	0.942	0.907	0.921	0.831	0.855	0.835	0.874	0.867	0.886	**0.114**	0.864	**0.136**
Turanose	0.847						0.873	0.860					0.847	**0.153**	0.867	**0.133**
Galactinol	0.905						0.882						0.905	**0.095**	0.882	**0.118**
Digalactosylglycerol	0.915	0.904					0.930						0.910	**0.090**	0.930	**0.070**

Table S4.6 Summarised NTFD output (M+0) data for *A. aspera* host under control (C) and thermal stress (HS) conditions at 9 d

Group	M+0 9C						M+0 9HS						9C		9HS	
													M+0	M+X	M+0	M+X
Glycerol	0.534	0.561	0.690	0.551	0.629		0.729	0.670	0.673	0.805	0.684	0.753	0.593	**0.407**	0.719	**0.281**
Serine	0.841	0.878	0.883				0.918	0.914	0.928				0.867	**0.133**	0.920	**0.080**
Proline	0.837	0.855	0.811	0.917	0.906								0.865	**0.135**		
Glyceric acid	0.713	0.666					0.841						0.689	**0.311**	0.841	**0.159**
Butyric acid	0.858	0.856	0.891				0.926						0.868	**0.132**	0.926	**0.074**
Erythronic acid	0.898	0.879	0.887	0.938	0.935	0.923	0.913						0.910	**0.090**	0.913	**0.087**
Unknown sugar_16.18	0.808	0.838	0.750	0.895	0.892	0.926							0.851	**0.149**		
Unknown sugar_16.49	0.796	0.692	0.874	0.904									0.816	**0.184**		
Glutarate_16.66	0.887												0.887	**0.113**		
Glutamate	0.772	0.778	0.860	0.894			0.934	0.934	0.946				0.826	**0.174**	0.938	**0.062**
Glutarate_17.20	0.747	0.782	0.699	0.857	0.848	0.890	0.921						0.804	**0.196**	0.921	**0.079**
Arabinose	0.845	0.918	0.911	0.914			0.937	0.919					0.897	**0.103**	0.928	**0.072**
Ribose	0.763	0.723	0.797				0.843						0.761	**0.239**	0.843	**0.157**
??Diaminovalerolactam	0.726	0.754	0.843	0.829	0.879		0.901	0.934	0.942	0.949	0.948		0.806	**0.194**	0.935	**0.065**
Arabitol	0.922	0.947	0.944	0.945			0.893						0.939	**0.061**	0.893	**0.107**
C14:4	0.747	0.785	0.844	0.843			0.921	0.930					0.805	**0.195**	0.925	**0.075**
C14:0	0.785												0.785	**0.215**		
Fructose							0.767	0.675							0.721	**0.279**

													9C		9HS	
Group	M+0 9C						M+0 9HS						M+0	M+X	M+0	M+X
Galactose	0.274	0.278	0.435	0.309	0.236		0.514	0.421	0.419	0.292	0.334		0.306	**0.694**	0.396	**0.604**
Glucose	0.754	0.642	0.778	0.790	0.828		0.764	0.396	0.378	0.689	0.697	0.728	0.758	**0.242**	0.609	**0.391**
Inositol, scyllo_21.89	0.489												0.489	**0.511**		
Inositol, scyllo_22.85	0.829	0.907	0.918	0.880	0.913	0.936	0.809						0.897	**0.103**	0.809	**0.191**
C16:0	0.896	0.860	0.890	0.930									0.894	**0.106**		
Inositol, myo-	0.916	0.941	0.930										0.929	**0.071**		
Galactosylglycerol_25.56	0.172	0.241	0.290	0.259	0.230		0.190	0.471	0.215	0.403	0.393		0.238	**0.762**	0.334	**0.666**
Galactosylglycerol_26.05	0.150	0.278	0.244	0.228									0.225	**0.775**		
Galactosylglycerol_26.45	0.859	0.815	0.860	0.802	0.846	0.859	0.846						0.840	**0.160**	0.846	**0.154**
Monopalmitoylglycerol	0.728												0.728	**0.272**		
Monohexadecanoylglycerol	0.740												0.740	**0.260**		
Sucrose							0.616								0.616	**0.384**
Maltose	0.836	0.891	0.891	0.896			0.732	0.727					0.878	**0.122**	0.729	**0.271**
Turanose	0.834	0.895	0.892										0.874	**0.126**		
Galactinol	0.920	0.921	0.935										0.925	**0.075**		
Digalactosylglycerol	0.922	0.931											0.926	**0.074**		

Table S4.7 Summarised MassHunter output abundance data for *Aiptasia* symbiont under control (C) and thermal stress (HS) conditions at 7 d

													7C		7HS	
Compound	7C								7HS				Mean	SE	Mean	SE
1-Monohexadecanoylglycerol	0.0886	0.0975	0.0934	0.0897	0.0764	0.0761	0.0862	0.0738	0.0631	0.0789	0.0864	0.0640	0.0869	0.0036	0.0754	0.0042
1-Monooctodecanoylglycerol	0.0331	0.0288	0.0236	0.0324	0.0226	0.0209	0.0375	0.0252	0.0187	0.0284	0.0239	0.0184	0.0269	0.0021	0.0254	0.0029
Adenosine	0.0013	0.0014	0.0011	0.0012	0.0013	0.0010	0.0013	0.0008	0.0008	0.0008	0.0007	0.0007	0.0012	0.0001	0.0009	0.0001
C12:0	0.0029	0.0051	0.0063	0.0033	0.0030	0.0069	0.0014	0.0018	0.0018	0.0015	0.0025	0.0016	0.0046	0.0007	0.0017	0.0002
C14:0	0.0334	0.0525	0.0584	0.0376	0.0348	0.0566	0.0202	0.0238	0.0201	0.0185	0.0308	0.0209	0.0456	0.0047	0.0224	0.0018
C16:0	0.0969	0.1193	0.1282	0.0937	0.1010	0.1134	0.1164	0.1242	0.1243	0.1172	0.1169	0.1307	0.1088	0.0056	0.1216	0.0023
C16:1	0.0046	0.0050	0.0065	0.0044	0.0041	0.0047	0.0031	0.0031	0.0033	0.0033	0.0055	0.0039	0.0049	0.0004	0.0037	0.0004
C18:0	0.0411	0.0552	0.0534	0.0425	0.0387	0.0492	0.0417	0.0406	0.0318	0.0375	0.0488	0.0335	0.0467	0.0028	0.0390	0.0025
C18:1	0.0007	0.0013	0.0027	0.0010	0.0016	0.0011	0.0018	0.0015	0.0016	0.0016	0.0029	0.0029	0.0014	0.0003	0.0020	0.0003
C20:0	0.0007	0.0008	0.0007	0.0007	0.0006	0.0008	0.0008	0.0007	0.0005	0.0007	0.0008	0.0006	0.0007	0.0000	0.0007	0.0001
C22:6	0.0065	0.0041	0.0063	0.0066	0.0066	0.0069	0.0102	0.0068	0.0054	0.0080	0.0095	0.0060	0.0062	0.0004	0.0076	0.0008
Citrate	0.0012	0.0017	0.0033	0.0014	0.0023	0.0022	0.0022	0.0014	0.0017	0.0018	0.0021	0.0021	0.0020	0.0003	0.0019	0.0001
Galactose	0.0149	0.0168	0.0165	0.0178	0.0169	0.0140	0.0187	0.0156	0.0219	0.0159	0.0185	0.0142	0.0162	0.0006	0.0174	0.0011
Galactosylglycerol_25.59	0.0113	0.0112	0.0087	0.0110	0.0082	0.0069	0.0070	0.0083	0.0081	0.0066	0.0065	0.0055	0.0095	0.0008	0.0070	0.0004
Galactosylglycerol_26.48	0.0388	0.0599	0.0528	0.0361	0.0428	0.0555	0.0313	0.0488	0.0392	0.0267	0.0391	0.0389	0.0476	0.0040	0.0373	0.0031
Glucose	0.0782	0.0565	0.0841	0.0751	0.0801	0.0813	0.0703	0.0778	0.0842	0.0737	0.0781	0.0719	0.0759	0.0041	0.0760	0.0021
Hexadecanoic methyl ester	0.0013	0.0016	0.0015	0.0012	0.0012	0.0016	0.0016	0.0013	0.0015	0.0011	0.0014	0.0015	0.0014	0.0001	0.0014	0.0001
Inositol, scyllo-	0.0008	0.0006	0.0005	0.0008	0.0005	0.0004	0.0027	0.0040	0.0037	0.0033	0.0034	0.0023	0.0006	0.0001	0.0032	0.0003
Maltose	0.0014	0.0015	0.0014	0.0014	0.0015	0.0013	0.0011	0.0008	0.0007	0.0009	0.0011	0.0007	0.0014	0.0000	0.0009	0.0001
Monooctadecanoylglycerol	0.0037	0.0039	0.0043	0.0034	0.0028	0.0030	0.0013	0.0011	0.0008	0.0010	0.0013	0.0009	0.0035	0.0002	0.0011	0.0001
Monopalmitoylglycerol	0.0045	0.0059	0.0053	0.0046	0.0039	0.0040	0.0045	0.0038	0.0032	0.0039	0.0047	0.0033	0.0047	0.0003	0.0039	0.0003
Turanose	0.0014	0.0015	0.0013	0.0014	0.0013	0.0011	0.0013	0.0011	0.0012	0.0010	0.0012	0.0011	0.0013	0.0001	0.0011	0.0000
Unknown fatty acid_27.22	0.0011	0.0018	0.0018	0.0011	0.0010	0.0014	0.0006	0.0006	0.0005	0.0006	0.0009	0.0006	0.0014	0.0002	0.0006	0.0001
Unknown fatty acid_27.59	0.0163	0.0268	0.0277	0.0171	0.0150	0.0207	0.0090	0.0087	0.0081	0.0086	0.0130	0.0088	0.0206	0.0022	0.0094	0.0007

Table S4.8 Summarised MassHunter output and symbiont normalised relative abundance data for *Aiptasia* host under control conditions at 7 d

				7C			7C	
							Mean	SE
12C cells/mg protein	9516387	1E+07	8960805	1E+07	9535342	9270766	9616762	208877
Fructose	0.0174	0.0190	0.0189	0.0142	0.0008	0.0134	0.0139	0.0028
Galactose	0.0041	0.0024	0.0140	0.0044	0.0108	0.0031	0.0065	0.0019
Galactosylglycerol_25.60	0.4529	0.4018	0.4066	0.4083	0.4289	0.3802	0.4131	0.0102
Galactosylglycerol_26.48	0.0059	0.0057	0.0057	0.0068	0.0054	0.0047	0.0057	0.0003
Glucose	0.1349	0.0825	0.1229	0.1216	0.1994	0.0955	0.1261	0.0167
Glutamate	0.0007	0.0011	0.0014	0.0009	0.0007	0.0011	0.0010	0.0001
Glycerol	0.0275	0.0229	0.0244	0.0220	0.0213	0.0218	0.0233	0.0009
Inositol, myo-	0.0073	0.0057	0.0044	0.0056	0.0057	0.0028	0.0052	0.0006
Inositol, scyllo-	0.0448	0.0373	0.0356	0.0400	0.0395	0.0374	0.0391	0.0013
Maltose	0.0304	0.0216	0.0280	0.0460	0.0494	0.0266	0.0337	0.0046
Pyroglutamate	0.0024	0.0015	0.0011	0.0053	0.0005	0.0015	0.0020	0.0007

Symbiont normalised							Mean	SE
12C cells/mg protein	9516387	1E+07	8960805	1E+07	9535342	9270766	9616762	208877
Fructose	1.8E-09	1.9E-09	2.1E-09	1.4E-09	8.2E-11	1.4E-09	1.5E-09	3E-10
Galactose	4.4E-10	2.4E-10	1.6E-09	4.2E-10	1.1E-09	3.4E-10	6.9E-10	2.2E-10
Galactosylglycerol_25.60	4.8E-08	4E-08	4.5E-08	3.9E-08	4.5E-08	4.1E-08	4.3E-08	1.4E-09
Galactosylglycerol_26.48	6.2E-10	5.7E-10	6.4E-10	6.6E-10	5.7E-10	5E-10	5.9E-10	2.3E-11
Glucose	1.4E-08	8.2E-09	1.4E-08	1.2E-08	2.1E-08	1E-08	1.3E-08	1.8E-09
Glutamate	7.8E-11	1.1E-10	1.6E-10	9.1E-11	7.3E-11	1.2E-10	1.1E-10	1.3E-11
Glycerol	2.9E-09	2.3E-09	2.7E-09	2.1E-09	2.2E-09	2.4E-09	2.4E-09	1.2E-10
Inositol, myo-	7.6E-10	5.7E-10	4.9E-10	5.4E-10	5.9E-10	3E-10	5.4E-10	6.1E-11
Inositol, scyllo-	4.7E-09	3.7E-09	4E-09	3.9E-09	4.1E-09	4E-09	4.1E-09	1.4E-10
Maltose	3.2E-09	2.1E-09	3.1E-09	4.4E-09	5.2E-09	2.9E-09	3.5E-09	4.5E-10
Pyroglutamate	2.5E-10	1.4E-10	1.2E-10	5.1E-10	5.4E-11	1.6E-10	2.1E-10	6.6E-11

Table S4.9 Summarised MassHunter output and symbiont normalised relative abundance data for *Aiptasia* host under heat stress conditions at 7 d

			7HS				7HS	
							Mean	SE
12C cells/mg protein	3714115	5887214	5325545	4006971	4585953	5832258	4892009	379774
Fructose	0.0127	0.0147	0.0025	0.0120	0.0147	0.0094	0.0110	0.0019
Galactose	0.0013	0.0030	0.0077	0.0031	0.0018	0.0132	0.0050	0.0019
Galactosylglycerol_25.60	0.1852	0.2855	0.2944	0.2391	0.1999	0.2485	0.2421	0.0180
Galactosylglycerol_26.48	0.0039	0.0059	0.0080	0.0066	0.0036	0.0048	0.0055	0.0007
Glucose	0.0359	0.0891	0.1376	0.0783	0.0597	0.1020	0.0838	0.0143
Glutamate	0.0004	0.0009	0.0011	0.0012	0.0008	0.0013	0.0010	0.0001
Glycerol	0.0124	0.0198	0.0225	0.0162	0.0144	0.0204	0.0176	0.0016
Inositol, myo-	0.0041	0.0039	0.0034	0.0032	0.0043	0.0041	0.0038	0.0002
Inositol, scyllo-	0.2069	0.2687	0.2642	0.2673	0.2233	0.2712	0.2503	0.0113
Maltose	0.0055	0.0146	0.0125	0.0158	0.0074	0.0135	0.0115	0.0017
Pyroglutamate	0.0057	0.0029	0.0077	0.0071	0.0014	0.0044	0.0049	0.0010
Symbiont normalised							Mean	SE
12C cells/mg protein	3714115	5887214	5325545	4006971	4585953	5832258	4892009	379774
Fructose	3.42E-09	2.5E-09	4.7E-10	2.99E-09	3.21E-09	1.62E-09	2.4E-09	4.6E-10
Galactose	3.58E-10	5.17E-10	1.44E-09	7.67E-10	3.85E-10	2.26E-09	9.5E-10	3.1E-10
Galactosylglycerol_25.60	4.99E-08	4.85E-08	5.53E-08	5.97E-08	4.36E-08	4.26E-08	5E-08	2.7E-09
Galactosylglycerol_26.48	1.05E-09	1E-09	1.5E-09	1.65E-09	7.84E-10	8.15E-10	1.1E-09	1.5E-10
Glucose	9.66E-09	1.51E-08	2.58E-08	1.95E-08	1.3E-08	1.75E-08	1.7E-08	2.3E-09
Glutamate	1.17E-10	1.51E-10	2.09E-10	2.99E-10	1.81E-10	2.23E-10	2E-10	2.6E-11
Glycerol	3.33E-09	3.37E-09	4.23E-09	4.03E-09	3.15E-09	3.5E-09	3.6E-09	1.8E-10
Inositol, myo-	1.09E-09	6.56E-10	6.47E-10	8.07E-10	9.44E-10	7.04E-10	8.1E-10	7.3E-11
Inositol, scyllo-	5.57E-08	4.56E-08	4.96E-08	6.67E-08	4.87E-08	4.65E-08	5.2E-08	3.3E-09
Maltose	1.48E-09	2.48E-09	2.35E-09	3.93E-09	1.62E-09	2.31E-09	2.4E-09	3.6E-10
Pyroglutamate	1.53E-09	4.85E-10	1.45E-09	1.78E-09	3.05E-10	7.51E-10	1.1E-09	2.5E-10

Table S4.10 Summarised MassHunter output abundance data for *A. aspera* symbiont under control (C) and thermal stress (HS) conditions at 6 d

Group													6C		6HS	
Sample	6C								6HS				Mean	SE	Mean	SE
C12:0	0.0009	0.0011	0.0007	0.0012	0.0010	0.0007	0.0048	0.0080	0.0073	0.0041	0.0040	0.0046	0.0009	0.0001	0.0055	0.0007
C14:0	0.0099	0.0175	0.0118	0.0177	0.0169	0.0106	0.0495	0.0662	0.0693	0.0539	0.0415	0.0496	0.0141	0.0015	0.0550	0.0044
C16:0	0.0691	0.0915	0.0852	0.0904	0.0974	0.0839	0.1365	0.1322	0.1445	0.1255	0.1298	0.1751	0.0863	0.0040	0.1406	0.0074
C18:0	0.0093	0.0123	0.0122	0.0104	0.0264	0.0125	0.0219	0.0125	0.0183	0.0168	0.0121	0.0220	0.0138	0.0026	0.0173	0.0018
C18:1	0.0022	0.0041	0.0033	0.0042	0.0042	0.0018	0.0134	0.0118	0.0145	0.0235	0.0107	0.0172	0.0033	0.0004	0.0152	0.0019
C20:0	0.0016	0.0022	0.0017	0.0012	0.0011	0.0016	0.0016	0.0011	0.0013	0.0009	0.0006	0.0010	0.0016	0.0002	0.0011	0.0001
C20:5	0.0202	0.0328	0.0292	0.0313	0.0368	0.0297	0.0461	0.0442	0.0488	0.0564	0.0475	0.0699	0.0300	0.0022	0.0522	0.0039
C22:6	0.0133	0.0241	0.0208	0.0135	0.0229	0.0148	0.0200	0.0146	0.0191	0.0236	0.0099	0.0176	0.0182	0.0020	0.0175	0.0019
Cellotriose	0.0106	0.0007	0.0010	0.0027	0.0031	0.0028	0.0019	0.0001	0.0001	0.0063	0.0035	0.0056	0.0035	0.0015	0.0029	0.0011
Galactose	0.0159	0.0161	0.0056	0.0078	0.0132	0.0045	0.0385	0.0189	0.0110	0.0138	0.0147	0.0140	0.0105	0.0021	0.0185	0.0041
Galactosylglycerol	0.0581	0.0487	0.0345	0.0411	0.0346	0.0402	0.0772	0.0259	0.0175	0.0233	0.0318	0.0301	0.0429	0.0037	0.0343	0.0088
Glucose	0.0229	0.0107	0.0056	0.0074	0.0072	0.0043	0.0501	0.0121	0.0071	0.0189	0.0268	0.0184	0.0097	0.0028	0.0222	0.0062
Glycerol	0.0083	0.0165	0.0004	0.0136	0.0144	0.0095	0.0325	0.0358	0.0344	0.0398	0.0203	0.0271	0.0104	0.0024	0.0316	0.0028
Maltotriose	0.0070	0.0186	0.0082	0.0061	0.0136	0.0030	0.0216	0.0020	0.0013	0.0057	0.0032	0.0057	0.0094	0.0023	0.0066	0.0031
Monohexadecanoylglycerol	0.0155	0.0233	0.0180	0.0228	0.0258	0.0161	0.0531	0.0578	0.0588	0.0647	0.0411	0.0598	0.0203	0.0018	0.0559	0.0033
Monolinoleoylglycerol	0.0035	0.0067	0.0061	0.0051	0.0102	0.0034	0.0129	0.0158	0.0172	0.0095	0.0102	0.0151	0.0059	0.0010	0.0135	0.0013
Monopalmitoylglycerol	0.0021	0.0027	0.0016	0.0023	0.0024	0.0011	0.0049	0.0041	0.0040	0.0045	0.0029	0.0043	0.0020	0.0002	0.0041	0.0003
Unknown sugar_38.7	0.0015	0.0047	0.0042	0.0053	0.0077	0.0075	0.0041	0.0034	0.0032	0.0092	0.0049	0.0096	0.0052	0.0009	0.0057	0.0012

Table S4.11 Summarised MassHunter output abundance data for *A. aspera* symbiont under control (C) and thermal stress (HS) conditions at 9 d

Group	9C						9HS						9C		9HS	
Sample													Mean	SE	Mean	SE
C12:0	0.0015	0.0012	0.0006	0.0007	0.0010	0.0011	0.0047	0.0104	0.0114	0.0037	0.0034	0.0051	0.0010	0.0001	0.0065	0.0014
C14:0	0.0137	0.0184	0.0090	0.0109	0.0144	0.0172	0.0450	0.0647	0.0701	0.0462	0.0362	0.0531	0.0139	0.0015	0.0526	0.0052
C16:0	0.0709	0.0938	0.0568	0.0649	0.0918	0.1099	0.1325	0.1269	0.1202	0.1271	0.1895	0.2000	0.0813	0.0083	0.1494	0.0145
C18:0	0.0091	0.0100	0.0105	0.0079	0.0108	0.0122	0.0192	0.0160	0.0146	0.0178	0.0184	0.0203	0.0101	0.0006	0.0177	0.0009
C18:1	0.0015	0.0048	0.0025	0.0027	0.0038	0.0032	0.0140	0.0063	0.0051	0.0217	0.0155	0.0224	0.0031	0.0005	0.0142	0.0030
C20:0	0.0010	0.0017	0.0014	0.0015	0.0017	0.0013	0.0012	0.0010	0.0008	0.0010	0.0009	0.0009	0.0014	0.0001	0.0010	0.0001
C20:5	0.0084	0.0311	0.0266	0.0205	0.0321	0.0290	0.0402	0.0329	0.0313	0.0445	0.0541	0.0594	0.0246	0.0036	0.0437	0.0046
C22:6	0.0047	0.0228	0.0175	0.0136	0.0180	0.0135	0.0169	0.0110	0.0091	0.0184	0.0164	0.0162	0.0150	0.0025	0.0147	0.0015
Cellotriose	0.0000	0.0002	0.0004	0.0018	0.0019	0.0019	0.0019	0.0000	0.0000	0.0030	0.0024	0.0039	0.0010	0.0004	0.0019	0.0006
Galactose	0.0154	0.0078	0.0114	0.0082	0.0067	0.0059	0.0215	0.0057	0.0065	0.0125	0.0058	0.0068	0.0092	0.0015	0.0098	0.0026
Galactosyl-glycerol	0.0858	0.0294	0.0317	0.0326	0.0468	0.0481	0.0483	0.0148	0.0135	0.0138	0.0202	0.0324	0.0457	0.0087	0.0238	0.0057
Glucose	0.0263	0.0092	0.0083	0.0081	0.0061	0.0051	0.0445	0.0079	0.0096	0.0359	0.0330	0.0529	0.0105	0.0032	0.0306	0.0075
Glycerol	0.0119	0.0156	0.0146	0.0102	0.0109	0.0109	0.0282	0.0223	0.0236	0.0230	0.0161	0.0225	0.0124	0.0009	0.0226	0.0016
Maltotriose	0.0031	0.0048	0.0119	0.0042	0.0147	0.0066	0.0116	0.0007	0.0006	0.0025	0.0022	0.0024	0.0075	0.0019	0.0033	0.0017
Monohexa-decanoylglycerol	0.0137	0.0278	0.0114	0.0181	0.0234	0.0240	0.0555	0.0385	0.0368	0.0648	0.0492	0.0746	0.0197	0.0026	0.0532	0.0061
Monolinol-eoylglycerol	0.0008	0.0061	0.0046	0.0021	0.0043	0.0056	0.0113	0.0103	0.0106	0.0060	0.0074	0.0121	0.0039	0.0008	0.0096	0.0010
Monopalmit-oylglycerol	0.0017	0.0029	0.0033	0.0025	0.0038	0.0029	0.0047	0.0028	0.0027	0.0043	0.0030	0.0053	0.0028	0.0003	0.0038	0.0005
Unknown sugar_38.7	0.0014	0.0024	0.0019	0.0028	0.0032	0.0060	0.0032	0.0013	0.0009	0.0044	0.0075	0.0091	0.0030	0.0007	0.0044	0.0014

Table S4.12 Summarised MassHunter output relative abundance data for *A. aspera* host under heat stress conditions at 6 d

Sample	6C					6HS							6C		6HS	
													Mean	SE	Mean	SE
	5.28	4.90	5.53	4.20	4.78	5.26	3.73	2.46	2.43	2.75	3.62	3.16	4.99	0.19	3.02	0.23
Counts x 10^6																
Butyrate	0.0021	0.0021	0.0018	0.0042	0.0021	0.0020	0.0016	0.0011	0.0022	0.0035	0.0037	0.0028	0.0024	0.0004	0.0025	0.0004
C12:0	0.0029	0.0020	0.0021	0.0049	0.0026	0.0012	0.0018	0.0015	0.0032	0.0061	0.0078	0.0041	0.0026	0.0005	0.0041	0.0010
C14:0	0.0049	0.0051	0.0045	0.0108	0.0062	0.0032	0.0032	0.0026	0.0052	0.0071	0.0077	0.0042	0.0058	0.0011	0.0050	0.0008
C14:4	0.0040	0.0033	0.0055	0.0047	0.0030	0.0025	0.0053	0.0013	0.0033	0.0052	0.0064	0.0071	0.0038	0.0005	0.0048	0.0009
C16:0	0.0156	0.0106	0.0102	0.0259	0.0180	0.0112	0.0057	0.0086	0.0087	0.0177	0.0208	0.0099	0.0152	0.0025	0.0119	0.0024
Diaminovalerolactum	0.0086	0.0122	0.0124	0.0153	0.0147	0.0066	0.0119	0.0125	0.0129	0.0168	0.0186	0.0100	0.0116	0.0014	0.0138	0.0013
Digalactosylglycerol	0.0004	0.0005	0.0003	0.0006	0.0008	0.0005	0.0004	0.0001	0.0005	0.0002	0.0003	0.0006	0.0005	0.0001	0.0003	0.0001
Erythronate	0.0014	0.0030	0.0012	0.0018	0.0022	0.0051	0.0013	0.0010	0.0012	0.0011	0.0010	0.0030	0.0025	0.0006	0.0014	0.0003
Fructose	0.0005	0.0002	0.0003	0.0005	0.0005	0.0002	0.0004	0.0002	0.0005	0.0003	0.0003	0.0015	0.0004	0.0001	0.0005	0.0002
Galactinol	0.0013	0.0011	0.0006	0.0006	0.0010	0.0025	0.0019	0.0006	0.0010	0.0007	0.0013	0.0027	0.0012	0.0003	0.0014	0.0003
Galactose	0.0352	0.0275	0.0350	0.0349	0.0505	0.0232	0.0573	0.0451	0.0371	0.0375	0.0405	0.0285	0.0344	0.0038	0.0410	0.0039
Galactosylglycerol_25.60	0.1374	0.1658	0.1447	0.2209	0.1480	0.1015	0.0546	0.0670	0.0596	0.0917	0.0599	0.0478	0.1531	0.0161	0.0634	0.0062
Galactosylglycerol_26.05	0.0081	0.0103	0.0065	0.0099	0.0081	0.0051	0.0025	0.0023	0.0024	0.0037	0.0024	0.0019	0.0080	0.0008	0.0025	0.0003
Galactosylglycerol_26.45	0.0014	0.0033	0.0022	0.0025	0.0021	0.0016	0.0012	0.0021	0.0017	0.0022	0.0021	0.0012	0.0022	0.0003	0.0018	0.0002
Glucose	0.1157	0.0460	0.0642	0.0829	0.0732	0.0446	0.1000	0.1116	0.1146	0.0726	0.0917	0.0849	0.0711	0.0108	0.0959	0.0066
Glutamate_16.758	0.0044	0.0024	0.0015	0.0005	0.0022	0.0026	0.0038	0.0008	0.0007	0.0008	0.0018	0.0027	0.0023	0.0005	0.0018	0.0005
Glutarate_17.196	0.0072	0.0064	0.0053	0.0052	0.0069	0.0122	0.0081	0.0019	0.0031	0.0060	0.0052	0.0162	0.0072	0.0011	0.0068	0.0021
Glycerate	0.0006	0.0007	0.0004	0.0005	0.0006	0.0009	0.0004	0.0003	0.0003	0.0005	0.0005	0.0007	0.0006	0.0001	0.0004	0.0001
Glycerol	0.0173	0.0171	0.0198	0.0282	0.0294	0.0090	0.0117	0.0133	0.0221	0.0142	0.0156	0.0193	0.0201	0.0031	0.0160	0.0016
Inositol, myo_21.89	0.0004	0.0002	0.0002	0.0003	0.0002	0.0002	0.0031	0.0006	0.0005	0.0007	0.0008	0.0006	0.0003	0.0000	0.0011	0.0004
Inositol, scyllo-_22.86	0.0005	0.0000	0.0006	0.0006	0.0003	0.0000	0.0001	0.0009	0.0002	0.0008	0.0007	0.0001	0.0003	0.0001	0.0005	0.0002
Maltose	0.0038	0.0194	0.0098	0.0043	0.0092	0.0082	0.0050	0.0040	0.0024	0.0043	0.0148	0.0052	0.0091	0.0023	0.0060	0.0018
Monohexadecanoylglycerol	0.0046	0.0060	0.0037	0.0206	0.0085	0.0028	0.0011	0.0004	0.0041	0.0061	0.0128	0.0072	0.0077	0.0027	0.0053	0.0018
Monopalmitoylglycerol	0.0007	0.0011	0.0009	0.0030	0.0017	0.0005	0.0003	0.0001	0.0007	0.0012	0.0025	0.0014	0.0013	0.0004	0.0010	0.0003

	6C							6HS					6C		6HS	
Sample													Mean	SE	Mean	SE
Proline	0.0020	0.0011	0.0021	0.0023	0.0016	0.0008	0.0017	0.0009	0.0013	0.0023	0.0021	0.0014	0.0016	0.0002	0.0016	0.0002
Ribitol	0.0010	0.0012	0.0011	0.0009	0.0008	0.0006	0.0009	0.0011	0.0008	0.0009	0.0008	0.0007	0.0009	0.0001	0.0009	0.0001
Ribose	0.0009	0.0006	0.0007	0.0005	0.0008	0.0005	0.0019	0.0007	0.0007	0.0009	0.0011	0.0009	0.0007	0.0001	0.0010	0.0002
Serine	0.0014	0.0004	0.0004	0.0007	0.0015	0.0010	0.0015	0.0009	0.0011	0.0015	0.0015	0.0003	0.0009	0.0002	0.0011	0.0002
Turanose	0.0010	0.0042	0.0019	0.0009	0.0017	0.0019	0.0012	0.0009	0.0008	0.0009	0.0030	0.0014	0.0020	0.0005	0.0014	0.0003
unknown sugar_16.18	0.0029	0.0028	0.0028	0.0080	0.0027	0.0024	0.0017	0.0029	0.0031	0.0058	0.0046	0.0024	0.0036	0.0009	0.0034	0.0006
unknown sugar_16.496	0.0009	0.0009	0.0009	0.0024	0.0008	0.0008	0.0005	0.0009	0.0010	0.0018	0.0014	0.0008	0.0011	0.0003	0.0011	0.0002

Table S4.13 Summarised MassHunter output relative abundance normalised to symbiont density for *A. aspera* host under heat stress conditions at 6 d

	Relative abundance (x10^{-9})												6C		6HS	
Sample	6C						6HS						Mean	SE	Mean	SE
Butyrate	0.41	0.43	0.32	0.99	0.43	0.38	0.42	0.46	0.90	1.26	1.03	0.87	0.49	0.10	0.82	0.13
C12:0	0.54	0.42	0.37	1.16	0.55	0.22	0.47	0.59	1.30	2.23	2.16	1.29	0.54	0.13	1.34	0.30
C14:0	0.92	1.05	0.80	2.58	1.30	0.60	0.85	1.07	2.14	2.58	2.13	1.32	1.21	0.29	1.68	0.28
C14:4	0.76	0.67	1.00	1.13	0.64	0.47	1.42	0.53	1.34	1.91	1.78	2.26	0.78	0.10	1.54	0.24
C16:0	2.95	2.17	1.84	6.15	3.76	2.12	1.52	3.51	3.56	6.46	5.73	3.15	3.17	0.66	3.99	0.74
Diaminovalerolactum	1.62	2.49	2.24	3.64	3.07	1.25	3.20	5.09	5.32	6.14	5.14	3.17	2.39	0.36	4.68	0.50
Digalactosylglycerol	0.07	0.11	0.06	0.15	0.16	0.09	0.10	0.04	0.20	0.07	0.08	0.19	0.11	0.02	0.11	0.03
Erythronate	0.27	0.61	0.23	0.44	0.46	0.97	0.36	0.40	0.50	0.41	0.28	0.96	0.50	0.11	0.48	0.10
Fructose	0.09	0.05	0.05	0.12	0.10	0.05	0.11	0.10	0.20	0.10	0.10	0.46	0.08	0.01	0.18	0.06
Galactinol	0.25	0.23	0.10	0.14	0.21	0.47	0.52	0.23	0.41	0.26	0.36	0.86	0.23	0.05	0.44	0.09
Galactose	6.66	5.60	6.33	8.30	10.57	4.40	15.38	18.34	15.26	13.66	11.18	9.03	6.98	0.89	13.81	1.35
Galactosylglycerol_25.60	26.01	33.84	26.15	52.53	30.98	19.30	14.66	27.25	24.53	33.39	16.53	15.15	31.47	4.68	21.92	3.13
Galactosylglycerol_26.05	1.54	2.10	1.17	2.36	1.69	0.97	0.67	0.94	1.00	1.35	0.66	0.59	1.64	0.22	0.87	0.12

	Relative abundance ($x10^{-9}$)												6C		6HS	
Sample	6C							6HS					Mean	SE	Mean	SE
Galactosylglycerol_26.45	0.27	0.67	0.40	0.59	0.45	0.31	0.32	0.83	0.71	0.80	0.59	0.38	0.45	0.06	0.61	0.09
Glucose	21.89	9.39	11.61	19.72	15.33	8.48	26.85	45.39	47.15	26.44	25.31	26.92	14.40	2.26	33.01	4.21
Glutamate_16.758	0.83	0.49	0.27	0.11	0.47	0.49	1.02	0.33	0.28	0.28	0.49	0.87	0.44	0.10	0.54	0.13
Glutarate_17.196	1.36	1.31	0.96	1.24	1.45	2.32	2.17	0.77	1.29	2.20	1.44	5.14	1.44	0.19	2.17	0.64
Glycerate	0.11	0.15	0.08	0.12	0.12	0.17	0.11	0.13	0.13	0.17	0.13	0.22	0.12	0.01	0.15	0.02
Glycerol	3.28	3.49	3.58	6.71	6.16	1.70	3.13	5.42	9.11	5.18	4.32	6.10	4.15	0.78	5.54	0.83
Inositol, myo_21.89	0.08	0.04	0.04	0.07	0.04	0.05	0.84	0.23	0.22	0.27	0.23	0.19	0.05	0.01	0.33	0.10
Inositol, scyllo-_22.86	0.10	0.00	0.11	0.14	0.06	0.00	0.02	0.37	0.10	0.31	0.20	0.02	0.07	0.02	0.17	0.06
Maltose	0.72	3.95	1.77	1.02	1.92	1.55	1.34	1.64	1.01	1.57	4.08	1.66	1.82	0.46	1.88	0.45
Monohexadecanoylglycerol	0.86	1.23	0.67	4.91	1.78	0.54	0.30	0.18	1.70	2.22	3.53	2.29	1.66	0.67	1.70	0.52
Monopalmitoylglycerol	0.14	0.23	0.17	0.72	0.36	0.09	0.08	0.05	0.31	0.44	0.68	0.44	0.29	0.09	0.33	0.10
Proline	0.37	0.22	0.37	0.54	0.34	0.15	0.45	0.37	0.54	0.85	0.58	0.46	0.33	0.06	0.54	0.07
Ribitol	0.19	0.24	0.19	0.22	0.17	0.12	0.25	0.46	0.34	0.32	0.22	0.21	0.19	0.02	0.30	0.04
Ribose	0.17	0.12	0.13	0.13	0.17	0.09	0.50	0.28	0.27	0.33	0.30	0.29	0.13	0.01	0.33	0.04
Serine	0.27	0.08	0.08	0.17	0.31	0.18	0.39	0.35	0.45	0.55	0.41	0.10	0.18	0.04	0.38	0.06
Turanose	0.20	0.86	0.35	0.22	0.36	0.36	0.33	0.35	0.32	0.33	0.84	0.45	0.39	0.10	0.44	0.08
unknown sugar_16.18	0.54	0.57	0.51	1.89	0.56	0.46	0.45	1.17	1.27	2.12	1.27	0.77	0.76	0.23	1.17	0.23
unknown sugar_16.496	0.17	0.18	0.16	0.57	0.17	0.15	0.15	0.36	0.40	0.65	0.38	0.26	0.24	0.07	0.37	0.07

Table S4.14 Summarised MassHunter output relative abundance data for *A. aspera* host under heat stress conditions at 9 d

													9C		9HS	
Sample	9C						9HS						Mean	SE	Mean	SE
Counts x10^6	4.47	4.99	4.66	3.77	4.10	5.51	2.46	0.83	0.54	1.14	1.90	1.70	4.58	0.25	1.43	0.29
Butyrate	0.0021	0.0030	0.0025	0.0024	0.0020	0.0020	0.0017	0.0020	0.0025	0.0022	0.0029	0.0029	0.0023	0.0002	0.0024	0.0002
C12:0	0.0031	0.0043	0.0032	0.0020	0.0020	0.0009	0.0020	0.0035	0.0021	0.0016	0.0095	0.0025	0.0026	0.0005	0.0035	0.0012
C14:0	0.0044	0.0089	0.0073	0.0039	0.0044	0.0020	0.0042	0.0045	0.0035	0.0025	0.0050	0.0032	0.0052	0.0010	0.0038	0.0004
C14:4	0.0038	0.0030	0.0038	0.0028	0.0036	0.0079	0.0030	0.0032	0.0010	0.0035	0.0062	0.0023	0.0042	0.0008	0.0032	0.0007
C16:0	0.0117	0.0220	0.0209	0.0087	0.0144	0.0061	0.0120	0.0109	0.0098	0.0112	0.0161	0.0097	0.0140	0.0026	0.0116	0.0010
Diaminovalerolactum	0.0103	0.0126	0.0152	0.0081	0.0148	0.0088	0.0115	0.0084	0.0116	0.0081	0.0195	0.0087	0.0116	0.0012	0.0113	0.0018
Digalactosylglycerol	0.0002	0.0002	0.0003	0.0002	0.0004	0.0001	0.0002	0.0001	0.0001	0.0001	0.0001	0.0002	0.0002	0.0000	0.0001	0.0000
Erythronate	0.0018	0.0022	0.0016	0.0022	0.0013	0.0010	0.0011	0.0008	0.0007	0.0008	0.0004	0.0011	0.0017	0.0002	0.0008	0.0001
Fructose	0.0003	0.0002	0.0002	0.0002	0.0003	0.0004	0.0004	0.0004	0.0002	0.0003	0.0004	0.0002	0.0003	0.0000	0.0003	0.0000
Galactinol	0.0006	0.0003	0.0004	0.0010	0.0009	0.0009	0.0007	0.0002	0.0001	0.0003	0.0003	0.0005	0.0007	0.0001	0.0004	0.0001
Galactose	0.0298	0.0294	0.0253	0.0148	0.0348	0.0361	0.0433	0.0116	0.0092	0.0324	0.0329	0.0281	0.0284	0.0032	0.0263	0.0054
Galactosylglycerol_25.60	0.1669	0.2163	0.1841	0.1586	0.1918	0.1650	0.0334	0.0200	0.0167	0.0448	0.0469	0.0549	0.1804	0.0088	0.0361	0.0063
Galactosylglycerol_26.05	0.0094	0.0114	0.0097	0.0083	0.0095	0.0077	0.0013	0.0007	0.0007	0.0016	0.0017	0.0022	0.0094	0.0005	0.0014	0.0002
Galactosylglycerol_26.45	0.0013	0.0025	0.0030	0.0019	0.0023	0.0016	0.0012	0.0024	0.0025	0.0022	0.0018	0.0015	0.0021	0.0003	0.0019	0.0002
Glucose	0.1024	0.0458	0.0518	0.0439	0.0724	0.0658	0.0847	0.1232	0.1142	0.0555	0.0984	0.0689	0.0637	0.0090	0.0908	0.0107
Glutamate_16.758	0.0051	0.0013	0.0006	0.0007	0.0015	0.0027	0.0036	0.0008	0.0001	0.0012	0.0010	0.0011	0.0020	0.0007	0.0013	0.0005
Glutarate_17.196	0.0074	0.0055	0.0037	0.0060	0.0069	0.0128	0.0076	0.0067	0.0029	0.0061	0.0066	0.0052	0.0070	0.0013	0.0059	0.0007
Glycerate	0.0006	0.0005	0.0004	0.0004	0.0004	0.0004	0.0004	0.0002	0.0002	0.0003	0.0002	0.0003	0.0005	0.0000	0.0003	0.0000
Glycerol	0.0145	0.0147	0.0180	0.0120	0.0192	0.0177	0.0104	0.0142	0.0147	0.0087	0.0227	0.0155	0.0160	0.0011	0.0144	0.0020
Inositol, myo_21.89	0.0004	0.0002	0.0002	0.0002	0.0002	0.0002	0.0023	0.0006	0.0007	0.0006	0.0009	0.0008	0.0002	0.0000	0.0010	0.0003
Inositol, scyllo-_22.86	0.0007	0.0005	0.0003	0.0001	0.0006	0.0004	0.0004	0.0007	0.0003	0.0006	0.0013	0.0001	0.0004	0.0001	0.0005	0.0002
Maltose	0.0009	0.0147	0.0171	0.0079	0.0149	0.0049	0.0015	0.0007	0.0011	0.0012	0.0036	0.0050	0.0101	0.0026	0.0022	0.0007
Monohexadecanoylglycerol	0.0041	0.0116	0.0120	0.0020	0.0024	0.0011	0.0006	0.0011	0.0008	0.0008	0.0029	0.0072	0.0056	0.0020	0.0022	0.0010
Monopalmitoylglycerol	0.0010	0.0019	0.0030	0.0004	0.0007	0.0004	0.0003	0.0003	0.0002	0.0003	0.0006	0.0013	0.0012	0.0004	0.0005	0.0002
Proline	0.0016	0.0015	0.0017	0.0012	0.0019	0.0025	0.0015	0.0014	0.0008	0.0016	0.0030	0.0011	0.0017	0.0002	0.0016	0.0003
Ribitol	0.0008	0.0009	0.0011	0.0008	0.0009	0.0008	0.0008	0.0008	0.0008	0.0008	0.0010	0.0007	0.0009	0.0000	0.0008	0.0000

Sample	9C						9HS						9C Mean	9C SE	9HS Mean	9HS SE
Ribose	0.0010	0.0006	0.0008	0.0005	0.0011	0.0010	0.0015	0.0004	0.0003	0.0006	0.0008	0.0004	0.0008	0.0001	0.0007	0.0002
Serine	0.0012	0.0006	0.0006	0.0003	0.0010	0.0008	0.0025	0.0024	0.0021	0.0024	0.0015	0.0013	0.0007	0.0001	0.0021	0.0002
Turanose	0.0004	0.0026	0.0031	0.0018	0.0025	0.0011	0.0005	0.0003	0.0003	0.0003	0.0007	0.0013	0.0019	0.0004	0.0006	0.0002
unknown sugar_16.18	0.0024	0.0056	0.0040	0.0035	0.0033	0.0023	0.0015	0.0028	0.0032	0.0033	0.0053	0.0035	0.0035	0.0005	0.0033	0.0005
unknown sugar_16.496	0.0007	0.0017	0.0012	0.0011	0.0010	0.0008	0.0004	0.0009	0.0010	0.0010	0.0016	0.0012	0.0011	0.0001	0.0010	0.0002

Table S4.15 Summarised MassHunter output relative abundance normalised to symbiont density for *A. aspera* host under heat stress conditions at 9 d

	Relative abundance ($x10^{-9}$)												9C		9HS	
Sample	9C						9HS						Mean	SE	Mean	SE
Butyrate	0.47	0.60	0.54	0.63	0.50	0.37	0.67	2.44	4.56	1.90	1.50	1.70	0.52	0.04	2.13	0.54
C12:0	0.70	0.86	0.68	0.54	0.48	0.16	0.81	4.17	3.80	1.37	4.98	1.47	0.57	0.10	2.77	0.72
C14:0	0.99	1.79	1.57	1.03	1.07	0.36	1.69	5.39	6.51	2.20	2.62	1.90	1.13	0.20	3.38	0.83
C14:4	0.86	0.60	0.81	0.74	0.89	1.43	1.21	3.79	1.91	3.03	3.23	1.32	0.89	0.12	2.42	0.44
C16:0	2.62	4.41	4.49	2.30	3.51	1.11	4.90	13.12	17.92	9.85	8.48	5.67	3.07	0.54	9.99	2.00
Diaminovalerolactum	2.31	2.53	3.26	2.15	3.61	1.60	4.66	10.11	21.34	7.11	10.24	5.09	2.58	0.30	9.76	2.51
Digalactosylglycerol	0.05	0.04	0.06	0.05	0.09	0.02	0.09	0.10	0.12	0.13	0.06	0.15	0.05	0.01	0.11	0.01
Erythronate	0.41	0.44	0.35	0.59	0.31	0.19	0.44	0.95	1.27	0.70	0.23	0.67	0.38	0.05	0.71	0.15
Fructose	0.07	0.05	0.05	0.05	0.08	0.08	0.16	0.52	0.36	0.23	0.19	0.14	0.06	0.01	0.27	0.06
Galactinol	0.14	0.06	0.08	0.26	0.23	0.16	0.29	0.20	0.27	0.25	0.16	0.31	0.15	0.03	0.25	0.02
Galactose	6.67	5.89	5.43	3.92	8.50	6.55	17.58	13.97	16.94	28.41	17.30	16.48	6.16	0.62	18.45	2.06
Galactosylglycerol_25.60	37.37	43.34	39.53	42.05	46.80	29.91	13.56	24.06	30.57	39.28	24.63	32.25	39.83	2.38	27.39	3.58
Galactosylglycerol_26.05	2.11	2.29	2.09	2.21	2.32	1.40	0.55	0.84	1.25	1.43	0.91	1.27	2.07	0.14	1.04	0.14
Galactosylglycerol_26.45	0.28	0.51	0.64	0.51	0.56	0.30	0.48	2.84	4.66	1.90	0.96	0.90	0.47	0.06	1.96	0.64
Glucose	22.92	9.19	11.12	11.64	17.68	11.93	34.42	148.07	209.76	48.69	51.65	40.45	14.08	2.12	88.84	29.68
Glutamate_16.758	1.13	0.27	0.14	0.17	0.37	0.49	1.45	0.90	0.25	1.07	0.50	0.63	0.43	0.15	0.80	0.18
Glutarate_17.196	1.65	1.11	0.80	1.58	1.68	2.32	3.09	8.05	5.35	5.33	3.49	3.06	1.52	0.21	4.73	0.79
Glycerate	0.14	0.10	0.08	0.12	0.10	0.07	0.14	0.29	0.34	0.25	0.12	0.18	0.10	0.01	0.22	0.04
Glycerol	3.24	2.94	3.87	3.19	4.70	3.21	4.23	17.03	26.97	7.59	11.90	9.11	3.52	0.27	12.81	3.33
Inositol, myo_21.89	0.08	0.04	0.04	0.05	0.05	0.04	0.94	0.76	1.21	0.57	0.48	0.45	0.05	0.01	0.73	0.12

	Relative abundance ($x10^{-9}$)												9C		9HS	
Sample	9C							9HS					Mean	SE	Mean	SE
Inositol, scyllo-_22.86	0.16	0.10	0.06	0.03	0.16	0.08	0.14	0.84	0.50	0.53	0.67	0.03	0.10	0.02	0.45	0.13
Maltose	0.20	2.95	3.67	2.08	3.63	0.90	0.61	0.90	2.07	1.04	1.87	2.95	2.24	0.59	1.57	0.36
Monohexadecanoylglycerol	0.92	2.33	2.59	0.53	0.59	0.20	0.25	1.35	1.42	0.68	1.52	4.21	1.19	0.41	1.57	0.57
Monopalmitoylglycerol	0.22	0.38	0.64	0.11	0.17	0.07	0.11	0.35	0.38	0.29	0.30	0.75	0.27	0.09	0.37	0.09
Proline	0.36	0.31	0.35	0.31	0.46	0.46	0.59	1.74	1.49	1.42	1.58	0.67	0.38	0.03	1.25	0.20
Ribitol	0.19	0.19	0.23	0.22	0.21	0.14	0.32	0.93	1.46	0.72	0.52	0.41	0.19	0.01	0.73	0.17
Ribose	0.22	0.13	0.18	0.12	0.27	0.17	0.60	0.51	0.51	0.53	0.44	0.23	0.18	0.02	0.47	0.05
Serine	0.26	0.13	0.14	0.07	0.24	0.14	1.03	2.94	3.91	2.10	0.77	0.79	0.16	0.03	1.92	0.53
Turanose	0.10	0.53	0.67	0.48	0.60	0.19	0.22	0.32	0.54	0.25	0.37	0.75	0.43	0.09	0.41	0.08
unknown sugar_16.18	0.53	1.12	0.86	0.92	0.80	0.43	0.62	3.38	5.89	2.90	2.80	2.06	0.78	0.11	2.94	0.71
unknown sugar_16.496	0.16	0.34	0.25	0.30	0.25	0.14	0.18	1.08	1.85	0.90	0.86	0.69	0.24	0.03	0.93	0.22